

**University of Alberta**

**Dual Function Sensorimotor Neurons Mediate a Behavioral Response to  
Hypoxia in Embryos of *Helisoma trivolvis***

by

**Shihuan Kuang**



A thesis submitted to the Faculty of Graduate Studies and Research in partial  
fulfillment of the requirements for the degree of Doctor of Philosophy

in

Physiology and Cell Biology

Department of Biological Sciences

Edmonton, Alberta

Fall 2002



National Library  
of Canada

Acquisitions and  
Bibliographic Services

395 Wellington Street  
Ottawa ON K1A 0N4  
Canada

Bibliothèque nationale  
du Canada

Acquisitions et  
services bibliographiques

395, rue Wellington  
Ottawa ON K1A 0N4  
Canada

*Your file Votre référence*

*Our file Notre référence*

The author has granted a non-exclusive licence allowing the National Library of Canada to reproduce, loan, distribute or sell copies of this thesis in microform, paper or electronic formats.

The author retains ownership of the copyright in this thesis. Neither the thesis nor substantial extracts from it may be printed or otherwise reproduced without the author's permission.

L'auteur a accordé une licence non exclusive permettant à la Bibliothèque nationale du Canada de reproduire, prêter, distribuer ou vendre des copies de cette thèse sous la forme de microfiche/film, de reproduction sur papier ou sur format électronique.

L'auteur conserve la propriété du droit d'auteur qui protège cette thèse. Ni la thèse ni des extraits substantiels de celle-ci ne doivent être imprimés ou autrement reproduits sans son autorisation.

0-612-81213-8

**Canada**

**University of Alberta**

**Library Release Form**

**Name of Author:** Shihuan Kuang

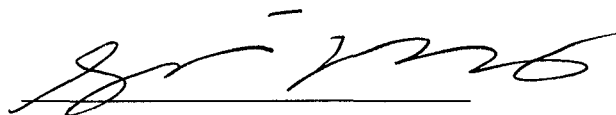
**Title of Thesis:** Dual Function Sensorimotor Neurons Mediate a Behavioral Response to Hypoxia in Embryos of *Helisoma trivolvis*.

**Degree:** Doctor of Philosophy

**Year this Degree Granted:** 2002

Permission is hereby granted to the University of Alberta Library to reproduce single copies of this thesis and to lend or sell such copies for private, scholarly, or scientific research purposes only.

The author reserves all other publication and other rights in association with the copyright in the thesis, and except as herein before provided, neither the thesis nor any substantial portion thereof may be printed or otherwise reproduced in any material form whatever without the author's prior written permission.



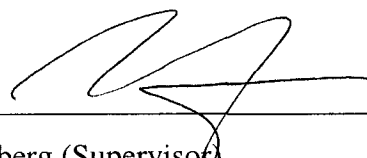
Department of Biological Sciences,  
CW315 Biological Sciences Center  
University of Alberta,  
Edmonton, Alberta,  
Canada T6G 2E9

August 29, 2002

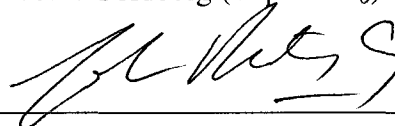
University of Alberta

Faculty of Graduate Studies and Research

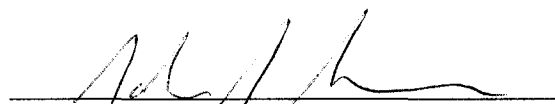
The undersigned certify that they have read, and recommend to the Faculty of Graduate Studies and Research for acceptance, a thesis entitled **Dual Function Sensorimotor Neurons Mediate a Behavioral Response to Hypoxia in Embryos of *Helisoma trivolvis*** submitted by **Shihuan Kuang** in partial fulfillment of the requirements for the degree of **Doctor of Philosophy in Physiology and Cell Biology**.



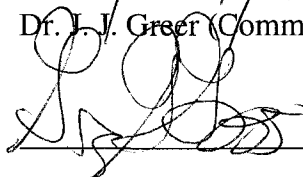
Dr. J. I. Goldberg (Supervisor)




Dr. J. P. Chang (Committee Member)



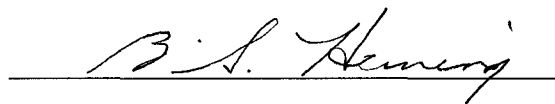
Dr. J. J. Greer (Committee Member)



Dr. G. G. Goss (Department Appointee)



Dr. W. K. Milsom (External Examiner)



Dr. B. S. Heming (Examination Chairman)

Aug. 15, 2002



## **Dedication**

This thesis is dedicated to my late grandmother, Yuanying Deng (1920-1998), whose endless encouragement led to the successful completion of this Ph. D. thesis.

## Abstract

Encapsulated embryos of *Helisoma trivolvis* display a cilia-driven rotational behavior. This thesis elucidates the physiological importance, cellular components and molecular mechanisms of this behavior through laser stimulation, laser ablation, anatomical, developmental, pharmacological and electrophysiological experiments.

Since several studies in this thesis required embryos to be removed from egg capsules, experimentally manipulated and then monitored as they continue to develop, I established a transplantation technique to achieve long-term growth and development of de-capsulated embryos. To investigate the physiological importance of embryonic rotation, I tested the hypothesis that this behavior functions to mix the capsular fluid and improve O<sub>2</sub> diffusion to the embryo. Structural components of encapsulation conferred diffusional barriers, resulting in an O<sub>2</sub> gradient from the exterior to the center of the egg capsule. Hypoxia elicited a long-lasting, dose-dependent and reversible enhancement of embryonic rotation and a relocation of embryos to the egg capsule periphery.

To study the neuronal basis of the rotational behavior, I tested the hypothesis that ENC1s, a pair of early developing serotonergic neurons, function to detect O<sub>2</sub> levels and stimulate ciliary activity accordingly. Laser stimulation of ENC1 enhanced the activity of specific target cilia that generate the embryonic rotation. In contrast, bilateral laser ablation of ENC1s reduced the rate of embryonic rotation. Furthermore, embryos displayed no behavioral response to hypoxia after ablation of ENC1s. Lastly, hypoxia elicited membrane depolarization and action potential activity in cultured ENC1s.

To explore the molecular mechanisms underlying the hypoxia-elicited response, I tested the hypothesis that serotonin, K<sup>+</sup> channels and mitochondrial function are involved

in O<sub>2</sub> sensing and hypoxic signaling. The rotational response to hypoxia was attenuated in the presence of a serotonin receptor antagonist. In addition, inhibitors of K<sup>+</sup> channels and the mitochondrial electron transport chain mimicked the rotational response to hypoxia.

Together, these results demonstrate that the ENC1-ciliary neuronal circuit functions to detect environmental O<sub>2</sub> and produce behavioral responses to hypoxia. Since homologues of ENC1 commonly exist in other invertebrate larvae, this unique system provides excellent opportunities to examine not only developmental and mechanistic, but also comparative and evolutionary aspects of O<sub>2</sub> sensing.

## Acknowledgments

First of all, I thank my supervisor, Dr. Jeffrey Goldberg for his excellent supervision. Jeff not only taught me how to appreciate snails, but also exemplified excellence in research, teaching, scientific communication and family life. I will always remember the wonderful time that I had in his lab and will try to practice the fishing skills he taught me on our way back from the CSZ meeting in Lethbridge.

My next big thanks go to a number of professors and students who have directly or indirectly involved in this thesis work. I appreciate the enormous input from members of my supervisory committee: Drs. John Greer (Dept. of Physiology), Dave Pilgrim and John Chang. Dr. Chang also allowed me to use his equipment and chemicals. I appreciate and will not forget his critical thinking skills, talent and generosity. Dr. Greg Goss, who assumed his faculty position a few months before I started my program, has been always ready to help. He not only helped me set up the hypoxic and hypercapnic experiments, but also acted as an examiner in my candidacy and final defense. I will remember the questions you have asked me, Greg! As the external examiner, Dr. Bill Milsom traveled from University of British Columbia to attend my thesis defense and brought me a pile of questions! Thank you Bill for the hard work. Dr. Bruce Heming acted as the chair of my defense and did a fantastic job! Future Dr. Shandra Doran carried out some control experiments on the cultured ciliated cell for me. Shandra liberated me from the snail room by taking over my lab captain title (I was the captain of myself most of the time before she came to the lab) and brought to the lab lots of joy and telephone rings. Murette Regnier tested the effects of pH and EGF on embryonic development. Thank you Dr. Declan Ali for helping me patch clamp ENC1s in culture. Dr. Rich Wilson (Dept. of Physiology, Univ. of Calgary) measured the oxygen gradient across egg capsules. Dr. Calvin Wong helped with automatic analysis of ciliary beating and was very helpful throughout my program of study. Rakesh Bhatnagar, Randy Mandryk and George Braybrook assisted with the confocal, light and electron microscopy. I am thankful to Dr. Steven Archer for discussion on the current view of O<sub>2</sub>-sensing mechanisms and generously providing me with some chemicals. Dr. Andy Bulloch (Dept. of Cell Biology, Univ. of Calgary) provided the *Lymnaea* EGF tested in my study.

It has always been my great pleasure to be acquainted with other colleagues, graduate and undergraduate students. Every one of them will leave a long-lasting memory in my mind. Here I list some of them: Kee-Chan Ahn, Yuka Asai, Geoff Boddy, Dr. Li Chen, Angela Cole, Cagla Esicioglu, Kevin Friesen, Dr. Fern Galvez, Guy Hawkings, Zhigang Jin, Dr. James Johnson, Dawn Kieller, Bin Li, Dr. James Lin, Dr. Xinwei Lin, Dr. Helen Mao, Sabeen Mapra, Aniseh Mashkournia, Elizabeth Orr, Shawn Parries, Sarah Robbins, James Stafford, Keith Todd, Nina Tran, Suraj Unniappan, Aubrey Uretsky, Brain Weiss, Kevin Young, Warren Yunker. Thank you all for correcting my English and appreciating my accent.

I am grateful to the University of Alberta for sponsoring me with an F. S. Chia Scholarship. My study was also partially funded by scholarships from the Faculty of Science and Department of Biological Sciences.

Finally, I would like to express my heartfelt gratitude to my parents, my wife Jun and my son Randy for their consistent love and support.

## Table of Contents

<b>Introduction .....</b>	<b>1</b>
1. Overview .....	1
2. Development of embryos and serotonergic neurons in <i>Helisoma</i> .....	1
2.1 Environmental and developmental characteristics of encapsulated embryos .....	1
2.2 Development and possible role of serotonergic neurons in <i>Helisoma</i> .....	3
3. Serotonergic modulation of animal behavior .....	5
3.1 Sensory-motor integration and animal behavior .....	5
3.2 Organization of chemosensory systems in adult gastropods .....	6
3.3 Distribution of serotonergic neurons in apical sensory organs of larval gastropods..	8
3.4 Serotonin stimulates ciliary beating .....	8
3.5 Modulation of rhythmic swimming behavior by serotonergic neurons .....	9
3.6 Central serotonergic neurons modulate rhythmic feeding behavior in gastropods..	11
3.7 Serotonin-mediated forms of behavioral plasticity .....	12
4. O <sub>2</sub> sensing and responses to hypoxia .....	13
4.1 Comparative respiratory physiology .....	13
4.2 Control of respiration by central pattern generators .....	15
4.3 Modulation of respiration by central and peripheral chemosensory afferents .....	16
4.4 Mechanisms of O <sub>2</sub> sensing and hypoxia signaling .....	18
4.5 Behavioral, physiological and developmental responses to hypoxia .....	20
4.6 Serotonin-related plasticity in respiration .....	23
5. Use of ablation technique in the study of cellular function .....	24
5.1 Methods for cell ablation .....	24
5.2 Principles and applications of laser ablation .....	25
6. Objectives .....	26
6.1 To establish a method for long-term culture of de-capsulated embryos .....	26
6.2 To test the motor function of ENC1 .....	27
6.3 To examine the sensory function of ENC1 .....	27
6.4 To investigate the hypoxia-signaling pathway in <i>Helisoma</i> embryos .....	28

<b>Materials and methods</b> .....	<b>31</b>
1. Animals .....	31
2. <i>Ex ovo</i> culture of isolated embryos .....	31
3. Transplantation of early embryos .....	32
4. Scanning electron microscopy .....	33
5. Mounting and dismounting live embryos on glass slides .....	33
6. ENC1 identification .....	34
7. Laser treatment .....	34
8. Serotonin immunohistochemistry .....	35
9. Measurement of ciliary activity and embryonic rotation .....	36
10. Culture of Embryonic Cells and Tissues .....	37
11. Measurement of O <sub>2</sub> Partial Pressure .....	38
12. Hypoxic Treatment .....	38
13. Patch-clamp Recording of ENC1 .....	39
14. Pharmacological treatments .....	40
15. Statistical analysis .....	40
<b>Results</b> .....	<b>42</b>
1. Culture of isolated embryos .....	42
1.1 <i>Ex ovo</i> culture of de-capsulated embryos .....	42
1.2 Transplantation of de-capsulated embryos .....	44
2. ENC1 regulates the activity of specific target cilia .....	45
2.1 Effectiveness and specificity of laser ablation .....	46
2.2 Different groups of cilia display distinct basal ciliary activity .....	48
2.3 Laser stimulation of ENC1 has different effects on different groups of cilia .....	48
2.4 Laser-induced enhancement of ciliary activity involves serotonin .....	49
2.5 Laser ablation of ENC1 abolishes spontaneous rotational surges .....	50
3. <i>Helisoma</i> embryos display an adaptive behavioral response to hypoxia .....	51
3.1 Structural basis of encapsulation renders a diffusional barrier .....	52
3.2 Hypoxia elicits prolonged acceleration of embryonic rotation .....	54
3.3 Po <sub>2</sub> dependency and behavioral plasticity of hypoxia-elicited embryonic rotation .....	55
3.4 Effect of CO <sub>2</sub> on embryonic rotation .....	55

3.5	Hyperoxia also elicits dose-dependent acceleration of rotation .....	57
3.6	Interaction between O <sub>2</sub> and CO <sub>2</sub> .....	57
3.7	Effects of other environmental factors on embryonic rotation .....	58
4.	ENC1 mediates O <sub>2</sub> sensing and the rotational response to hypoxia .....	59
4.1	Hypoxia has no direct effect on ciliary beating .....	59
4.2	Rotational responsiveness to hypoxia correlates to ENC1 development .....	60
4.3	Laser ablation of ENC1s abolishes hypoxia-elicited acceleration of embryonic rotation .....	60
4.4	Hypoxia induces excitatory responses in ENC1 .....	60
5.	The hypoxia signaling pathways .....	61
5.1	Involvement of serotonin receptor activation .....	62
5.2	Involvement of 4-AP sensitive potassium channels .....	62
5.3	Involvement of the mitochondrial electron transport chain .....	63
	<b>Discussion .....</b>	<b>113</b>
1.	Embryonic environment during encapsulated development .....	113
1.1	Diffusional barriers resulting from encapsulation .....	113
1.2	Function of ciliary beating and embryonic rotation .....	114
2.	Possible environmental factors affecting embryonic rotation .....	115
2.1	O <sub>2</sub> as a major environmental regulator of embryonic behavior .....	115
2.2	Behavioral plasticity of hypoxia-elicited embryonic rotation .....	116
2.3	Effect of CO <sub>2</sub> variations on embryonic rotation .....	117
2.4	Interaction between O <sub>2</sub> and CO <sub>2</sub> .....	117
3.	<i>Ex ovo</i> culture and transplantation of de-capsulated early embryos .....	118
3.1	De-capsulated early embryos fail to develop normally <i>ex ovo</i> .....	119
3.2	Embryo transplantation is an effective strategy for culturing de-capsulated embryos .....	121
3.3	Potential applications of the embryo transplantation technique .....	122
4.	Laser treatment of cells in <i>Helisoma</i> embryos .....	123
4.1	Laser treatment paradigms .....	123
4.2	Advantages of laser ablation .....	124
4.3	Laser-induced cell death .....	125



5. ENC1 as a cilioexcitatory motor neuron .....	126
5.1 Laser treatment directly demonstrates the cilioexcitatory motor function of ENC1 .....	126
5.2 ENC1 regulates ciliary activity through release of serotonin .....	127
5.3 How are ciliary activity and embryonic rotation regulated in <i>Helisoma</i> embryos? .....	128
6. ENC1 as an O <sub>2</sub> -sensitive chemosensory neuron .....	130
6.1 Multiple lines of evidence suggest ENC1 as the O <sub>2</sub> sensor .....	130
6.2 The dendritic knob is the possible site of O <sub>2</sub> sensing .....	130
7. Signaling pathways involved in the adaptive response to hypoxia .....	132
7.1 Mechanisms of O <sub>2</sub> sensing .....	132
7.2 Hypoxia-elicited signal transduction .....	134
8. General significance of ENC1-ciliary circuits in <i>Helisoma</i> .....	135
<b>Footnotes</b> .....	<b>143</b>
<b>References</b> .....	<b>144</b>

## List of Tables

<b>Table 1.</b> Acute and chronic responses to hypoxia .....	21
--	----

## List of Figures

<b>Figure 1.</b>	Mechanisms of O <sub>2</sub> sensing .....	30
<b>Figure 2.</b>	DIC micrograph of scratches made by single laser pulses on a glass coverslip .....	41
<b>Figure 3.</b>	Embryonic development after 3 days of culture <i>in ovo</i> and <i>ex ovo</i> at 23°C ....	64
<b>Figure 4.</b>	Growth and development of <i>in ovo</i> control embryos, transplanted embryos and <i>ex ovo</i> cultured embryos at 23 °C .....	66
<b>Figure 5.</b>	Effect of pH on growth and development of <i>ex ovo</i> cultured embryos .....	68
<b>Figure 6.</b>	Survival and hatching rates of transplanted and control embryos at 23 °C ....	69
<b>Figure 7.</b>	Morphological development of control and transplanted stage E1-E2 (2-4 cell stages) embryos at 20.5 °C .....	70
<b>Figure 8.</b>	Growth and development of control and transplanted stage E1-E2 (2-8 cell stage) embryos at 20.5 °C .....	71
<b>Figure 9.</b>	Anatomical evidence for the motor function of ENC1 .....	72
<b>Figure 10.</b>	Morphological changes in ENC1 after laser treatment .....	73
<b>Figure 11.</b>	Laser ablation of ENC1's primary neurite .....	74
<b>Figure 12.</b>	Loss of serotonin immunoreactivity in ENC1 6-24 h after laser ablation .....	75
<b>Figure 13.</b>	Laser treatment causes cell-specific elimination .....	76
<b>Figure 14.</b>	Anatomical relationship between ENC1 and the major ciliary bands of <i>Helisoma</i> embryos .....	77
<b>Figure 15.</b>	Temporal profiles of ciliary beat frequency in different groups of cilia before and after unilateral laser stimulation of ENC1 .....	78
<b>Figure 16.</b>	Effects of ENC1 laser stimulation on ciliary activity .....	80
<b>Figure 17.</b>	Laser treatment of ENC1 causes transient increases in ciliary beat frequency of dorsolateral and pedal cilia .....	81
<b>Figure 18.</b>	Effect of serotonin on beat frequency of different groups of cilia .....	82
<b>Figure 19.</b>	Effect of ENC1 laser stimulation on the temporal pattern of CBF in the presence of mianserin (50 µM) .....	83
<b>Figure 20.</b>	Effect of mianserin (50 µM) on basal and ENC1 laser stimulation-induced ciliary activity .....	84

<b>Figure 21.</b> Bilateral laser ablation of ENC1s provides direct evidence for the cilioexcitatory function of these cells .....	85
<b>Figure 22.</b> Structural components involved in embryonic rotation behavior .....	86
<b>Figure 23.</b> Diffusional barriers associated with encapsulation in <i>Helisoma</i> embryos .....	87
<b>Figure 24.</b> Ultrastructure of egg capsule membrane in <i>Helisoma</i> .....	88
<b>Figure 25.</b> Ultrastructure of egg capsule membrane in <i>Lymnaea</i> .....	89
<b>Figure 26.</b> O <sub>2</sub> gradient from surface to interior of egg mass .....	90
<b>Figure 27.</b> Experimental demonstration of the diffusional barrier associated with encapsulation .....	91
<b>Figure 28.</b> Hypoxia stimulates the embryonic rotational behavior in <i>Helisoma</i> .....	92
<b>Figure 29.</b> Effect of extracellular pH on embryonic rotation .....	93
<b>Figure 30.</b> Translocation of embryos during hypoxia .....	94
<b>Figure 31.</b> Hypoxia stimulates the embryonic rotational behavior in <i>Lymnaea</i> .....	95
<b>Figure 32.</b> The rotational response to hypoxia is Po <sub>2</sub> dependent and reversible .....	97
<b>Figure 33.</b> Effect of hypercapnia on embryonic rotational behavior .....	98
<b>Figure 34.</b> Effect of hyperoxia on the embryonic rotational behavior .....	99
<b>Figure 35.</b> Interactive effect of CO <sub>2</sub> and O <sub>2</sub> on embryonic rotation .....	100
<b>Figure 36.</b> Glutamine stimulates embryonic rotation .....	101
<b>Figure 37.</b> Effect of low extracellular Ca <sup>2+</sup> concentration on basal and hypoxia-induced embryonic rotation .....	102
<b>Figure 38.</b> Isolated ciliated cells do not respond to hypoxia .....	103
<b>Figure 39.</b> Correlation of embryonic rotational response to hypoxia to ENC1 development .....	104
<b>Figure 40.</b> ENC1s mediate the rotational response to hypoxia .....	105
<b>Figure 41.</b> Identification of ENC1 in culture .....	107
<b>Figure 42.</b> Electrophysiological responses of ENC1 to hypoxia as indicated by membrane currents in a cell-attached patch-clamp recording .....	108
<b>Figure 43.</b> Electrophysiological responses of ENC1 to hypoxia as indicated by membrane potential in a whole-cell patch-clamp recording .....	109
<b>Figure 44.</b> Involvement of serotonin in mediating the rotational response to hypoxia ...	110
<b>Figure 45.</b> Involvement of K <sup>+</sup> channels in mediating embryonic rotation .....	111

<b>Figure 46.</b> Involvement of the mitochondrial electron transport chain in mediating embryonic rotation .....	112
<b>Figure 47.</b> Visualization of current flow generated by ciliary beating in <i>Helisoma</i> embryos .....	138
<b>Figure 48.</b> Laser treatment paradigms .....	140
<b>Figure 49.</b> Model of the function of the embryonic rotational behavior .....	142

## Abbreviations

4-AP	4-aminopyridine
5-HT	5-hydroxytryptamine; serotonin
AHS	antibiotic <i>Helisoma</i> saline
APW	artificial pond water
ASO	apical sensory organ
ATP	adenosine triphosphate
BDNF	brain derived neurotrophic factor
BSA	bovine serum albumin
CB	carotid body
CBF	ciliary beat frequency
CF	capsular fluid
cAMP	cyclic adenosine monophosphate
cGMP	cyclic guanosine monophosphate
CNS	central nervous system
CO <sub>2</sub>	carbon dioxide
CPG	central pattern generator
DIC	Nomarski differential interference contrast microscopy
DLB	dorsolateral band of cilia
EGF	epidermal growth factor
EGTA	ethylene glycol-bis( $\beta$ -aminoethyl ether)-N,N,N',N'-tetraacetic acid
ENC1	embryonic neurons C1
EPO	erythropoietin
EPSP	excitatory postsynaptic potential
ET	endothelin
ETC	mitochondrial electron transport chain
GABA	$\gamma$ -aminobutyric acid
h-EGF	human recombinant epidermal growth factor
H <sub>2</sub> O <sub>2</sub>	peroxide
HDM	<i>Helisoma</i> defined medium
HIF	hypoxia inducible factor
HRE	hypoxia response elements
HS	<i>Helisoma</i> saline
IGF	insulin-like growth factor
I <sub>K(Ca)</sub>	Ca <sup>2+</sup> -dependent K <sup>+</sup> current

l-EGF	<i>Lymnaea</i> epidermal growth factor
IPAS	inhibitory PAS domain protein
ITC	isolated tufts of cilia
LTF	long-term facilitation
M199	medium 199
NADPH	nicotinamide adenine dinucleotide phosphate
NEB	neuroepithelial body
NH <sub>4</sub> <sup>+</sup>	ammonium
NMDA	N-methyl-D-aspartate
NO	nitric oxide
O <sub>2</sub>	molecular oxygen
O <sub>2</sub> <sup>•</sup>	oxygen free radical
O <sub>2</sub> <sup>-</sup>	superoxide
OK channel	O <sub>2</sub> -sensitive potassium channel
PAS	Per/Arnt/Sim domain protein
PB	pedal band of cilia
PBS	phosphate buffered saline
PH	prolyl hydroxylase
PKA	cAMP dependent protein kinase
PKG	cGMP dependent protein kinase
P <sub>O<sub>2</sub></sub>	partial pressure of O <sub>2</sub>
ROS	reactive oxygen species
S. E. M.	standard error of the mean
sAHP	spike afterhyperpolarization
SEM	scanning electron microscopy
SOD	superoxide dismutase
STP	short-term potentiation
TEA	tetraethylammonium
UL	ubiquitin ligase
VEGF	vascular endothelial growth factor
VHL	von Hippel-Lindau protein

## Introduction

### 1. Overview

The neural mechanisms underlying animal behavior are a fundamental yet not well-understood question in neurobiology. Even less is known at cellular and molecular levels how neural circuits incorporate certain environmental stimuli and generate specific adaptive responses, especially during development. Taking advantage of the simplicity and accessibility, both *in vivo* and *in vitro*, of molluscan neural circuits (Bulloch and Syed, 1992; Goldberg, 1998), I try to address these issues in embryos of the pond snail *Helisoma trivolvis* (Mollusca, Gastropoda, Pulmonata, Basommatophora, Planorbidae).

Pond snail embryos develop in individual egg capsules within egg masses, where they display a cilia-driven rotational behavior early in development (Diefenbach et al., 1991). Concomitant with the initiation of the rotational behavior, a pair of bipolar serotonergic neurons, named ENC1s, develops bilaterally in close association with target ciliary cells (Goldberg and Kater, 1989; Diefenbach et al., 1998; Koss et al., 2002). Each of the ENC1s has an ascending dendrite that penetrates the embryonic surface and terminates with a chemosensory-like structure, suggestive of a sensory function. Each ENC1 also projects a primary neurite towards specific target ciliary cells that drive the embryonic rotation, indicating a motor function. However, direct evidence for the sensory and motor functions of ENC1s is lacking. One objective of this study is to demonstrate the sensory and motor functions of these unique serotonergic cells. Another objective is to test the hypothesis that the ENC1-ciliary neural circuits mediate a respiratory behavioral response to hypoxia in embryos. Finally, the molecular mechanisms involved in oxygen (O<sub>2</sub>) sensing and the hypoxia-signaling pathway are explored.

In light of these objectives, I will review some related background in the rest of this section.

### 2. Development of embryos and serotonergic neurons in gastropods

#### 2.1. Environmental and developmental characteristics of encapsulated embryos

Embryos of pulmonate gastropods undergo direct development from fertilized egg to juvenile snail inside egg capsules filled with albuminous perivitelline fluid, also known as capsular fluid (CF). The nutrition required for normal development of embryos is



provided by the CF, which is a secretory product of the albumen gland (Raven, 1958; Morrill et al., 1964; Beadle, 1969; Goudsmit, 1976; Morrill, 1982; Stockmann-Bosback and Althoff, 1989; Heras et al. 1998). Early studies have largely identified carbohydrates such as galactogen and proteins as two major categories of nutrition in CF, which together make up more than 94 % of its dry weight in the freshwater pond snail *Lymnaea stagnalis* (Horstmann, 1956; Morrill et al., 1964; Wijsman and van Wijck-Batenburg, 1987). However, the specific key nutritive components for the growth and development of early embryos are yet unknown. In addition, there are several other unique features of the microenvironment of egg capsules that can hardly be mimicked *in vitro*. It has been reported that there is a positive hydrostatic pressure (2.1 atmospheres) and negative equilibrium potential (-23 mV) inside newly laid egg capsules of *Lymnaea* (Raven, 1958; Taylor, 1973; Morrill, 1982; Pechenik et al., 1984). There is also a report of antibacterial factors in the CF of the sea slug *Aplysia kurodi* (Kamiya et al., 1984). Recent studies have further identified an epidermal growth factor (EGF) and various enzymes such as phosphatases and trypsin inhibitors in the CF of several species (Stockmann-Bosback and Althoff, 1989; Hermann et al., 2000; Nagle et al., 2001). These complex structural and compositional features of egg capsules appear to be critical for embryonic development, as attempts to achieve normal development of early stage embryos *ex ovo* have been largely unsuccessful in many species (Morrill, 1982; Pechenik et al., 1984; Stockmann-Bosback and Althoff, 1989; Meshcheryakov, 1990).

Encapsulation has important physiological consequences on embryos. Compared to free swimming larvae, encapsulated embryos are well protected from bacterial invasion and don't need to move a lot in search of food, but they have to overcome problems arising from limited space and multilayer diffusional barriers. In *Helisoma*, normally 10-25 sibling egg capsules are housed in a jelly matrix, together called an egg mass. As revealed by scanning electron microscopy of freeze-fractured egg masses (refer to **Results, 3.1**), there are at least four layers of diffusional barriers surrounding each embryo. From inside to outside, these include a vitelline membrane that covers the embryo prior to gastrulation, a viscous CF, a capsular membrane, a gelatinous matrix in which the egg capsule is embedded, and an outer envelope that surrounds the whole egg mass (refer to Beadle, 1969 for similar structures in other pulmonates). Furthermore,

unstirred boundary layers surrounding the embryo and on either side of both capsular and egg mass membranes severely impede the exchange of materials (Wither, 1992).

Although results from the current and other studies have shown that these structural components inherent to egg masses are collectively permeable to water, inorganic ions and low molecular weight solutes, their presence nevertheless retards the rates of diffusion (Beadle, 1969; Taylor, 1973). The retarded diffusional rate could result in severe physiological consequences under certain circumstances, such as when O<sub>2</sub> availability falls due to metabolic consumption or environmental constraints (Derry, 1993).

Another physiological challenge that encapsulated embryos constantly encounter is to maintain ionic and osmotic homeostasis within their egg capsules. It has been suggested that CF maintains a higher level of cations, including Ca<sup>2+</sup>, Na<sup>+</sup>, K<sup>+</sup> and Mg<sup>2+</sup>, by a Donnan equilibrium (Taylor, 1973), but it is unclear how embryos actively achieve ionic and osmotic balance. Although other unknown mechanisms may be involved, ciliary beating could function to maintain the homeostasis and O<sub>2</sub> supply by reducing the intracapsular boundary layers, thus facilitating the inward diffusion of cations and O<sub>2</sub> and outward diffusion of metabolic wastes such as CO<sub>2</sub> and NH<sub>4</sub><sup>+</sup>. A major part of this thesis examines the neural circuit that controls ciliary beating and the environmental cue that stimulates its activity.

## **2.2. Development and possible role of serotonergic neurons in *Helisoma***

The first pair of serotonergic neurons, identified as embryonic neurons C1 (ENC1s), develops at the early trochophore stage, or stage E15, in embryonic *Helisoma* (Goldberg and Kater, 1989; Diefenbach et al., 1995; 1998). The somata of ENC1s are found bilaterally among large ectodermal cells at the lateral margins of the apical plate in an anterior-lateral superficial orientation (Diefenbach et al., 1998). Each ENC1 has a relatively large ovoid cell body (12-15 μm in length) which contains a smooth nucleus and prominent nucleolus, as well as numerous large granules in the apical cytoplasm (Diefenbach et al., 1998). During development, each ENC1 projects a primary neurite ventrally to the region of the pedal band of ciliated cells, where extensive neuritic branching occurs (Goldberg and Kater, 1989; Diefenbach et al., 1995; 1998; Koss et al.,

2002). Furthermore, as each descending primary neurite passes below the dorsolateral ciliary band, short processes extend from the basal surface of dorsolateral ciliated cells to closely appose the primary neurite and small secondary neurites of ENC1 (Koss et al., 2002). This anatomical association of ENC1 with the dorsolateral and pedal ciliated cells implies that ENC1s function to regulate ciliary activity. In addition, each ENC1 projects an apical dendrite that penetrates the dorsal epidermis and terminates with a non-motile ciliary structure (Diefenbach et al., 1998). This structure is very similar to the "dendritic knob" of vertebrate olfactory neurons and chemosensory neurons in adult molluscs (Emery, 1975; 1976; 1992; Muller and Marc, 1984; Menini, 1999), suggesting that ENC1 also functions as a chemosensory cell to detect certain environmental cues.

In several recent studies, the physiological mechanisms and possible involvement of ENC1 in cilia-driven embryonic rotation have begun to be elucidated. Pharmacological experiments demonstrated that embryonic rotation is regulated by serotonin. Addition of exogenous serotonin accelerates the rate of embryonic rotation in egg capsules (Diefenbach et al., 1991). In contrast, the serotonin receptor antagonist, mianserin, abolishes the action of serotonin and, when applied alone, reduces the rate of embryonic rotation by eliminating the periodic surges in rotation that occur normally (Diefenbach et al., 1991). These key experiments suggest that endogenously released serotonin generates periodic surges of embryonic rotation. Cell culture experiments have confirmed the cilioexcitatory action of serotonin (Goldberg et al., 1994) and have begun to elucidate the underlying signal transduction mechanisms (Christopher et al., 1996; 1999). Taken together, these results suggest that endogenous serotonin plays a role in regulating ciliary function. Given that ENC1s are the only pair of neurons expressing the serotonin phenotype in early-stage embryos, it appears that ENC1s release serotonin to regulate embryonic rotation. However, direct functional evidence linking ENC1 to ciliary activity is lacking. It is also unclear what environmental cue stimulates ENC1 to release serotonin. Lastly, it remains to be determined whether and how ENC1s act selectively on the different groups of cilia; the pedal band of cilia, the dorsolateral bands of cilia, and the isolated tufts of cilia that are diffusely distributed all over the embryonic surface.

Interestingly, ENC1 loses its serotonin immunoreactivity at around stage E65 but the morphology of ENC1 persists throughout embryonic development (Diefenbach et al.,

1998). Following development of ENC1, which is a peripheral neuron that resides just anterior to the developing cerebral ganglia, several clusters of central serotonergic neurons occur first in the cerebral, and then pedal ganglia by stage E50 (Goldberg and Kater, 1989). At later stages of embryonic development and through hatching to adulthood, the number of serotonergic neurons increases gradually. By the stage of sexual maturation, there are 30-70 serotonergic neurons in each of the cerebral, pedal, parietal and visceral ganglia, and 3 serotonergic neurons in each of the buccal and pleural ganglia (Goldberg and Kater, 1989). The abundant presence of serotonergic neurons in every ganglion of the central nervous system (CNS) implies that serotonin is a major neurotransmitter system involved in many aspects of neural function in *Helisoma*. While the cerebral ganglion neuron C1 is the only adult serotonergic cell to be studied extensively in *Helisoma* (reviewed in Murphy, 2001), the homologues of C1 and other serotonergic neurons have been characterized in other gastropod species (elaborated below in 3.6).

### **3. Serotonergic modulation of animal behavior**

#### **3.1. Sensory-motor integration and animal behavior**

In all animals other than sponges, which don't have a true nervous system, simple and complex animal behaviors are generated by the integrated output of sensory and motor signals from the nervous system. In cnidarians, such as hydras, corals and jellyfish, specialized sensory neurons in the outside epidermal layer detect environmental stimuli and signal either directly to effector cells or to motor neurons, which in turn innervate effector cells (Swanson et al., 1999). In most other higher animals, sensory inputs are carried to a centralized aggregation of neurons called a ganglion or brain, where they are integrated and processed to generate specific motor outputs and behavioral responses.

Extraordinary examples of how nerve cells integrate environmental information to produce coordinated behavior have been studied in numerous invertebrates, such as worms, leeches, snails, slugs, flies, bees, ants, lobster and crayfish, because of their simplified neural circuits and wide diversity (Nicholls et al., 2001). Ants and bees wander miles away from their home in search of food without getting lost. Their amazing ability to navigate by integrating information provided by polarized sunlight or magnetic fields

exemplifies how a simple nervous system can nonetheless control complex behavior (Nicholls et al., 2001). Sensory-motor integration can be best studied in less complex behaviors, such as leech swimming. Although the basic rhythmic swimming pattern is established by inhibitory and excitatory synaptic interactions within each ganglion, peripheral receptors serve to trigger, enhance, depress, or halt the swimming behavior (Brodfuehrer et al., 1995). Similarly, feeding behavior in gastropods is an integrated output of basic rhythmic activity and sensory modulation (Kemenes, 1994). The neural circuits generating feeding behavior are subjected to positive and negative modulation from serotonergic and FMRFamide interneurons, respectively, which receive sensory information from peripheral receptors (Murphy, 2001; elaborated in 3.6).

Embryos of *Helisoma* provide an excellent system to study the mechanism of sensory-motor integration underlying a simple behavior. *Helisoma* embryos develop within individual transparent egg capsules where they display a rotational behavior. Using time-lapse videomicroscopy, this behavior can be readily quantified in terms of the average rate of rotation and frequency of periodic accelerations in rotation (Diefenbach et al., 1991). Moreover, essentially the cellular components underlying this rotational behavior are limited to a pair of serotonergic neurons, ENC1s, and several target ciliary cells (Koss et al., 2002). The simple structure of this circuit enables one to dissect the whole signaling pathway from the sensory input to motor output. Finally, the neurotransmitter phenotypes, developmental course and synaptic connections of ENC1, and parts of the intracellular signaling pathways involved in regulation of ciliary activity have been elucidated (Goldberg, 1989, Goldberg et al., 1994; 1995; 1998; Christopher et al., 1996; 1999; Koss et al., 2002). However, the environmental factor that stimulates the ENC1-ciliary neural circuit remains unknown. Identification of the environmental stimulant will allow for detailed analysis of molecular events and signaling pathways involved in the sensory-motor integration process as embryos modify their behavior in response to external influences and internal programs.

### **3.2. Organization of chemosensory systems in adult gastropods**

The sensory system functions to provide the CNS with a representation of the external environment so that proper behavioral responses can be generated. Given their

poor hearing and vision, many gastropods detect environment stimuli mainly by means of chemical sensing. Therefore, chemical sensing plays critical roles in feeding, respiration, mating, reproduction and social organization. In transduction of chemical sensing, chemical stimuli bind to specific chemoreceptors, interacting with specific moieties within the receptors to generate broad spectra of signaling cascades that usually result in a depolarizing sensory current response (Mac Leish et al., 1999). Studies on olfaction indicate that  $\text{Ca}^{2+}$  plays an important role in mediating the initial excitation and subsequent adaptation of olfactory receptors (Menini, 1999; Zufall and Leinders-Zufall, 2000).

Chemoreceptors are distributed all over the skin of adult gastropods, with a higher concentration in the tentacles, mouth area, and osphradia, functioning to detect distant stimuli, taste, and changes in  $\text{O}_2$  and osmolarity, respectively (Zaitseva, 1999). Most receptor cells have a single peripheral sensory process that terminates on the epithelial surface with microvilli and cilia (Yi and Emery, 1991; Emery, 1992; Boudko, 1999; Zaitseva, 1999). Chemical cues presumably bind to receptor proteins in the microvilli or cilia and trigger a sensory response that is propagated to the CNS directly or through a peripheral ganglion (Emery, 1992). Electrophysiological studies on isolated olfactory receptor cells of squid show that the sensory cells are excitable and contain voltage-gated  $\text{K}^+$ ,  $\text{Na}^+$  and  $\text{Ca}^{2+}$  channels (Lucero et al., 1992). Blockage of  $\text{K}^+$  channels, which increases cell excitability and broadens action potentials (Lucero et al., 1992), may be a common mechanism underlying chemosensory responses.

The role of serotonin in mediating or modulating chemosensory responses is not well understood. Cells with serotonin-like immunoreactivity have been detected in the osphradial ganglion of *Lymnaea* (Nezlin and Voronezhskaya, 1997). In other gastropods, including *Cryptomphalus aspersa*, *Pleurobranchaea californica* and *Tritonia diomedea*, abundant serotonin immunoreactive neuronal processes were present in the sensory epithelia of the rhinophore, tentacle and mouth, but serotonergic cell bodies were found only in the CNS (Flores et al., 1986; Moroz et al., 1997). Together, these studies suggest a role for serotonergic neurons in sensory signaling.

### **3.3 Distribution of serotonergic neurons in apical sensory organs of larval gastropods**

The apical sensory organ (ASO) is a larval neural structure present in a variety of marine invertebrate larvae, including gastropods (For a list, see Marois and Carew, 1997a). It is comprised of a ciliated sensory epithelium near the larval apex and an underlying cluster of neurons that are referred to as the apical ganglion. Serotonergic sensory cells have been universally found in the ASO of many gastropods. In larvae of the patellogastropod *Tectura scutum*, three serotonergic sensory cells are found in the ASO, all having an apical sensory process and descending neurites that extend beneath ciliated prototrochal cells that drive larval swimming (Page, 2002). In the ASO of the caenogastropods *Euspira lewisii*, *Lacuna vincta*, *Trichotropis cancellata*, and *Amphissa versicolor*, three to six serotonin-immunoreactive neurons are found, with only some of them displaying sensory features (Page and Parries, 2000). In the ASO of the larval opisthobranches *Aplysia californica*, *Berghia verrucicornis*, *Phestilla sibogae*, *Melibe leonina*, and *Tritonia diomedea*, three of five serotonergic cells are para-ampullary type sensory cells that extend a ciliated apical dendrite to the pretrochal epithelium and a descending axon into the CNS (Kempf et al., 1997; Marois and Carew, 1997b; 1997c). This arrangement suggests a role for these serotonergic neurons in the integration of sensory information to achieve proper motor adaptation to variable environmental conditions. Whereas photoinactivation of the ASO of *Phestilla* confirmed its role in detecting metamorphic cues (Hadfield et al., 2000), the specific function of the serotonergic neurons could not be determined. Since it has been suggested that ENC1s in early-stage embryos of *Helisoma* are homologous to serotonergic neurons in the ASO of other gastropods (Marois and Carew, 1997a), elucidation of the sensory and motor function of ENC1 has evolutionary and phylogenetic significance.

### **3.4 Serotonin stimulates ciliary beating**

Ciliary beating plays various roles in different animal systems. In aquatic animals, beating of specific cilia drives locomotion (Chia et al, 1984). In addition, cilia in the gut and on the gill surface of aquatic animals plays important roles in feeding (Richoux and Thompson, 2001). Finally, mammalian tracheal cilia and gill surface cilia in aquatic

animals function in respiration (van der Baan, 2000). Although cilia are generally capable of spontaneous beating, their activities are often under neuronal and neurohumoral control (Aiello, 1957; Murakami and Takahashi, 1975; Mackie et al., 1976; Audesirk, 1978).

Serotonin or serotonergic neurons have been predominantly shown to stimulate ciliary beating through a signaling pathway that involves a rise in intracellular  $\text{Ca}^{2+}$  concentration (reviewed in Murakami, 1989; Walczak and Nelson, 1994). Exogenous serotonin has a cilioexcitatory action on the lateral gill cilia of the bivalve *Mytilus edulis* and *Modiolus demissus* (Aiello, 1957; Gosselin, 1961; Gosselin et al., 1962), cilia of several embryonic gastropods (Koshtoyants et al., 1961, Goldberg et al., 1994), cilia of sea urchin larvae (Soliman, 1983), and tracheal cilia in mammalian respiratory tracts (Tsuchiya and Kensler, 1959). More recently, serotonergic neurons have been implicated in control of ciliary activity in *Helisoma* embryos (Diefenbach et al., 1991; Goldberg et al., 1994; refer to 2.2). Furthermore, in adults of a closely related pond snail *Lymnaea*, a cluster of serotonergic neurons in the pedal ganglia innervates ciliary cells on the base of the foot (Syed and Winlow, 1989). Finally, in the nudibranch *Tritonia*, stimulation of an identified serotonergic neuron in the pedal ganglia, or serotonin injection, elicits an increase in pedal ciliary activity (Audesirk, 1978; Audesirk et al., 1979). The results from these functional studies are supported by a recent comparative anatomical study showing that serotonergic projections towards locomotory cilia commonly occur in most invertebrate phyla ranging from platyhelminthes to echinoderms (Hay-Schmidt, 2000).

### **3.5 Modulation of rhythmic swimming behavior by serotonergic neurons**

In vertebrates, rhythmic swimming is generated by neuronal networks called central pattern generators (CPGs) that are located in the spinal cord. Although CPGs display intrinsic activity, the motor output of the CPG is subjected to inhibitory and excitatory modulation by neurotransmitters so that the speed, strength, direction and coordination of the movement can be finely tuned (Katz, 1996; Sillar et al., 1997). Serotonergic projections from the raphe nuclei in the ventral medulla of the brain stem mediate the excitatory modulation of CPG output. In *Xenopus*, the rostrocaudal development of the swimming rhythm is coincident with the axial growth of serotonergic



raphespinal projections into the spinal cord (van Mier et al., 1986). Serotonin mainly increases the timing and intensity of motoneuronal discharge during locomotion (Sillar et al., 1997). In lamprey, serotonin blocks a  $\text{Ca}^{2+}$ -dependent  $\text{K}^+$  current ( $I_{\text{K}(\text{Ca})}$ ) that contributes to the slow spike afterhyperpolarization (sAHP) that negatively regulates the firing frequency of neurons (el Manira et al., 1994). Since reduction of  $I_{\text{K}(\text{Ca})}$  by serotonin also impairs burst termination (Sillar et al., 1997), serotonin increases both burst duration and firing frequency within the burst. Presynaptically, serotonin reduces glycinergic reciprocal inhibition during swimming in *Xenopus* tadpoles through a reduction of voltage-activated  $\text{Ca}^{2+}$  currents (Sillar et al., 1997). This leads to an increase in the strength of excitatory synaptic connectivity as well as the amplitude and duration of bursts. Finally, in CPGs of *Rana* and *Xenopus*, serotonin plays a role in NMDA receptor-mediated intrinsic oscillations of membrane potential by enabling the repolarizing phase of each oscillation (Sillar et al., 1997).

In invertebrates, serotonin affects leech swimming through its effect on the membrane properties of swim-initiating interneurons and several swim motor neurons (Brodfuefrer et al., 1995). Swimming leeches have higher levels of serotonin in the blood than do quiescent ones. Moreover, stimulation of the serotonergic Retzius cells promotes swimming (Nicholls et al., 2001), whereas chemical ablation of these serotonergic neurons during embryonic development results in a deficiency in swimming movements during adulthood (Glover and Kramer, 1982). In crayfish, the afferent synaptic transmission to a pair of escape command neurons is under serotonergic modulation. The modulatory effect is either facilitatory or inhibitory, depending on the dose, rate and duration of serotonin application, as well as on the social status of the animals (Yeh et al., 1996; Teshiba et al., 2001). Finally, both exogenous serotonin and central serotonergic neurons increase swimming activity in marine opisthobranchs (McPherson and Blankenship, 1991; Satterlie and Norekian, 1996). In *Clione limacina*, for example, central serotonergic neurons in the cerebral and pedal ganglia directly modulate swimming by increasing the swimming CPG cycle frequency (Norekian and Satterlie, 1996; Satterlie et al., 2000). These studies demonstrate that serotonin plays an important role in modulating the swimming behavior of both vertebrate and invertebrate species.

### 3.6 Central serotonergic neurons modulate rhythmic feeding behavior in gastropods

The rhythmic feeding behaviors in some gastropods are generated by CPGs in the buccal ganglia (Kemenes, 1997; Perrins and Weiss, 1998; Murphy, 2001). Similar to the swimming CPG, activity of the feeding CPG is subject to CNS modulation so that specific feeding patterns can be generated in response to food stimuli at the lip. The predominant evidence suggests that serotonergic modulation plays a stimulatory role in feeding behavior. In *Helisoma*, the feeding CPG is composed of three interconnected subunits, S1, S2 and S3, each containing a group of interneurons. Each subunit semi-independently generates rhythmic oscillations and innervates a subset of motor neurons that directly control the feeding pattern. Stimulation of S1 sequentially activates S2 and S3, resulting in a triphasic feeding pattern composed of protraction, retraction, and hyper-retraction, respectively (Murphy, 2001). The activity of this CPG is under direct facilitatory modulation by a pair of giant serotonergic interneurons (C1) located in the cerebral ganglia (Granzow and Kater, 1977). Both bath application of serotonin and stimulation of C1 either electrophysiologically or with food stimulants to the lip consistently elicit rhythmic activities in S2 and S3, resulting in a rhythmic swallowing behavior (Murphy, 2001). In *Lymnaea*, the feeding CPG is similarly composed of three interneurons, N1, N2, and N3, which control the protraction, rasping and swallowing phases of the feeding behavior, respectively (Kemenes, 1997). The feeding rhythm is gated and facilitated by a pair of giant serotonergic interneurons in the cerebral ganglia that are homologous to C1 in *Helisoma* (Bulloch and Ridgway, 1995). Neurotoxin treatment or laser photoinactivation of these serotonergic neurons significantly reduced the rate and responsiveness of feeding behavior (Yeoman et al., 1994; Kemenes, 1997). Likewise, *Aplysia* contains a pair of homologous cerebral serotonergic neurons that play a role in controlling feeding arousal (Weiss et al., 1982). Morphologically, physiologically and functionally similar pairs of serotonergic neurons have also been identified in several other gastropods (Reviewed in Bulloch and Ridgway, 1995). As compared to what is known from studies on vertebrate swimming CPGs, less detail is known how serotonin modulates the firing properties and the synaptic connectivity of CPG interneurons and motor neurons in gastropods.

### 3.7 Serotonin-mediated forms of behavioral plasticity

Several studies by Kandel and colleagues on the molecular mechanisms of a simple form of behavioral plasticity, sensitization of the gill-withdraw reflex in the sea hare *Aplysia*, demonstrate that serotonin plays a central role in this process (reviewed in Kandel, 2001). *Aplysia* responds to otherwise innocuous stimuli with enhanced gill withdrawal upon an aversive shock to the tail, a learned behavior termed sensitization. *In vivo* studies and *in vitro* experiments on reconstructed neural circuits delineate that the sensitization results from an enhancement of synaptic transmission induced by a serotonin-elicited signaling cascade (Kandel, 2001). Upon a shock to the tail, serotonin is released from certain interneurons onto presynaptic terminals of the sensory-motor circuit that generates gill withdrawal. Binding of serotonin to its receptors on the presynaptic terminals results in an increase in levels of intracellular cAMP and its downstream target protein kinase A (PKA). PKA either directly activates the neurotransmitter release machinery or phosphorylates certain K<sup>+</sup> channels, resulting in reduced K<sup>+</sup> currents and increased cell excitability and spike duration. Together, these modulations by PKA result in a short-term enhancement of synaptic transmission and a sensitization of the gill-withdraw response. Furthermore, prolonged increases in PKA upon repeated stimulation of the tail result in a long-term enhancement of synaptic transmission and behavioral responses through signaling pathways that involve gene transcription and growth of new synapses (Kandel, 2001).

In leech, photo or mechanosensory stimuli trigger a defensive whole-body shortening response that displays certain forms of behavioral plasticity. During sensitization, the excitability of an identified interneuron (S-cell) increases. In contrast, during habituation, where animals learn to decrease the strength of responses to repetitive stimuli, the S-cell activity decreases (Burrell et al., 2001). Bath application of serotonin or stimulation of the serotonergic Retzius cells increases the excitability of the S-cell (Burrell et al., 2001). In contrast, serotonin depletion attenuates both the sensitization and classical conditioning of the body-withdraw reflex (Ehrlich et al., 1992; Sahley, 1994). Finally, serotonin has also been shown to mediate changes in behavioral state associated with food deprivation in the leech (Groome et al., 1993). Together, these studies suggest that serotonin plays a role in non-associative and associative learning in leech.

In *Caenorhabditis elegans*, when food-deprived animals are reintroduced with food, they move more slowly to ensure that they don't leave the feast too soon. This starving experience-dependent behavior plasticity is mediated by serotonergic transmission. Destruction of biogenic amine synthesis, through mutation or laser ablation of serotonergic sensory neurons, abolishes this form of behavioral plasticity, whereas exogenous serotonin rescues the behavioral plasticity in mutants and laser-ablated animals (Sawin et al., 2000). In addition, the behavioral plasticity is potentiated by the selective serotonin reuptake inhibitor fluoxetine in wild-type animals (Sawin et al., 2000). Serotonin also modulates the temporal coordination between two alternative behavior states, locomotion and egg-laying, by acting on decision-making brain interneurons to facilitate the latter (Waggoner et al., 1998; Hardaker et al., 2001). Therefore, these types of behavioral plasticity, referred to as behavioral arousal or alternation in behavioral state (Sawin et al., 2000), are serotonin-dependent in *C. elegans*.

#### **4. O<sub>2</sub> sensing and responses to hypoxia**

##### **4.1. Comparative respiratory physiology**

Mitochondrial electron transport is an evolutionary conserved process that generates high-energy phosphate (ATP), the most important source of energy for cellular metabolism (Voet and Voet, 1995; Ratcliffe et al., 1998). As the final electron acceptor in the mitochondrial electron transport process, O<sub>2</sub> is absolutely required for the survival of all aerobic organisms. Therefore, animals have evolved various strategies to maintain an adequate supply of O<sub>2</sub> to all cells in their bodies. The active process in which animals obtain environmental O<sub>2</sub> and discharge the metabolic waste carbon dioxide (CO<sub>2</sub>) is called respiration.

Monocellular and small multicellular organisms often don't need true respiratory function since environmental O<sub>2</sub> readily diffuses through the whole organism due to the large surface to volume ratio (Withers, 1992). However, cellular respiration often results in localized O<sub>2</sub> depletion from the medium immediately surrounding each organism. This O<sub>2</sub>-depleted layer, or boundary layer (Withers, 1992), cannot be readily replenished with O<sub>2</sub> through passive diffusion. As a consequence, small organisms display certain 'respiratory or ventilatory behaviors' that facilitate O<sub>2</sub> diffusion. In particular, small

organisms often move themselves to preferable ambient environments where higher O<sub>2</sub> levels occur (Taylor et al., 1999). Alternatively, the organisms use movements to actively mix the O<sub>2</sub>-depleted boundary layer and facilitate O<sub>2</sub> diffusion (Burggren, 1985; Hunter and Vogel, 1986). The embryos of *Helisoma*, for example, display a rotational behavior within their egg capsules during development (Diefenbach et al., 1991). One of the hypotheses tested in this thesis is that this rotational behavior serves to reduce the boundary layer and facilitate O<sub>2</sub> exchange between the embryo and its environment.

Larger organisms, including most animals, actively regulate O<sub>2</sub> uptake through respiration. In addition, many animals have a circulatory system functioning to deliver O<sub>2</sub> from the site of respiration to distant tissues. There are three general types of respiratory systems: gills, lungs and tracheae (Withers, 1992). Lungs are invaginated, highly vascularized epithelial structures that mammals and birds use for respiration. O<sub>2</sub> inhaled into small cavities (alveoli) of the lung is taken up into their neighboring blood vessels in exchange with CO<sub>2</sub>. O<sub>2</sub> binds to red blood cells in the blood vessel and is then transported via the circulatory system to distant tissues. In contrast, gills are evaginated, highly folded structures that aquatic animals and some terrestrial invertebrates use for respiration. O<sub>2</sub> circulating around the gill surface diffuses into the blood vessel underlying the gill and is then similarly transported to distant destinations. Tracheae, mostly occurring in arthropods, are air-filled, highly branched tubular systems that extend to different locations of the body from common openings at the body surface (Withers, 1992). Since tracheae directly reach various tissues and cells, a circulatory system is not needed to deliver O<sub>2</sub>.

Most molluscan species utilize gills for respiration. However, respiration of adult pulmonate snails takes place in a vascularized mantle cavity that is sometimes called a lung. Air or water is inhaled into the mantle cavity and expelled into the environment via the pneumostome, a respiratory orifice at the body surface. As in conventional lungs, O<sub>2</sub> uptake and CO<sub>2</sub> discharge occur across the wall of the mantle cavity (Fretter and Peake, 1975).

## 4.2. Control of respiration by central pattern generators

Like other rhythmic activities, respiratory rhythm is driven by CPGs that are usually composed of many pacemaker neurons. These neurons display spontaneous oscillatory activity. Once initiated, the oscillation propagates through the CPG and generates motor output to the muscles involved in respiration (Feldman and McCrimmon, 1999). In vertebrates, most pacemaker cells are found in the brain stem within a region of the ventral medulla called the pre-Botzinger complex (Smith et al., 1991; Rekling and Feldman, 1998). However, the neuronal components of vertebrate respiratory CPGs are very complicated and thus not well delineated (Rekling and Feldman, 1998; Koshiya and Smith, 1999).

Invertebrate respiratory CPGs consist of fewer cells. In the adult pond snail *Lymnaea*, respiration is a rhythmic behavior (Syed et al., 1991). To replenish O<sub>2</sub> supply, snails periodically move to water surface, where the respiration takes place. Upon reaching the surface, the pneumostome opens while air is expelled from the lung cavity. After expiration, fresh air is inhaled into the lung cavity, followed by closure of the pneumostome. This rhythmic opening and closure of the pneumostome can be repeated several times before the animal submerges again (Syed et al., 1991). The CPG controlling the respiratory behavior mainly consists of three interconnected interneurons, RPeD1, IP3I, and VD4 (Syed and Winlow, 1991). VD4 connects to both IP3I and RpeD1 with reciprocal inhibitory synapses, whereas IP3I and RpeD1 are mainly interconnected with reciprocal excitatory synapses. When RpeD1, a giant dopaminergic neuron, is stimulated, it inhibits VD4 and excites IP3I neuron, which in turn causes opening of pneumostome, coupled with expiration. As VD4 subsequently recovers from inhibition, it fires a burst of action potentials, causing inhibition of both IP3I and RpeD1 and closure of the pneumostome, accompanied by inspiration. Therefore, the oscillatory firing of IP3I and VD4 interneurons, controlled by RPeD1, generates the respiratory rhythm in *Lymnaea*. Very remarkably, *in vitro* reconstruction of the whole CPG and *in vivo* transplantation of one of the interneurons following ablation functionally restored the rhythmic activity (Syed et al., 1990; 1992). In contrast to this well-characterized system, the neural mechanisms mediating respiratory behaviors in smaller animals or embryos, where O<sub>2</sub> uptake depends solely on diffusion, are unknown.

### **4.3. Modulation of respiration by central and peripheral chemosensory afferents**

Although CPGs intrinsically generate respiratory motor output, the final pattern of respiration is subject to modulation by sensory afferents from specialized chemoreceptors that monitor changes of O<sub>2</sub> and CO<sub>2</sub> levels. These chemoreceptors detect decreases in O<sub>2</sub> or increases in CO<sub>2</sub> and signal to CPG or local effectors to increase ventilation so that an adequate supply of O<sub>2</sub> can be maintained. Whereas all vertebrate O<sub>2</sub> chemoreceptors are peripherally located, CO<sub>2</sub> chemoreceptors may be centrally or peripherally located.

Based on their distribution and function, there are at least three types of O<sub>2</sub> sensors in air-breathing vertebrates. First, the principle chemoreceptors that monitor systemic blood O<sub>2</sub> levels are found in the carotid body (CB) of mammals. Since the brain is extremely sensitive to O<sub>2</sub> deprivation, the CB is strategically located at the bifurcation of the common carotid artery through which O<sub>2</sub> is carried into the brain (Feldman and McCrimmon, 1999). It is generally believed that the type I or glomus cells in the CB are O<sub>2</sub> chemoreceptors (Prabhakar, 2000). Hypoxia activates the glomus cells by a mechanism involving closure of K<sup>+</sup> channels. The glomus cells subsequently signal to the CPG through the sinus nerve to increase its bursting frequency and therefore the rate of respiration (Prabhakar, 2000). A second type of O<sub>2</sub>-sensitive chemoreceptor is found in the neuroepithelial bodies (NEB) that are distributed throughout the airway mucosa of the lung. These chemoreceptors function to detect environmental O<sub>2</sub> levels in the airway. NEBs are composed of clusters of innervated aminergic and peptidergic cells and likely play a role in optimizing ventilation-perfusion matching, via both local vasoconstriction and ascending inputs to the CPG (Youngson et al., 1993; Cutz and Jackson, 1999). O<sub>2</sub> sensing in the NEB is mediated by NADPH oxidase and closure of the acid sensitive hTASK type K<sup>+</sup> channels (Youngson et al., 1993; Fu et al., 2000; Hartness et al., 2001). Reduction in K<sup>+</sup> currents increases chemoreceptor excitability and Ca<sup>2+</sup> influx, leading to secretion of neurotransmitters involved in modulating respiration. Third, aortic bodies containing O<sub>2</sub> chemoreceptors are widely distributed in arterial networks and monitor local O<sub>2</sub> levels in the blood stream. Instead of NADPH oxidase, the mitochondrial electron transport chain may function as the O<sub>2</sub> sensor in the pulmonary artery in mice (Acher et al., 1999).

Much less is known about the peripheral O<sub>2</sub> chemoreceptors in invertebrates and aquatic vertebrates. In fish, chemoreceptors sensitive to both internal (blood) and external (water) O<sub>2</sub> levels are primarily found in all the gill arches and are innervated by the glossopharyngeal nerve, or the cranial nerve IX (Burleson and Milsom, 1990; 1993; Gilmour, 2001). The discharge frequency in the afferent nerve increases with moderate hypoxia (P<sub>O<sub>2</sub></sub> > 40 torr), but decreases when P<sub>O<sub>2</sub></sub> falls below 40 torr (Burleson and Milsom, 1993). Likewise, in *Lymnaea*, O<sub>2</sub>-sensitive chemoreceptors are located in the periphery, mainly in the mantle area (Janse et al., 1985; Inoue et al., 2001). These chemoreceptors respond to moderate hypoxia and signal to interneuron RPeD1, the modulatory command neuron of the CPG, which in turn increases the frequency of respiratory discharge (Inoue et al., 2001). Similar to what is seen in fish, extreme hypoxia decreases the respiratory discharge (Inoue et al., 2001). Additional regions that are sensitive to environmental O<sub>2</sub> have also been reported in other invertebrates (Crabtree and Page, 1974; Thompson and Page, 1975; Taylor, 1982). Although these studies have revealed O<sub>2</sub> sensitivity in specific structures, identification of individual O<sub>2</sub> sensors at the cellular level has not been reported, let alone dissection of the signaling pathways.

Sensory afferents from CO<sub>2</sub> chemoreceptors also function to modulate respiration. High levels of CO<sub>2</sub>, or hypercapnia, stimulate ventilation in mammals (Bainton et al., 1978; Bruce and Cherniack, 1987). In air-breathers, specialized chemoreceptors in CB and aortic bodies detect not only decreases of O<sub>2</sub>, but also increases in CO<sub>2</sub> levels, both resulting in enhanced respiratory activity (Prabhakar, 2000). In addition, central chemoreceptors in the brainstem and certain serotonergic neurons in medulla of vertebrates are sensitive to changes in brain CO<sub>2</sub> levels (Feldman and McCrimmon, 1999; Ballantyne and Scheid; 2000; Richerson et al., 2001; Bradley et al., 2002). Similarly, specific CO<sub>2</sub> chemoreceptor cells have been identified in the brain of two terrestrial pulmonates, *Helix pomitia* and *Helix aspersa* (Erlichman and Leiter, 1993; 1994; 1997). Focal hypercapnia or electrophysiological stimulation of these CO<sub>2</sub> chemoreceptors results in opening of the pneumostome and inspiration. Furthermore, loss-of-function studies have demonstrated that these chemoreceptors are required for the hypercapnia-induced opening of the pneumostome. In contrast, environmental CO<sub>2</sub> levels have long been thought to play very little role in modulating respiration of aquatic



animals due to the high solubility of CO<sub>2</sub> in water. Actually, elevated CO<sub>2</sub> levels often have no effect on respiration, or they may even inhibit respiration through inhibitory effects on nerves and muscles involved in respiration (Fretter and Peake, 1975; Withers, 1992; Inoue et al., 2001). However, recent studies have begun to challenge this idea by showing that sensory afferents from both external and internal CO<sub>2</sub> chemoreceptors modulate respiration in fish (Milsom, 1995; Gilmour, 2001).

#### **4.4. Mechanisms of O<sub>2</sub> sensing and hypoxia signaling**

While specialized chemoreceptors detect systemic O<sub>2</sub> levels and mediate acute ventilatory responses that function to maintain an adequate supply of O<sub>2</sub>, all other types of cells respond to local O<sub>2</sub> variations so that short- and long-term physiological adaptations can be achieved (Semenza, 1999). As a result, different cells have evolved different O<sub>2</sub>-sensing mechanisms and hypoxia-induced signal transduction pathways (Lopez-Barneo et al., 2001). Three hypoxia-elicited signaling pathways are relatively conserved among different animals. First, almost all O<sub>2</sub>-sensitive chemosensory cells respond to hypoxia via a closure of K<sup>+</sup> channels, leading to activation of neural afferents that increase the motor output of CPGs (Lopez-Barneo et al., 1988; Haddad and Jiang, 1997). However, K<sup>+</sup> channels *per se* don't seem to be the O<sub>2</sub> sensor, rather, K<sup>+</sup> channels seem to be associated with or located downstream of the O<sub>2</sub> sensor (Lopez-Barneo, 1996). Second, most of the long-term physiological responses to hypoxia are mediated through a signaling pathway that involves activation of gene transcription by hypoxia inducible factors (HIF) (Zhu and Bunn, 2001). Third, the NO-cGMP signaling pathway has been shown to mediate O<sub>2</sub> sensing in both invertebrates and vertebrates (O'Farrell, 2001).

Several putative O<sub>2</sub> sensors and O<sub>2</sub> sensing mechanisms have been proposed. One of the most widely postulated O<sub>2</sub> sensors is a heme-based protein (Goldberg et al., 1988; Bunn and Poyton, 1996; Semenza, 1999; Wenger, 2000; Lopez-Barneo et al., 2001). Under this hypothesis, the heme-based sensor detects O<sub>2</sub> variations either through direct ligand binding or by modification of the cytosol redox state (Fig. 1A). In the ligand-binding model, the heme-based sensor binds O<sub>2</sub> reversibly with moderate affinity. Under hypoxic conditions, the heme molecule unloads O<sub>2</sub> and switches to the reduced 'deoxy'

conformation. Deoxy heme, the active state of the sensor, subsequently signals hypoxia to the effectors (Fig. 1A). The most powerful evidence for this model comes from studies on the hypoxia signal transduction of mammalian erythropoietin-secreting cells and nitrogen-fixing bacteria (Goldberg et al., 1988; Bunn and Poyton, 1996; Pellequer et al., 1999). FixL, a hemoprotein with kinase activity in bacteria, and heme protein in human hepatoma cells both play important roles in regulating gene transcription in response to hypoxia.

In the redox model, membrane-bound NADPH oxidases or other oxidases located in the mitochondrial electron transport chain are postulated to be the O<sub>2</sub> sensors (Fig. 1A). Both NADPH oxidase and mitochondrial oxidases contain heme groups and catalyze O<sub>2</sub>-dependent production of superoxide (O<sub>2</sub><sup>-</sup>). O<sub>2</sub><sup>-</sup> can be further catalyzed to peroxide (H<sub>2</sub>O<sub>2</sub>) by the enzyme superoxide dismutase (SOD). Both O<sub>2</sub><sup>-</sup> and H<sub>2</sub>O<sub>2</sub> affect cytosolic redox status, which in turn modifies the function of hypoxia-signaling molecules or K<sup>+</sup> channel proteins (Semenza, 1999; Hoshi and Heinemann, 2001; Lopez-Barneo et al., 2001). NADPH oxidases have been shown to mediate O<sub>2</sub> sensing in NEB chemoreceptors (Youngson et al., 1993; Fu et al., 2000). Cytochrome c oxidase, on the other hand, is a key component of the mitochondrial electron transport chain and may also play a role in O<sub>2</sub> sensing by mitochondria (Lopez-Barneo et al., 2001).

Specific thiol-rich proteins have been proposed as a second class of O<sub>2</sub> sensors (Lopez-Barneo et al., 2001). According to this hypothesis, O<sub>2</sub> level directly changes the redox status of cysteine residues in the sensor protein. Specifically, a reduced O<sub>2</sub> level facilitates the reduced state of the thiol-based sensor, which in turn alters channel function and signals the hypoxia status (Fig. 1B). This hypothesis has been supported by studies demonstrating that redox-related modification of cysteine residues alters the function of recombinant K<sup>+</sup> channels and skeletal muscle Ca<sup>2+</sup> release channels (Ruppersberg et al., 1993; Eu et al., 2000). Recent studies have also shown that methionine oxidation and reduction by ROS are implicated in regulation of the *shaker* type K<sup>+</sup> channel function (reviewed in Hoshi and Heinemann, 2001).

Finally, recent studies have identified a prolyl hydroxylase (PH) as the O<sub>2</sub> sensor involved in HIF-mediated gene transcription (Ivan et al., 2001; Jaakkola et al., 2001; Epstein et al., 2001). In both vertebrates and invertebrates, long-term regulation of O<sub>2</sub>

homeostasis is mediated by HIF, a heterodimer transcriptional complex that contains HIF- $\alpha$  and HIF- $\beta$  subunits (Nambu et al., 1996; Bacon et al., 1998; Epstein et al., 2001, Zhu and Bunn, 2001). HIF- $\alpha$  is the O<sub>2</sub>-dependent regulatory subunit, whereas HIF- $\beta$  is the constitutive subunit. Under normoxic conditions, HIF- $\alpha$  subunits are constantly subjected to enzymatic cleavage via mechanisms involving the ubiquitin-proteasome pathway (Ratcliffe et al., 1998; Wenger, 2000). Thus, transcriptionally active HIF complexes cannot form. Under hypoxic conditions, however, the enzymatic destruction of HIF- $\alpha$  is suppressed, so that the HIF- $\alpha$  binds to HIF- $\beta$  and forms active HIF heterodimers. HIF complexes subsequently translocate to the nucleus where they bind to the hypoxia response elements and regulate gene transcription (**Fig. 1C**).

What remains unclear is how hypoxia protects HIF- $\alpha$  from enzymatic destruction. Two recent studies have shown that prolyl hydroxylation is the key O<sub>2</sub>-sensitive regulatory event that targets HIF- $\alpha$  subunits for proteasomal destruction via the von Hippel-Lindau ubiquitylation complex (**Fig. 1C**). In mammals, PH is directly involved in this process and acts as the O<sub>2</sub> sensor (Ivan et al., 2001; Jaakkola, 2001). In *C. elegans*, a dioxygenase (EGL-9) is the key enzyme mediating prolyl hydroxylation of HIF- $\alpha$ , thus acting as the O<sub>2</sub> sensor (Epstein et al., 2001). More recently, a negative regulator (IPAS) of HIF-mediated gene expression was identified and found to be expressed in Purkinje cells of the cerebellum and in the corneal epithelium of the eye (Makino et al., 2001). The anti-angiogenesis effect of IPAS represents a novel mechanism for negative regulation of HIF function. Together, these studies delineated unique molecular O<sub>2</sub>-sensors and signal transduction pathways that are involved in hypoxia-induced gene transcription.

#### **4.5. Behavioral, physiological and developmental responses to hypoxia**

Because O<sub>2</sub> plays such an important role in cellular respiration and physiological functions, a narrow range of O<sub>2</sub> homeostasis must be maintained. When the environmental O<sub>2</sub> level is low, animals adjust their behavior, development and physiological processes so that an adequate O<sub>2</sub> supply can be maintained and adaptations to the lower O<sub>2</sub> level can be achieved.

The animal behavioral responses to hypoxia generally involve an increase or decrease in motor activities. Juvenile and adult fishes display avoidance behaviors to

specific levels of hypoxia (van Raaij et al., 1996; Wannamaker and Rice, 2000). In contrast, adult flies lose coordination, fall and then stay motionless in response to acute anoxic challenges, but they nevertheless survive hours of anoxia with a recovery of normal behavior (Haddad, 2000). Within 2 minutes from the onset of hypoxia, rat embryos display a 3-phase behavioral response, including an initial suppression in motor activity, a brief period of hyperactivity, and a secondary suppression of movement (Smotherman and Robinson, 1987). In larval *Drosophila*, hypoxia treatment rapidly induces exploratory behavior (Wingrove and O'Farrell, 1999). Perturbing nitric oxide (NO) levels or the nucleotide sequence at a genetic locus encoding protein kinase G (PKG) attenuates this larval response to hypoxia (Wingrove and O'Farrell, 1999). In salamander, the effective surface area of egg capsules increases under hypoxia, likely serving to increase O<sub>2</sub> conductance and enhance O<sub>2</sub> transport (Mills et al., 2001). However, the behavioral responses of the encapsulated embryos to hypoxia were not characterized in that study.

**Table 1. Acute and chronic responses to hypoxia (modified from Lopez-Barneo et al., 2001).**

<b>Acute responses (s to min)</b>	<b>Chronic responses (h to day)</b>
Respiration/Ventilation ↑	Erythropoiesis (EPO ↑)
Heart Output ↑	Angiogenesis (VEGF ↑)
Systemic arterial vasodilation	Tissue hypertrophy (IGF ↑, ET ↑)
Pulmonary vasoconstriction	Tyrosine Hydroxylase ↑; Vasodilators ↑
Glucose uptake ↑	Glucose metabolism ↑ (Glycolytic enzymes ↑)

The physiological responses to hypoxia are classified as either acute or chronic (**Table 1**). The acute responses occur in a time-scale of seconds to minutes and involve post-translational changes in the activities of enzymes, growth factors, transporters and ion channels. At the systemic level, acute hypoxia elicits an immediate increase of ventilation and blood circulation, thereby increasing O<sub>2</sub> loading and transportation. These events are modulated by excitatory afferent inputs from O<sub>2</sub> chemoreceptors in the CB, NEB and aortic body (Haddad and Jiang, 1997; Lopez-Barneo et al., 2001). At the cellular level, acute hypoxia elicits metabolic changes that result in enhanced O<sub>2</sub>-

independent glycolytic energy production (**Table 1**). For example, hypoxia rapidly induces translocation of glucose transporters from intracellular stores to the cell membrane (Lopez-Barneo et al., 2001), thus facilitating O<sub>2</sub>-independent energy production. Meanwhile, O<sub>2</sub> consumption is reduced to 20% of control and muscle-evoked potentials are completely silenced under anoxia (Haddad, 2000). Similarly, neurons in the brain are exceptionally vulnerable to acute hypoxia. Reversible unconsciousness occurs within seconds following cerebral hypoxia induced by sudden, complete arrest of blood flow to the brain (Rossen et al., 1943). Minutes of hypoxia exposure may cause irreversible neuronal damage or even cell death, leading to severe mental disorders (Lipton, 1999). A recent study has indicated that the earliest response (within 15-30 seconds) of neocortical neurons to hypoxia is an increase in spontaneous neurotransmitter release that leads to disruption of normal circuit function (Fleidervish et al., 2001).

The chronic physiological responses to hypoxia, occurring in a time-scale of hours to days, involve HIF-mediated by gene transcription and protein translation (**Table 1**). They are essentially global physiological adaptations to low O<sub>2</sub>. The peritubular cells of the adult kidney and fetal hepatocytes respond to hypoxia with pronounced erythropoietin (EPO) production (Semenza et al., 1991), thereby stimulating the production of red blood cells. Since the glomus cells release dopamine during hypoxia, chronic hypoxia increases gene transcription of tyrosine hydroxylase, the rate-limiting enzyme in the synthesis of dopamine. In addition, chronic hypoxia causes chemoreceptor hypertrophy by increasing the size, number and excitability of cells (Stea et al., 1992; Lopez-Barneo et al., 2001). Finally, chronic hypoxia upregulates the expression of glucose transporters and enzymes involved in glucose metabolism (Lopez-Barneo et al., 2001).

Hypoxia also affects developmental process in several ways. In larval *Drosophila*, hypoxia induces an arrest of the cell cycle at S phase (Wingrove and O'Farrell, 1999; DiGregorio et al., 2001). In addition, the development of trachea is also upregulated by the protein BRANCHLESS and its receptor BREATHLESS under hypoxic pressure (O'Farrell, 2001). This regulatory pattern is in parallel to the hypoxia-induced upregulation of lung and endothelial angiogenesis by vascular endothelial growth factor (VEGF) in mammals (**Table 1**). During the encapsulated development of the frogs, *Rana* and *Crinia Georgiana*, moderate hypoxia (> 5% O<sub>2</sub>) has no effect on the rate of

development, but embryos consistently hatch at earlier stages under lower  $P_{O_2}$  (Mills and Barnhart, 1999; Seymour et al., 2000). Severe hypoxia ( $< 2\% O_2$ ), however, delays both growth and development of embryos and causes morphological anomalies in both salamanders and frogs (Mills and Barnhart, 1999; Seymour et al., 2000).

#### **4.6. Serotonin related plasticity in respiration**

Like other motor activities, respiratory behaviors display plasticity that is modulated by sensory activity and neurotransmitters. A temporary (lasting minutes) increase in respiratory motor output and ventilation is termed short-term potentiation (STP), whereas a long-lasting (hours) increase is referred to as long-term facilitation (LTF) (Feldman and McCrimmon, 1999).

Short-term exposure to hypoxia or electrical stimulation of the carotid sinus nerve often elicits a STP of respiration, followed by a slow decay to base-line levels (Wagner and Eldridge, 1991). STP is associated with facilitation of EPSPs and prolonged depolarization of individual phrenic motoneurons (McCrimmon et al., 1997), and functions to produce smooth respiratory changes in response to large and rapid changes in sensory afferent input (Feldman and McCrimmon, 1999).

LTF of ventilation can be experimentally induced by intermittent exposure to hypoxia or episodic electrical stimulation of carotid chemoafferent neurons in anesthetized animals (Millhorn et al., 1980a; Baker and Mitchell, 2000, Fuller et al., 2000; Mitchell et al., 2001). In patients with chronic recurrent apnea, periodic breathing arrests during sleep produce episodic hypoxia, resulting in LTF due to repeated activation of peripheral chemoreceptors and serotonergic neurons in the raphe nuclei (Feldman and McCrimmon, 1999). LTF is generated centrally since it can be induced by stimulation of the carotid sinus nerve without activating peripheral chemoreceptors. Recent studies have begun to elucidate the mechanisms of respiratory LTF induced by intermittent hypoxia. First, serotonin itself and central serotonergic neurons have been implicated in the initiation of respiratory LTF (Fuller et al., 2001). Serotonin is sufficient to elicit a  $5-HT_3$  receptor dependent long-lasting enhancement of rhythmic respiratory activity in the turtle brain stem in vitro (Johnson et al., 2001). In cats, electrical stimulation of raphe nuclei induces LTF of phrenic motor activity (Millhorn, 1986). In contrast, LTF induced by

electrical activation of the sinus nerve is blocked or reduced in the presence of a serotonergic neurotoxin, 5, 7-dihydroxytryptamine, or a serotonin depleter, *p*-chlorophenylalanine (Millhorn et al., 1980b). Second, activation of serotonin receptors is necessary for the induction of respiratory LTF. In rats, episodic hypoxia-induced LTF requires activation of serotonin receptors, probably of the 5-HT<sub>2</sub> subtype located in the spinal cord (Bach and Mitchell, 1996; Kinkead and Mitchell, 1999; Mitchell et al., 2001). Likewise, stimulation of sinus nerve-induced LTF is attenuated by the serotonin receptor antagonist, methysergide (Millhorn et al., 1980b). It has been proposed that activation of serotonin receptors initiates a signaling cascade that results in increased PKC levels and BDNF transcription. Either of these events could enhance glutamate-dependent respiratory neurotransmission through phosphorylation of glutamate receptors (Mitchell et al., 2001). Finally, serotonin is involved in a novel type of respiratory plasticity, where chronic training with intermittent hypoxia enhances the subsequent phrenic motor responses to hypoxia (Ling et al., 2001). Together, these studies suggest that serotonin plays an important role in the formation of respiratory LTF.

## **5. Use of ablation technique in the study of cellular function**

### **5.1. Methods for cell ablation**

There are several different ways to ablate or knock out cells. First, cells can be genetically knocked out by mutation of certain key cellular components (e. g. Bernhardt et al., 1992), or by genetically engineered expression of toxin in target cells (reviewed in Shah and Jay, 1993). This ablation technique requires long time periods since it involves targeting gene transcription at early embryonic stages. Genetic knockout of cells also requires that the DNA sequence of the target protein or transcriptional regulatory region is known for specific cell types. In addition, genetic ablation usually causes death or malfunction of a population of cells that expresses the common target component. The second way to knock out certain types of cells is to kill cells pharmacologically, whereby certain toxic molecules are incorporated into the target cells through injection, immunobinding, or other uptake mechanisms. For example, by virtue of its structural similarity to serotonin, the neurotoxin 5, 6(7)-dihydroxytryptamine is specifically taken up by serotonergic neurons to induce cell death or perturb cellular function (Glover and

Kramer, 1982; Goldberg and Kater, 1989; Diefenbach et al., 1995; Kemenes, 1997). This technique acts relatively quickly, but in most cases affects a group of cells. The third cell ablation technique is physical ablation, in which a specific cell is killed by mechanical destruction, resection, dye photo-inactivation, or laser ablation (reviewed in Shah and Jay, 1993). This technique kills cells rapidly and precisely, often at the single cell level. In the dye photo-inactivation procedure, a fluorescent dye is incorporated into the target cell by injection, immunological binding or genetic engineering. The dye-loaded target cell, together with other unloaded cells, are then irradiated by laser at a wavelength that would maximally excite the fluorescent dye. Energy and toxic free radicals associated with the fluorescence emission, rather than the irradiating laser, subsequently kills the target cells. The laser ablation procedure is different from dye photo-inactivation in that it doesn't require dye-loading. Instead, high-intensity laser beams are directly focused on the target cell or cellular components to achieve ablation.

## **5.2. Principles and applications of laser ablation**

In one of the commonly used laser ablation systems, a nitrogen pumped dye laser is introduced, via a coupling unit, into a compound microscope and focused onto cells through Differential Interference Contrast (DIC) optics (Bargmann and Avery, 1995). As compared to other ablation methods, laser ablation induces rapid cell death on the order of minutes to hours. High intensity laser irradiation deposits relative high energy into the target cell, resulting in increased temperature and pressure. Either of these can denature protein, break DNA and subsequently cause cell death. In addition, laser ablation effectively reduces collateral damage to neighboring cells for three reasons. First, only cells at the focal plane are killed as cells above and below don't receive sufficient laser energy to be damaged. Second, since the diameter (~ 400 nm) of the laser spot is much smaller than any cell, the laser can be easily focused inside a cell, or even on specific cellular components, ensuring that neighboring cells are not irradiated. Third, transportation of laser-induced heat and pressure waves to neighboring cells is greatly reduced by application of brief laser pulses less than 70 ns in duration (Bargmann and Avery, 1995). Taken together, laser ablation has the advantages of rapid cell elimination and high spatial resolution, and is very useful for ablating single cells both *in vivo* and *in*



*vitro*. However, laser ablation is not useful for ablating many cells simultaneously, or cells that are invisible under DIC microscopy.

Because of its high efficiency and spatial resolution, laser ablation is frequently used for selective cell elimination. In recent years, laser beams have been used to kill specific cells in *C. elegans*, *Drosophila*, amphibians, grasshoppers, zebra fish and various plants to investigate cell function, cell regeneration, cell-cell interactions, and neuronal path-finding (Balak et al., 1990; Kuwada, 1993; Shah and Jay, 1993; Bargmann and Avery, 1995; Chang and Keshishian, 1996; Berger, 1998). Laser ablation has also been used to study microtubule function in cultured dorsal root ganglion cells (Kurachi et al., 1999). Finally, a chromophore-assisted laser inactivation technique has been used to damage specific dye-labeled proteins *in vivo* to test the function of cell adhesion molecules during axonogenesis of grasshopper pioneer neurons (Jay and Keshishian, 1990; Beermann and Jay, 1994).

## **6. Objectives**

### **6.1. To establish a method for long-term culture of de-capsulated embryos**

Encapsulated *Helisoma* embryos naturally develop in CF, from which the embryos absorb nutrients until hatching. Since the composition of CF and the properties of the capsular environment are largely unknown, many previous attempts to maintain normal development of early embryos after they have been removed from egg capsules have been unsuccessful.

In this thesis, identified embryonic neurons will be transiently perturbed or permanently killed with laser beams in order to test the sensory and motor functions of these cells. Thus, encapsulated snail embryos must be isolated and immobilized for laser treatment, followed by a recovery period under conditions that promote normal embryonic development and function. The first objective of this study is to establish a method for long-term culture of decapsulated embryos. The effects of pH, epidermal growth factors, various culture media and culture environments on the development and growth of decapsulated embryos will be tested. In addition, the feasibility of transplanting experimental embryos into egg capsules that contain host embryos will be tested.

## **6.2. To test the motor function of ENC1**

Previous anatomical and pharmacological experiments have provided indirect evidence for ENC1's motor function (Diefenbach et al., 1991; Goldberg et al., 1994). The second objective of the thesis is to provide direct functional evidence that ENC1 regulates ciliary activity through the release of serotonin. Since it is technically difficult to perturb ENC1 with electrical stimulation, laser beams will be used to stimulate ENC1 and the activity of different groups of cilia will be measured with time-lapse videomicroscopy. Several morphological characteristics make ENC1 readily identifiable under DIC optics and experimentally amenable for laser stimulation studies. The idea is that laser treatment deposits heat and pressure into target ENC1s, resulting in cellular swelling (Bargmann and Avery, 1995), increase of membrane permeability (Lee et al., 1996), depolarization and release of the cilioexcitatory neurotransmitter serotonin. I will test the hypothesis that laser stimulation of ENC1 results in enhanced beating of those ciliary cells that are innervated by ENC1. Combined laser stimulation and pharmacological experiments will be conducted to test if ENC1 regulates ciliary activity by releasing serotonin. Furthermore, the occurrence of rotational surges and the average rate of embryonic rotation will be examined after bilateral laser ablation of ENC1s. It is hypothesized that ENC1-ablation will abolish the occurrence of rotational surges and reduce the average rate of embryonic rotation.

## **6.3. To examine the sensory function of ENC1**

The third objective of this thesis is to examine the sensory function of ENC1. The chemosensory-like dendritic knob of ENC1 suggests that this cell also functions to detect certain environmental cues during development. Since it has been established in the previous objective that ENC1 directly stimulates ciliary beating and embryonic rotation, chemosensory stimulation of ENC1 should result in an enhanced cilia-driven embryonic rotation. As an initial step, embryonic rotation in response to different chemosensory stimulants will be tested.

Since low levels of intracapsular O<sub>2</sub> may occur frequently due to metabolic O<sub>2</sub> consumption and environmental hypoxia, I hypothesize that O<sub>2</sub> is the major chemical cue

that activates ENC1 and the rotational surges. Specifically, I will test the effect of hypoxia on the rotational behaviors of control- and ENC1-ablated embryos. In addition, ENC1 will be isolated in culture and its response to hypoxia will be examined electrophysiologically. Finally, the effect that other chemical cues, including amino acids, odorant compounds, CO<sub>2</sub>, have on embryonic rotation will be examined. The reasons for choosing these chemicals are that many aquatic animals are able to detect certain amino acids and organic compounds (Leinders-Zufall et al., 1998a; b; Mac Leish et al., 1999), and that CO<sub>2</sub> is an important factor regulating respiratory behavior in other animal systems.

#### **6.4. To investigate the hypoxia signaling pathway in snail embryos**

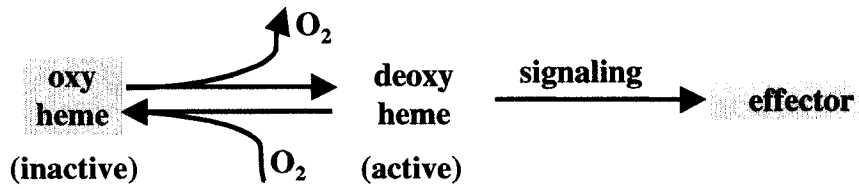
My experiments addressing the previous objective identified hypoxia as an environmental stimulus that increases ENC1-mediated rotational surges. To understand the mechanisms of sensory-motor integration within ENC1, the hypoxia-signaling pathway will be investigated as the final objective of this thesis. First, the involvement of serotonin in hypoxia-induced enhancement of embryonic rotation will be examined pharmacologically with a specific serotonin receptor antagonist, mianserin. Potassium channels and mitochondrial electron transport chain (ETC) have been implicated in O<sub>2</sub> sensing and hypoxia-induced behavioral responses in other animal systems (Lopez-Barneo et al., 2001). The involvement of these signaling pathways in hypoxia-induced rotational responses will also be examined pharmacologically. Specifically, embryonic rotation and responses to hypoxia will be determined in the presence of inhibitors of O<sub>2</sub>-sensitive K<sup>+</sup> channels and the mitochondrial ETC.

Together, these experiments will delineate not only the neural circuit underlying a behavioral response to hypoxia in pond snail embryos, but also the signal transduction pathway and the molecular mechanisms of sensory-motor integration within a simple embryonic neural circuit.

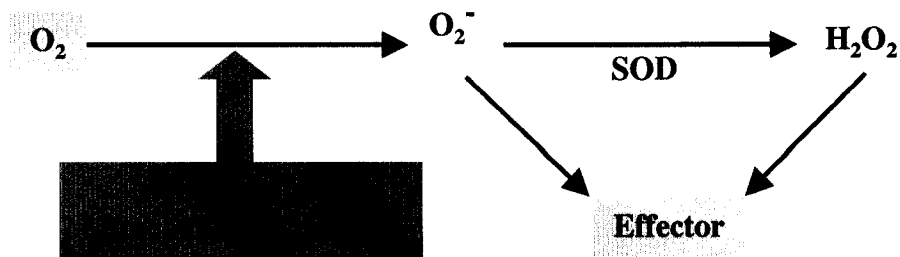
**Figure 1. Mechanisms of O<sub>2</sub> sensing. A.** A heme based molecule acts as the O<sub>2</sub> sensor. In the ligand model, the heme based sensor directly binds O<sub>2</sub> reversibly. As O<sub>2</sub> level falls, the deoxy state of the sensor signals directly or through a signaling cascade to the effector. In the redox model, reactive oxygen species (ROS), such as O<sub>2</sub><sup>-</sup> and H<sub>2</sub>O<sub>2</sub>, alter the redox state of signaling molecules and/or the function of effectors. In this scenario, NADPH oxidase or mitochondrial cytochrome oxidases, heme based enzymes catalyzing the production of ROS, would act as the O<sub>2</sub> sensor (Modified from Semenza, 1999; Lopez-Barneo et al., 2001). SOD: superoxide dismutase. **B.** Thiol based proteins associated with potassium or other ion channels are the O<sub>2</sub> sensors. Under hypoxic stress, disulfide bonds between cysteine residues are reduced, allowing movement or further modification of the protein, which in turn affects channel function and generates a hypoxia-induced current response (Modified from Ruppertsberg et al., 1991; Eu et al., 2000). **C.** The enzyme prolyl hydroxylase (PH) acts as the O<sub>2</sub> sensor. Hypoxia induced gene transcription is mediated through a transcription factor, the Hypoxia Inducible Factor (HIF). Functionally active HIF is a heterodimer of HIF $\alpha$  and HIF $\beta$  subunits. When the intracellular O<sub>2</sub> level is high, HIF $\alpha$  subunit is subjected to hydroxylation by PH, an Fe- and O<sub>2</sub>-dependent process that adds a hydroxyl (OH) group on a specific proline residue (P) within HIF $\alpha$ . This modification is required and sufficient for binding of HIF $\alpha$  to a tumor suppressor von Hippel-Lindau protein (VHL), which recruits a Ubiquitin Ligase (UL) complex. Ubiquitination of HIF $\alpha$  labels the subunit for degradation by proteasomes. When the O<sub>2</sub> level decreases below a critical threshold, the proline is not hydroxylated so that HIF $\alpha$  escapes degradation and dimerizes with HIF $\beta$  subunit. The active HIF heterodimer subsequently translocates to the nucleus and binds to Hypoxia Response Elements (HRE) in genes that are switched on by hypoxia (Modified from Zhu and Bunn, 2001).

## A. Heme based O<sub>2</sub> sensor

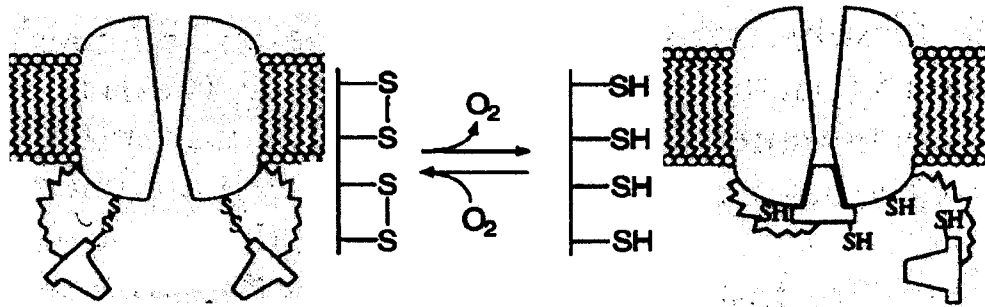
### 1. Ligand model



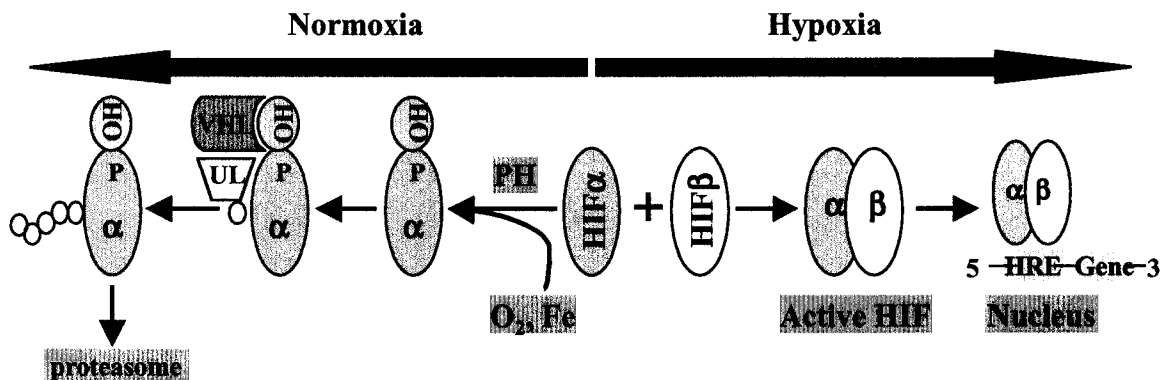
### 2. Redox model



## B. Thiol based O<sub>2</sub> sensor



## C. Prolyl hydroxylase as O<sub>2</sub> sensor



## MATERIALS AND METHODS

### 1. Animals

Adult *Helisoma trivolvis* were maintained in flow-through aquaria containing dechlorinated water (~ 25 °C) and alternatively fed with lettuce and trout pellets (NU-WAY: United Feeds). Since pond snails preferentially lay eggs on a smooth surface, plastic petri dishes (150 mm diameter) were placed in the aquaria to facilitate egg-laying and egg mass collection. Egg masses were removed from the petri dishes with a razor blade and transferred into artificial pond water (APW: 0.025 % Instant Ocean, pH 7.2-7.3; Aquarium Systems) for experimental use. Embryos were staged as a percentage of the whole intracapsular development, with E0 corresponding to 0 % development (zygote) and E100 corresponding to 100 % development (hatching) (Goldberg and Kater, 1989; Goldberg, 1995; Diefenbach et al., 1998). In this study, egg masses containing embryos at stages E2 to E30 were used.

### 2. *Ex ovo* culture of isolated embryos

Clean and intact egg masses containing embryos of appropriate stages were washed 3 X 30 min in antibiotic APW (150 µg Gentamicin/ml, Sigma) to disinfect the egg mass surface. Embryos were then isolated in antibiotic *Helisoma* saline (AHS: 51.3 mM NaCl, 1.7 mM KCl, 4.1 mM CaCl<sub>2</sub>, 1.5 mM MgCl<sub>2</sub>, 5.0 mM Hepes, 150 µg Gentamicin/ml, pH 7.30-7.35, 115-119 mOsm) under sterile conditions. The egg mass and capsular membranes were ruptured with a 30-gauge surgical needle and the embryos were gently blown or sucked out with a refined and heat-polished Pasteur pipette.

The isolated embryos were then cultured in 2 ml of various media in 35 mm petri dishes (Falcon 3001). The media tested included AHS, antibiotic APW, *Helisoma* defined medium (HDM: 50% Leibovitz-15 (Gibco), 40.0 mM NaCl, 1.7 mM KCl, 4.1 mM CaCl<sub>2</sub>, 1.5 mM MgCl<sub>2</sub>, 5.0 mM Hepes, 50 µg Gentamicin/ml, 150 µg L-glutamine/ml, pH 7.30-7.40, 143 mOsm), 30% M199 (GIBCO, pH 7.20-7.30, 91 mOsm), 5% galactose in AHS, 1.5% CF in AHS, and albumen gland conditioned AHS. The 1.5% CF was harvested by releasing all intracapsular contents from 60 egg capsules into 2 ml AHS with a pipette and subsequently removing the embryos. The average volume of egg capsules was

estimated to be  $0.47 \mu\text{l}$  based on their near oval shape and maximal height ( $916 \pm 49 \mu\text{m}$ ,  $n = 7$ ) and length ( $1066 \pm 16 \mu\text{m}$ ,  $n = 26$ ). The albumen gland conditioned AHS was made by incubating isolated albumen glands in AHS (2 glands/ml, 2 – 12 h at room temperature) in the presence of  $100 \mu\text{M}$  forskolin (Sigma), a cyclic AMP activator previously shown to stimulate release of proteins and polysaccharides from the albumen gland (Morishita et al., 1998).

To mimic the capsular environment, isolated embryos were cultured in hanging droplets of culture media and in culture media with increased viscosity (1% gelatin), separately. To test the effect of pH on growth and development, isolated embryos were cultured in HDM of different pH (6.4, 7.4 and 8.4). To test the effect of epidermal growth factors (EGF) on growth and development, isolated embryos were cultured either in HDM plus human recombinant EGF (h-EGF, Sigma;  $0.1 \mu\text{g/ml}$ ), or HDM plus a novel EGF purified from the CF-secreting albumin gland of *Lymnaea* (l-EGF, a generous gift from Dr. A. Bulloch, Univ. of Calgary;  $0.1 \mu\text{g/ml}$ ) (Hermann et al., 2000).

The cultured embryos were viewed under an inverted microscope (Zeiss Axiovert) and digital images were captured by a CCD video camera (Paultek Imaging). Embryo length was analyzed with NIH Image.

### **3. Transplantation of early embryos**

Isolated embryos were washed twice in AHS and placed in AHS for at least 1 h, or experimentally manipulated, before they were transplanted into new host capsules. In transplantation of stage E15- E25 embryos, the host egg capsules contained younger embryos ( $\leq$  stage E10) so that host and transplanted embryos could easily be distinguished. For transplantation of embryos at the 2-cell to 8-cell stages (E1 – E2), isolated embryos were transplanted into capsules whose host embryos (stage E10-15) were killed by heat shock (water bath at  $48 \text{ }^\circ\text{C}$  for 25 min).

Prior to transplantation, the host egg mass was stabilized at the center of a 35 mm petri dish (Falcon 1008) with a strip of dental wax surrounding the egg mass edge. The host egg mass was then immersed in filtered APW. Transplantation was performed through a  $150 - 300 \mu\text{m}$  incision near the edge of the host capsule using a Sigmacote (Sigma)-coated, heat-polished glass micropipette (tip diameter:  $120 - 250 \mu\text{m}$  depending

on the stage of embryos to be transferred). The micropipette was operated by hand and pressure control was exerted with a 0.2 ml calibrated micrometer syringe (Gilmont). In each donor egg mass, half of the embryos were isolated for transplantation, whereas the remaining embryos were kept as *in ovo* controls. The transplanted and control embryos were viewed under an inverted microscope (Nikon Eclipse TE300) and digital images were captured with a CCD camera (Cooke SensiCam). Embryo length was analyzed with image analysis software (Slidebook).

#### **4. Scanning electron microscopy**

To characterize the membrane structures surrounding *Helisoma* and *Lymnaea* embryos, whole egg masses were frozen in liquid nitrogen and vertically fractured through the middle planes. The freeze-fractured egg masses were then mounted on a cryostage, surface-thawed, and viewed with a field emission scanning electron microscope (JEOL JSM6301FXV) under an accelerating voltage of 5 kV. The size of capsules and the thickness of each layer comprising egg capsule and egg mass membranes were analyzed with NIH Image.

#### **5. Mounting and dismounting live embryos on glass slides**

Because embryos normally rotate, they must be stabilized for ENC1 identification, laser treatment and measurement of ciliary activity *in vivo*. To do this, around 5 isolated embryos in a drop of AHS were placed on a glass slide coated with Sigmacote and covered by an 18×18 mm coverslip raised by dental wax on each corner. Pressure was then appropriately applied to each corner of the coverslip so that the embryonic rotation was stopped but the embryos were not crushed. For prolonged treatment (> 30 min), each border of the coverslip was sealed with Vaseline to prevent evaporation.

Not all the embryos on each slide received the same treatment since the orientation of the embryos sometimes prevented the identifiability and laser accessibility of ENC1s. To separate embryos receiving different laser treatment for confirmation of laser ablation with immunohistochemistry, or for further experiments on ENC1-ablated and sham-operated embryos, embryos were individually dismounted after laser treatment. Specifically, the whole slide with embryos receiving different treatments was immersed



in AHS and the coverslip was gently removed without disturbing the relative location of each embryo. The embryos on the slides were then sorted out with a Sigmacote-coated suction micropipette according to the actual treatment applied.

## **6. ENC1 identification**

For laser stimulation, laser ablation and electrophysiological experiments, ENC1 must be first identified *in vivo* or in culture under Nomarski Differential Interference Contrast (DIC) optics. ENC1s were reliably identified *in vivo* based on several morphological characteristics. The stereotypic position of the ENC1 soma and superficial dendritic knob provided the most important cues for ENC1 identification. Each dendritic knob is composed of a tuft of non-motile cilia and is consistently located 2-3 cells dorsal to the anterior end of the dorsolateral ciliary band. The ENC1 soma was normally identified by first locating the dendritic knob and then focusing approximately 20  $\mu\text{m}$  below the embryonic surface. The ENC1 soma lies anterior to the large flame cell of the protonephridium and has distinct morphological features. Each ENC1 has a smooth nucleus with a central, prominent nucleolus, as well as numerous granules concentrated in the apical cytoplasm (Diefenbach et al., 1998; Koss et al., 2002). Finally, each ENC1 projects a primary neurite ventrally, which can often be detected under DIC optics (refer to **Fig. 9** in **Results** section).

## **7. Laser treatment**

Laser irradiation of cells caused a transient excitation followed by cell death in 6 – 24 h. Taking advantage of this laser-induced biphasic cellular response, laser treatment was used in this study for two purposes. First, to test if ENC1 directly innervates ciliary cells, laser beams were used to stimulate ENC1 while ciliary activity was being monitored. Second, to test the O<sub>2</sub> chemosensory function of ENC1, both ENC1s in each embryo were killed with laser beams and the behavioral response of ENC1-ablated embryos to hypoxia was tested.

Pulsed laser beams generated by a VSL-337 nitrogen laser (Laser Science, Inc.) were delivered to a coupling unit (Photonic Instruments, Inc.) via a low-loss multimode fiber. The coupling unit contained a dye laser module (5 mM coumarin 440, emitting at

420-475 nm wavelength) and laser beam tuning controls. The resulting dye laser pulses were then introduced into the incident-light illuminator (arc lamp) port of a Zeiss Axioskop compound microscope (Carl Zeiss). Laser beams were finally reflected off a dichroic mirror and focused with a 100× oil immersion Plan-Neofluar DIC objective onto specific cells. Laser pulses had a peak wavelength of 445 nm, a pulse length of 3 ns and pulse energy of 60 μJ (assuming 50% energy loss at the DIC analyzer; Bargmann and Avery, 1995). These laser beams, further attenuated to a strength that was just able to scratch glass coverslips with a single pulse (**Fig. 2**), were applied at a frequency of 8-10 Hz to ablate or treat cells in embryos. The laser microbeams were focused on the nucleolus and transected around the perinucleolar region to ablate the cell. In control experiments, unidentified cells neighboring ENC1 were ablated. To ablate whole cells, pulses were applied until visible scars or blebs were apparent on the nucleolus, the nuclear boundary became obscure and the cell started to swell. Depending on the orientation of the embryo, 200 – 300 pulses were required.

## **8. Serotonin immunohistochemistry**

Serotonin immunohistochemistry on wholemounts was used to confirm the laser-induced cell death of ENC1 and the identification of ENC1 in tissue culture. Embryos were fixed overnight at 4 °C with 2× Zamboni's fixative (Goldberg and Kater, 1989) in 96-well tissue culture plates (Falcon), followed by 4 X 20 min washes in phosphate buffered saline (PBS: 12.06 g/L Na<sub>2</sub>HPO<sub>4</sub>•7H<sub>2</sub>O, 7.20 g/L NaCl, pH 7.2). These washes and the following steps were carried out at room temperature with agitation (80 - 100 rpm, American Rotator V) unless otherwise stated. Embryos were incubated in 10% horse serum (Sigma) in PBS and 0.4 % Triton X-100 to block non-specific binding and improve penetration, respectively. They were then incubated in primary antibody (rabbit anti-serotonin, Sigma) diluted 1:1000 in PBS with 0.4 % Triton X-100, 1 % horse serum and 3.3 mg/ml bovine serum albumin (BSA, Sigma) at 4 °C for 24 – 72 h. The unbound primary antibody was washed out with 0.4 % Triton X-100 in PBS for 6 X 20 min. Embryos were then incubated in secondary antibody (goat anti-rabbit immunoglobulin G conjugated to tetramethyl rhodamine, Sigma) that was diluted 1:400 in PBS plus 0.4 % Triton X-100 for 2 h. The unbound secondary antibodies were washed out with PBS plus

0.4 % Triton X-100 for 5 X 15 min and PBS for 6 X 15 min. Finally, embryos were dehydrated in ascending ethonal concentrations (70 %, 85%, 95% and 100 %, 10 min each) and mounted in methyl salicylate (Sigma) on glass slides.

A modified procedure using the same solutions and antibodies as described above was employed to immunostain ENC1 in tissue culture. Briefly, pieces of attached embryonic tissues (30-50  $\mu\text{m}$  in size) in glass bottom culture dishes were fixed for 1 h, followed by 3  $\times$  10 min washes in PBS and a 30 min wash in 10% horse serum. Tissues were then incubated with the primary antibody for 12 h and washed with 0.4% Triton X-100 in PBS for 4  $\times$  7 min. Tissues were then incubated with the secondary antibody for 1 h and then washed in 0.4% Triton X-100 in PBS for 4  $\times$  5 min and in PBS for 2  $\times$  10 min. Finally, stained tissues were clear-mounted in 80% glycerol in PBS.

The serotonin immunostained embryos or tissues were examined with an epifluorescence microscope (Nikon diaphot-TMD or Ziess Axioskop) or a laser-scanning confocal microscope (Multiprobe 200, Molecular Dynamics).

## **9. Measurement of ciliary activity and embryonic rotation**

To measure ciliary activity *in vivo*, an activated charcoal powder (BDH Chemicals) suspension was used to label cilia and facilitate visualization of ciliary movements (Audesirk et al., 1979). To prepare the suspension, 0.03 g of charcoal powder was mixed in 1 ml of *Helisoma* saline and washed by centrifuging the suspension at 10,000 g for 4 X 10 min. The supernatant was discarded and the pellet was resuspended with saline after each centrifugation. The charcoal-saline mixture was then centrifuged at 1,000 g for 2 min. After the resulting supernatant was autoclaved, it was ready for ciliary labelling. A drop of this charcoal suspension was mixed with 100  $\mu\text{l}$  of saline containing isolated embryos. After 5 min of incubation, most embryos had some of the cilia randomly labeled by charcoal particles. They were then mounted on Sigmacote-coated slides for laser treatment and analysis of ciliary activity.

Preliminary experiments indicated that there was no relationship between ciliary beat frequency and the attached charcoal particle. The ciliary movement, as indicated by attached charcoal particles, was captured with a CCD video camera (JVC model TK-860U) under 100 $\times$  DIC optics. The analog signal captured by the CCD camera was then

recorded by a time-lapse video cassette recorder (Panasonic model AG-6720) at 60 frames/sec. Finally, the ciliary beat frequency (CBF) was determined by replaying the video at 5 frames/sec and manually counting ciliary beats.

To measure the CBF of isolated ciliary cells, unlabelled ciliary cell cultures were viewed under phase contrast optics (Nikon Diaphot - TMD) using a 40X objective. The CBF was recorded at 60 fields/s and replayed at 5 fields/s for quantification. For each time point, the CBF was measured by counting ciliary beats in a 5 s time window.

Embryonic rotation was monitored with a CCD video camera (see above) mounted on a dissecting microscope (Zeiss, StemiSR) and recorded with a time-lapse videocassette recorder as described above. Rotational behavior was recorded at 2.5 fields/s and replayed at 60 fields/s for quantification. The average rate of rotation in each 10-min interval was analyzed by counting the total number of rotations in 6 – 8 min.

## **10. Culture of embryonic cells and tissues**

Embryonic ciliated cells were cultured as previously described (Christopher et al., 1999). Briefly, intact egg masses containing stage E20 – E35 embryos were disinfected in 35% ethanol and the embryos were removed. Isolated embryos were treated with 0.2% trypsin and mass dissociated by passing them repeatedly through a 63  $\mu\text{m}$  nylon mesh (Small Parts Inc.). Dissociated cells were cultured in poly-L-lysine coated (1  $\mu\text{g}/\text{ml}$ , hydrobromide, MW 8,800 – 14,400; Sigma) culture dishes (Falcon 3001) containing HDM. The cultures were maintained in a humidified box at room temperature (20-22°C) for 20-24 h to allow for attachment of isolated cells.

To characterize the electrophysiological responses of ENC1 to hypoxia, embryonic tissue explants that contained ENC1s were isolated and cultured. Stage E25 embryos were disinfected by 3 X 15 min washes in antibiotic APW and isolated from egg capsules under sterile conditions. Isolated embryos were then transferred to 35 mm petri dishes (Falcon 3001) and viewed under an inverted compound microscope (Nikon diaphot). Micropipettes pulled from thin wall glass (World Precision Instruments, TW 120-3) with a tip size of about 30  $\mu\text{m}$  were used to isolate embryonic tissue. Pieces of epidermis in the vicinity of ENC1 were sucked into the micropipettes with a 0.2 ml calibrated micrometer syringe (Gilmont) and surgically removed from the rest of the embryos with

a 30-gauge needle. The isolated pieces of embryonic tissue were transferred to poly-L-Lysine coated glass bottom culture dishes (10 – 15 pieces/dish) and cultured overnight in HDM in the dark for attachment. ENC1s were identified in 20 – 30% of the tissue explants under DIC microscopy, based on the presence of the dendritic knob, apical granules, smooth nucleus and prominent nucleolus. Furthermore, the identification of ENC1s in culture was verified with anti-serotonin immunostaining (see Results).

### **11. Measurement of O<sub>2</sub> partial pressure**

To measure O<sub>2</sub> levels in the egg mass, the partial pressure of O<sub>2</sub> (P<sub>O<sub>2</sub></sub>) was recorded with a Clark-style microelectrode with guard cathode (tip diameter 25-30 μm, Model 737GC, Diamond General) and a polarographic amplifier (Model 1900, A-M systems). The P<sub>O<sub>2</sub></sub> electrode was calibrated with APW saturated with 100% O<sub>2</sub> (P<sub>O<sub>2</sub></sub> = 640 mm Hg), 100% N<sub>2</sub> and 100% air prior to, and after, experiments. Egg masses were stabilized in a superfusion chamber (Wilson et al., 1999) and perfused with APW equilibrated with 20% O<sub>2</sub> and 80 % N<sub>2</sub>. The P<sub>O<sub>2</sub></sub> at positions outside, inside near the surface, and inside near the center of the egg capsules was measured.

To test whether the egg mass membrane retards the rate of intracapsular P<sub>O<sub>2</sub></sub> change in response to P<sub>O<sub>2</sub></sub> changes in the perfusate, a pair of electrodes was used to simultaneously monitor P<sub>O<sub>2</sub></sub> levels inside egg capsules and in the perfusate. The APW saturated with 20% O<sub>2</sub> + 80% N<sub>2</sub> and 100% N<sub>2</sub> were alternately perfused to egg masses at 4-min durations, using a fast perfusion system (Wilson et al., 1999). Axograph software (version 4.6) was used to quantify the time constants of P<sub>O<sub>2</sub></sub> changes after introduction of hypoxic and normoxic APW, respectively.

### **12. Hypoxic treatment**

Whole embryos and cultured cells were exposed to hypoxic APW to test behavioral responses to hypoxia and the underlying cellular mechanisms. Calibrated ratios of air and N<sub>2</sub> were mixed using a flow meter (Advanced Specialty Gas Equipment) and bubbled into a Petri dish (150 × 25 mm, LabTek), which was sealed with parafilm and tilted (~5°) to elevate one side. The experimental egg mass was stabilized by dental wax close to the edge of the lower side of the dish. Gas mixtures were introduced continuously throughout

the experiments using an air stone located near the center and exhausted through a pore located on the elevated side of the dish. Measurements were taken at 10-min intervals, starting 4 min after the initiation of aeration.

For hypoxic treatments in the presence of pharmacological agents, egg masses were stabilized by wax in a 2.8 ml sealed perfusion chamber. Normoxic or hypoxic (equilibrated with different levels of air and N<sub>2</sub>) solutions were perfused by gravity at a flow rate of 6.5 ml/min through the chamber. To test the behavioral sensitization of embryonic rotation to hypoxic treatments, egg masses were presented with 3 sequential cycles of intermediate hypoxia (20% air, 20 min)/normoxia (100% air, 30 min). To construct the dose-response curve of hypoxia-stimulated embryonic rotation, APW saturated with different levels of O<sub>2</sub> was perfused to the embryos in the sealed chamber. Measurements were taken at 10 min intervals.

Culture dishes containing ciliated cells were modified to enable perfusion of hypoxic *Helisoma* saline (HS: the same compositions with AHS without gentamicin). The dishes were initially filled with normoxic HS and sealed. Following the recording of basal CBF, the solution within the culture dish was replaced with hypoxic (100% N<sub>2</sub> equilibrated) HS and CBF was recorded again.

### **13. Patch-clamp recording of ENC1**

To test the electrophysiological responses of ENC1 to hypoxia, standard whole-cell recording techniques (Hamill et al., 1981) were performed under normoxic (air saturated) and hypoxic (N<sub>2</sub> saturated) bathing solutions distributed via gravity perfusion. ENC1s were cultured overnight and identified as described previously (refer to 2.6), under a 40X water immersion DIC lens on an upright compound microscope (Leica DMLFSA) equipped with an infrared videocamera (Dage MTI). Because the cell body of ENC1 was normally located below the surface of the explant, digestive enzymes (0.2 % trypsin in HS, 15 min) were sometimes focally applied to partially digest the connective tissue surrounding ENC1. Patch-clamp electrodes were pulled from borosilicate glass (type 1BBL, World Precision Instruments) with a Flaming Brown horizontal puller (Model P-97, Sutter Instruments) and filled with a CsCl intracellular solution [(in mM): CsCl 130, MgCl<sub>2</sub> 2, HEPES 10, EGTA 10, Na<sub>4</sub>ATP 4, pH 7.2, 290 mOsm](Ali et al., 2000) that was

diluted to about 40% to match the osmolarity of the extracellular solution (HS, 115 mOsm). Positive pressure was applied to the CsCl filled electrodes to facilitate penetration of the epithelium. The electrode resistance was 8 – 12 M $\Omega$ , and whole-cell recordings were performed in the I = 0 mode in order to record cell membrane potentials.

Membrane potentials were recorded with an Axopatch 200B patch clamp amplifier (Axon Instruments) at room temperature. The traces were filtered at 5 kHz, digitized at 25 – 30 kHz, and captured with pClamp software (version 8.02, Axon Instruments). Results were analyzed offline with Axograph (version 4.6, Axon Instruments) and pClamp software.

#### **14. Pharmacological treatments**

All chemicals were from Sigma unless otherwise specified. All solutions were pH balanced to pH 7.2-7.4 unless otherwise specified. To test the role of serotonin in ENC1-mediated ciliary activity, serotonin or 5-hydroxytryptamine (5-HT) was used as a serotonin receptor agonist and mianserin as a serotonin receptor antagonist. 1 mM stock solutions of serotonin creatinine sulfate complex and mianserin hydrochloride (RBI) were made in HS. The solutions were made fresh each day and kept in the dark at 4 °C.

To test the involvement of K<sup>+</sup> channels and the mitochondrial electron transport chain (ETC) in hypoxia signaling, the K<sup>+</sup> channel blocker 4-aminopyridine (4-AP) and tetraethylammonium (TEA) chloride, and the mitochondrial ETC inhibitor rotenone were used. Stock solutions of 4-AP (0.5 M) and TEA (1 M) were made in H<sub>2</sub>O. Stock solutions of rotenone (10 mM) were made in DMSO. Intracellular acidification was induced by 20 mM sodium butyrate.

#### **15. Statistical analysis**

Data were expressed as mean  $\pm$  standard error of the mean (S. E. M.). Unless otherwise specified, the statistical significance of differences among groups was evaluated using the Student's *t*-test or an ANOVA (Analysis of Variance) followed by the Fisher's PLSD (Protected Least Significant Difference) test.

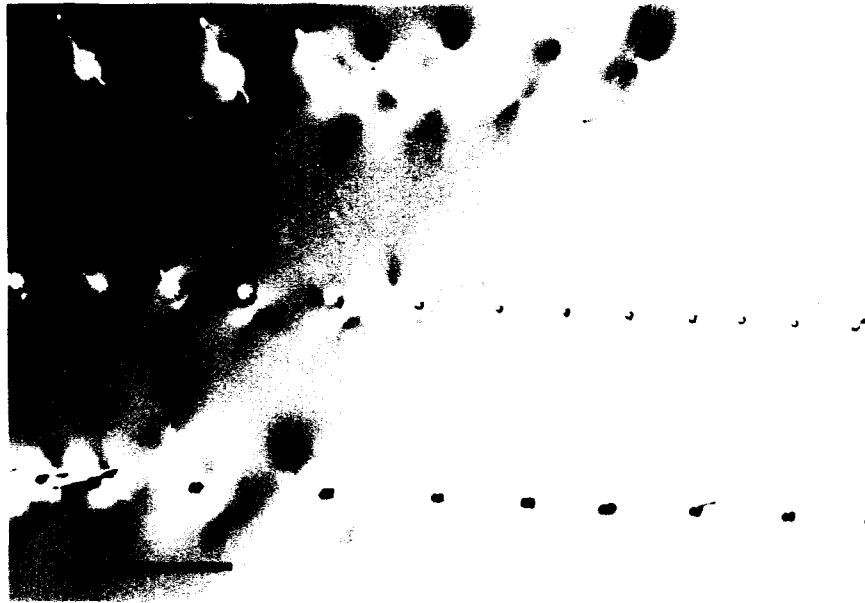


**Figure 2.** DIC micrograph of scratches made by single laser pulses on a glass coverslip. **Top:** Laser pulses with higher-than-threshold intensity were fired on a plane that was below the plane of view. Out-of-focus scratches and cracks were seen. **Middle:** Laser intensity was attenuated to a threshold intensity so that a single pulse of laser was just able to scratch the glass. Laser pulses were focused on the plane of view. Scratches and very small cracks were seen. **Bottom:** Laser pulses with a slightly higher intensity produced larger scratches and more cracks on the coverslip. Scale bar: 15 $\mu$ m.



## Results

### 1. Culture of isolated embryos <sup>1</sup>

In experiments that involve perturbation of embryonic development and function, embryos must be isolated from egg capsules for experimental treatments and then monitored as they continue to develop. However, many previous attempts to culture de-capsulated early-stage embryos *ex ovo* have been unsuccessful in many encapsulated species (Morrill, 1982; Pechenik et al., 1984; Stockmann-Bosback and Althoff, 1989; Meshcheryakov, 1990). Two major objectives of this thesis are to elucidate the sensory and motor roles of ENC1s by perturbing their function *in vivo* with laser beams, a process requiring the encapsulated embryos to be isolated from egg capsules and immobilized under the laser-ablation microscope. Therefore, successful culture of isolated *Helisoma* embryos provides not only the foundation for the rest of the studies of this thesis, but also valuable insights into the culture of other encapsulated species in general. Initially, the growth and development of isolated early-stage embryos cultured in different media, under different chemical and physical conditions, and with the addition of EGFs were compared. As an alternative to the *ex ovo* approach, an embryo transplantation technique was developed. The results indicate that transplantation is an extremely effective method for achieving long-term continual growth and development of previously de-capsulated embryos. This transplantation technique will facilitate studies of embryonic cell function, lineage and development of encapsulated species.

#### 1.1. *Ex ovo* culture of de-capsulated embryos <sup>2</sup>

Initial attempts to achieve sustained development *ex ovo* were made with stage E15, E20 and E25 embryos, corresponding to the period of development of the rotational behavior and underlying ENC1-ciliary neural circuits (Diefenbach et al., 1991; Diefenbach et al., 1998; Koss et al., 2002). A variety of different culture media were tested, including AHS, APW, HDM, 30% M199, 5% galactose in AHS, 1.5% CF in AHS, and albumen gland-conditioned AHS. Although short-term growth and development was observed in all the media tested, none of them supported sustained growth, probably due to the absence of crucial nutritive components or growth-promoting

factors. Of all the media tested, 30% M199, 1.5% CF in AHS, and albumen gland conditioned AHS produced the best development, with stage E15, E20 and E25 embryos sometimes reaching stages that display features of normal stage E25, E30 and E40 embryos, respectively, after 3 d of culture (**Fig. 3**). At the same time point, the control embryos developing *in ovo* consistently reached stages E35, E45, and E50, respectively, when egg masses were incubated in APW or HS (**Fig. 3**).

Generally, embryos cultured *ex ovo* displayed abnormal features (**Fig. 3**) and slower development (**Fig. 4**) in comparison to *in ovo* controls. In particular, shell formation was either stunted or absent in the *ex ovo* embryos (**Fig. 3**). Furthermore, accumulation of particles was always found in the canaliculus of the protonephridia (**arrows in Fig. 3**). Finally, embryos were often hydropic after 72 h of culture *ex ovo*. Although embryos often survived in culture for more than 30 days, no significant development was observed after the first 5 days of *ex ovo* cultivation (**Fig. 4**). The average increases in the length of embryos over this time period were  $54 \pm 13 \mu\text{m}$  ( $N = 7$ ) and  $69 \pm 11 \mu\text{m}$  ( $N = 7$ ) for the stage E15 and E20 groups, respectively. In contrast, control embryos exhibited significantly greater increases in length over the same time periods (**Fig. 4**).

To test whether the high viscosity or other physical properties within egg capsules are important factors promoting embryonic development, embryos were cultured in AHS containing 1% gelatin or in hanging droplets of AHS. Neither of these conditions resulted in improved *ex ovo* embryonic development (data not shown).

Next, the effect of pH on the growth of isolated embryos was tested. Egg mass matrix and capsular fluid had a pH of  $6.6 \pm 0.1$  ( $N = 4$ ), suggesting that low pH may promote embryonic development. The growth and development of stage E20 embryos were assessed after three days of culture in HDM adjusted to pH 6.4, 7.4 or 8.4. Whereas none of these groups exhibited significantly improved embryonic development as compared to the previous treatments, embryonic development improved inversely with pH, both in terms of embryo length (**Fig. 5A**) and percent of embryos displaying stage E30 features, including larval kidney shape, muscle contraction of the body wall, and shell deposition (**Fig. 5B**). This effect of pH was not observed when embryos were cultured in

30% M199 (data not shown), a medium that generally promoted greater embryonic development than HDM, as described above.

Since a novel EGF has recently been identified in the capsular fluid secreting albumen gland of *Lymnaea stagnalis* (Hermann et al., 2000), I also tested if EGF can promote the growth and development of *Helisoma* embryos *ex ovo*. Stage E20 embryos cultured for 3 days in HDM at pH 6.4 developed similarly in the presence or absence of human recombinant EGF (450 ng/ml) or *Lymnaea* EGF (100 ng/ml)(data not shown). While EGF may still be an important factor, other key components are clearly required to sustain normal growth and development of embryos *ex ovo*.

## 1.2. Transplantation of de-capsulated embryos

As an alternative to *ex ovo* culture of embryos, I tested the feasibility of transplanting de-capsulated embryos into egg capsules already containing host *Helisoma* embryos. Stage E15 and E20 embryos were transplanted into host egg capsules containing much younger embryos ( $\leq$  stage E10) to minimize mechanical interactions between host and transplant, and to ensure that they could be easily distinguished. Furthermore, younger egg capsules provide greater nutrition since the nutritive components of CF become depleted as embryonic development proceeds (Morrill, 1982; Stockmann-Bosbach and Althoff, 1989). In most cases, the incision in the capsule membrane re-sealed within 12 h after transplantation.

In striking contrast to the *ex ovo* trials, the growth and development of transplanted embryos was very similar to that displayed by control embryos within intact egg capsules (**Fig. 4**). At 23 °C, the growth and development of transplanted stage E15 embryos were identical to the controls in the first 3–4 days but slightly slower thereafter (**Fig. 4A and 4C**). When transplanted at stage E20 or older, however, the lengths (**Fig. 4B**) and embryonic stages (**Fig. 4D**) reached by transplanted embryos at various days were identical to controls (t-test,  $p > 0.05$  at any time point,  $N = 7$ ). Although embryos transplanted at stage E15 had a marginally lower survival rate 8 days after transplantation (**Fig. 6A**, chi square test,  $p < 0.05$ ), the survival rate of embryos transplanted at stage E20 was not different from that of control (**Fig. 6A**, chi square test,  $p > 0.05$ ). However, transplantation caused a slight decrease in the percentage of embryos hatched at day 8

post-transplantation (Fig 6B); 91% stage E15 (n = 23) and 89% stage E20 (n = 18) control embryos hatched by this time, as compared to 70% stage E15 (n = 28) and 62% stage E20 (n = 29) transplanted embryos, respectively (chi square test,  $p < 0.05$  for both stages). Nonetheless, transplanted embryos grew normally in APW after hatching (data not shown). These data suggest that transplantation into host egg capsules is an extremely effective technique for achieving a normal course of embryonic development for previously de-capsulated stage E15 or older embryos.

To test if this transplantation technique can be applied to embryos at cleavage stages, I transplanted 2-cell to 8-cell stage embryos (stage E1-E2) into capsules whose hosts were killed previously with heat shock (48 °C for 25 min). Approximately two thirds of the successfully transplanted embryos died around stage E10, at the time of gastrulation. However, the remaining third survived and displayed normal embryonic growth and development (Fig. 7 and 8).

## 2. ENC1 regulates the activity of specific target cilia<sup>3</sup>

Previous studies have demonstrated that serotonin is a cilioexcitatory neurotransmitter in *Helisoma* (Diefenbach et al., 1991; Goldberg et al., 1994; Christopher et al., 1996; 1999) as well as other animal systems (Aiello, 1957; Tsuchiya and Kensler, 1959; Gosselin, 1961; Koshtoyants et al., 1961; Gosselin et al., 1962; Soliman, 1983; Auderirk, 1978; Auderirk et al., 1979; Syed and Winlow, 1989; Hay-Schmidt, 2000). Given the anatomical association of ENC1's neurites with the dorsolateral and pedal bands of cilia in *Helisoma* (Fig. 9; Diefenbach, 1995; Diefenbach et al., 1998; Koss et al., 2002), it is likely that ENC1 regulates ciliary activity through the release of serotonin. Specifically, it has been hypothesized that the periodic surges of cilia-driven embryonic rotation in *Helisoma* result from the release of serotonin from ENC1s (Diefenbach et al., 1991; Diefenbach, 1995). One way to directly test this hypothesis is to examine whether stimulation of ENC1 transiently increases the activity of target ciliary cells and whether knockout of ENC1s abolishes the rotational surges. Because it is technically difficult to stimulate ENC1 with electrical stimulation protocols, laser beams were used to both transiently excite ENC1s and permanently kill them. In this part of the Results, I first show that the laser ablation technique is effective in killing specific cells in *Helisoma*

embryos. I then demonstrate that the laser ablation treatment of ENC1 initially causes a transient increase in the activity of cilia that are anatomically associated with ENC1. Furthermore, I show that laser-induced transient excitation of ciliary activity is reduced by an effective serotonin receptor antagonist, mianserin. Finally, I show that after the laser-induced cell death of both ENC1s, embryos no longer display rotational surges. Together, these results demonstrate that ENC1s are cilioexcitatory motor neurons that regulate ciliary activity through the release of serotonin.

### **2.1. Effectiveness and specificity of laser ablation**

The laser treatment used in this study was sufficient to cause morphological changes in ENC1 indicative of a gradual cell death ( $n > 25$  embryos). The most apparent morphological change initially was laser-induced scars on the nucleolus. The intact ENC1 nucleolus had a very smooth appearance, whereas after laser treatment it became very scarred (**Fig. 10B**). In contrast, less scarring was apparent in the perinucleolar region, even though it also received laser pulses. A few minutes after laser treatment, the wounded cell started to swell and the nuclear boundary became unclear (**Fig. 10B**). This indicated that the cell started a systematic cell death process. Subsequently, the laser treated cells completely lost their integrity and disappeared in 6-24 h (**Fig. 10B**).

The laser treatment also caused morphological changes in the dendritic knob of ENC1 within 30 minutes (**Fig. 10A**). Usually, the stiff non-motile cilia of the dendritic knob became flaccid as the ablated cell underwent cell death (data not shown). In some cases, laser treatment caused the dendritic knob to round up and detach from the embryonic surface (**Fig. 10A**). In addition, cytoplasm escaping from the apical dendrite was occasionally detected. In contrast to the dendritic knob, the morphology of ENC1's primary neurite appeared normal for up to 2 hours following laser treatment (data not shown). Finally, laser treatment of ENC1's primary neurite at a proximal site induced cell death (data not shown), whereas laser ablation of distal neurites had no effect on the survival of ENC1 (**Fig. 11**).

Serotonin immunohistochemistry of embryos before and after ENC1 laser treatment was also examined to confirm laser-induced cell elimination. ENC1s are the only serotonergic neurons in stage E20-30 embryos (Goldberg and Kater, 1989;

Diefenbach et al., 1998) and can be reliably labeled with antibodies against serotonin (**Fig. 12A**). Although serotonin immunoreactivity persisted in the first 6 h after laser treatment of ENC1, a significant loss of serotonin immunoreactivity occurred in a period 6–24 h post ablation (**Fig. 12B and C**). During this time period, 70% of the embryos (n = 89 embryos from 7 experiments) that received unilateral laser treatment of ENC1 lost their 5-HT immunoreactivity in the laser-treated cells (**Fig. 12B**). Similarly, 82% of the embryos (n = 78 embryos from 7 experiments) lost their 5-HT immunoreactivity in both ENC1s after bilateral laser treatment of ENC1s (**Fig. 12C**). Taken together, laser treatment of ENC1 substantially decreased the cell's serotonin immunoreactivity in 6-24 h, coincident with laser-induced cell elimination observed under DIC microscopy (**Fig. 10**).

In addition to observing the direct effect of laser treatment on ENC1 morphology, the morphology of untreated neighboring cells was also evaluated (n > 20 embryos). The laser-treated ENC1 and its adjacent cells were closely watched for 5-10 minutes after treatment and then periodically examined over the next 3 days under the DIC microscope. Normally, no obvious damage to nearby cells was observed unless the laser microbeam caused explosion of ENC1. When ENC1 explosion occurred, the embryos were excluded from further analysis of morphology and ciliary activity.

Laser treatment of cells neighboring ENC1 (n=11 embryos) was also conducted for two reasons. First, this served as a laser operation control to show that the laser-induced effects on ciliary activity were specific for ENC1 treatment. Next, a neighboring cell of ENC1 was ablated and the morphology and serotonin immunoreactivity of ENC1 were examined to assess the secondary effects of laser treatment on adjacent cells. The laser treated cells adjacent to ENC1 underwent similar morphological changes and cell death as seen in ENC1 (**Fig. 13**). As expected, ablation of cells adjacent to ENC1 didn't cause any visible damage to ENC1, as monitored with DIC microscopy (**Fig. 13**). Serotonin immunohistochemistry confirmed that there was no loss of 5-HT immunoreactivity or change in neurite morphology after laser treatment of ENC1 neighbor cells. This indicated that laser treatment caused only target-specific cell damage.

## **2.2. Different groups of cilia display distinct basal ciliary activity**

In stage E20-E30 embryos, ENC1s are associated with all three major ciliary bands, the left and right dorsolateral bands and the pedal band (**Fig. 9A** and **14**; also see Koss et al., 2002). In contrast, there is no evidence that ENC1s are anatomically associated with the isolated tufts of cilia found near the shell gland or sparsely distributed over other regions of the embryonic surface (**Fig. 14**). Surprisingly, these three groups of cilia displayed different ciliary beat patterns (**Fig. 15**) and different CBF (**Fig. 16**). In most embryos, the cilia of dorsolateral (**Fig. 15A**) and pedal (**Fig. 15B**) bands beat at a slow basal level with periodic surges of fast beating. Here, a surge is operationally defined as a transient rise of CBF to a peak at least 2 fold higher than the initial rising point. Statistical analysis showed that 72 % (n = 18) and 71 % (n = 28) of the stage E20-30 embryos exhibited periodic beat surges in pedal and dorsolateral bands, respectively, over the 2 min measurement period (**Fig. 16C**). In contrast, the isolated tufts of cilia always beat more rapidly without apparent surges (**Fig. 15C**). In addition, these various groups of cilia had significantly different overall rates of beating (**Fig. 16A**). The average CBF of the dorsolateral band, pedal band and isolated tufts of cilia were  $3.6 \pm 0.6$  Hz (n = 21),  $6.9 \pm 0.8$  Hz (n = 26) and  $12.0 \pm 0.4$  Hz (n = 24), respectively (ANOVA followed by Fisher PLSD,  $p < 0.01$  between any two groups).

## **2.3. Laser stimulation of ENC1 has different effects on different groups of cilia**

To test whether ENC1s regulate the activity of different groups of cilia, ENC1s were unilaterally stimulated with laser beams and the ciliary activity was subsequently measured. Embryos that met the following two criteria were used. First, the embryo must have some normally beating cilia that were labeled by a charcoal particle. Second, the embryo must be in an orientation in which at least one ENC1 can be detected under DIC optics so that the cell is accessible to laser beams. Before laser treatment, the basal activities of different groups of cilia (if applicable) were recorded for at least 2 min. Every 10 min in the first hour after laser treatment of ENC1, the activity of selected cilia were video taped for a 2-min period.

Results showed that unilateral laser treatment of ENC1 caused a very significant increase in CBF of pedal and the ipsilateral dorsolateral cilia (paired t-test, dorsolateral: p

< 0.01, n = 14; pedal: p < 0.01, n = 15; **Fig. 15A, B and 16A**). In contrast, the contralateral dorsolateral cilia and the isolated tufts of cilia were not affected by laser treatment of ENC1 (paired t-test, p > 0.05, n = 4 for the contralateral dorsolateral cilia; n = 9 for the isolated tufts of cilia; **Fig. 15C, 16A and B**). The responses in pedal and ipsilateral dorsolateral cilia were transient, as the CBF returned to normal levels within 50 minutes after laser treatment (**Fig. 17**). As laser operation controls, laser treatment of the ENC1-neighbor cells did not affect the CBF of dorsolateral and pedal cilia (paired t-test p > 0.05, n = 7 for dorsolateral, n = 11 for pedal; **Fig. 16A**). These results suggest that laser treatment of ENC1 cause enhanced ciliary beating specifically in ciliary cells with which it is anatomically associated.

Besides the increase in CBF, the ciliary beat pattern in the dorsolateral and pedal ciliary bands was also transiently affected by laser treatment of ENC1. Before laser treatment of ENC1, 72% (n = 18) and 71% (n = 28) of the embryos exhibited periodic CBF surges in the pedal and dorsolateral bands, respectively, over the 2-min measurement period. After laser treatment of ENC1, however, the percentage of embryos exhibiting CBF surges in pedal and dorsolateral bands decreased to 22% (Chi-square test, p < 0.01; n = 9) and 47% (Chi-square test, p = 0.10; n = 17), respectively (**Fig. 16C**). In most cases, the CBF elevated to a less variable rate without distinct surges (**Fig. 15A and B**). In contrast, CBF surges were absent in the isolated tufts of cilia, both before and after laser treatment (**Fig. 15C**).

#### **2.4. Laser-induced enhancement of ciliary activity involves serotonin**

In previous pharmacological studies, exogenous serotonin stimulated embryonic rotation *in vivo* and ciliary beating in cultured ciliated cells, and these effects of serotonin were blocked by the serotonin receptor antagonist mianserin (Diefenbach et al., 1991; Goldberg et al., 1994). Given the abovementioned results showing that the serotonergic ENC1s regulate ciliary activity *in vivo*, it is very likely that ENC1s do so by releasing of the cilioexcitatory neurotransmitter serotonin.

As a first step to test this hypothesis, the effects of exogenous 5-HT on the CBF of the different groups of cilia *in vivo* were examined. The CBF of pedal and dorsolateral cilia was significantly increased after addition of 50  $\mu$ M serotonin (**Fig. 18**; t-test, p <



0.01 for both dorsolateral and pedal bands). In contrast, the CBF of isolated tufts of cilia was not affected by serotonin (**Fig. 18**; t-test,  $p > 0.05$ ). Thus, only ciliated cells that were anatomically associated with ENC1 were responsive to the application of serotonin.

As the next step to test the hypothesis, the effects of mianserin on the ciliary activity of the pedal and dorsolateral bands were examined. Mianserin (50  $\mu\text{M}$ ) reduced the expression of ciliary beat surges in both pedal and dorsolateral bands (**Fig. 19A, B and 20A**). Whereas 72% of control embryos exhibited CBF surges in the pedal band in the 2-min measurement period, only 8 % of embryos incubated in mianserin displayed CBF surges (**Fig. 20A**; Chi-square test,  $p < 0.01$ ). Similarly, 71% of the control embryos exhibited CBF surges in the dorsolateral band, while only 36% of embryos exhibited CBF surges in the presence of mianserin (**Fig. 20A**; Chi-square test,  $p < 0.05$ ). Associated with the mianserin-induced reduction in surge events was a significant reduction in the CBF of the pedal ciliary band, but not the dorsolateral band (**Fig. 20B**). These results suggest that surges in CBF result from the action of endogenous serotonin.

In a final test of the hypothesis that ENC1 releases serotonin to stimulate ciliary activity, the effect of mianserin on the laser-induced enhancement of CBF was examined. Mianserin reduced the laser-induced increase in CBF in the dorsolateral and pedal cilia (**Fig. 20C**; t-test,  $p < 0.05$  for pedal,  $p = 0.05$  for dorsolateral cilia), whereas the CBF of isolated tufts of cilia was unaffected by mianserin and laser treatment (**Fig. 19C**). Compared to the pretreatment level, the pedal CBF increased by 63% in control embryos in response to laser treatment, but only by 7% in the presence of mianserin (**Fig. 20C**). Similarly, dorsolateral CBF increased by 89% in control embryos, but only by 34% in mianserin (**Fig. 20C**). Therefore, mianserin partly blocked the transient increase in ciliary activity induced by laser treatment of ENC1. Taken together, these results provide the first direct evidence suggesting that ENC1 regulates ciliary activity through the release of serotonin.

## **2.5. Laser ablation of ENC1 abolishes spontaneous rotational surges**

Although the above experiments confirm that ENC1s are serotonergic cilio-excitatory motor neurons, they only indirectly suggest that ENC1s generate the rotational surges. To directly test this hypothesis, both ENC1s in each embryo were ablated with

laser beams (**Fig. 21A**). Embryos (stage E25) with both ENC1s knocked out or two random cells adjacent to each ENC1 knocked out (sham ablation) were then transplanted to new host egg capsules (**Fig. 21A**). After overnight recovery from laser ablation and transplantation treatments, the rate of embryonic rotation and the frequency of rotational surges (Diefenbach et al., 1991) were analyzed.

Embryos with both ENC1s ablated displayed a slower average rate of rotation (**Fig. 21B**). Whereas sham operated embryos ( $n = 9$ ) rotated at an average rate of  $0.59 \pm 0.10$  rotation/min, ENC1-ablated embryos ( $n = 7$ ) rotated at a rate of  $0.22 \pm 0.07$  rotation/min (t-test,  $p < 0.05$ ). Moreover, bilateral laser ablation of ENC1 nearly abolished the intrinsic rotational surges occurring in control embryos (**Fig. 21C**). In the sham operated embryos, an average of  $6.3 \pm 0.6$  surges were generated in each 10-min period ( $n = 11$ ), whereas only  $0.6 \pm 0.3$  surges ( $n = 7$ ) were detected in embryos with both ENC1s ablated (t-test,  $p < 0.01$ ). Finally, embryonic rotational behaviors were affected by laser ablation of ENC1. Permanent arrest of embryonic movement was found in 50 % of the embryos ( $n = 14$ ) with both of their ENC1s ablated. In contrast, only 21 % ( $n = 14$ ) of the sham ablated embryos displayed arrested movements (Chi-square test,  $p = 0.11$ ; embryos with arrested movement were not used in the above quantification of rotational rate and surge frequency). When only one of their ENC1s was ablated, embryos ( $n = 3$ ) displayed uncoordinated or aberrant movements not found in normal embryos, including reversal of rotation and swimming in circular patterns within their egg capsules. Together, these results supported the hypothesis that ENC1s generate the periodic surges of embryonic rotation and coordinate embryonic movement.

### **3. *Helisoma* embryos display an adaptive behavioral response to hypoxia <sup>4</sup>**

Provided that ENC1s generate periodic rotational surges by releasing serotonin onto cilia, the dendritic knobs of ENC1s may function to detect certain environmental cues inside the egg capsule and subsequently regulate embryonic rotation according to the level of these cues. The next question to ask is “what environmental factor(s) elicits increases in ciliary beating and embryonic rotation?” There are strong reasons to assume that the membrane structures surrounding each embryo produce a diffusional barrier for certain metabolically important molecules so that any changes in the levels of these

molecules would elicit enhanced rotation to promote diffusion. Since the levels of the nutrition and energy sources in the capsular fluid do not oscillate (Morrill, 1982; Meshcheryakov, 1990), they are unlikely to be stimulants of embryonic rotation. Instead, factors that elicit embryonic rotation should be exogenous to the capsular fluid. During growth and development, embryonic metabolism tends to deplete O<sub>2</sub> and build up CO<sub>2</sub> as well as ammonium in the capsular fluid. Therefore, one of the purposes of embryonic rotation may serve to reduce the diffusional barrier to these gaseous molecules. The effects of O<sub>2</sub>, CO<sub>2</sub> and ammonia on the embryonic rotation were examined in this section. Results showed that there is an O<sub>2</sub> gradient surrounding each encapsulated embryo rendered by the structural composition of egg capsule and egg mass membranes. More importantly, hypoxia elicited dose-dependent accelerations of embryonic rotation, suggesting that O<sub>2</sub> is a major environmental factor that stimulates embryonic rotation.

### **3.1. Structural basis of encapsulation renders a diffusional barrier**<sup>5</sup>

*Helisoma* embryos develop within transparent egg masses, with each sibling embryo housed in an individual egg capsule (**Fig. 22A**). The first behavior displayed by embryos is a rotational movement that is driven by three bands of motile cilia (**Fig. 22B**<sup>6</sup>; Diefenbach et al., 1991) and regulated by the serotonergic ENC1 neurons (**Fig 22C**; elaborated in **Results 2.3-2.5**). Since cellular respiration tends to deplete O<sub>2</sub> surrounding each embryo, one of the purposes of embryonic rotation may serve to facilitate inward diffusion of environmental O<sub>2</sub>. This hypothesis predicts that there is an O<sub>2</sub> gradient from the surface of the egg mass to the center of each egg capsule due to the metabolic consumption of O<sub>2</sub> by embryos and the O<sub>2</sub> diffusional barrier conferred by the physical structure of egg capsules.

As a first attempt to test this hypothesis, the membrane structures that surround each embryo were examined. Whole egg masses were freeze-fractured along a cross-sectional plane that roughly bisected the entire egg mass (**Fig. 23A**). The membrane structures within each egg mass were examined with scanning electron microscopy (SEM) (**Fig. 23B**). There were two major layers of membrane surrounding each embryo (**Fig. 23C**). The inner layer comprised the egg capsule membrane and had a thickness of 0.3–0.5 μm. The outer layer comprised the envelope of the whole egg mass and had a

thickness of 2– 8  $\mu\text{m}$ . Between these two membranous structures was a gelatinous porous material with a thickness of at least 10  $\mu\text{m}$  (**Fig. 23C**). The egg mass and capsular membranes were filled with channel-like pores that were less than 100 nm in diameter (**Fig. 24**). Together, these results suggest that the membranes surrounding each embryo confer diffusional barriers that only allow the passage of molecules smaller than 100 nm.

In order to determine if a similar diffusional barrier exists in another pond snail species, *Lymnaea stagnalis*, the ultrastructure of the *Lymnaea* egg mass was examined similarly. Instead of flat and globular shaped, *Lymnaea* egg masses had a sausage-like shape (**Fig. 25A**). SEM of freeze-fractured cross sections of *Lymnaea* egg masses revealed that the egg mass envelope had a thickness of about 150  $\mu\text{m}$  (**Fig. 25B**). This envelope was composed of a very permeable spongy material (**Fig. 25B and D**). In contrast to the single layer of membrane surrounding the *Helisoma* egg capsule, there were multilayers of porous membranes surrounding each *Lymnaea* egg capsule (**Fig. 25C**). The estimated pore size in these membranous structures was 0.5–1.5  $\mu\text{m}$ . Thus, although there are several layers of membrane surrounding each *Lymnaea* embryos, these barriers may allow the passage of much larger molecules.

As a second test of the  $\text{O}_2$  diffusion hypothesis, the  $\text{O}_2$  gradient across egg capsules was examined by measuring the partial pressure of  $\text{O}_2$  ( $\text{Po}_2$ ) at different positions around stage E20–E25 egg masses under normoxic conditions, using an  $\text{O}_2$ -sensitive microelectrode (**Fig. 26**). As the electrode moved towards the embryo, the  $\text{Po}_2$  just below the egg mass surface was only 69% of the perfusate, and there was a further drop to 42% of the perfusate  $\text{Po}_2$  levels at the center of the capsule (**Fig. 26 and 27B**). Conversely,  $\text{O}_2$  levels increased as the electrode moved away from the center of the egg capsule (**Fig. 26**).

Another indication of the diffusional barrier was that the rate of change in  $\text{O}_2$  levels upon introduction of hypoxic perfusate was slower inside the egg capsule as compared to the bath (**Fig. 27A and C**). Outside the egg mass,  $\text{O}_2$  levels changed at a time constant of  $10 \pm 2$  sec, reflecting the time taken to replace the perfusate. In contrast,  $\text{O}_2$  levels within the egg mass changed at a time constant of  $61 \pm 10$  sec (**Fig. 27C**; t-test,  $p < 0.05$ ,  $n = 6$ ). Similarly, the average rate of  $\text{O}_2$  level rise inside the egg capsule was much slower than that in the perfusate upon reintroduction of normoxic perfusate (**Fig. 27C**; t-test,  $p < 0.05$ ,

n = 6). These results suggest that the physical construction of the egg mass membranes and the gelatinous egg mass materials comprise O<sub>2</sub> diffusional barriers, such that the consumption of O<sub>2</sub> by the embryo causes an O<sub>2</sub> gradient from the egg mass surface to the embryo.

### **3.2. Hypoxia elicits prolonged acceleration of embryonic rotation** <sup>7</sup>

The hypothesis that embryonic rotation serves to facilitate inward diffusion of environmental O<sub>2</sub> also predicts that experimental reduction of O<sub>2</sub> levels should increase embryonic rotation. This prediction was tested by measuring embryonic rotation under reduced levels of environmental O<sub>2</sub>. Hypoxia (100% N<sub>2</sub> saturated APW) induced an increase in the rate of rotation that reached a peak in 30 min and gradually returned to basal levels after 2.75 h during continued hypoxia (**Fig. 28**). Interestingly, reoxygenation with 100% air following the hypoxic treatment transiently inhibited embryonic rotation, followed by a return to the basal level (**Fig. 28**). All embryos (n = 29) survived the 3-hour hypoxic treatment, indicating their good tolerance to O<sub>2</sub> depletion.

Since the 100% N<sub>2</sub> saturated APW had an elevated pH (about 9.0, as compared to pH 7.2 of normoxic APW), it was possible that the hypoxia-enhanced embryonic rotation was due to medium alkalization. To rule out this possibility, the rates embryonic rotation at pH 7.3 and pH 9.1 were compared. There was no difference in the rate of embryonic rotation under these pH levels (**Fig. 29**), suggesting that medium alkalization doesn't contribute to the hypoxia-elicited enhancement in embryonic rotation.

Accompanying the increase in rotational rate, the relative position of each embryo within its egg capsule also changed in response to hypoxia. Prior to hypoxic treatment, embryos inside individual egg capsules tended to occupy the region towards the center of the whole egg mass (**Fig. 30A**). There was no net movement of embryos caused by the constitutive rotation under normoxia. In contrast, there was a clear migration towards the egg mass periphery during the hypoxic treatment in all egg massed examined (N > 30; **Fig. 30B**). This behavioral response to hypoxia may serve to relocate embryos into a more favorable microenvironment within the egg capsules where higher levels of O<sub>2</sub> occur (**Fig. 26**). To determine if the migration was actively mediated by an O<sub>2</sub>-chemotaxis mechanism or passively generated by the fluid dynamics inside the egg

capsule, egg masses were immersed in normoxic APW containing the cilio-excitatory neurotransmitter serotonin (100  $\mu\text{M}$ ). Accompanying the serotonin-stimulated embryonic rotation, similar outward migration was observed (data not shown). This suggests that the fluid dynamics resulting from enhanced embryonic rotation generates the outward migration under hypoxia.

In a closely related pond snail species, *Lymnaea stagnalis*, hypoxia also elicited increases in embryonic rotation, but in a more transient manner (**Fig. 31**). Return to normoxia also transiently inhibited embryo rotation, followed by a rebound that was not seen in *Helisoma* (**Fig. 31**).

### **3.3. $\text{Po}_2$ dependency and behavioral plasticity of hypoxia-elicited embryonic rotation**

The amplitude of the rotational response to hypoxia was  $\text{Po}_2$  dependent (**Fig. 32A**). The  $\text{Po}_2$  for threshold, half-maximal and maximal responses were 60, 28, and 13 mmHg, respectively. At the maximal response, the rotation rate was about 4 times the basal rate (**Fig. 32A**). In addition, the response to hypoxia was reversible and displayed behavioral sensitization to repeated hypoxic treatments (**Fig. 32B**). Upon each repeated cycle of hypoxia and normoxia, embryonic rotation displayed a similar pattern of stimulation, transient inhibition and recovery (**Fig. 32B**). However, the embryonic rotational response to the same levels of hypoxia ( $\text{Po}_2 = 22$  mm Hg) was enhanced after two cycles of hypoxic/normoxic treatment. During the third hypoxic treatment, the rate of embryonic rotation was higher than those during the initial two episodes of hypoxic treatment (t-test,  $p < 0.05$  between responses at 50 and 90 min; also  $p < 0.05$  between responses at 10 and 90 min,  $n = 19$ ).

### **3.4. Effect of $\text{CO}_2$ on embryonic rotation**

The effect of  $\text{CO}_2$  on embryonic rotation was examined for two reasons. First, in air-breathers, tissue or blood  $\text{CO}_2$  levels are also important regulators of ventilation because slight changes in  $\text{CO}_2$  levels may significantly affect tissue pH and intracellular pH ( $\text{pH}_i$ ) (Erlichman and Leiter, 1993; Gonzalez et al., 1995; Fitzgerald et al., 1999). Second, the hypoxic medium used in the studies described above also had reduced levels of  $\text{CO}_2$  because they were made by mixing air with different levels of  $\text{N}_2$ . It was possible

that the increases in embryonic rotation actually resulted from decreased CO<sub>2</sub> levels instead of decreased O<sub>2</sub> levels.

If ambient CO<sub>2</sub> is involved in the regulation of ventilation in *Helisoma* embryos as in air-breathers, increases of CO<sub>2</sub> levels (hypercapnia) would be expected to increase the ventilatory embryonic rotation. To test this possibility, embryos were exposed to media equilibrated with 1% CO<sub>2</sub> and 99% air, a level of hypercapnia similar to that seen in eutrophic ponds (Derry, 1993). Elevated Pco<sub>2</sub> transiently reduced the rate of embryonic rotation by about 30%, whereas return to normal CO<sub>2</sub> levels transiently increased the rate of rotation (**Fig. 33A**; ANOVA followed by Fisher's PLSD,  $p < 0.05$ ,  $n = 15$ ). These responses were much smaller and opposite to those noted for hypoxia, suggesting that CO<sub>2</sub> is not a major regulator of the adaptive ventilation in embryonic pond snails.

Since hypercapnia causes acidosis both extra- and intracellularly (Erichman and Leiter, 1997), the CO<sub>2</sub> response seen above is likely mediated by alterations in pH. Elevations in Pco<sub>2</sub> to 1% reduced the pH of the extracellular medium from 7.2 to 6.3. Experimental reduction of the medium to pH 5.0 with HCl had no effect on embryonic rotation (**Fig. 29**). Assuming an intracellular buffering capacity of 20 mM/pH unit, 1% CO<sub>2</sub> would reduce pH<sub>i</sub> by 0.2 units. To test if the effect of CO<sub>2</sub> are associated changes in pH<sub>i</sub>, a similar ~ 0.2 unit reduction in pH<sub>i</sub> was induced with 20 mM sodium butyrate (Muller et al., 2000). Addition and washout of the sodium butyrate decreased and increased the rate of embryonic rotation, respectively, in a manner similar to that induced by changes in Pco<sub>2</sub> (**Fig. 33B**; ANOVA,  $p < 0.05$ ,  $n = 15$ ). These results suggest that the small response to elevated CO<sub>2</sub> occurs through changes in pH<sub>i</sub>.

The effect of reduced CO<sub>2</sub> levels on embryonic rotation was also examined. Embryonic rotation in air-saturated APW (20.9% O<sub>2</sub>, 0.2% CO<sub>2</sub>, 78% N<sub>2</sub> and 0.9% other inert gases) and in APW equilibrated with 21% O<sub>2</sub> and 79% N<sub>2</sub> was compared. In contrast to what occurred under hypercapnia, removal of CO<sub>2</sub> from the medium while keeping O<sub>2</sub> unchanged transiently increased the embryonic rotation by about 30% in the first 20 min, with a return to the normal rate of rotation by 30 min (**Fig. 34**). This transient increase was mimicked by ammonium-induced intracellular alkalization (data not shown), but was not produced by increasing the pH of bathing medium with NaOH (**Fig. 29**). These results suggest that transient increase in embryonic rotation induced by

removal of CO<sub>2</sub> is likely mediated through intracellular alkalization. However, decreased CO<sub>2</sub> alone cannot account for the robust and prolonged increase of embryonic rotation observed under hypoxic conditions.

### **3.5. Hyperoxia also elicits dose-dependent acceleration of rotation**

Results from the hypoxic treatments suggest that when the intracapsular O<sub>2</sub> level falls to a critical point, embryos increase their rate of rotation to facilitate O<sub>2</sub> diffusion so that adequate supplies of O<sub>2</sub> are maintained. Although the occurrence of hyperoxia (high levels of O<sub>2</sub>) is not likely in the natural environment, it would be interesting to test whether hyperoxia has any effect on embryonic rotation. Since high levels of O<sub>2</sub> increase the production of harmful reactive oxygen species (ROS), it is hypothesized that embryos will increase their rate of rotation in order to eliminate the excess ROS under hyperoxia.

When the ambient O<sub>2</sub> level was doubled from 21% to 41%, the rate of embryonic rotation transiently increased by about 20% (**Fig. 34**). As the ambient O<sub>2</sub> level was further increased to 100%, the rate embryonic rotation increased to 160% of that under 21% O<sub>2</sub> (**Fig. 34**). Reintroduction of the air-saturated medium transiently inhibited embryo rotation (**Fig. 34**), a phenomenon similar to the post-hypoxia inhibition described above (**Fig. 28**). These results, together with those observed in response to hypoxia, suggest that the intracapsular O<sub>2</sub> levels are actively maintained at a certain range through regulation of embryonic rotation.

### **3.6. Interaction between O<sub>2</sub> and CO<sub>2</sub>**

Given the contradictory effects between hypoxia and hypercapnia, as well as between hypercapnia and hyperoxia, it is interesting to examine the interplay between these factors. Exposure of embryos to combined hyperoxic and hypercapnic treatment (99.7 % O<sub>2</sub> plus 0.3 % CO<sub>2</sub>) caused no change in the rate of embryonic rotation (**Fig. 35A**). However, restoration of normal levels of O<sub>2</sub> and CO<sub>2</sub> resulted in an increased rate of embryonic rotation (**Fig. 35A**), as would have occurred after hypercapnia treatment alone (**Fig. 34**). When embryos were simultaneously challenged by hypercapnia and hypoxia (99.7 % N<sub>2</sub> plus 0.3 % CO<sub>2</sub>) followed by a return to normal levels, the changes in the rate of embryonic rotation were very similar to those elicited by a hypoxic



challenge alone (**Fig. 35B** as compared to **Fig. 28**). Together, these data suggest that hypoxia is the most predominant factor affecting embryonic rotation, followed by hypercapnia and hyperoxia.

### **3.7. Effects of other environmental factors on embryonic rotation**

Since many aquatic animals are able to detect certain amino acids and odorant compounds (Leinders-Zufall et al., 1998a; b; Mac Leish et al., 1999), the effect of these chemical cues on embryonic rotation was examined. Whole egg masses were incubated in 5 mM (in APW) of glutamine, histidine, aspartic acid, GABA, isoamyl acetate, cineole and acetophenone, separately. Embryonic rotation was examined before and 10 min after incubation with these chemicals. Glutamine had a stimulatory effect on the embryonic rotation (**Fig. 36**). This stimulatory effect lasted for 2.5 h during continued incubation (**Fig. 36**). Moreover, preliminary studies showed that both glutamate and glutamine had a chemoattractant effect on de-capsulated stage E25 embryos (data not shown). In contrast, other amino acids and all the odorant compounds tested had very little effect on the rotational behavior (data not shown).

Since a major component of the capsular fluid is galactogen, polymers of galactose (Morrill, 1982), the effect of 5 mM galactose on embryonic rotation was also examined. Galactose had no effect on the rotational behavior (data not shown). Similarly, variation of extracellular pH had no effect on embryonic rotation (**Fig. 29**). In other experiments, 7.4 mg total-N/L ammonium increased embryonic rotation by 82% (n = 20), whereas 2.5 mg total-N/L ammonium had no effect on embryonic rotation (data not shown). Finally, the effect of extracellular  $\text{Ca}^{2+}$  on basal and hypoxia-induced embryonic rotation was tested. Low extracellular  $\text{Ca}^{2+}$  concentration in the presence of 10 mM EGTA reduced the basal rate of embryonic rotation and abolished hypoxia-induced enhancement of the rotational behavior (**Fig. 37**). Twenty minutes after washout of EGTA, embryonic rotation under normoxia recovered to control level (**Fig. 37**). However, only partial recovery of the rotational response to hypoxia was observed (**Fig. 37**), suggesting depletion of extracellular  $\text{Ca}^{2+}$  has a prolonged effect on the  $\text{O}_2$  sensing mechanism.

#### **4. ENC1 mediates O<sub>2</sub>-sensing and the rotational response to hypoxia**

The robust rotational response to hypoxia and the apical chemosensory structure of ENC1 (**Fig. 10**) provide the foundation for a hypothesis that ENC1 mediates O<sub>2</sub> sensing and the behavioral response to hypoxia in *Helisoma* embryos. This part of the Results tests this hypothesis. First, the direct effect of hypoxia on the activity of isolated ciliary cells was examined. The results showed that hypoxia did not change the ciliary beat frequency in cultured ciliary cells, suggesting that the hypoxia-induced enhancement of embryonic rotation requires cells upstream of the motile cilia. Second, developmental analysis indicated that the embryonic rotational response to hypoxia is correlated to the development of ENC1, suggesting a link between ENC1 and hypoxia-induced behavioral response. Third, bilateral ablation of ENC1s with laser beams abolished the hypoxia-elicited enhancement of embryonic rotation. Therefore, ENC1s are necessary in mediating the behavioral response to hypoxia in the embryos. Fourth, electrophysiological experiments demonstrated that hypoxia caused an excitation of ENC1 in culture, suggesting that ENC1 directly responds to hypoxia. Together, these results provide strong evidence that ENC1 mediates O<sub>2</sub> sensing and embryonic rotation in *Helisoma*.

##### **4.1. Hypoxia has no direct effect on ciliary beating**<sup>8</sup>

To demonstrate that the behavioral response to hypoxia is specifically mediated by O<sub>2</sub> chemoreceptors upstream of the motile ciliary cells, the response of isolated ciliary cells to hypoxia was tested. Ciliary cells did not respond to hypoxia with an increase in CBF (**Fig. 38**). The CBF before, during and after hypoxia were  $11.23 \pm 0.78$ ,  $10.78 \pm 0.60$  and  $11.03 \pm 0.73$  Hz, respectively (ANOVA,  $p > 0.05$ ,  $n = 5$ ). The lack of response to hypoxia in isolated ciliary cells could not be due to their insensitivity to chemical stimuli since it has been shown that both serotonin and NO stimulate ciliary beating (Goldberg et al., 1994; 2000). The lack of direct response to hypoxia in ciliary cells suggests that hypoxia stimulates other cells upstream to increase the activity of these ciliary cells.

#### **4.2. Rotational responsiveness to hypoxia correlates to ENC1 development**

The ability to study the development of O<sub>2</sub> sensing is an important feature of this animal system. Constitutive rotational behavior of the embryo is initiated at stage E15 (Diefenbach et al., 1991). At this stage, the ENC1 – ciliary cell circuit is not fully developed (Goldberg et al., 1996; Koss et al., 2002). Embryos at stage E15 had a delayed (40 min) and attenuated response to hypoxia, whereas the older (stage E20-E30) embryos responded more rapidly and with a greater magnitude (**Fig. 39**). Furthermore, the stage E15 embryos did not show inhibition of rotation in response to reoxygenation following hypoxia (**Fig. 39**). These data suggest that development of the behavioral response to hypoxia is correlated to the development of ENC1s.

#### **4.3. Laser ablation of ENC1s abolishes hypoxia-elicited acceleration of embryonic rotation**

Each ENC1 bears a superficially located chemosensory structure (**Fig. 22B and C inset**; Diefenbach et al., 1998) and innervates the ciliary bands (refer to **2.3- 2.5 of the Results**). To test whether the hypoxia-induced enhancement of embryonic rotation is mediated through the sensory-motor ENC1s, the rotational response to hypoxia was examined after both ENC1s were ablated with laser beams. The laser-treated embryos were transplanted back into intact host egg capsules and the rate of embryonic rotation was measured after 16 h of recovery. Control ablated embryos (ablation of a random cell near each ENC1) responded normally to hypoxia and reoxygenation by increasing and transiently decreasing the rate of rotation, respectively (**Fig. 40**). In contrast, embryos with both ENC1s ablated did not respond to hypoxia, nor did they respond to the reoxygenation following hypoxia (**Fig. 40**). These results demonstrate that ENC1s are required for the embryonic response to hypoxia.

#### **4.4. Hypoxia induces excitatory responses in ENC1<sup>9</sup>**

The most direct way to test whether ENC1s directly respond to hypoxia is to record its electrical activity. Since direct electrophysiological recording of ENC1 *in vivo* is technically difficult, an alternative approach was used to record its electrical activity in culture. As previous attempts to identify ENC1 in mass-dissociated embryonic cell

culture were unsuccessful, a new tissue culture method was developed for this experiment. Embryonic tissue explants containing ENC1s were surgically isolated (**Fig. 41A**) and cultured in poly-L-Lysine coated glass-bottom petri dishes. ENC1s were identified in 20–30 % of the attached tissue explants under DIC microscopy, based on presence of the dendritic knob, apical granules, smooth nucleus and prominent nucleolus (**Fig. 41C and D**). Furthermore, ENC1s identified using DIC were verified with anti-serotonin immunostaining (**Fig. 41B**).

Patch-clamp recordings were performed on the identified ENC1's under normoxia and hypoxia. While voltage clamping in the cell-attached configuration, spontaneous electrical activity was rarely seen in ENC1 under control conditions (**Fig. 42A**). However, introduction of hypoxic medium induced action potential activity, seen in this recording as action potential associated current spikes (**Fig. 42B**). Return to normoxia after the hypoxic treatment reduced the spiking frequency (**Fig. 42C**). Under the whole-cell recording configuration in current clamp mode, hypoxia initially elicited a large depolarization and a burst of action potentials, followed by a prolonged reduction of membrane potential (**Fig. 43**). Upon return to normoxia, the membrane potential repolarized partially to the pretreatment level (**Fig. 43**). A second application of hypoxic medium again produced an excitatory response in ENC1 (**Fig. 43**). Similar responses were observed in 3 additional ENC1s tested. Together, these results support the hypothesis that ENC1 functions as an O<sub>2</sub> chemosensory neuron that mediates the embryonic rotational response to hypoxia.

## 5. The hypoxia signaling pathways <sup>10</sup>

Given the simplicity of the nervous system and the robust hypoxia-induced behavioral response in stage E25 *Helisoma* embryos, the ENC1-ciliary reflex circuit may provide one of the best models for the examination of hypoxia signaling pathways. In mammals, acute responses to hypoxia are mediated by the closure of O<sub>2</sub>-sensitive potassium (OK) channels in both O<sub>2</sub>-sensitive chemosensory cells and central neurons (Barneo-Lopez, 1996; Haddad and Jiang, 1998; Barneo-Lopez et al., 2001). It has also been proposed that certain components in the mitochondrial electron transport chain (ETC) are sites of O<sub>2</sub> sensing and thus mediate hypoxia signaling (Acher et al., 1999;

Lopez-Barneo et al., 2001). In the present study, the involvement of OK channels in the initiation of hypoxia signaling was examined pharmacologically with 4-aminopyridine (4-AP), which preferentially blocks OK channels in several mammalian systems (Archer et al., 1999). To test whether the mitochondrial ETC is involved in the hypoxia signaling in *Helisoma*, the effect of an ETC inhibitor, rotenone, on the embryonic rotation was examined. At the level of motile ciliary cells, it has been shown that serotonin receptor activation is involved in regulation of ciliary beating (Goldberg et al., 1994). The involvement of serotonergic signaling pathway in hypoxia-induced acceleration of embryonic rotation was also investigated.

### **5.1. Involvement of serotonin receptor activation**

Since ENC1 releases serotonin to regulate ciliary activity (refer to **2.5** of the **Results**), it is very likely that hypoxia-induced enhancement of embryonic rotation results from the action of serotonin on ciliary cells. To test this possibility, the embryonic rotational response to hypoxia was examined in the presence of an effective serotonin receptor antagonist, mianserin. At maximally effective doses (100  $\mu$ M; Goldberg et al., 1994), mianserin reduced the rotational response to hypoxia by 33 % (**Fig. 44**; ANOVA followed by Fisher PLSD,  $p < 0.05$ ,  $n = 15$ ). A partial recovery of the mianserin inhibition was noted after 30 min of washout (**Fig. 44**; ANOVA followed by Fisher PLSD,  $p < 0.05$ ,  $n = 15$ ). Together, these experiments suggest that ENC1 mediates the behavioral response to hypoxia in part through a serotonin signaling pathway.

### **5.2. Involvement of 4-AP sensitive potassium channels**

The molecular mechanism of O<sub>2</sub> sensing has been a topic of dispute (Semenza, 1999; Prabhaker, 2000; Lopez-Barneo et al., 2001). Whereas long-term responses to hypoxia require activation of hypoxia inducible factors and expression of relevant genes (Bunn and Poyton, 1996), short-term cellular responses to hypoxia involve a closure of O<sub>2</sub> sensitive K<sup>+</sup> channels and depolarization of O<sub>2</sub>-sensitive cells (Lopez et al., 1988; Haddad and Jiang, 1997). The behavioral responses of embryos to the potassium channel blocker 4-AP (5mM) were examined. 4-AP increased the rate of embryonic rotation (**Fig. 45A**), but had no significant effect on the beating of isolated ciliated cells (**Fig. 45B**).

These results indicate that closure of K<sup>+</sup> channels in cells other than cilia is sufficient to mimic the hypoxic response in these embryos, therefore implicating a common mechanism to other described O<sub>2</sub>-sensing systems.

### **5.3. Involvement of the mitochondrial electron transport chain**

Although a closure of K<sup>+</sup> channels is a common feature of hypoxia-induced short-term responses, the actual O<sub>2</sub> sensor is believed to be a protein linked to, or upstream of, the channel protein in the signaling cascade (Youngson et al., 1993; Archer et al., 1999; Fu et al., 1999). Some studies have suggested that the mitochondrial electron transport chain (ETC) is the O<sub>2</sub> sensor (Archer et al., 1999). According to the 'mitochondria hypothesis', hypoxia inhibits ETC function and causes over-production of electron donors (NADPH), which in turn shifts the redox state of certain cysteine groups in K<sup>+</sup> channel proteins and causes closure of the channel (Ruppesberg et al., 1991). Thus, if a similar mechanism was involved in O<sub>2</sub> sensing in *Helisoma* embryos, then inhibition of the ETC should mimic the response to hypoxia. Rotenone (10 μM), an inhibitor of NADH dehydrogenase of the ETC, caused a delayed increase in the rate of embryonic rotation (**Fig. 46A**). In contrast, it had no effect on the beating of isolated ciliary cells (**Fig. 46B**), supporting the argument that the mitochondrial ETC in cells upstream of ciliary cells is part of the signal transduction pathway involved in O<sub>2</sub> sensing.

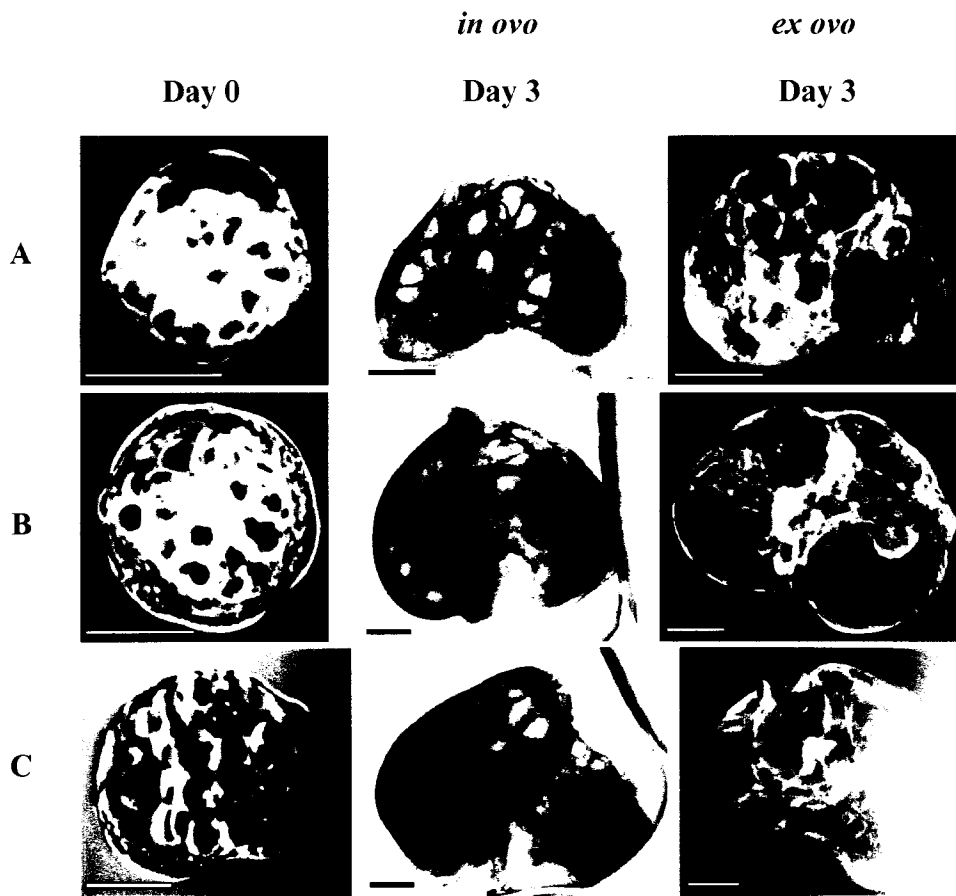
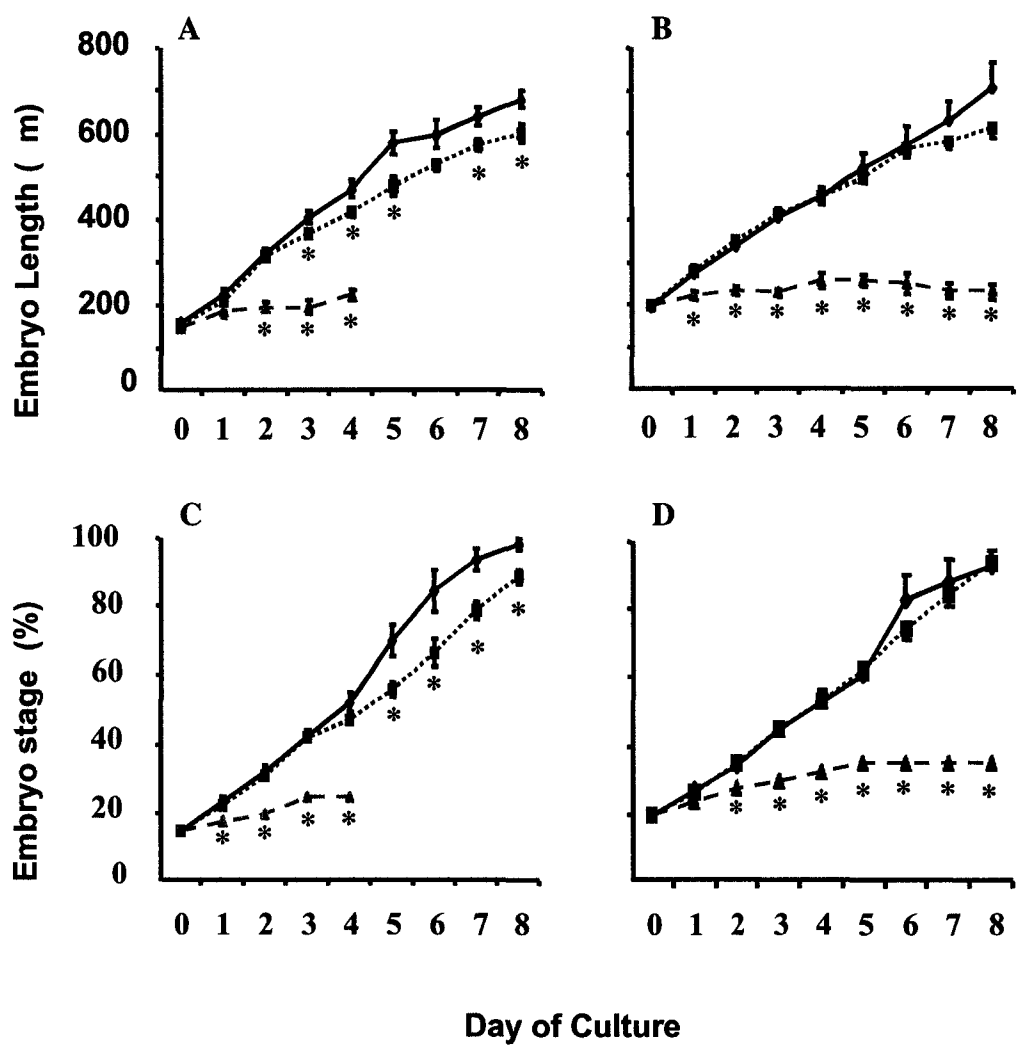


**Figure 3.** Embryonic development after 3 days of culture *in ovo* and *ex ovo* at 23°C. Examples of stage E15 (A), E20 (B) and E25 (C) embryos before culture (Day 0), and after 3 days of culture in host egg capsules (*in ovo*) and or in AHS plus 1.5% CF (*ex ovo*). Embryos cultured *in ovo* reached stages E40 (A), E45 (B), and E50 (C), whereas embryos cultured *ex ovo* only developed to stage E30 (A and B) or E35 (C). Arrows: Accumulation of particles in the protonephridium. Scale bars: 100 µm.

**Figure 4.** Growth and development of *in ovo* control embryos, transplanted embryos and *ex ovo* cultured embryos at 23 °C. The growth of stage E15 (**A**) and E20 (**B**) embryos cultured *ex ovo* in AHS plus 1.5% CF was significantly slower than that of control embryos (t-test,  $p < 0.05$  at time points marked by asterisks,  $n = 7$  for each of the *ex ovo* culture groups,  $n = 6$  and  $5$  for control stage E15 and E20 embryos, respectively). In contrast, growth of transplanted stage E15 and E20 embryos was very similar to their control counterparts. Slight differences were only seen at later stages of culture in transplanted E15 embryos (marked by asterisks, t-test,  $p < 0.05$ ,  $n = 6$ ). There was no significant difference in the growth of control and transplanted stage E20 embryos at any time points (t-test,  $p > 0.05$ ,  $n = 6$ ). The development of the same stage E15 (**C**) and E20 (**D**) embryos cultured *ex ovo* was much slower than that of control embryos (Asterisks:  $p < 0.05$ , t-test). In transplanted stage E15 and E20 embryos, however, the development was very similar to their control counterparts. Small differences were only seen at later stages of culture in transplanted E15 embryos (Asterisks, t-test,  $p < 0.05$ ). There was no significant difference in the development of control and transplanted stage E20 embryos at any time point (t-test,  $p > 0.05$ ).

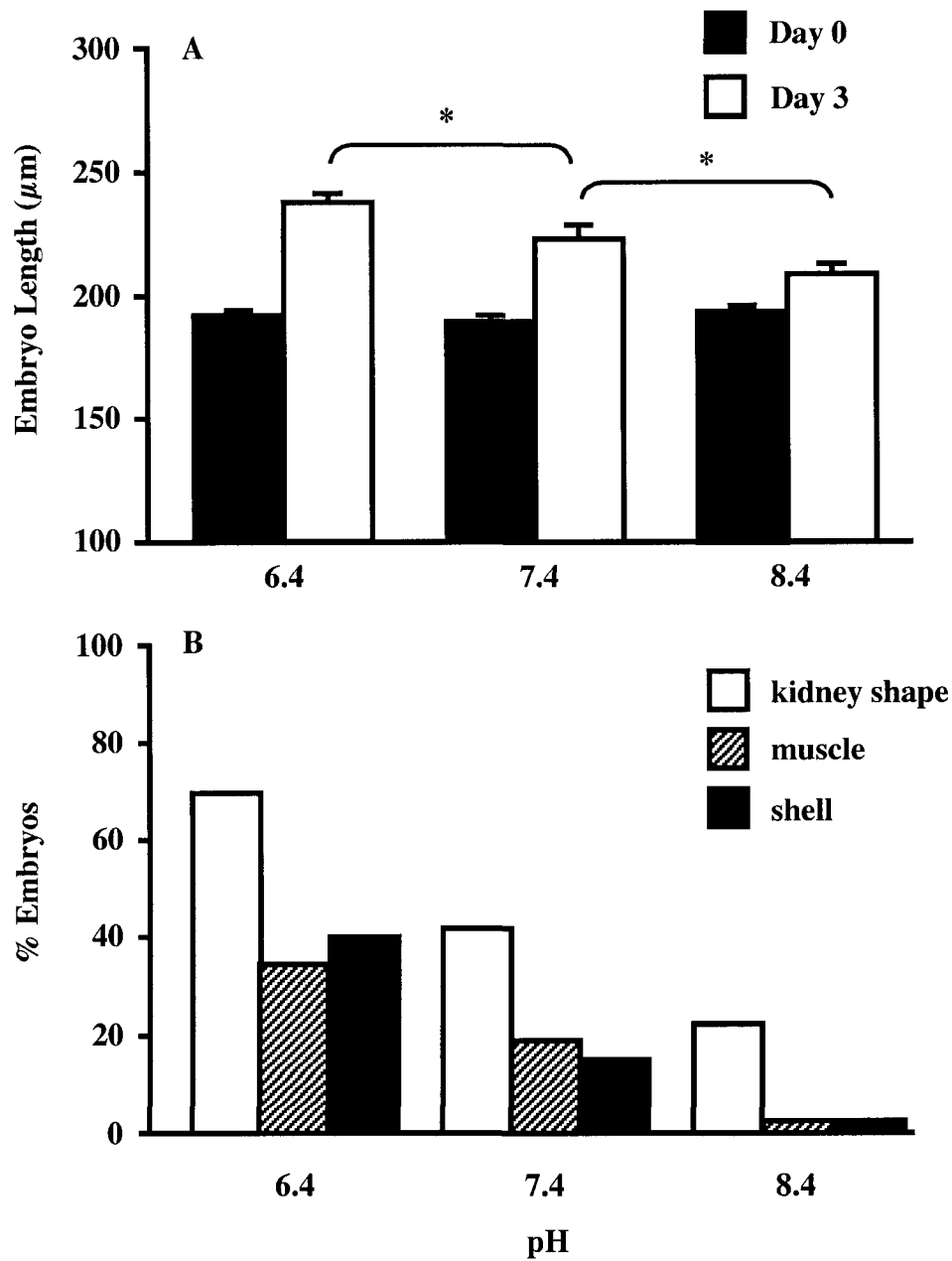


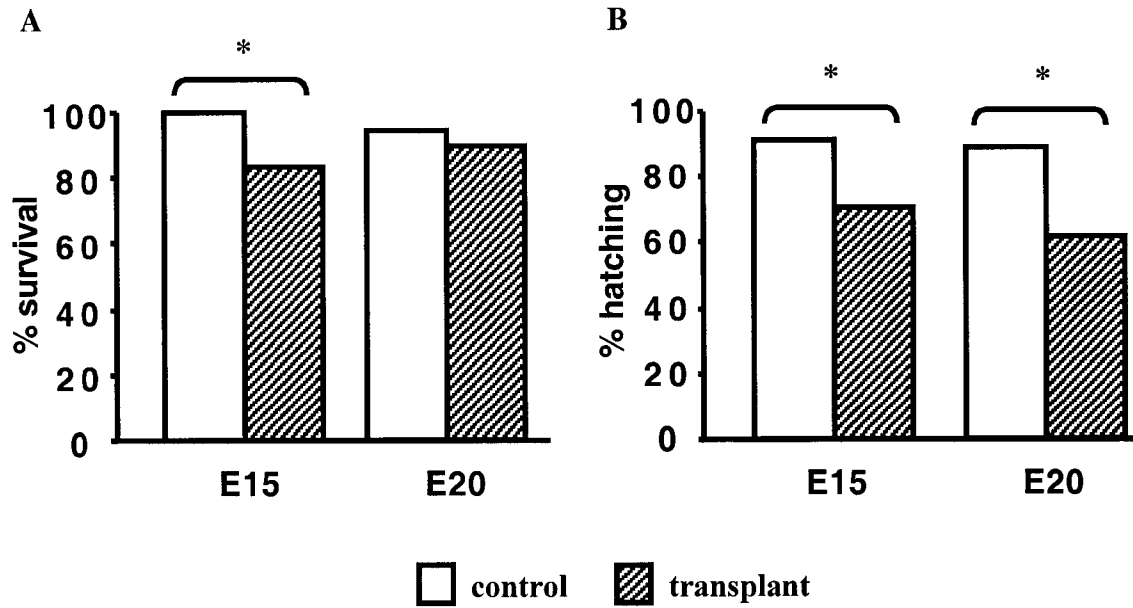
—◆— control    ···■··· transplant    -▲- ex ovo



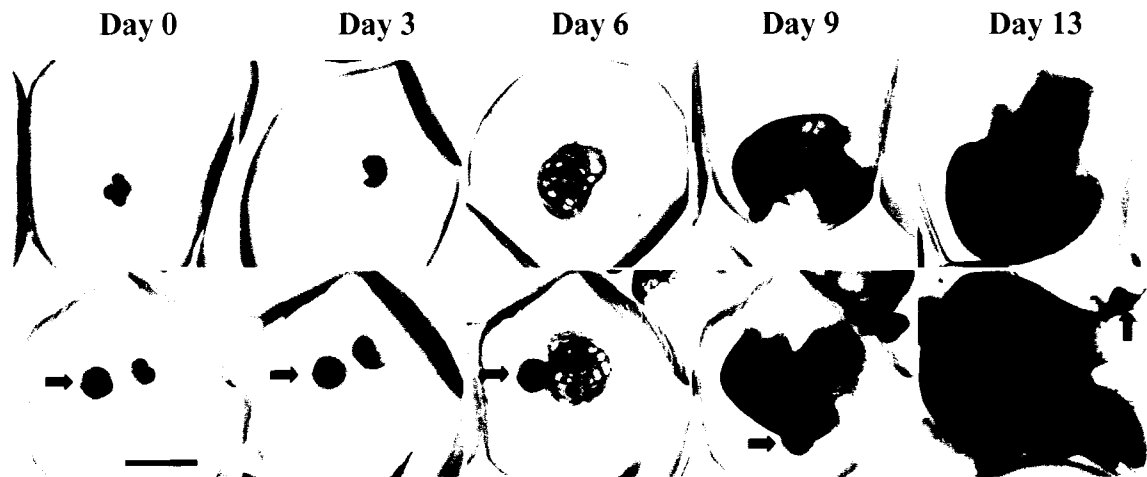
**Figure 5.** Effect of pH on growth and development of *ex ovo* cultured embryos.

**A.** Embryonic length before and after 3-day culture of stage E20 embryos. At each pH, there was a significant difference in the average embryonic length between Day 0 and Day 3 (t-test,  $p < 0.05$ ,  $n = 44 - 66$  embryos in 3 replicates). Whereas there were no differences in embryonic length at different pH at Day 0, there were significant differences in embryonic length at Day 3 (asterisks:  $p < 0.05$ , t-test). **B.** Percent of embryos expressing specific features of control stage E30 embryos, including larval kidney shape, muscle contraction and shell deposition, at different pHs. The percentage expression of each feature was significantly different at these three pHs (G-test,  $p < 0.01$ ,  $n = 51 - 68$  embryos from 3 replicates).

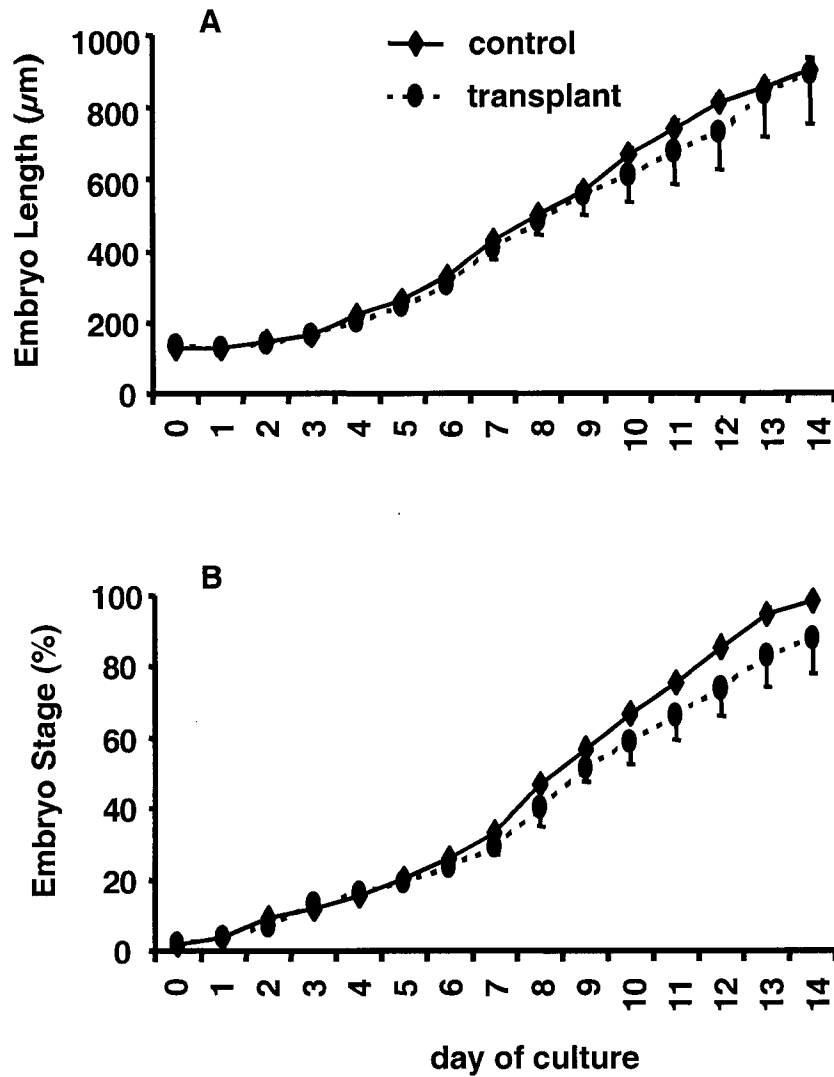




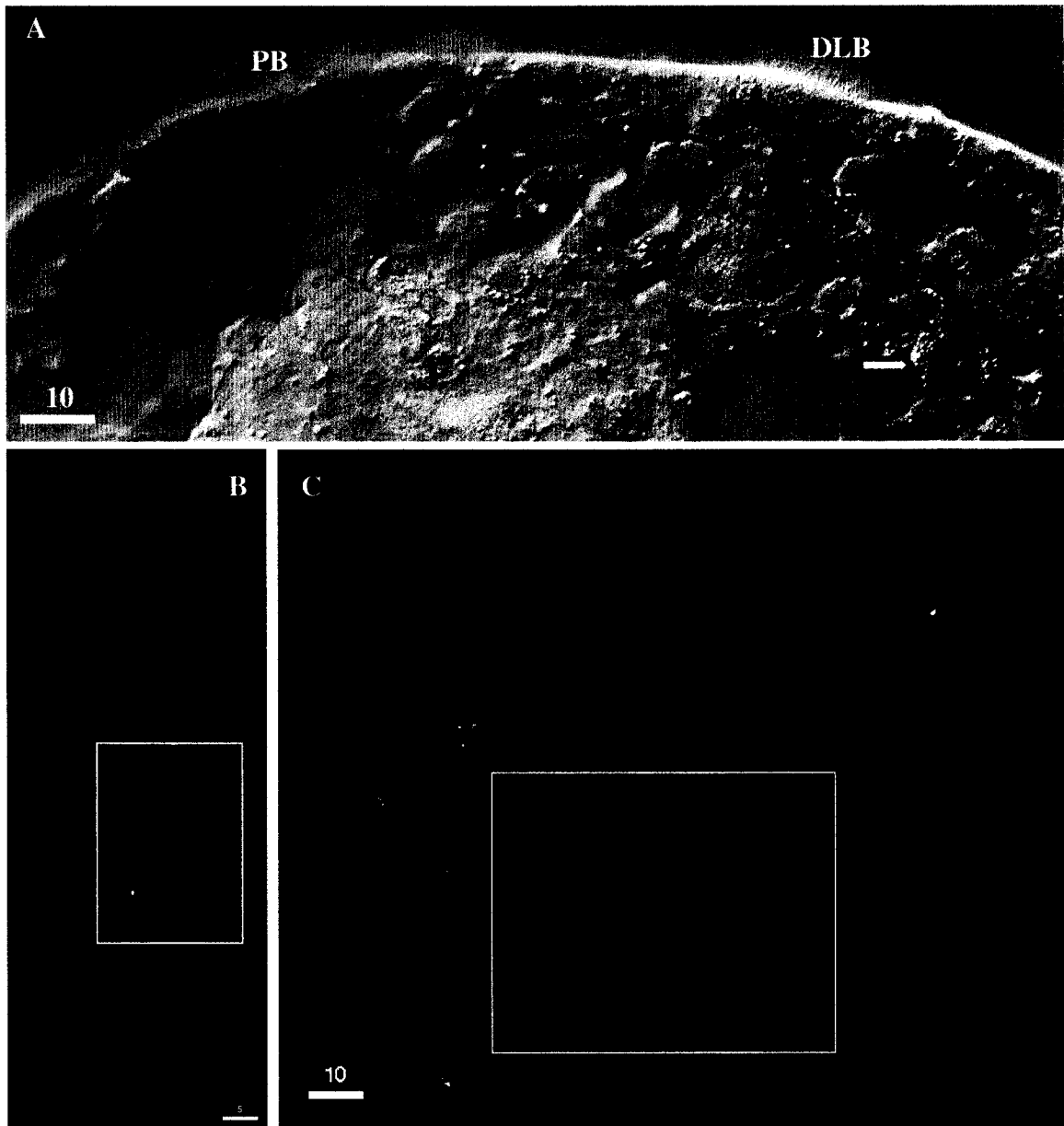
**Figure 6.** Survival and hatching rates of transplanted and control embryos at 23 °C. The survival rate was calculated as the total number of embryos alive at day 8 as a percentage of total embryos at the beginning of the experiment. The hatching rate was calculated as the total number of embryos hatched as a percentage of the total embryos alive at day 8. **A.** Survival rate of control and transplanted stage E15 and E20 embryos.  $n = 23$  (control E15), 30 (transplant E15), 19 (control E20) and 30 (transplant E20). Asterisk:  $p < 0.05$ , chi square test. **B.** Hatching rate of control and transplanted stage E15 and E20 embryos.  $n = 23$  (control E15), 28 (transplant E15), 18 (control E20) and 29 (transplant E20). Asterisks:  $p < 0.05$ , chi square test.



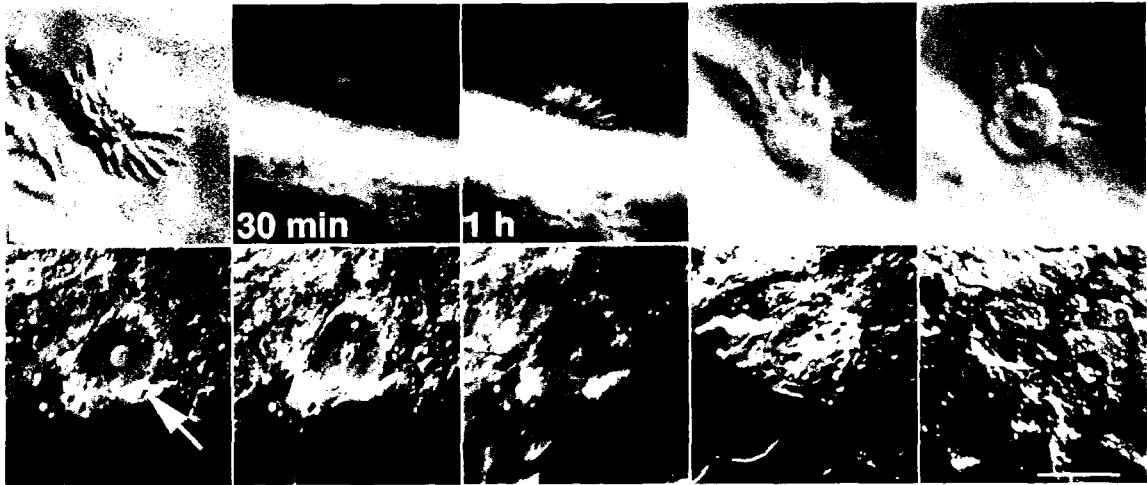
**Figure 7.** Morphological development of control and transplanted stage E1-E2 (2-4 cell stages) embryos at 20.5 °C. A control embryo developed from the 4-cell stage to hatching in 13 days (**Top panel**). Similarly, a transplanted embryo developed from the 2-cell stage to hatching at the same rate (**Bottom panel**). The transplanted embryo was isolated from the same egg mass as the control embryo. The transplanted embryos lagged behind the control embryo by 1 cleavage division at Day 0 because of the isolation and the 1 h incubation in saline prior to transplantation. The host embryo (**arrows**) in the transplantation group was killed by heat shock (45 °C, 25 min) prior to transplantation. Scale bar: 300  $\mu$ m.



**Figure 8.** Growth (A) and development (B) of control and transplanted stage E1-E2 (2-8 cell stage) embryos at 20.5 °C. No difference in growth or development was found between control and transplanted embryos ( $p > 0.05$  on each day,  $n = 22$  and 4 for control and transplanted embryos, respectively).

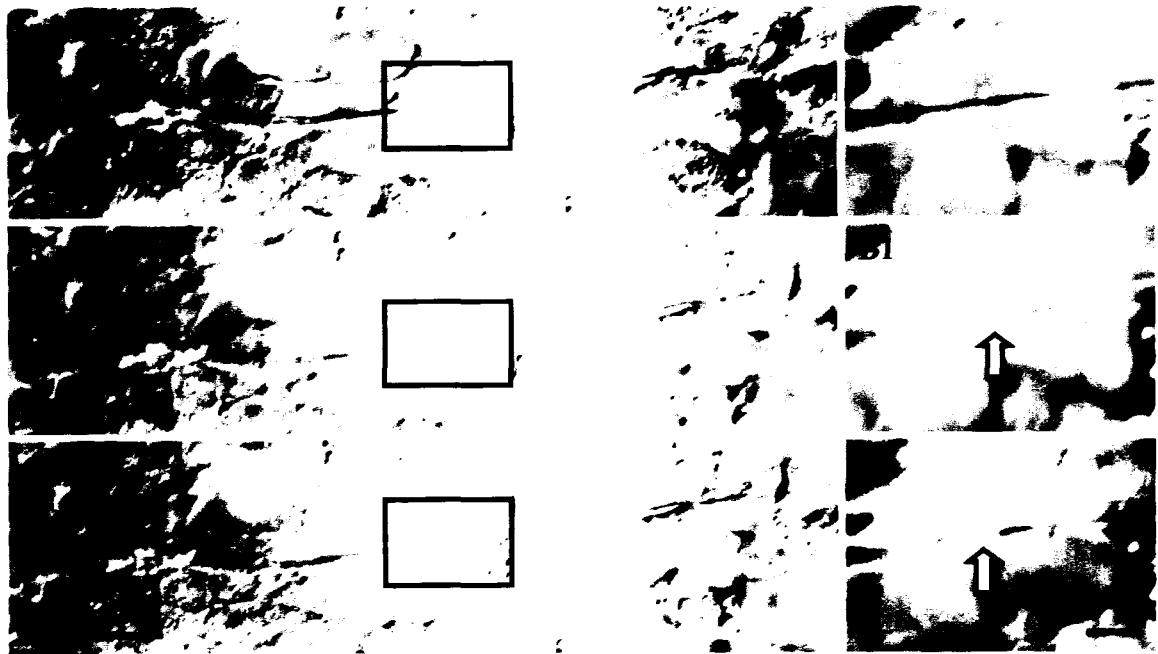


**Figure 9.** Anatomical evidence for the motor function of ENC1. **A:** DIC image indicates that ENC1 (**arrow**) projects its primary neurite towards the dorsolateral ciliary band (**DLB**) and the pedal ciliary band (**PB**). **B:** Serotonin immunohistochemistry combined with laser confocal imaging reveals that numerous neurite branches occur at the area where the **DLB** locate (**rectangle**). **C:** Similarly, extensive neurite branching occurs at the **PB** area (**rectangle**). Numbers on the scale bars are in  $\mu\text{m}$ .

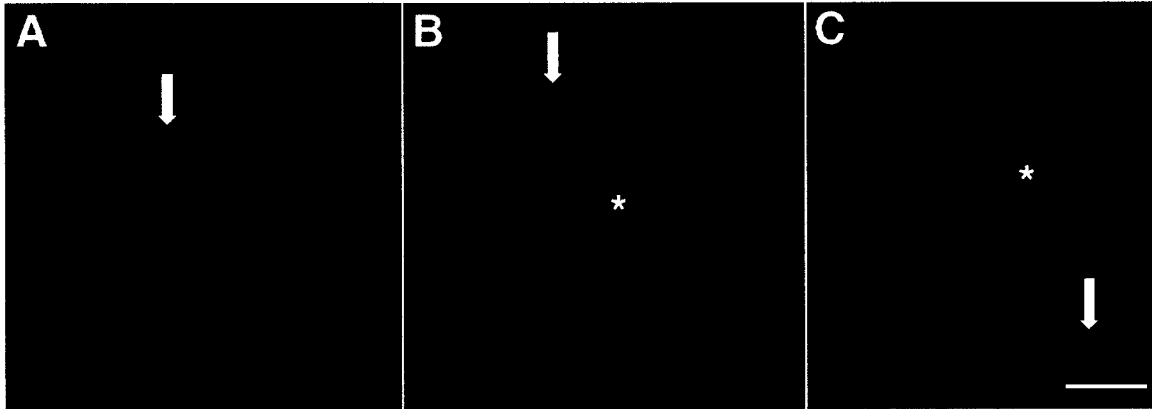


**Figure 10.** Morphological changes in ENC1 after laser treatment. **A.** Laser treatment of ENC1 nucleus caused the dendritic knob to detach from the embryonic surface. Furthermore, the stiff non-motile cilia of the dendritic knob usually became flaccid after laser treatment. **B.** Before treatment, ENC1 (arrow indicates the cell boundary) had a large nucleus and prominent nucleolus. Laser microbeams were focused onto the nucleolus and perinucleolar region. Immediately after laser treatment, nucleolar scars were observed (30 min). Subsequent morphological changes included swelling and blebbing of the cell, an obscured cell boundary, and nearly complete disruption by 6 hours. Scale bars: **A** = 4  $\mu\text{m}$ , **B** = 15  $\mu\text{m}$ .

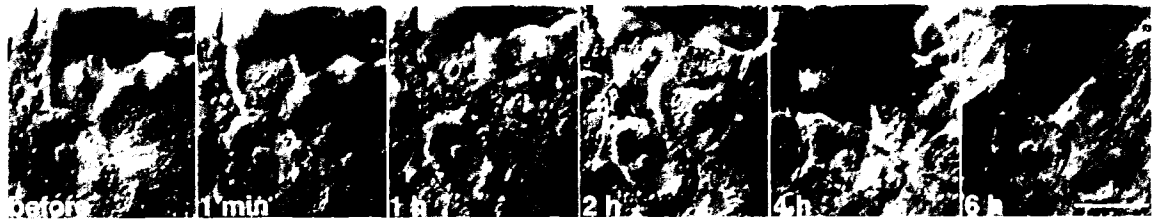




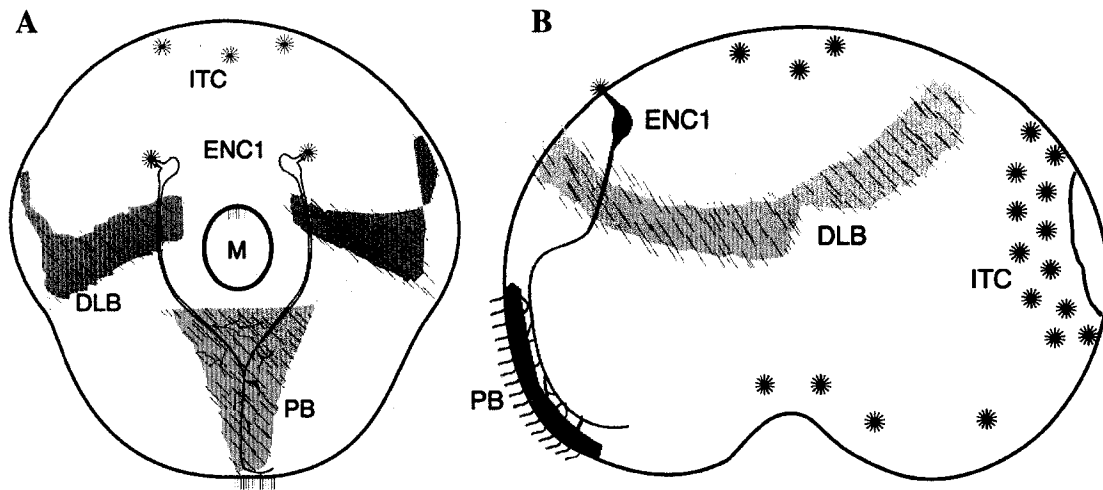
**Figure 11.** Laser ablation of ENC1's primary neurite. The morphology of ENC1's soma (the prominent cell at left upper corners) and its primary neurite before (**A**), during (**B**) and after (**C**) laser treatment (**arrows**). **A1, B1, C1:** Enlarged view of the rectangle areas in **A, B, C**, respectively. The morphology of ENC1's soma was not affected by the laser treatment in 72 h. Scale bars: 15  $\mu\text{m}$ .



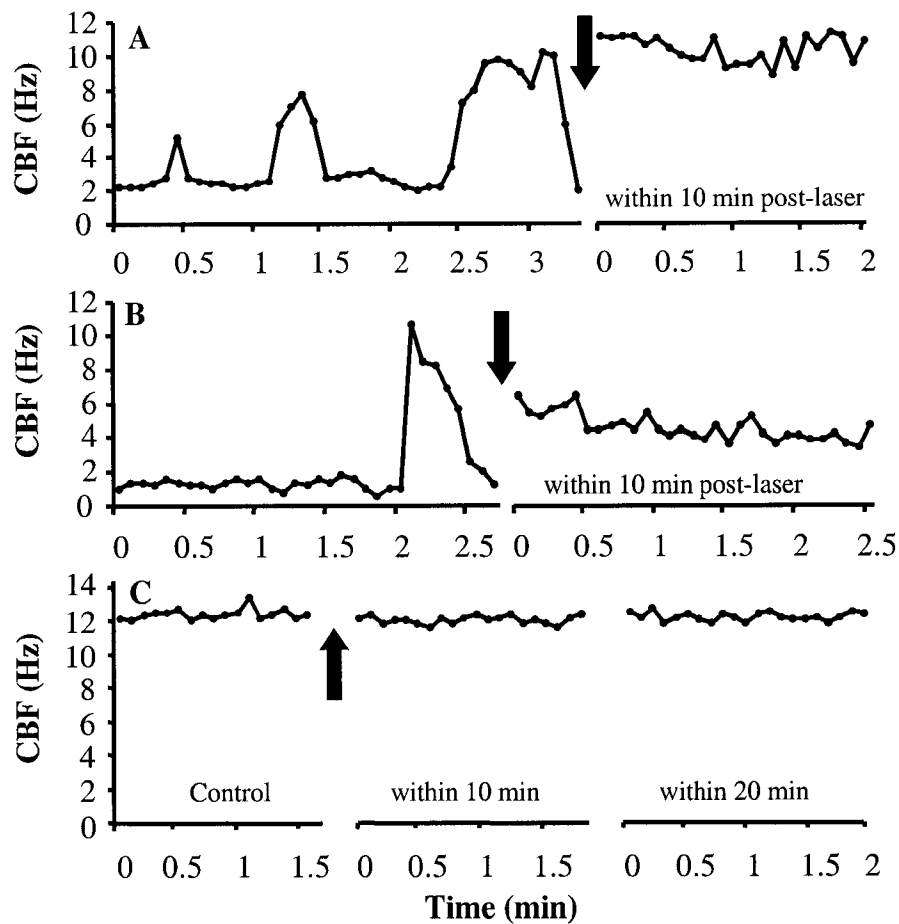
**Figure 12.** Loss of serotonin immunoreactivity in ENC1 6-24 h after laser ablation. **A.** In normal embryos, ENC1s are located dorsolateral to the mouth and send their primary neurite ventrally to the pedal ciliary band, where branching occurs. **B.** Single ENC1 laser treatment caused loss of 5-HT immunoreactivity in the soma and primary neurite of the treated cell. **C.** Serotonin immunoreactivity totally disappeared from both ENC1s after bilateral treatment. Widely distributed acellular serotonin immunoreactivity (**asterisk**) normally appeared after unilateral or bilateral laser treatment of ENC1. Arrows indicate the location of the embryonic mouth. Scale bars: 40  $\mu$ m.



**Figure 13.** Laser treatment causes cell-specific elimination. An adjacent cell (arrowhead) to ENC1 (**arrow**) was laser-treated and the morphology of ENC1 was monitored subsequently. The laser-treated neighboring cell underwent cell death and was eliminated in 6 h. In contrast, the morphology of ENC1 appeared intact during the same period. Serotonin immunohistochemistry indicated that ENC1 expressed serotonin immunoreactivity normally after neighbor cell ablation (data not shown). Scale bar: 15  $\mu$ m.

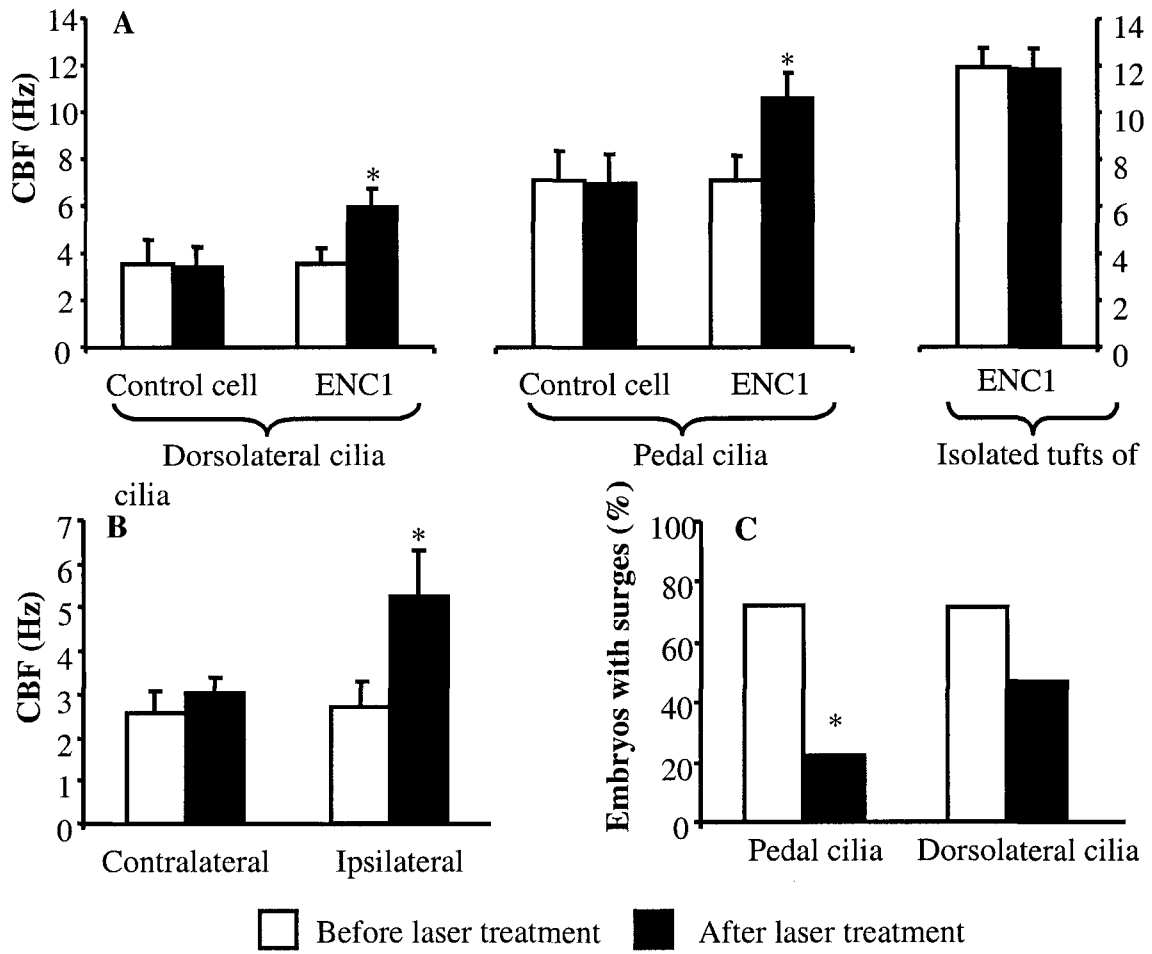


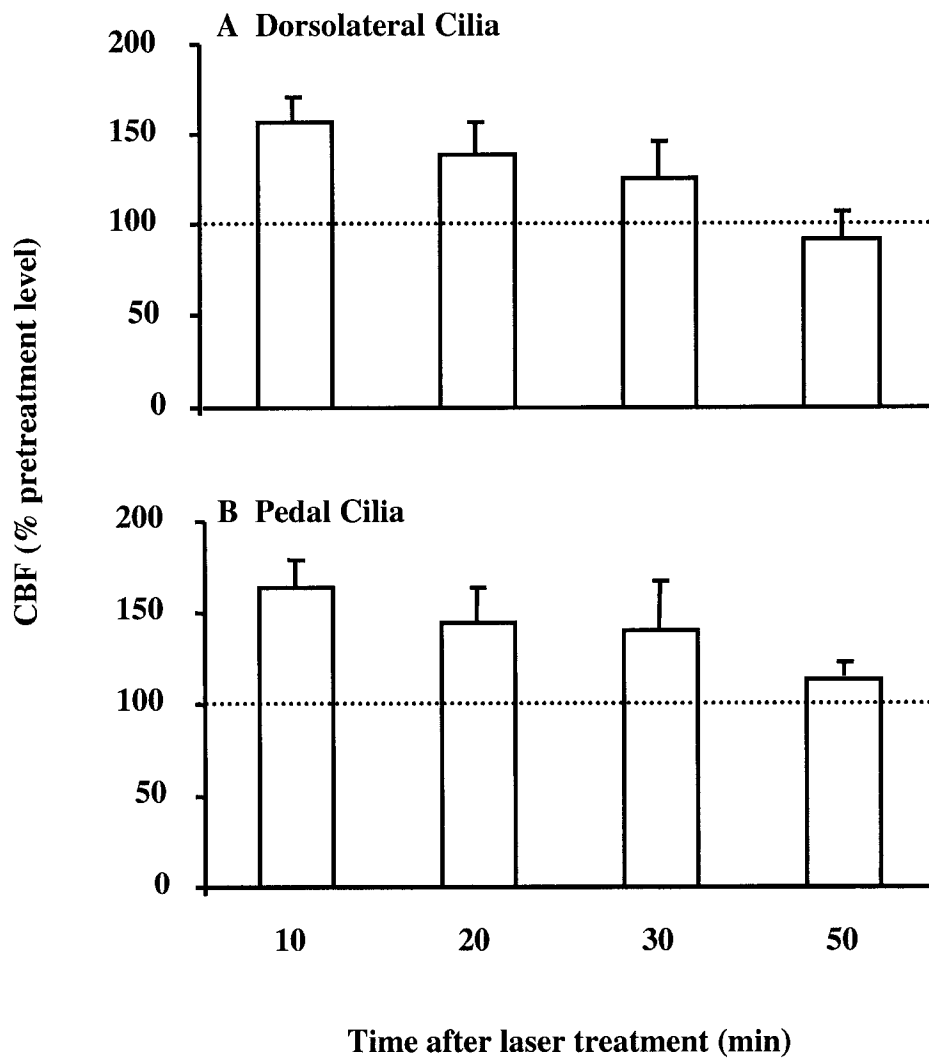
**Figure 14.** Anatomical relationship between ENC1 and the major ciliary bands of *Helisoma* embryos. **A.** Diagram showing the anterior view of a stage E25 embryo. Three distinct ciliary bands, the left and right dorsolateral bands (**DLB**) and pedal band (**PB**), generate the embryonic rotational behavior. The pair of ENC1s developed coincidentally with these three ciliary bands (Koss et al., 2002). The primary neurite of each ENC1 passes immediately below the ipsilateral dorsolateral band and proceeds ventrally to the pedal ciliary band. M; Mouth. **B.** Lateral view of stage E30 embryo. The primary neurite of ENC1 passes below the dorsolateral ciliary band and branches at the target pedal ciliated cells. Isolated tufts of cilia (**ITC**), distributed mainly along the shell gland and sparsely over other areas of the embryonic surface, are not anatomically associated with ENC1.



**Figure 15.** Temporal profiles of ciliary beat frequency (CBF) in different groups of cilia before and after unilateral laser stimulation of ENC1. Before laser treatment of ENC1, the pedal (A) and dorsolateral (B) cilia beat at a slow basal rate with periodic beat surges. Laser treatment of ENC1 changed this beat pattern to a continuously fast beat rate without beat surges. Isolated tufts of cilia (C) maintained a constant rapid CBF, with no apparent surges, both before and after laser treatment. Each point represents the average CBF in a 5-sec interval. **Arrows** indicate application of laser treatment to ENC1.

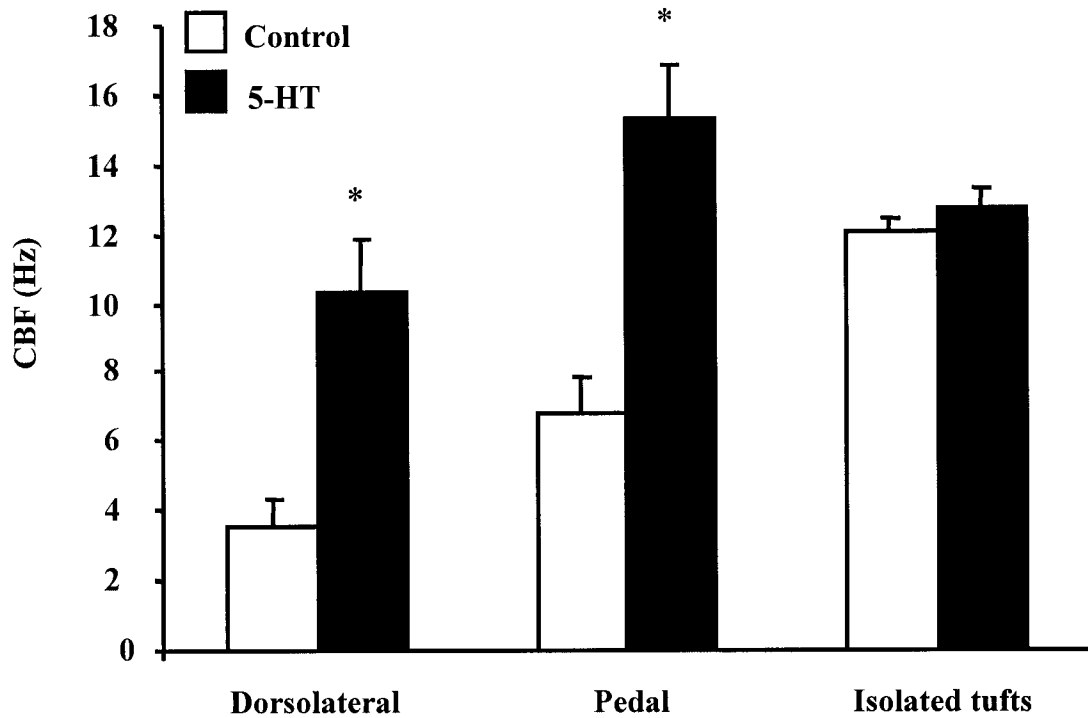
**Figure 16.** Effects of ENC1 laser stimulation on ciliary activity. **A.** The ciliary beat frequency (CBF) of dorsolateral and pedal cilia increased significantly (paired t-test,  $p < 0.01$ ,  $n = 14$  for dorsolateral;  $n = 15$  for pedal) after unilateral laser-treatment of ENC1. In contrast, laser treatment of an adjacent control cell didn't affect the CBF of dorsolateral ( $n = 7$ ) and pedal ( $n = 11$ ) cilia. Laser treatment of ENC1 had no effect on the CBF of isolated tufts of cilia ( $n = 9$ ,  $p > 0.05$ ). The basal CBF among different cilia were different (ANOVA,  $p < 0.01$ ). The CBF represented averages from 5-sec measurements over 2-min periods. **B.** Unilateral laser-treatment of ENC1 caused an increased CBF in the ipsilateral (paired t-test,  $n = 14$ ,  $p < 0.01$ ), but not the contralateral dorsolateral cilia (paired t-test  $n = 4$ ,  $p > 0.05$ ). **C.** Effect of ENC1 laser treatment on the ciliary beat pattern. Before laser treatment, more than 70% of the embryos exhibited beat surges in pedal cilia ( $n = 18$ ) and dorsolateral cilia ( $n = 28$ ) in a 2-min interval. After laser treatment, the percentage of embryos exhibiting beat surges in pedal and dorsolateral cilia decreased to 22% ( $n = 9$ , Chi square test  $p = 0.01$ ) and 47% ( $n = 17$ , Chi square test  $p = 0.10$ ), respectively.



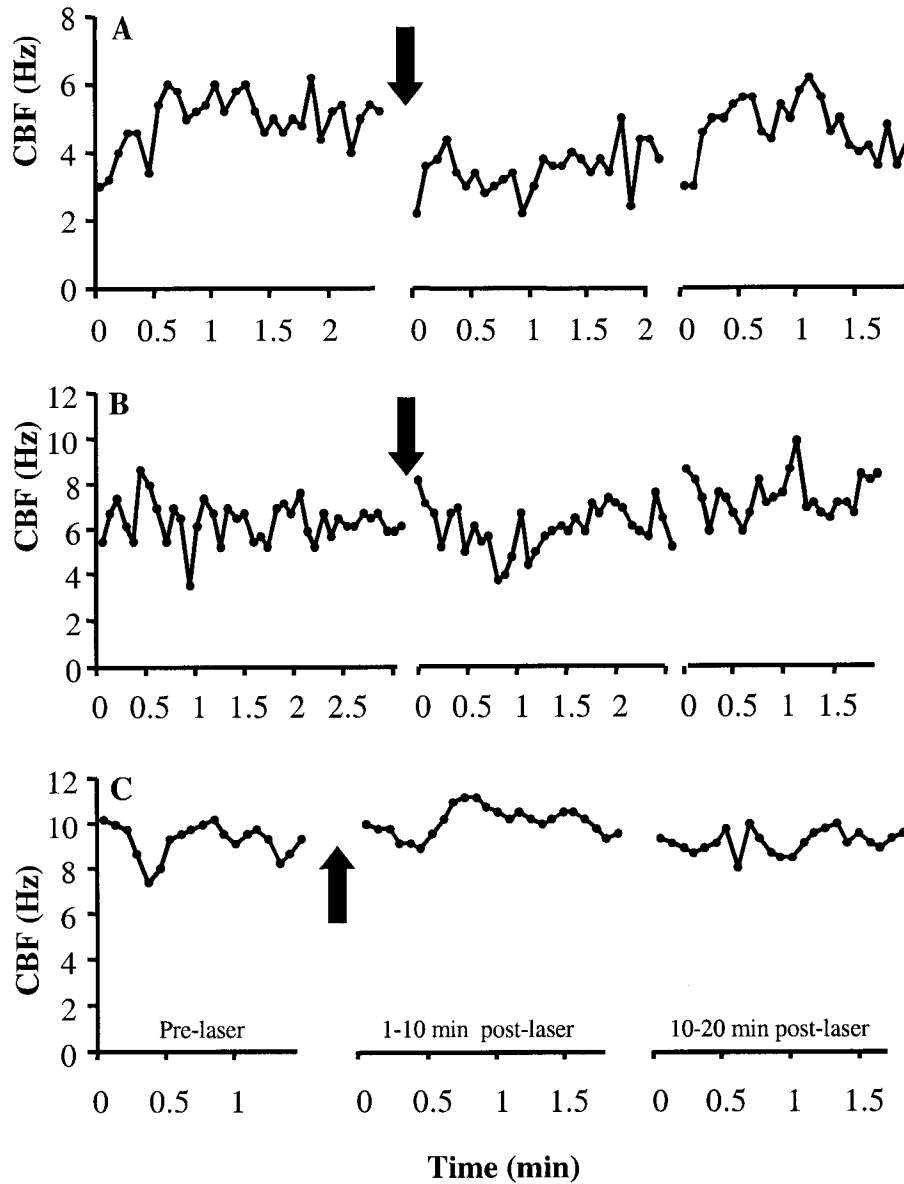


**Figure 17.** Laser treatment of ENC1 causes transient increases in ciliary beat frequency (CBF) of dorsolateral (A) and pedal (B) cilia. The bars represent the average CBF at different time intervals normalized to the pre-treatment level (indicated by the dotted lines). CBF returned to the pre-treatment level by 50 min post treatment. A: n = 3-19 embryos; B: n = 2-14 embryos.

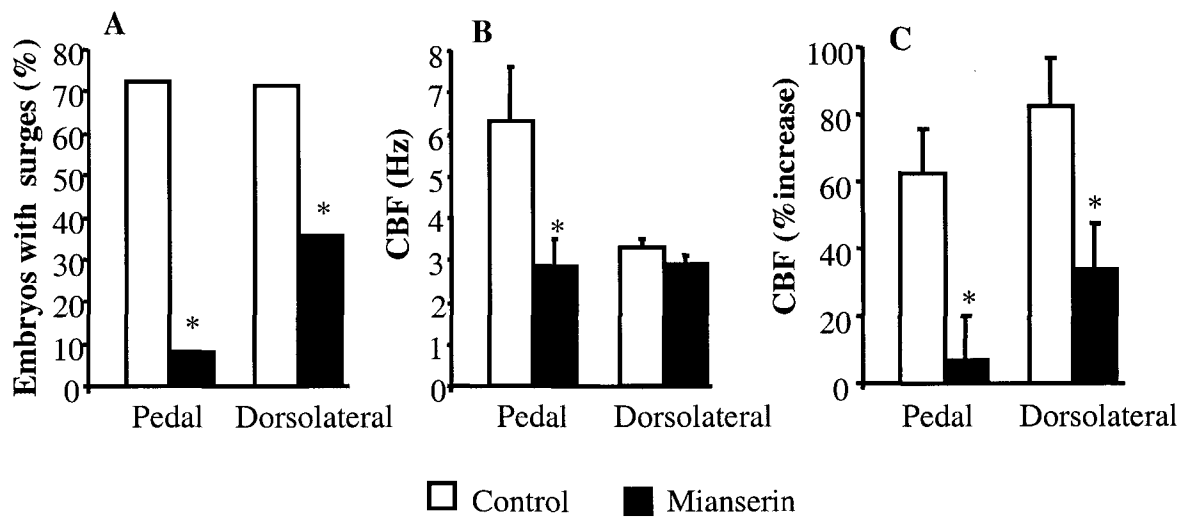




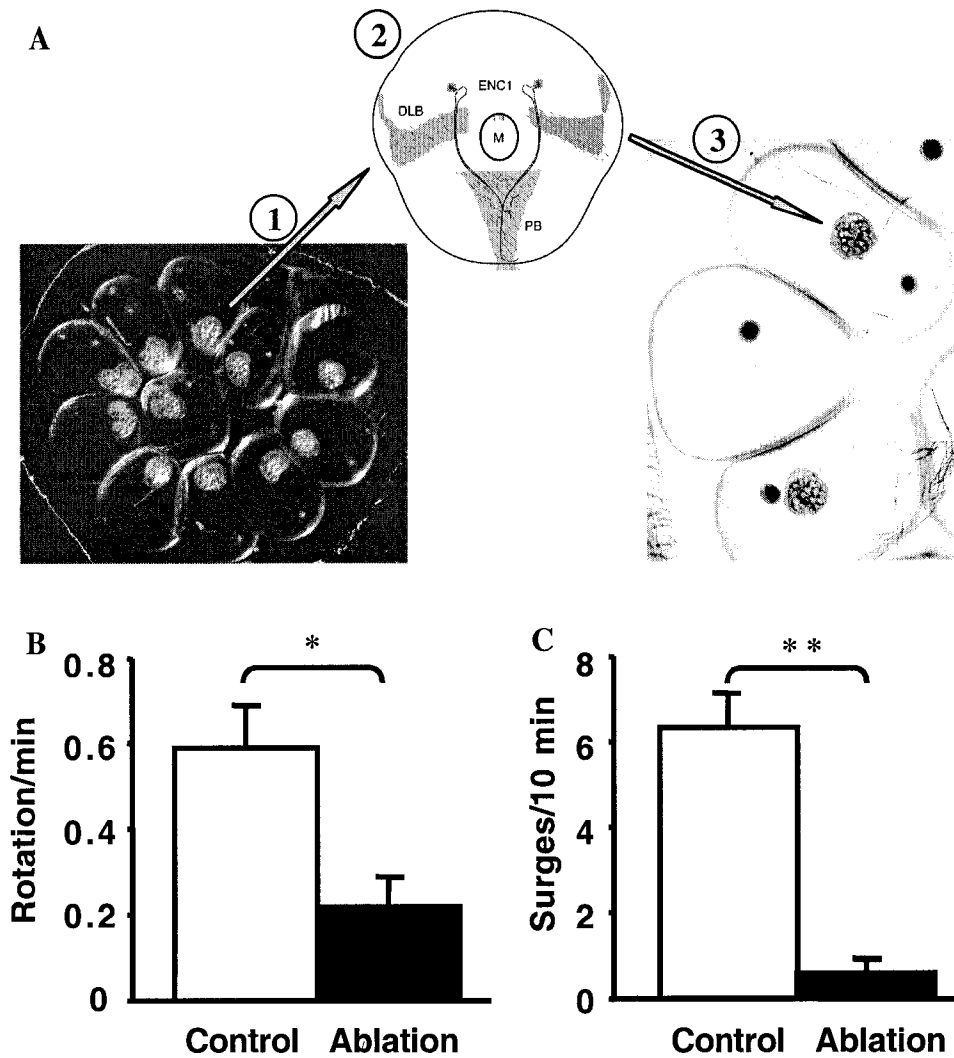
**Figure 18.** Effect of serotonin on beat frequency of different groups of cilia. Serotonin (50  $\mu$ M) significantly increased the CBF of dorsolateral and pedal cilia, by 189.1% and 117.8%, respectively. In contrast, the CBF of isolated tufts of cilia was not affected by serotonin. Asterisks denote significant increase over control level (ANOVA  $p < 0.01$ ;  $n = 15-28$  embryos in controls;  $n = 3-15$  embryos in serotonin treatment).



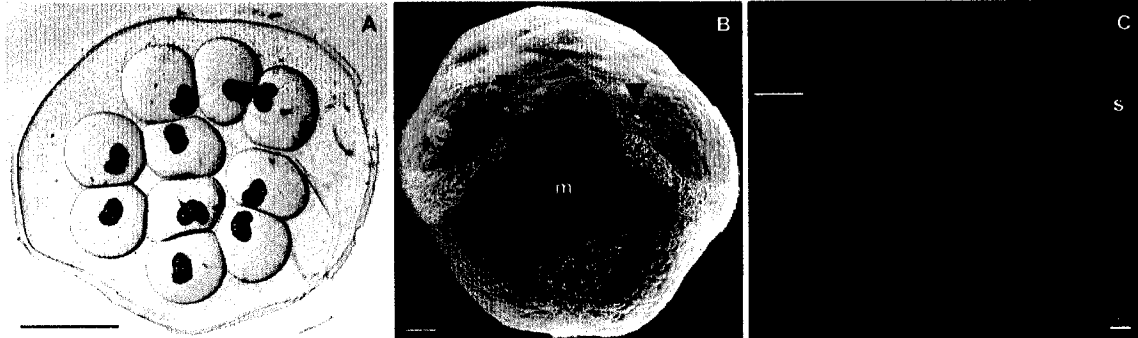
**Figure 19.** Effect of ENC1 laser stimulation on the temporal pattern of CBF in the presence of mianserin (50  $\mu$ M). In pedal (A) and dorsolateral (B) cilia, the ciliary beat surges usually seen before laser treatment, and the increase in CBF normally seen after laser treatment were both absent in the presence of mianserin. The isolated tufts of cilia (C) were not obviously affected by mianserin or laser treatment (as compared to Fig. 15C). Arrows indicated application of laser treatment to ENC1.



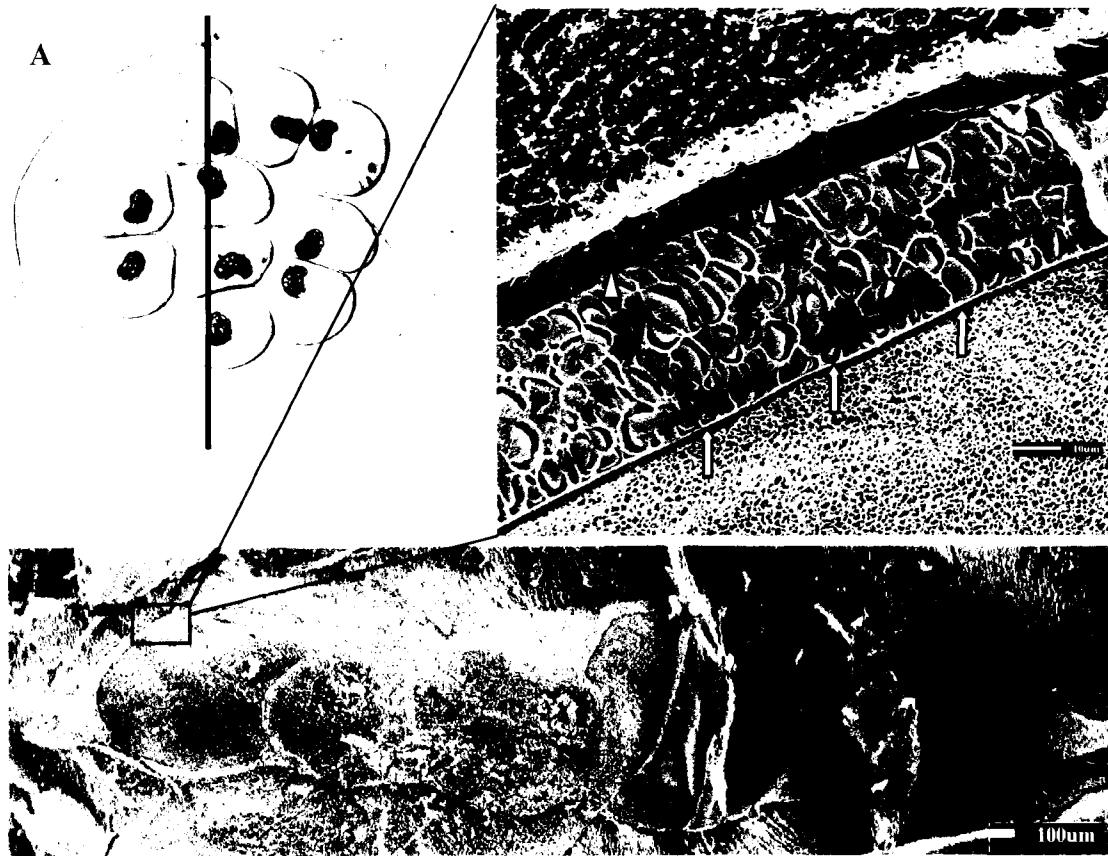
**Figure 20.** Effect of mianserin (50  $\mu$ M) on basal and ENC1 laser stimulation-induced ciliary activity. **A.** Percent of embryos exhibiting beat surges in 2-min periods. In control solution (saline), most of the embryos exhibited beat surges in pedal (71.4%,  $n = 18$ ) and dorsolateral (72.2%,  $n = 28$ ) cilia. After incubating the embryos in mianserin, however, only 8.3% ( $n = 12$ , \*: Chi-square test,  $p < 0.01$ ) and 35.7% ( $n = 14$ , \*: Chi-square test,  $p < 0.05$ ) of the embryos exhibited beat surges in pedal and dorsolateral cilia, respectively. **B.** Effect of mianserin on ciliary beat frequency of pedal and dorsolateral cilia. The CBF decreased significantly after mianserin treatment in pedal cilia (\*: ANOVA,  $p < 0.01$ ,  $n = 36$  embryos in control,  $n = 8$  in mianserin), but not in dorsolateral cilia (ANOVA,  $p > 0.05$ ,  $n = 33$  embryos in control,  $n = 12$  in mianserin). **C.** Mianserin reduced the cilioexcitatory response to laser stimulation of ENC1. Shown is the percent increase of CBF after unilateral ENC1 laser treatment in saline and in the presence of mianserin. After laser stimulation, the CBF of pedal and dorsolateral cilia increased by  $62.6 \pm 12.9\%$  ( $n = 15$ ) and  $82.8 \pm 14.3\%$  ( $n = 14$ ), respectively, in saline. These percentages decreased to  $6.9 \pm 13.4\%$  ( $n = 3$ ) and  $33.7 \pm 13.7\%$  ( $n = 4$ ) respectively, in the presence of mianserin (\* t-test,  $p < 0.05$  for both pedal and dorsolateral cilia).



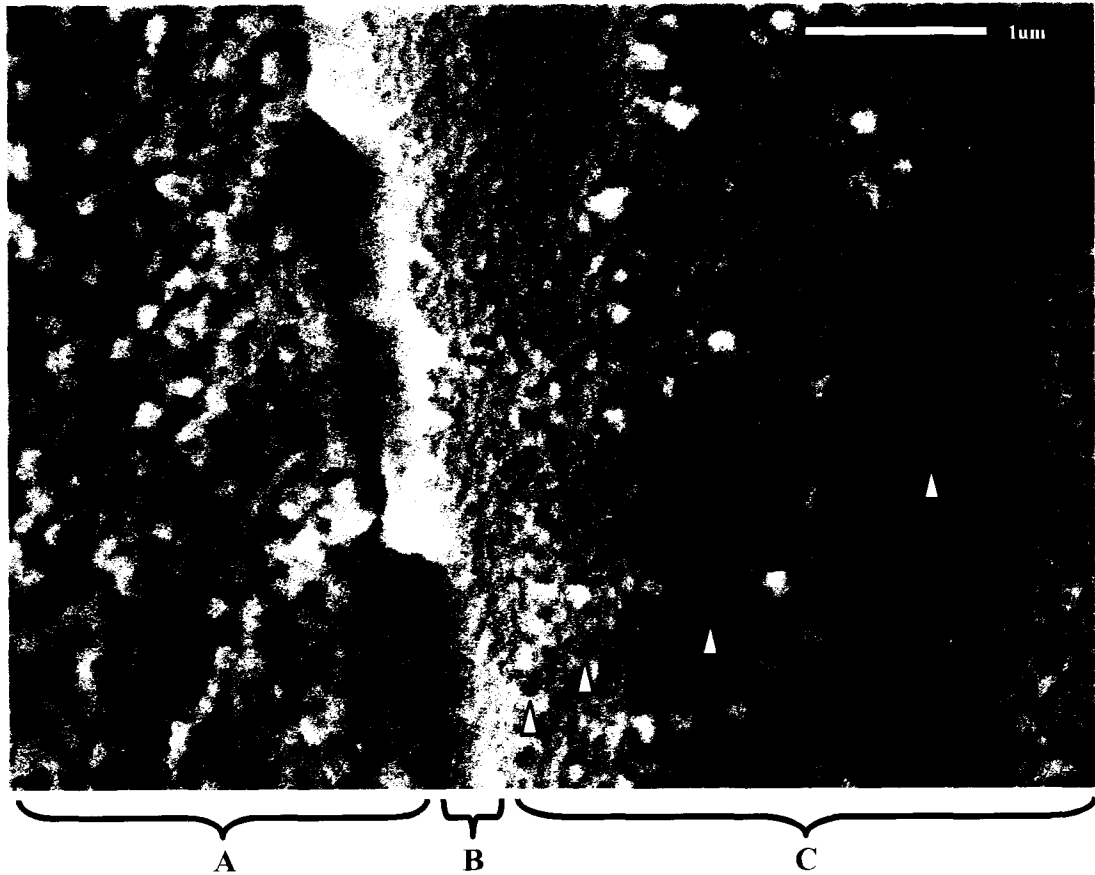
**Figure 21.** Bilateral laser ablation of ENC1s provides direct evidence for the cilioexcitatory function of these cells. **A.** Diagram showing the experimental design. Embryos were isolated from egg capsules ① and the ENC1s or control cells were ablated with laser beams under a compound microscope ②. The laser-operated embryos were transplanted into host egg capsules that contain much younger embryos ③. The embryonic rotational behavior was subsequently examined after overnight recovery. **DLB:** dorsolateral ciliary band; **PB:** pedal ciliary band. **B.** The average rate of rotation was reduced in embryos with both ENC1s ablated (\*: t-test,  $p < 0.05$ ,  $n = 9$  and 7 for control and ENC1 ablated embryos, respectively). **C.** The occurrence of rotational surges was almost abolished in embryos with both ENC1s ablated (\*\*: t-test,  $p < 0.01$ ,  $n = 11$  and 7 for control and ENC1 ablated embryos, respectively).



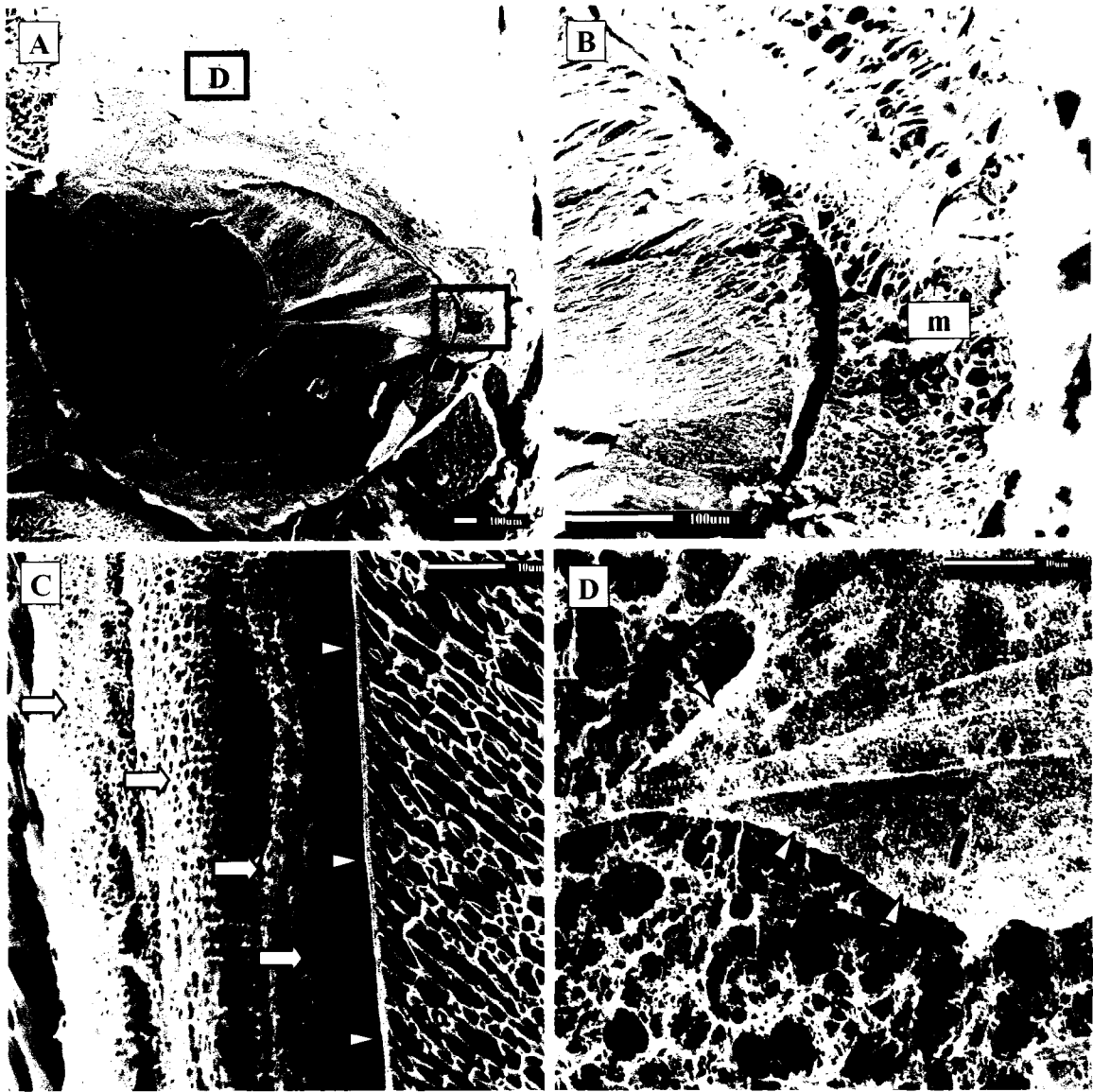
**Figure 22.** Structural components involved in embryonic rotation behavior. **A.** An egg mass containing stage E30 embryos. The embryos display a rotational behavior inside the egg capsules. Scale bar: 1 mm. **B.** Scanning Electron micrograph of a stage E25 embryo (anterior view). The bilateral dorsolateral ciliary bands (**dl**) and the pedal ciliary band (**p**) generate the rotational behavior (Diefenbach et al., 1991). The chemosensory dendritic knob of each ENC1 is indicated (arrow heads). **m**: mouth. Scale bar: 10  $\mu$ m. **C.** Left-anterior view of serotonin immunofluorescence in a stage E30 embryo showing a pair of serotonergic sensory-motor neurons (ENC1s) with extensive neurite branching in the region of the pedal cilia. Inset: the soma and the surface chemosensory structure of ENC1. **s**: shell. Scale bar: 10  $\mu$ m.



**Figure 23.** Diffusional barriers associated with encapsulation in *Helisoma* embryos. **A.** An egg mass was frozen in liquid nitrogen and fractured through a central plane (indicated by the vertical line). **B.** The cross section of the egg mass was ice-etched and viewed under SEM. Seen in this micrograph was five individual egg capsules encapsulated in the egg mass membrane. **C.** An enlarged view of the area indicated by the rectangle in **B**. Two major layers of membranes were seen, including the egg mass membrane (**arrow heads**) and the egg capsular membrane (**arrows**).

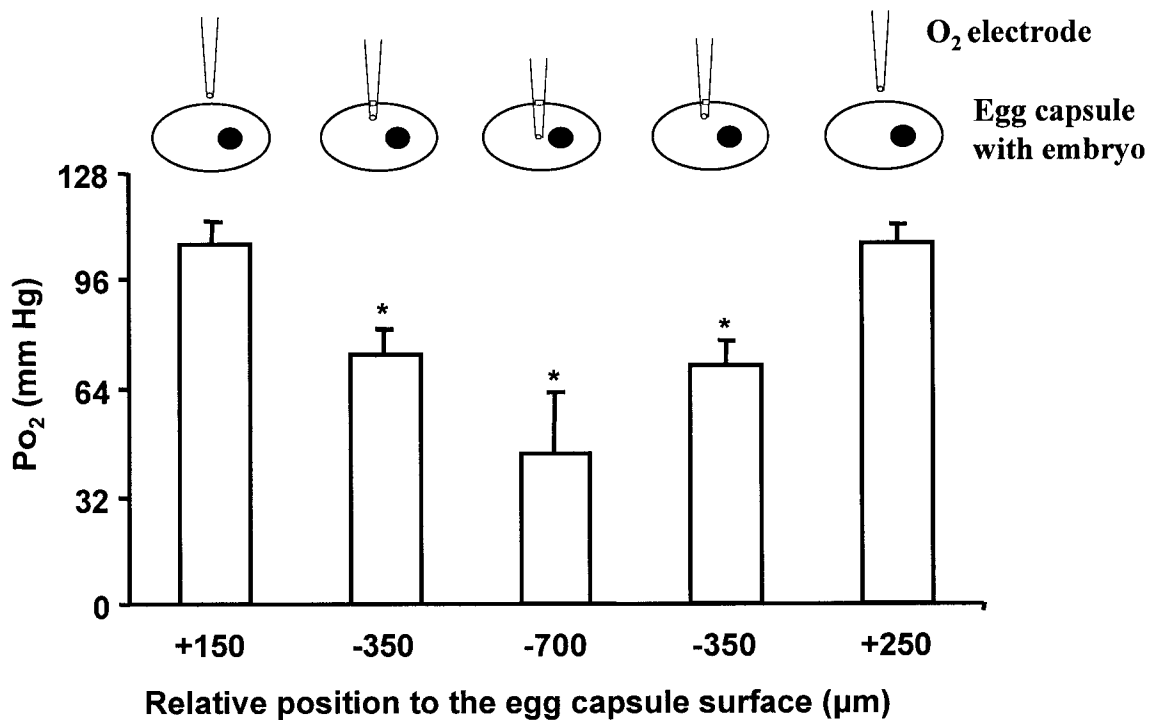


**Figure 24.** Ultrastructure of egg capsule membrane in *Helisoma*. **A.** Intracapsular material. **B.** Cross view of capsular membrane. **C.** The surface of the capsular membrane. Arrow heads indicate some of the pores on the egg capsule membrane.

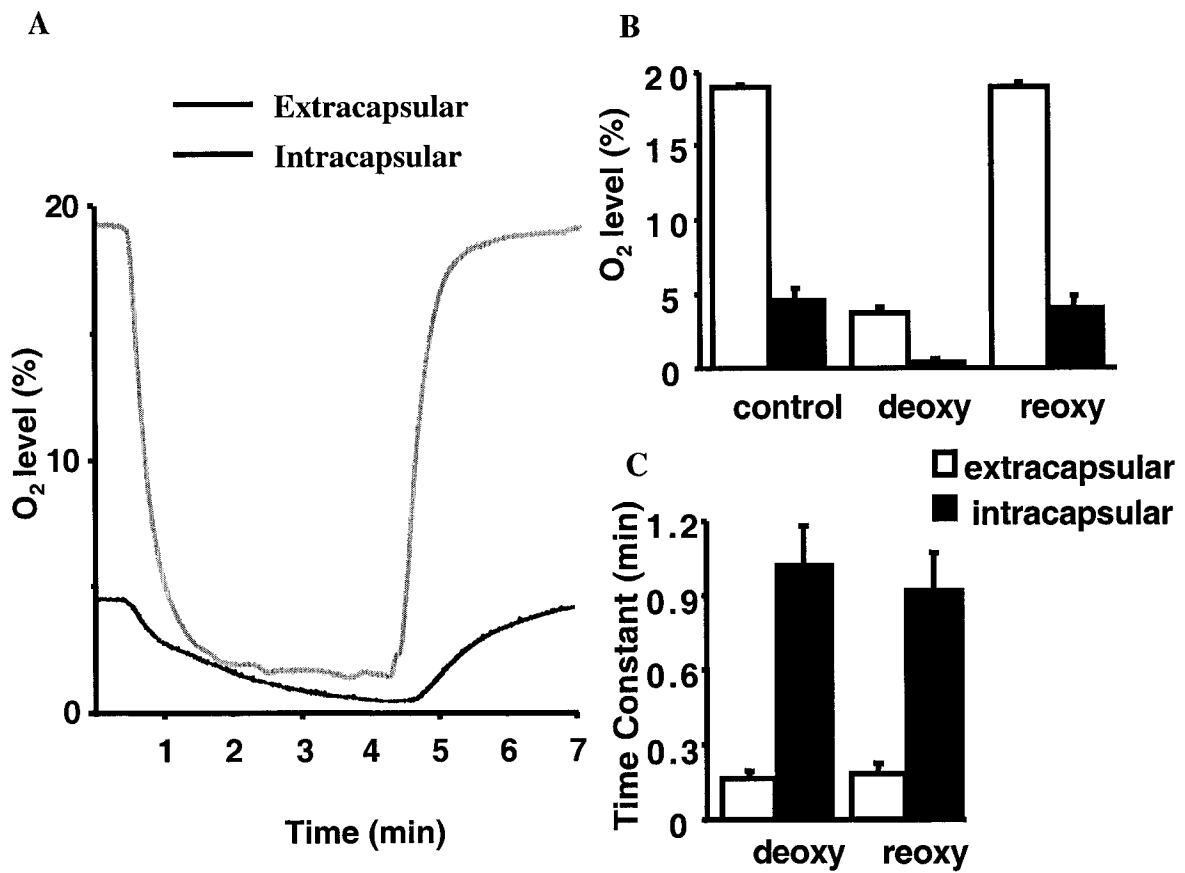


**Figure 25.** Ultrastructure of egg capsule membrane in *Lymnaea*. **A.** An egg mass was freeze-fractured through a cross section and view with SEM. Two egg capsules (indicated by asterisks) were seen in this plane. **B.** A cross section of the egg mass membrane (**m**). The porous nature of this membrane suggests that it is highly permeable to large molecules. **C.** Egg capsular membrane. This membrane was composed of multiple layers of outer spongy material (arrows) and a thin inner layer (arrow heads). **D.** Surface of the egg mass. A layer of mucus materials (arrow heads) was seen.

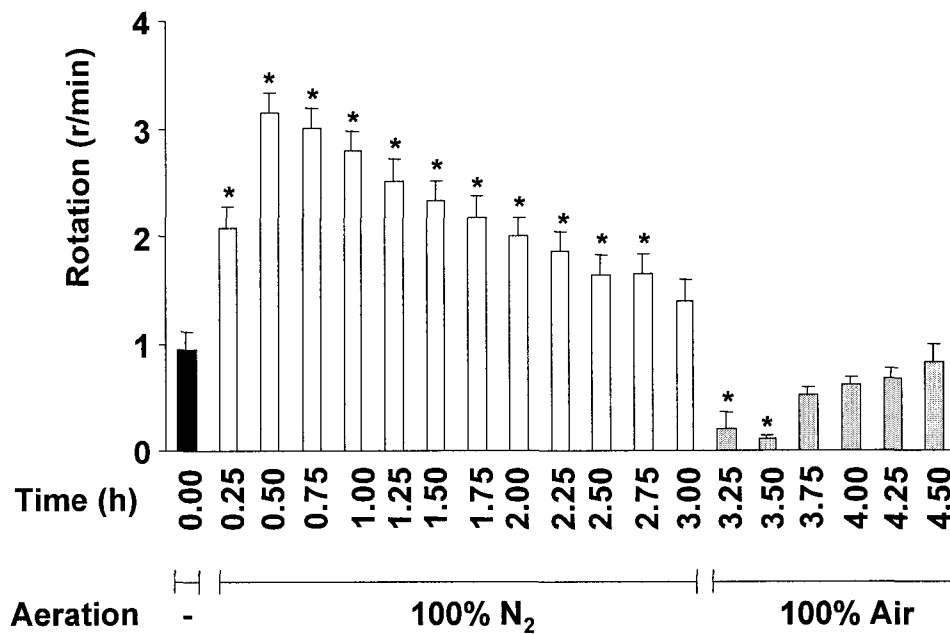




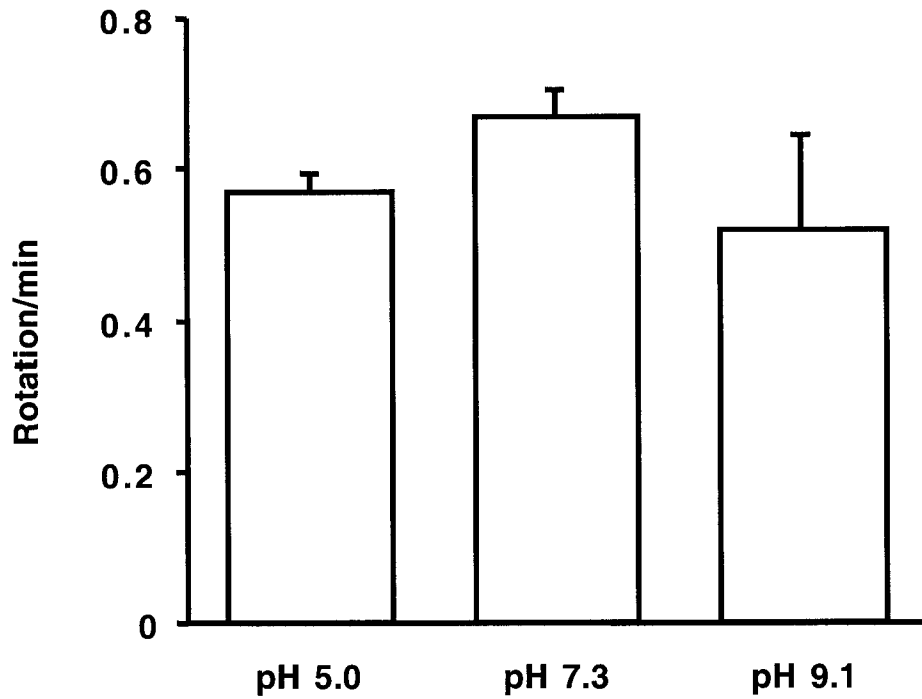
**Figure 26.**  $\text{O}_2$  gradient from surface to interior of egg mass. At 150  $\mu\text{m}$  above the egg capsule, the  $\text{Po}_2$  (mmHg) was equal to that in the bathing medium.  $\text{O}_2$  levels dropped steadily as the  $\text{O}_2$ -sensitive microelectrode was advanced into (-350  $\mu\text{m}$ ) and towards the center (-700  $\mu\text{m}$ ) of the egg capsule. The  $\text{O}_2$  levels recovered accordingly when the microelectrode was withdrawn from the center of the egg capsule (-350  $\mu\text{m}$  and 250  $\mu\text{m}$ ). The diagrams on the top of each bar indicate the microelectrode placements in relation to the egg capsule. Asterisks:  $p < 0.05$  (ANOVA followed by Fisher's PLSD) as compared to the  $\text{Po}_2$  value of the bathing medium;  $n = 7$  except for the -700 position, where  $n = 3$ .



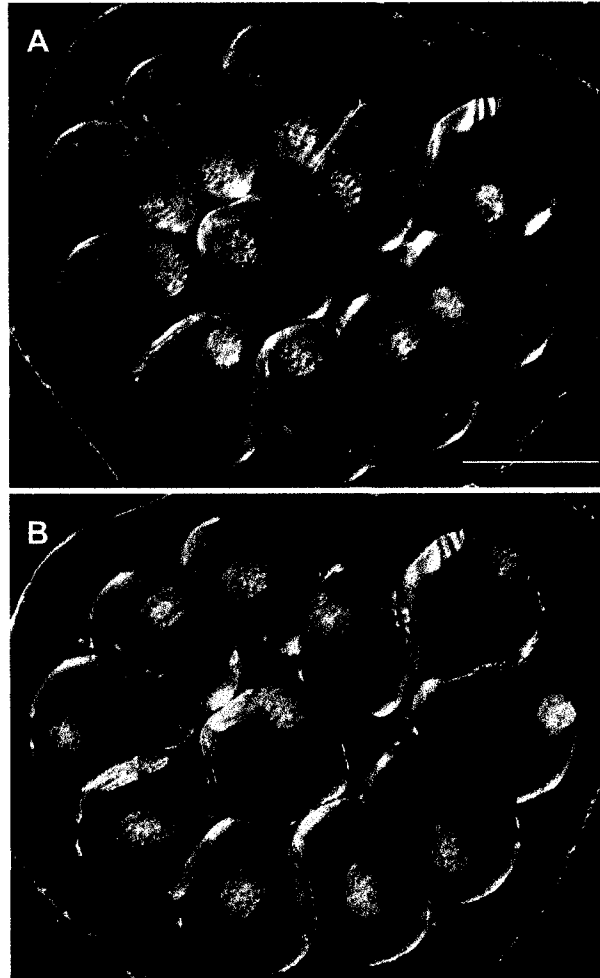
**Figure 27.** Experimental demonstration of the diffusional barrier associated with encapsulation. **A.** Example recordings of intracapsular O<sub>2</sub> level change (bottom trace) in response to extracapsular O<sub>2</sub> change (top trace). **B.** Levels of intra- and extracapsular O<sub>2</sub> levels under control, deoxygenation (**deoxy**) and reoxygenation (**reoxy**) treatments. **C.** The time constant of intracapsular and extracapsular O<sub>2</sub> changes under deoxygenation and reoxygenation treatment, respectively.



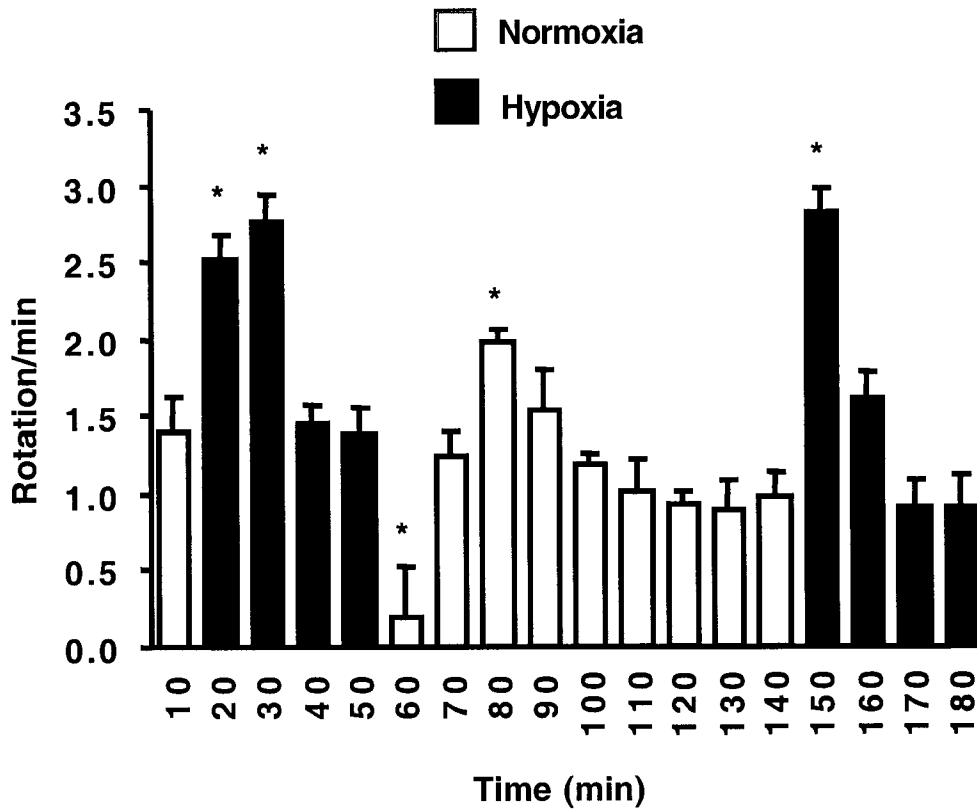
**Figure 28.** Hypoxia stimulates the embryonic rotational behavior in *Helisoma*. Removal of O<sub>2</sub> (100% N<sub>2</sub> aeration) caused a sustained elevation of rotation rate, whereas reintroduction of O<sub>2</sub> to normal levels (100% air aeration) caused a transient reduction of rotation rate below basal levels followed by a return to basal rotation. Asterisk, p < 0.05 (ANOVA followed by Fisher's PLSD) as compared to time point 0, n = 18. Each bar represents the average in a 6-min window prior to the time point shown.



**Figure 29.** Effect of extracellular pH on embryonic rotation. Egg masses were incubated in APW adjusted to pH 5.0, pH 7.3 and pH 9.1 with HCl or NaOH. The rate of embryonic rotation was examined after 10 min of incubation. There was no significant difference in the rate of rotation among these pH treatments (ANOVA,  $p > 0.05$ ,  $n = 18$  embryos (2 egg masses), 37 (5), 15 (3) for pH 5.0, pH 7.3 and pH 9.1, respectively).

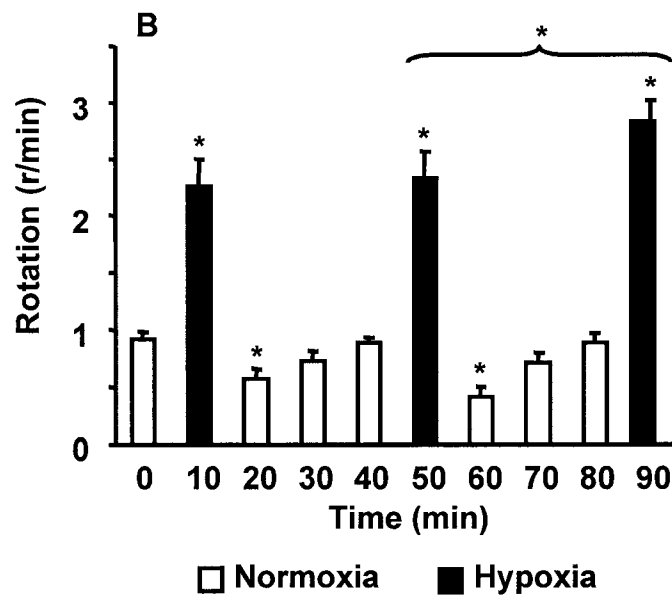
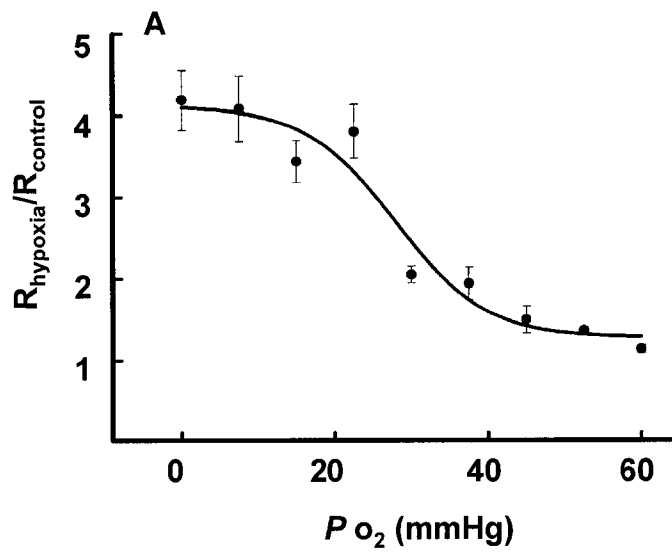


**Figure 30.** Translocation of embryos during hypoxia. **A.** Under normoxia, embryos inside individual egg capsules were most often found at positions near the center of the whole egg mass. **B.** During hypoxia, embryos displayed increased rate of rotation and migrated towards the periphery of the egg mass. Scale bar: 1 mm.



**Figure 31.** Hypoxia stimulates the embryonic rotational behavior in *Lymnaea*. Hypoxia (100% N<sub>2</sub> aeration) caused a transient elevation of rotational rate that lasted for 10 – 20 min, whereas restoration of normoxia with 100% air-saturated medium caused a transient reduction of rotational rate, followed by a return to basal rotation. Asterisk,  $p < 0.05$  (ANOVA followed by Fisher’s PLSD,  $n = 15$ ) as compared to time point 10. Each bar represents the average in a 6-min window prior to the time point shown.

**Figure 32.** The rotational response to hypoxia is  $\text{Po}_2$  dependent and reversible. **A.** The enhancement of embryonic rotation ( $R_{\text{hypoxia}}/R_{\text{control}}$ ) increased in a dose-dependent fashion with decreases in ambient  $\text{Po}_2$  (measured at 30 min time points of hypoxic treatments;  $n = 10 - 45$ ). The threshold, half-maximal and maximal responses occurred at 60, 28 and 13 mm Hg  $\text{Po}_2$ , respectively. **B.** The response to hypoxia was reversible and repeatable. Each repeated cycle of hypoxia ( $\text{Po}_2$ : 22 mmHg) and normoxia produced an elevation and transient depression of embryonic rotation, respectively. Asterisks,  $p < 0.05$  (ANOVA followed by Fisher's PLSD) as compared to time point 0,  $n = 19$ . The response at 90 min was significantly higher than the responses at 10 and 50 min ( $p < 0.05$ , paired t-test).





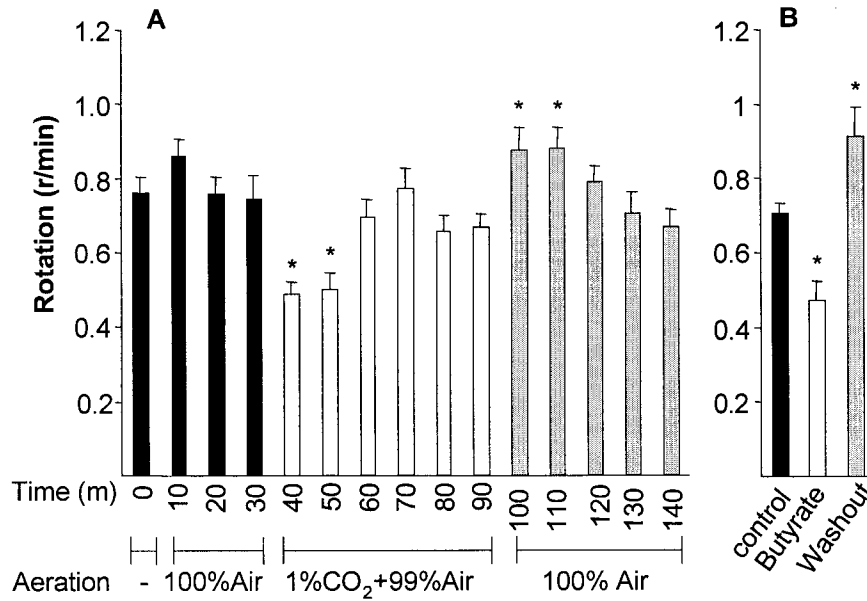


**Figure 33.** Effect of hypercapnia on embryonic rotational behavior. **A.** 1% CO<sub>2</sub> transiently decreased the rotation rate, whereas return to air transiently increased the rotation rate. Each bar represents the average in a 6 min window prior to the time point shown. **B.** Intracellular acidification of embryos with 20 mM sodium butyrate caused a similar change in rotation rate as 1% CO<sub>2</sub>. Each bar represents the average in a 6-min window 10 min after replacement of each solution. Asterisks,  $p < 0.05$  as compared to time point 0 or to control,  $n = 15$ ).

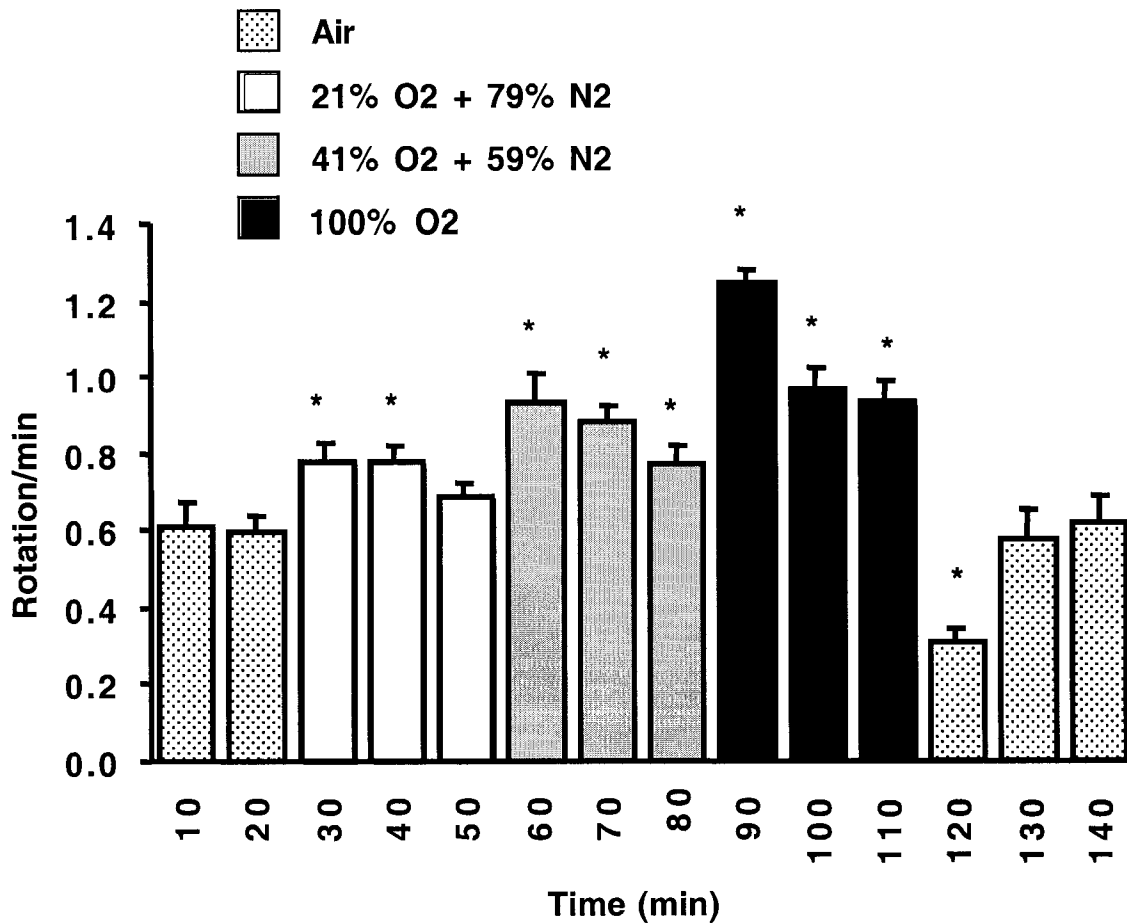


**Figure 34.** Effect of hyperoxia on the embryonic rotational behavior. Removal of CO<sub>2</sub> (aeration with a mixture of 21% O<sub>2</sub> and 79% N<sub>2</sub>) transiently increased embryonic rotation. Increasing O<sub>2</sub> level to 41% and 100% caused further elevations of the rotational rate in a dose dependent manner. Restoration of normoxia (100% air saturated medium) caused a transient reduction of rotational rate followed by a return to basal rotation. Asterisk,  $p < 0.05$  (ANOVA followed by Fisher's PLSD,  $n = 15$  embryos, 3 egg masses) as compared to the last time point of the previous treatment. Each bar represents the average in a 6-min window prior to the time point shown.

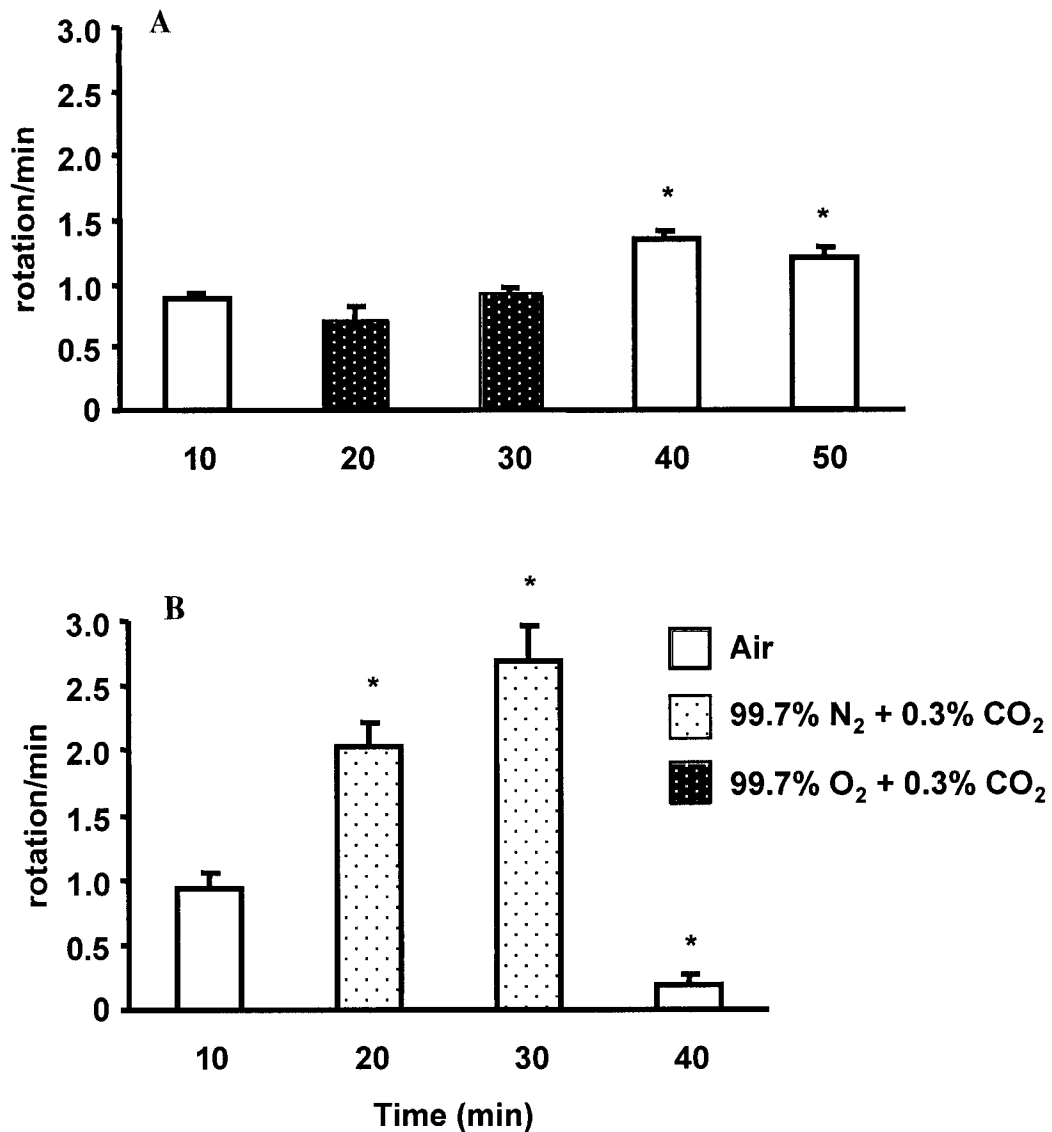


**Figure 35.** Interactive effect of CO<sub>2</sub> and O<sub>2</sub> on embryonic rotation. **A.** Combined hyperoxia and hypercapnia treatment (aeration with a mixture of 99.7% O<sub>2</sub> and 0.3% CO<sub>2</sub>) had no effect on embryonic rotation. However, the rate of embryonic rotation increased upon return to air-saturated medium. **B.** Combined hypoxia and hypercapnia treatment induced a 3-fold increase in embryonic rotation in 20 min. Restoration of normal O<sub>2</sub> and CO<sub>2</sub> levels (100% air-saturated medium) caused a reduction of rotational rate. Asterisk,  $p < 0.05$  (ANOVA followed by Fisher's PLSD,  $n = 15$  embryos, 3 egg masses) as compared to time point 10. Each bar represents the average in a 6-min window prior to the time point shown.

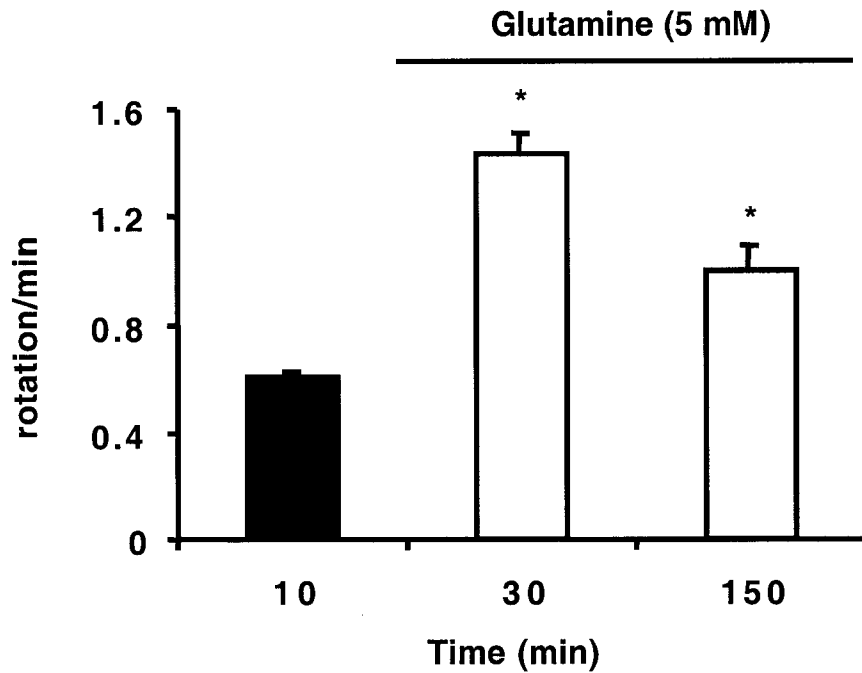


**Figure 36.** Glutamine stimulates embryonic rotation. Whole egg masses were incubated in 5 mM glutamine and the rates of embryonic rotation were examined at different time points. Each bar represents the average in 10 minutes prior to the time point shown. Asterisks:  $p < 0.05$  as compared to time point 0, ANOVA followed by Fisher's PLSD,  $n = 15$ .

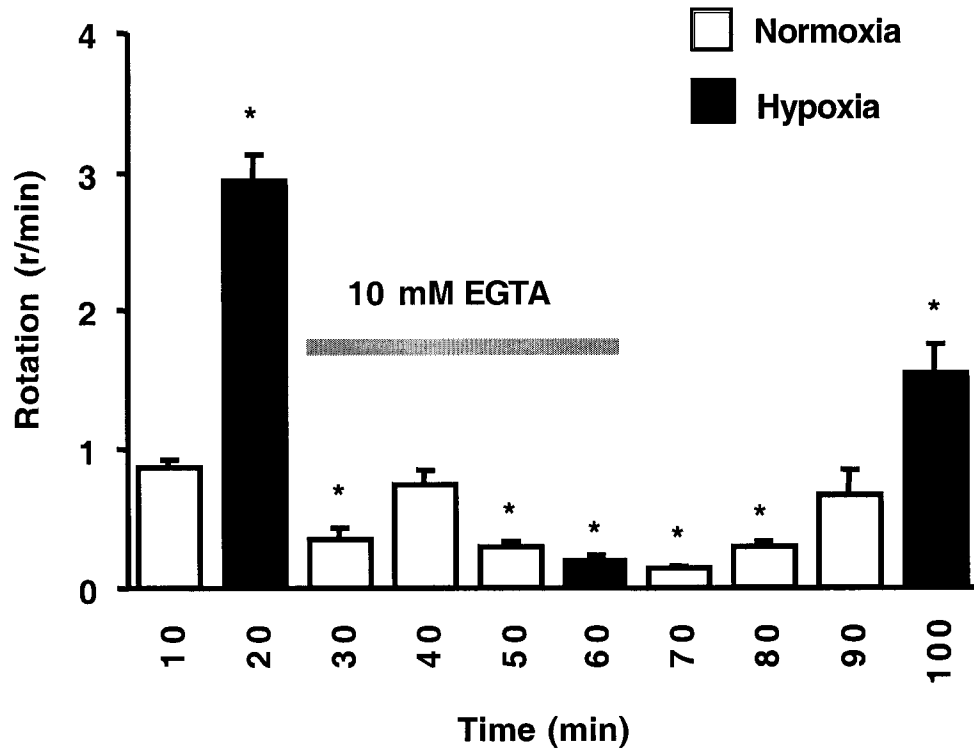


**Figure 37.** Effect of low extracellular  $\text{Ca}^{2+}$  concentration on basal and hypoxia-induced embryonic rotation. Whole egg masses were incubated sequentially in control APW, APW plus 10 mM EGTA and APW washout. Basal and hypoxia-induced embryonic rotation was examined at 10-min intervals. Asterisks:  $p < 0.05$  as compared to time point 0, ANOVA followed by Fisher's PLSD,  $n = 15$ .

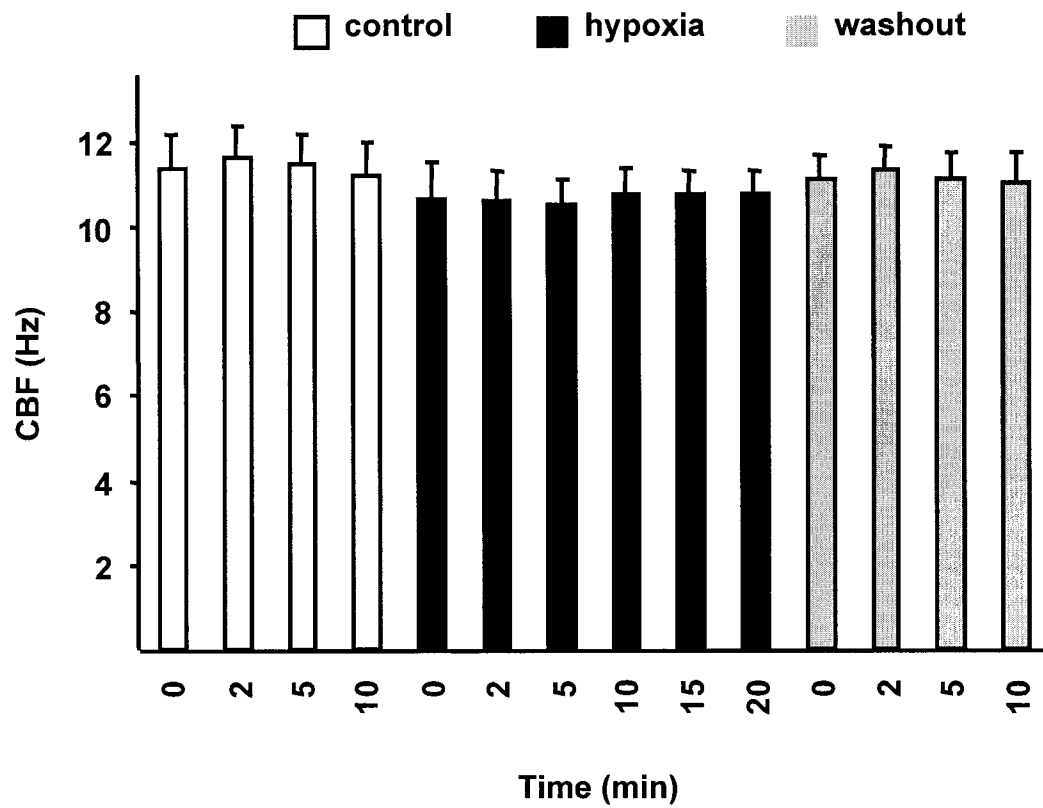


**Figure 38.** Isolated ciliated cells do not respond to hypoxia. Each bar represents the average in a 5-sec window at the time points shown;  $p > 0.05$ , ANOVA,  $n = 5$ .

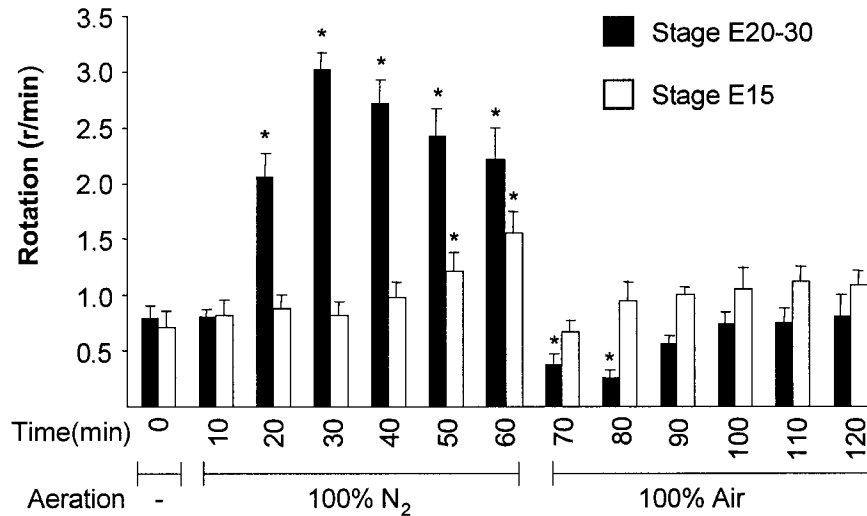


**Figure 39.** Correlation of embryonic rotational response to hypoxia to ENC1 development. At stage E15 (**open bars**, n = 8), when neuritic branching of ENC1s is incomplete (Koss et al., 2002), embryos displayed an attenuated and delayed response to hypoxia. Reoxygenation following hypoxia did not inhibit rotation in these embryos. In contrast, stage E20 – E30 embryos (**solid bars**, n = 45) responded to hypoxia more rapidly and with larger amplitudes. Rotation of the older embryos was also transiently inhibited by reoxygenation following hypoxia. Each bar represents the average in a 6-min window before the time point shown. Asterisks: p < 0.05 (ANOVA followed by Fisher’s PLSD) compared to the rotation rate at time = 0.

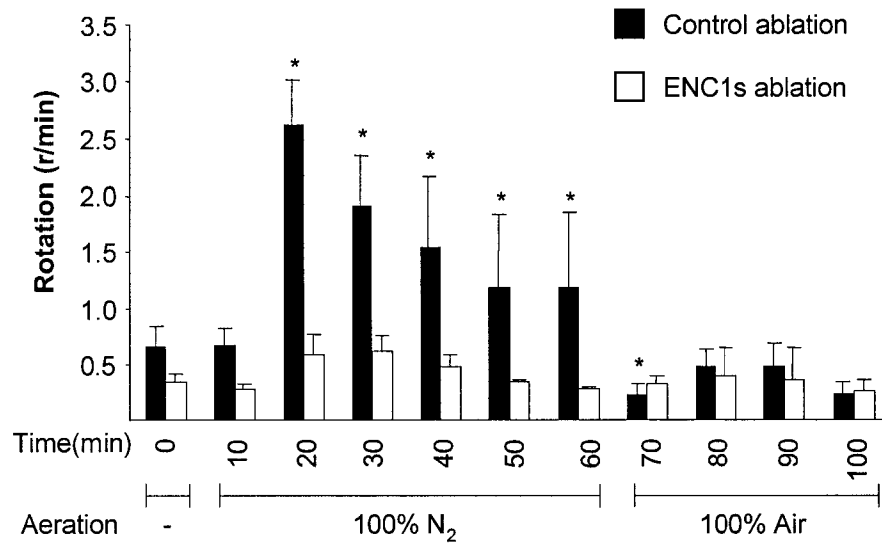
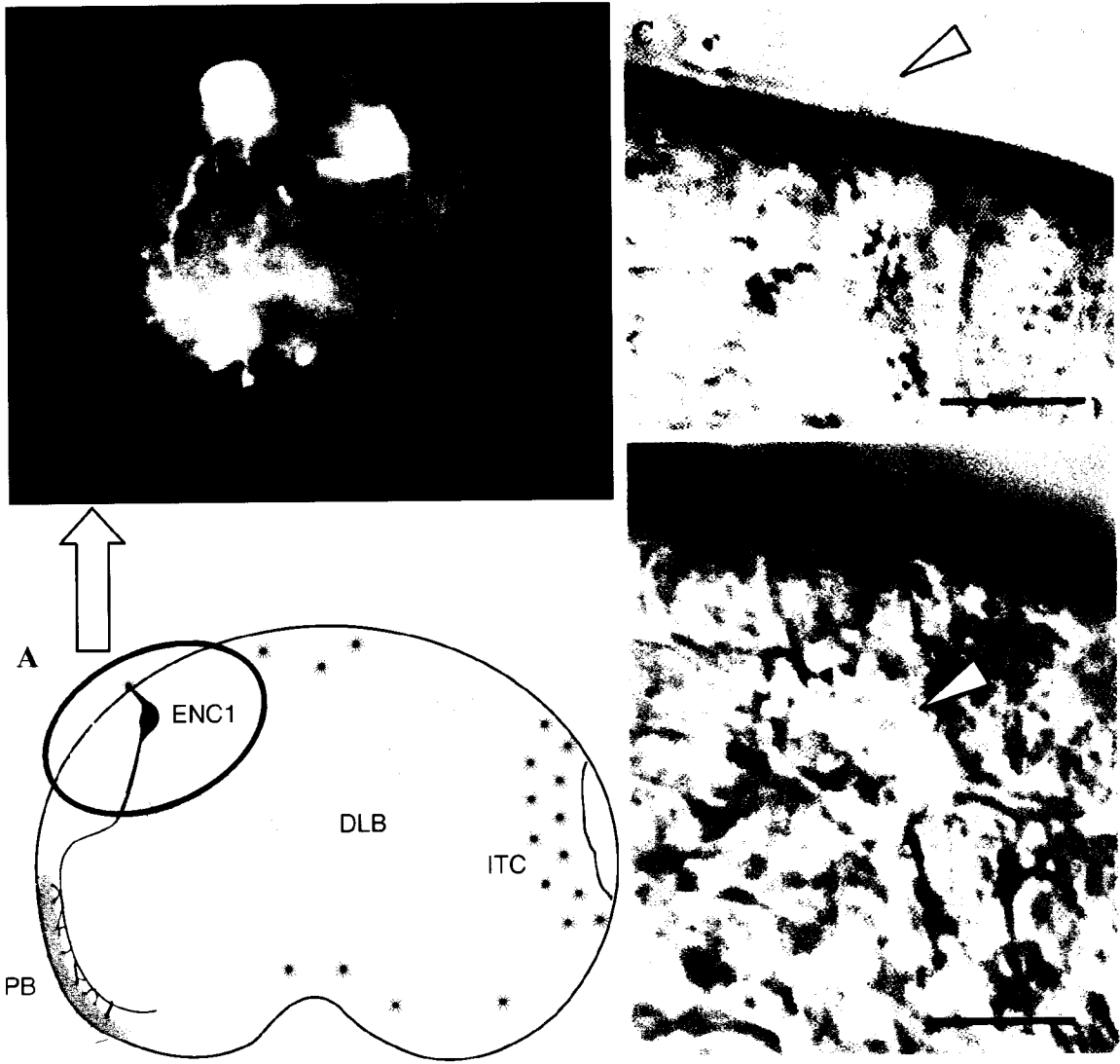


**Figure 40.** ENC1s mediate the rotational response to hypoxia. Embryos with both ENC1s ablated (**open bars**) didn't respond to hypoxia and reoxygenation, whereas control-ablated embryos (**solid bars**) responded normally (n = 4 for each treatment). Asterisks: p < 0.05 (ANOVA followed by Fisher's PLSD) compared to the rotation rate at time = 0.



**Figure 41.** Identification of ENC1 in culture. A small piece of embryonic tissue from an area in which ENC1 is located was surgically removed (**A**, encircled area) with a glass pipette and a needle. The embryonic tissue explant was subsequently cultured in HDM in a poly-l-lysine coated glass bottom petri dish. The presence of ENC1 in the explant culture was confirmed with anti-serotonin immunohistochemistry (**B**). Under DIC microscopy, ENC1 can be identified based on its terminal dendritic knob (**C**, arrow head) and large cell body with smooth nucleus and apical granules (**D**, arrow head). **C** and **D** represent different focal planes of the same piece of tissue. Scale bars: 10  $\mu\text{m}$ .



**A: normoxia**



**B: hypoxia**



**C: restoration of normoxia**



**Figure 42.** Electrophysiological responses of ENC1 to hypoxia as indicated by membrane currents in a cell-attached patch-clamp recording. **A.** Under normoxic conditions, no current spikes were recorded. **B.** Hypoxia elicited current spikes in ENC1's cell body. **C.** Upon restoration of normoxia, the frequency of membrane current spikes was reduced.

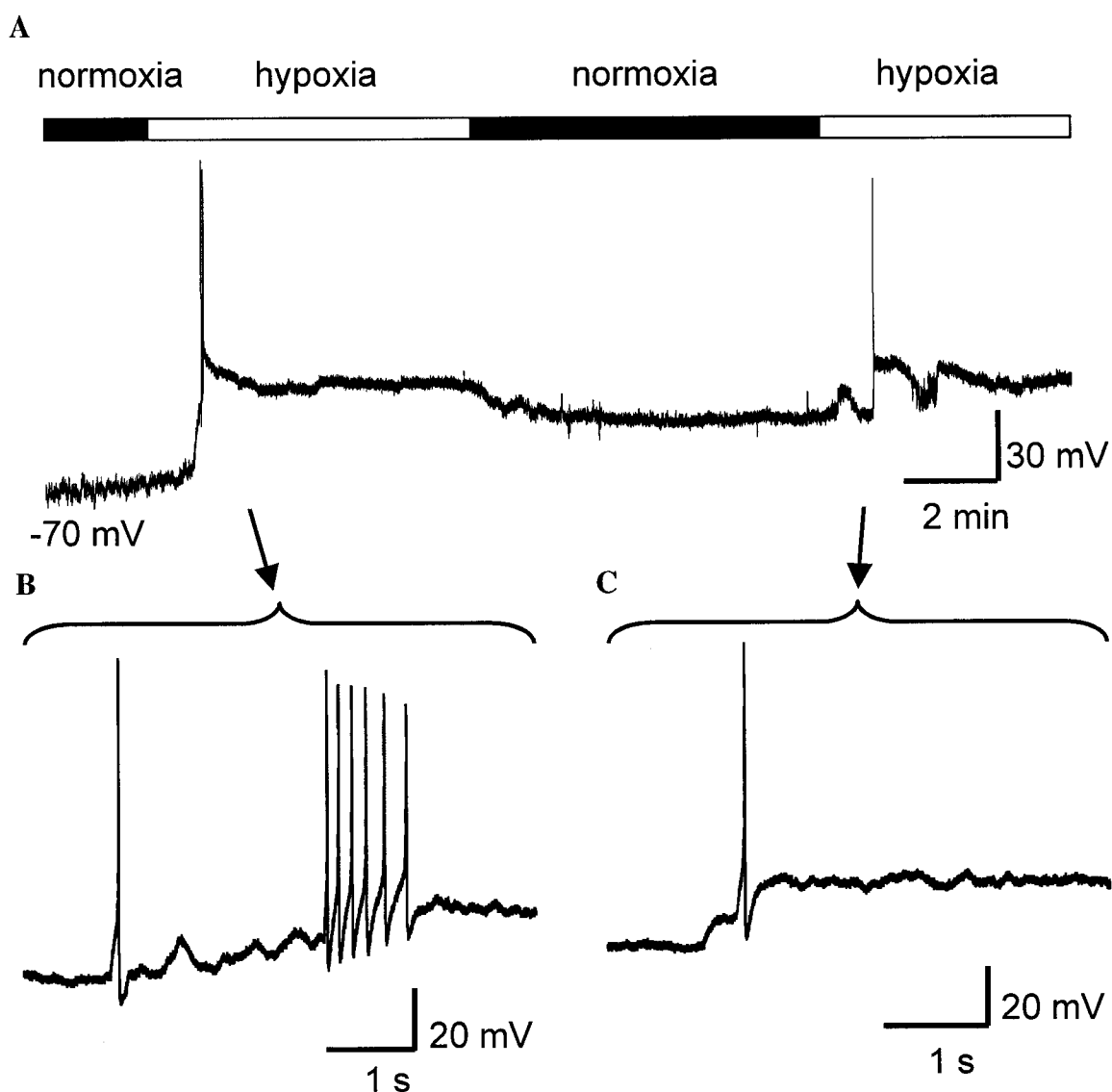


**Figure 43.** Electrophysiological responses of ENC1 to hypoxia as indicated by membrane potential in a whole-cell patch-clamp recording. **A.** Under normoxic conditions, ENC1's membrane potential was around  $-70$  mV. Hypoxia elicited membrane depolarization and a burst of action potentials, followed by sustained membrane depolarization. Restoration of normoxia partially repolarized the membrane potential. A second cycle of hypoxia again elicited membrane depolarization and an action potential. **B and C.** Enlarged view of the action potentials elicited by the first and second cycle of hypoxia, respectively.

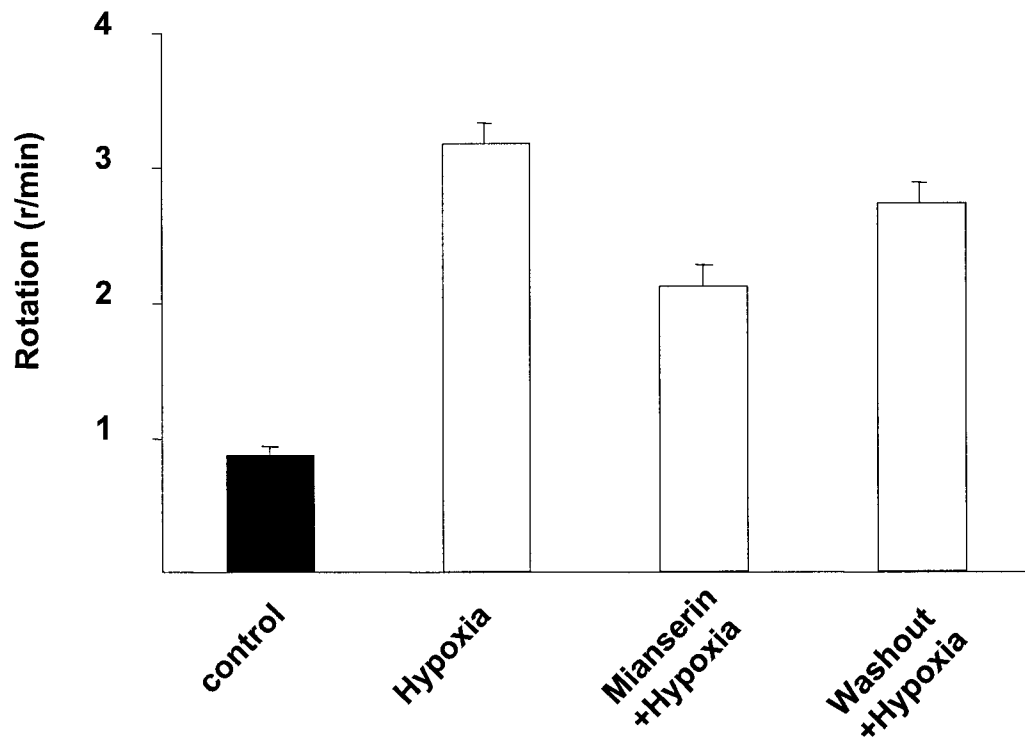


**Figure 44.** Involvement of serotonin in mediating the rotational response to hypoxia. Mianserin (100  $\mu$ M), a serotonin receptor antagonist, reduced the rotational response to hypoxia. Partial recovery of the response occurred after 30 min of washout. Each bar represents the average in a 6-min window 12 min after perfusion of media shown. Comparisons between any two treatments showed significant differences ( $p < 0.05$ , ANOVA followed by Fisher's PLSD,  $n = 15$ ).

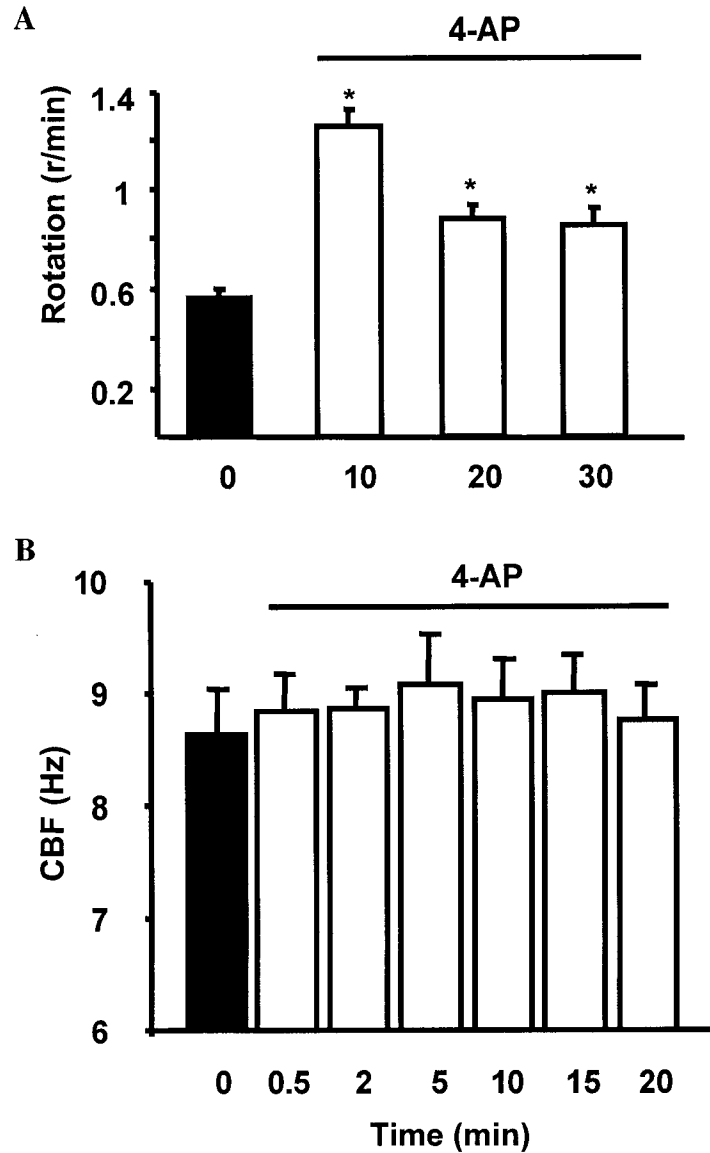


**Figure 45.** Involvement of  $K^+$  channels in mediating embryonic rotation. 4-Aminopyridine (4-AP, 5 mM), a  $K^+$  channel inhibitor, induced prolonged increases of embryonic rotation (**A**), but had no direct effect on the CBF of isolated ciliary cells (**B**). Asterisks:  $p < 0.05$  as compared to time point 0, ANOVA followed by Fisher's PLSD,  $n = 15$  in **A**, 5 in **B**.

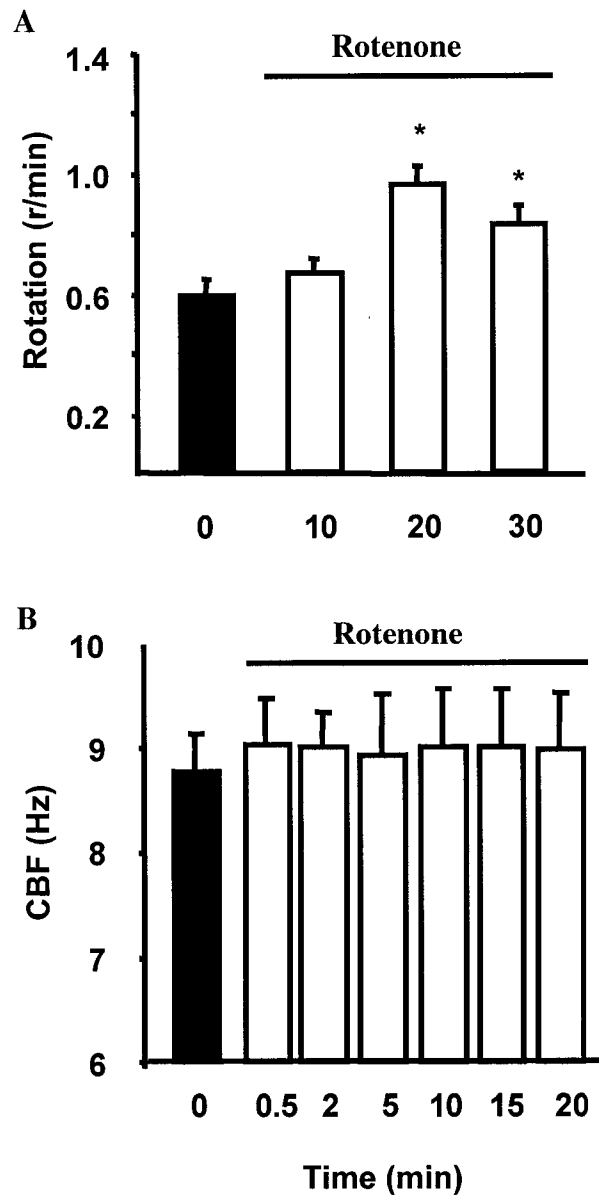


**Figure 46.** Involvement of the mitochondrial electron transport chain (ETC) in mediating embryonic rotation. Rotenone (10  $\mu$  M), an inhibitor of mitochondrial ETC, induced increases of embryonic rotation after 10 min of incubation (**A**), but had no direct effect on the CBF of isolated ciliary cells (**B**). Asterisks:  $p < 0.05$  as compared to time point 0, ANOVA followed by Fisher's PLSD,  $n = 15$  in **A**, 5 in **B**.

## Discussion

This thesis contains anatomical studies, laser ablation experiments, developmental analyses, pharmacological assays and electrophysiological recordings that provide direct evidence for the sensory and motor functions of a pair of early developing serotonergic neurons in *Helisoma trivolvis* embryos. The results suggest that ENC1s are dual-function sensory-motor neurons that both monitor O<sub>2</sub> levels and stimulate ciliary activity, resulting in enhanced embryonic rotation under hypoxic conditions. The increase in embryonic rotation may serve to mix intracapsular fluid, thus reducing the boundary layers and facilitating diffusion of environmental O<sub>2</sub> to the encapsulated embryos. In addition, a novel transplantation technique was developed to promote normal growth and development of previously de-capsulated and experimentally manipulated embryos. The simplicity of the ENC1-ciliary neural circuit, together with its amenability to laser ablation, embryo transplantation, behavioral and electrophysiological approaches, provide unique opportunities for examination of the mechanistic and evolutionary aspects of O<sub>2</sub> sensing and behavioral adaptation at both cellular and organismal levels.

### 1. Embryonic environment during encapsulated development

#### 1.1. Diffusional barriers resulting from encapsulation

Encapsulated embryos develop inside egg capsules, which aggregate into egg masses in many species. The evolution of this developmental strategy has several advantages, leading to a higher reproductive success. First, encapsulation provides embryos with sufficient nutrition from the CF for embryonic growth and development until the juvenile stage. Second, in contrast to larvae living in an open aquatic environment, encapsulated embryos don't need to move a lot to search for food, therefore reducing the energy cost of locomotion and exposure to predators. Third, encapsulated embryos live in relatively stable microenvironments that are well protected both physically and biochemically from microbial infection (Kamiya et al., 1984; Benkendorff et al., 2001). However, the egg capsule membrane and egg mass envelope form diffusional barriers that impede the flow of materials to and from the encapsulated embryos. Although small molecules (< 0.15 μm in *Helisoma* and < 1-2 μm in *Lymnaea*;



**Fig. 24 and 25**) theoretically pass through pores in these barriers freely (Beadle, 1969), the multiple membrane structures and the intervening egg mass materials should slow down the diffusion of these small molecules. Even within the egg capsules, diffusion of molecules would be further reduced by the high viscosity of the CF. These diffusional barriers were collectively demonstrated by the slow changes in O<sub>2</sub> content observed inside egg capsules, as compared to the O<sub>2</sub>-level changes in the bath (**Fig. 27**). As a result, *Helisoma* embryos display a cilia-driven rotational behavior that serves to facilitate diffusion of small molecules (elaborated below).

## **1.2. Function of ciliary beating and embryonic rotation**

Ciliary beating and embryonic rotation play important roles in normal embryonic development in several ways. First, ciliary beating functions as the driving force for embryonic locomotion (Chia et al., 1984) so that embryos can move to a preferred microenvironment. In *Helisoma*, one of the responses to hypoxia was an increase in the rate of embryonic rotation. The enhanced ciliary beating and embryonic rotation result in a translocation of embryos within their egg capsules towards the periphery of the egg mass (**Fig. 30**), where higher O<sub>2</sub> levels occur (**Fig. 26**). Second, embryonic rotation and ciliary beating serve to mix intracapsular fluid (**Fig. 47**) and reduce the thickness of the unstirred boundary layer surrounding each embryo (Withers, 1997). As a result, the gas and fluid exchange between embryos and their surrounding CF, as well as between the intracapsular and the external environment of the egg mass would be enhanced (Burggren, 1985; Hunter and Vogel, 1986). Whereas the results of this thesis are consistent with this interpretation, direct measurement of intracapsular O<sub>2</sub> level in the presence and absence of embryonic rotation are required to confirm the effect of rotation on diffusion. Third, ciliary beating and embryonic rotation may have specific effects on embryonic development. In mice, for example, the fluid flow pattern caused by ciliary beating determines the normal development of internal left-right asymmetry (Nonaka et al., 1998; Vogan and Tabin, 1999). Since embryonic rotation in *Helisoma* typically has a rightward tendency (Diefenbach, 1995), the bilateral asymmetry characteristic of pulmonate gastropods may be determined in part by ciliary activity.

## **2. Possible environmental factors affecting embryonic rotation**

Although the CF provides embryos with nutritive components such as polysaccharides and proteins (Morrill, 1982), O<sub>2</sub> and other small molecules necessary for embryonic development, such as trace elements, ions and vitamins, are acquired from environment through diffusion. In addition, metabolic wastes such as ammonia and CO<sub>2</sub> must diffuse away in order to prevent build-up of these harmful chemicals inside the egg capsules. Since one purpose of the embryonic rotation is to facilitate the bi-directional diffusion of wastes and nutritive molecules, any variations in the levels of these molecules may affect embryonic rotation. Results in this thesis demonstrate that variations in either O<sub>2</sub> or CO<sub>2</sub> affect embryonic rotation (discussed below). Several lines of evidence indicate that ammonium and glutamine (**Fig. 36**) also stimulate embryonic rotation. In contrast, other amino acids, odorant molecules or variations in pH have very little effect on embryonic rotation (**Fig. 29**). Although low Ca<sup>2+</sup> medium abolished the rotational behavior (**Fig. 37**), it remains to be determined whether fluctuations in ion concentration (such as Ca<sup>2+</sup>, K<sup>+</sup>, Na<sup>+</sup> and Cl<sup>-</sup>) affect embryonic rotation.

### **2.1. O<sub>2</sub> as a major environmental regulator of embryonic behavior**

As the final electron acceptor in the oxidative phosphorylation process (Voet and Voet, 1995), O<sub>2</sub> is absolutely required for survival of all aerobic animals. As such, variations in environmental O<sub>2</sub> or blood O<sub>2</sub> supplies have been shown to directly affect animal behavior. In both air breathers and aquatic animals, a drop in the environmental or bloodstream O<sub>2</sub> level is immediately detected by chemoreceptors and elicits enhanced ventilation (Burlison and Milsom, 1993; Inoue et al., 2001; Lopez-Barneo et al., 2001). In larval *Drosophila*, exposure to hypoxia induces increased larval motility, possibly to promote exploration for a more favorable microenvironment (Wingrove and O'Farrell, 1999). In *Helisoma* embryos, hypoxia elicits a prolonged enhancement of embryonic rotation that serves to facilitate O<sub>2</sub> diffusion and translocate embryos to a favorable microenvironment.

That O<sub>2</sub> is a major factor regulating embryonic behavior in *Helisoma* makes sense from an environmental-physiological perspective. Although the structural design of the egg mass and egg capsule provides the embryos with a protective shelter, it also forms an

O<sub>2</sub> diffusional barrier. The O<sub>2</sub> levels at the center of the egg capsule drops to less than 50% of the environmental levels surrounding the egg capsule (**Fig. 26 & 27**). This O<sub>2</sub> gradient is probably generated by the metabolic O<sub>2</sub> consumption of embryos and the diffusion barrier formed by the gelatinous egg mass and the capsular fluid surrounding the embryos. It can be assumed that the intracapsular O<sub>2</sub> level would be further reduced if the embryos stop rotating or if their metabolic rate increases under conditions such as high temperatures. Similarly, the intracapsular O<sub>2</sub> level would also decrease if the environmental O<sub>2</sub> level falls, as is often the case in an aquatic environment (Derry, 1993). Results from this thesis suggest that *Helisoma* embryos have evolved strategies to cope with short-term O<sub>2</sub> fluctuations, including mechanisms to detect variations in O<sub>2</sub> and respond accordingly. The early development of ENC1-ciliary neural circuits provides the neural machinery to accomplish these tasks.

## **2.2. Behavioral plasticity of hypoxia-elicited embryonic rotation**

An interesting finding of this study was that repeated treatment with hypoxia induced a behavioral sensitization of the embryonic response (**Fig. 32B**). The occurrence of sensitization suggests that the rotational response to hypoxia is adaptive, as this metabolically expensive response is not likely to be enhanced if it doesn't provide significant benefits to the embryo. Similar long-term facilitation of respiratory motor output induced by episodic hypoxia has been recently reported in anesthetized mammals (reviewed in Baker and Mitchell, 2000; Prabhakar, 2001) and shown to be serotonin-dependent (Ling et al., 2001; Mitchell et al., 2001). Since the rotational response to hypoxia is mediated by serotonergic ENC1s in *Helisoma*, it may be that the behavioral sensitization to repeated hypoxia is also serotonin-dependent. Serotonin-dependent behavioral plasticity has been reported in several other animal systems, including the gill-withdraw response in *Aplysia* (Brunelli et al., 1976; Kandel, 2001), locomotion in *Caenorhabditis elegans* (Sawin et al., 2000), non-associative learning in leech (Burrell et al., 2001), and the escape behavior in crayfish (Teshiba et al., 2001).

The transient inhibition of embryonic rotation upon restoration of normoxia following hypoxia may be caused by a sensory adaptation mechanism. In this scenario, reintroduction of normoxia initially produces a strong inhibition of the O<sub>2</sub> sensor that is

manifested as a transient inhibition of embryonic rotation. Subsequent adaptation to a tonic intermediate level of activity is seen as a return to basal rotation after 10 min. Similarly, transient post-hypoxic declines of respiratory sensory discharge have been observed in rodents (Bach et al., 1999; Dick and Coles, 2000).

### **2.3. Effect of CO<sub>2</sub> variations on embryonic rotation**

In air-breathers, both O<sub>2</sub> and CO<sub>2</sub> are major regulators of respiration (Erlichman and Leiter, 1993; Gonzalez et al., 1995; Fitzgerald et al., 1999). Similar to decreases in O<sub>2</sub> levels, increases in tissue or blood CO<sub>2</sub> levels lead to enhancement of ventilation through intracellular acidification (Erlichman and Leiter, 1997). In many cases, respiration of air-breathers is more sensitive to CO<sub>2</sub> since small variations in CO<sub>2</sub> levels often result in large changes in pH. Aquatic animals, however, generally rely much less on CO<sub>2</sub> for regulation of respiration (Fretter and Peake, 1975; Withers, 1992). Because CO<sub>2</sub> is highly soluble in water (Withers, 1992), tissue or blood CO<sub>2</sub> could diffuse away more readily in an aquatic environment. In this study, hypercapnic challenges cause small and very transient decreases of embryonic rotation that is opposite to hypoxia-elicited enhancement of rotation. In contrast, low CO<sub>2</sub> transiently enhanced embryonic rotation. Since these rotational responses don't serve to reduce or counteract the CO<sub>2</sub> variations, the physiological relevance of these behavioral responses is unclear. Interestingly, adults of another pond snail species, *Lymnaea*, directly breathe air despite living under water most of the time. As a result, the respiration of adult *Lymnaea* is affected by both hypercapnia and hypoxia, but in qualitatively different manners (Inoue et al., 2001). Specifically, hypoxia increases the frequency of ventilation, whereas hypercapnia increases the duration of inspiration (Inoue et al., 2001). Given that the ventilatory movements of early embryos are not sensitive to CO<sub>2</sub>, it would be interesting to examine when and how the CO<sub>2</sub> sensitivity is turned on at later stages of embryonic development.

### **2.4. Interaction between O<sub>2</sub> and CO<sub>2</sub>**

In air-breathers, hypoxia and hypercapnia interactively enhance each other's effect on stimulating ventilation (Lahiri and DeLaney, 1975; Fitzgerald and Dehghani, 1982, Saetta and Mortola, 1987; Daristotle and Bisgard, 1989; Teppema et al., 2001). In

contrast, hypoxia and hypercapnia exert opposing effects on the ventilatory rotation in *Helisoma* embryos. When embryos were challenged by combined hypercapnia and hypoxia, a response very similar to that induced by hypoxia alone was observed (**Fig. 28 and 35B**). This result suggests that hypoxia is the predominant environmental factor stimulating the ventilatory rotation. The overwhelming and prolonged effect of hypoxia also suggests that low O<sub>2</sub> level is detected by chemoreceptors and exerts its stimulatory effect through neural systems. In contrast, the small and transient inhibitory effect of hypercapnia and stimulatory effect of hypocapnia are probably mediated directly by effector cells through intracellular acidification (**Fig. 33**; Fretter and Peake, 1975; Withers, 1992).

Hyperoxia also stimulates embryonic rotation in a dose-dependent manner. This stimulatory effect is negated by hypercapnia. Moreover, upon restoration of normal air following a combined hyperoxic and hypercapnic treatment, a transient increase in embryonic rotation similar to the post-hypercapnia rebound is observed, suggesting that hypercapnia dominates the effect of hyperoxia. Like the response to hypercapnia, the hyperoxia-elicited transient enhancement of embryonic rotation doesn't seem to be a receptor-mediated response. Instead, the stimulatory effect of hyperoxia likely results from the oxidative effects of high O<sub>2</sub> levels on effector cells (Thom et al., 2002). In rats, hyperoxic challenge elicits hyper-reactivity of the airway smooth muscle to both endogenously-released and exogenously-administrated acetylcholine (Agani et al., 1997; Iben et al., 2000). In rodent cerebral cortex, elevations in O<sub>2</sub> levels increase free radical NO levels by stimulating the activity of NO synthase (Thom et al., 2002). Since NO has been shown to stimulate both ciliary beating and embryonic rotation in *Helisoma* (Goldberg et al., 2000; Cole et al., 2002), it is also possible that the hyperoxia-induced enhancement of embryonic rotation is mediated through production of NO.

### **3. *Ex ovo* culture and transplantation of de-capsulated embryos**

An embryonic transplantation technique for long-term sustained growth and development of previously de-capsulated embryos was reported in the present study. The *ex ovo* culture conditions that were also tested in this study were effective in the short-

term maintenance of embryonic growth and survival, but failed to promote normal development over the long-term.

### **3.1. De-capsulated early embryos fail to develop normally *ex ovo***

That embryos at early stages fail to develop normally under various *ex ovo* conditions suggests that some key growth promoting factors or certain environmental conditions are missing in *ex ovo* culture. It has been reported in several species that encapsulated embryos cannot develop normally if they are removed from the egg capsules at early stages of development (Morrill, 1982; Pechenik et al., 1984; Stockmann-Bosbach and Althoff, 1989; Meshcheryakov, 1990). This is because the environment in the capsular matrix is extremely complex and can hardly be mimicked *in vitro*. The situation is further complicated by the fact that there is substantial variation in the composition of CF in different species (Morrill et al., 1964; Morrill, 1982; Heras et al., 1998). Even less is known about the physical properties of the CF and the membranes surrounding the encapsulated embryos such as viscosity, electrical charge, pressure, osmolarity, and pH (Beadle, 1969; Taylor, 1973; Morrill, 1982). For instance, this study indicates that *Helisoma* embryos naturally develop in a slightly acidic environment. Furthermore, acidic pH promoted growth and development of early embryos cultured *ex ovo* in HDM. Likewise, hamster embryonic cells exhibit optimal clonal proliferation when cultured in medium with a pH of 6.70 (Leboeuf et al., 1989). It is unknown why embryonic growth was not promoted by acidic pH when cultured in 30% M199. Intracapsular hydrostatic pressure may also be an important factor for normal embryonic growth and development. In *Lymnaea palustris*, early stage embryos fail to develop normally if their egg capsules are punctured at 2-4 h intervals to relieve the intracapsular hydrostatic pressure (Morrill, 1982). Pechenik et al. (1984) reported increased survival when decapsulated prosobranch embryos were cultured in a pressurized syringe, yet they all failed to develop normally.

Various kinds of abnormal development were observed when embryos were cultured *ex ovo*. In the present study, embryos incubated in culture media always accumulated a large number of particles in the canaliculus of the protonephridia, suggesting either a malfunction of these embryonic kidneys or a precocious development

of nitrogen catabolism (Morrill, 1982). In addition, all embryos in culture failed to grow a shell, indicating incomplete development of the shell gland or lack of  $\text{CaCO}_3$  in the culture media tested. Taylor (1973) reported that a considerable amount of  $\text{Ca}^{2+}$  in CF is bound to calcium buffer. Given the reasonably high  $\text{Ca}^{2+}$  concentration in the culture medium, the bound  $\text{Ca}^{2+}$  that normally exists in the CF may be important for shell formation. Finally, *ex ovo* cultured embryos were sometimes hydropic after 72 h, suggesting that the osmoregulatory machineries are impaired in these embryos, or the osmolarity of the media is outside the range that embryos can handle.

Although *Helisoma* and other encapsulated pulmonates undergo direct development, they may still rely on chemical cues similar to those used by indirect developers to trigger settlement and metamorphosis (Morse, 1990). CF may contain cues that allow development to proceed from E30 – E50, the stages resembling the veliger to juvenile transition in metamorphosing gastropods (Raven, 1958; Morrill, 1982). That embryos develop normally when cultured after this transition lends support to this hypothesis (Pechenik et al., 1984). My preliminary trials also indicate that isolated stage E45 or later embryos grow and develop normally in APW. Since EGF has recently been found to be a major component in the albumen gland and CF in *Lymnaea* and has been implicated in development of the nervous system (Hermann et al., 2000), it may serve as a metamorphic factor in CF. However, neither human nor *Lymnaea* EGF promoted growth and development of *Helisoma* embryos. It is likely that EGF alone is not sufficient to compensate for other crucial factors that are missing in the culture media, or that the EGFs used in this study are highly species-specific.

Ignoring the physical properties of the intracapsular environment for the moment, CF intuitively seems to be the best medium for cultivation of de-capsulated embryos. However, it is technically difficult to harvest large quantities of concentrated CF since each capsule contains only about 0.47  $\mu\text{l}$  of CF. Moreover, when extracted from egg capsules, the highly viscous CF often clogged the micropipette or solidified in air. We have also tried to culture de-capsulated embryos in the liquid fraction of egg mass homogenates, with no apparent improvement in embryonic development. The degradation of certain essential components by enzymes released from homogenized embryonic cells or the inability to mimic the physical environment of the intact egg

capsule likely contributed to the poor development. Since the albumen gland secretes CF *in vivo*, stimulation of albumen gland secretion in tissue culture with cAMP (Morishita et al., 1998) would be a convenient way to produce an alternative medium to CF. In future studies, albumen gland-conditioned medium in combination with physical manipulations such as high pressure should be attempted.

### **3.2. Embryo transplantation is an effective strategy for culturing de-capsulated embryos**

Transplantation of previously de-capsulated gastrulated embryos yields a survival and growth rate similar to that of control embryos, suggesting that experimental manipulations and de-capsulation of gastrulated embryos do not permanently hinder embryonic development. It was observed that in most egg capsules, the ruptured openings on capsular membranes spontaneously sealed by 12 h after transplantation. Rich disulfide bonds previously reported in the egg covering of *Littorina saxatilis* (Losse and Greven, 1993) may have played a role in the self-sealing process. Alternatively, this self-sealing phenomenon might result from the solidification of CF along the suture. In addition, certain physical or chemical properties of the gelatinous matrix surrounding the exterior of the egg capsule membranes may facilitate the sealing process. The layer of polyanionic acid mucopolysaccharide on the surface of capsular membrane (Plesch et al., 1971) might be repelled by APW and therefore keep the ruptured membrane at a closely apposing state. The self-sealing of the ruptured capsular membrane is important in maintaining the physical, chemical, and electrical properties of the intracapsular environment that are essential for normal growth and development of embryos.

Roughly two-third of the embryos transplanted at the 2- or 4-cell stages died during gastrulation. Since the heat-treated host capsules resealed equally well as normal capsules after transplantation, the high mortality of transplanted early stage embryos cannot be attributed to a loss of hydrostatic pressure within the host egg capsules. Instead, this either indicates that embryos are especially vulnerable to experimental manipulation at early cleavage stages, or gastrulation is one of the most crucial processes during embryonic development. Early in development, each embryo is surrounded by a vitelline membrane that is cast off during gastrulation (Morrill, 1982). The vitelline membrane is



very sticky so that it tends to attach to petri dishes and glass pipettes during isolation and transplantation of embryos. Although Sigmacote-coated petri dishes and glass pipettes were used to prevent adhesion, it is still possible that the vitelline membranes of many embryos are ruptured during experimental manipulation. If the integrity of the vitelline membrane is crucial for the survival of embryos, then it may explain the high mortality of transplanted cleavage-stage embryos. Alternatively, it is likely that certain key ‘gastrulation factors’ in the host CF are denatured or inactivated during the heat-shock treatment used to kill the host embryos prior to transplantation. The host egg masses were incubated at 48 °C for 25 minutes, a treatment that would probably inactivate certain heat-labile proteins. Preliminary experiments indicated that more cleavage-stage embryos survived gastrulation (80%,  $n = 10$ ) when they were transplanted into non heat-shock treated host egg capsules. It remains to be determined, however, whether egg capsules contain heat-labile gastrulation factors.

### **3.3. Potential applications of the embryo transplantation technique**

The transplantation technique developed in this study provides a unique opportunity to assess the long-term effects of experimental manipulations on encapsulated embryos. For example, the loss of rotational surges after laser-ablation of both ENC1s provided an essential confirmation that these cells function as cilioexcitatory motor neurons (refer to **Results 2.5**). Through transplantation of ENC1-ablated embryos, I have demonstrated in this thesis that ENC1s mediate O<sub>2</sub> sensing and a rotational response to hypoxia (refer to **Results 4.3**). It is now possible to examine the long-term effect of ENC1 ablation on the survival of embryos, as well as respiratory function after hatching. The embryonic transplantation technique will also be useful in examining cell interactions during neuronal differentiation, neurite outgrowth, and synaptogenesis *in vivo*. Given the organizational simplicity of the ENC1-cilia circuit in *Helisoma* embryos, it is feasible to look into the interaction between ENC1 and its target ciliary cells by ablating either of them and examining the developmental consequences. Finally, studies involving cell lineage tracing or genetic manipulations are now possible, since molecular markers or genetic materials can be injected into early embryos, followed by transplantation of these embryos into host egg capsules for further development. With

the recent molecular cloning of serotonin receptors in *Helisoma* (Mapara et al., 2002), it is possible to look at the developmental and physiological consequences of over- and under- expression of these receptors. These are merely a few examples of how the transplantation technique can facilitate the investigation of physiological and developmental events in embryos of *Helisoma* and other encapsulated species.

#### **4. Laser treatment of cells in *Helisoma* embryos**

##### **4.1. Laser treatment paradigms**

When a laser beam is focused on a point inside a cell, it deposits light energy that causes damage to the area (Bargmann and Avery, 1995). Taking advantage of this principle, laser beams can be used to either excite or ablate cells, techniques called laser stimulation or laser ablation, respectively. Elimination of cells through laser ablation has been widely used to address questions regarding cell function, cell fate/origin, cell-cell interaction and cell regeneration (Bargmann and Avery, 1995; Chang and Keshishian, 1996; Balak et al., 1990; Kuwada, 1993; Shah and Jay, 1993). In this study, ENC1s were laser ablated to demonstrate their sensory and motor functions (discussed in detail later). This technique will also be very useful in examination of the long-term effects of ENC1 ablation, as well as the interactions between ENC1 and its target ciliary cells during neural circuit formation and synaptogenesis.

Over the short-term, laser treatment induced acute cellular responses include swelling and increased membrane permeability (Bargmann and Avery, 1995; Doukas and Flotte; 1996; Lee et al., 1996), which inevitably result in depolarization and excitation of the treated cells (**Fig. 48**). Taking advantage of these laser-induced acute responses, laser beams have been used to facilitate cell loading and drug delivery (Mulholland et al., 1999; Kodama et al., 2002), and to stimulate excitable cells *in vitro* (Fork, 1971; Farber and Grinvald, 1983; Hirase et al., 2002). In this thesis, a laser treatment protocol was adapted to stimulate a neuron *in vivo* in order to examine its cilioexcitatory actions (**Fig. 48**). Given the practical difficulty associated with electrophysiological stimulation of ENC1 in intact embryos, this laser treatment protocol was shown to be an effective technique to excite ENC1. The result of these experiments suggest that during the early stages of laser-induced cell death, ENC1s undergo prolonged release of serotonin (**Fig.**

48), as indicated by enhanced activity in ENC1's target ciliary cells for greater than 30 minutes (Fig. 17). The extended timecourse of this response may result from a continual release of serotonin as the cell loses its capability to regulate membrane potential, intracellular calcium concentration and other cellular factors. In addition, as ENC1 loses its serotonin re-uptake capability during cell death, the removal of released serotonin from the vicinity of ciliated cells may be reduced, again causing a prolonged response. Further experiments are required to fully characterize how serotonin is released in response to the laser treatment. It would be extremely useful if this technique could be adapted to stimulate ENC1 or other neurons without damaging the irradiated cells. Intriguing results from other studies on laser stimulation in combination with photostimulation probes (Farber and Grinvald, 1983) or caged compounds (Callaway and Katz, 1993; Katz and Dalva, 1994, Dodt et al., 1999), or on multiphoton laser stimulation (Hirase et al., 2002) provide directions for future development of this technique.

In the present study, a pulse intensity that is just able to scratch glass coverslips was applied (Fig. 2); stronger pulse intensities tended to cause cell explosion (personal observation). The laser treatment consisted of 200-300 pulses, comparable to that applied in killing *C. elegans* neurons (Bargmann and Avery, 1995). It has been reported that a single laser pulse was sufficient to kill a hair cell in axolotl, however, the pulse intensity used in that study was not clear (Jones and Corwin, 1996). In another study, 600-1800 laser pulses were used to kill a D blastomere in *C. elegans* embryos (Moerman et al., 1996). In general, the number of laser pulses required to kill a cell depends on pulse intensity and the location of the target cell: many fewer pulses are required to ablate a cell located in a surface epithelium than to ablate one located in deeper tissue. Practically, the number of laser pulses used was determined by the observed changes in cellular morphology caused by laser treatment (Chang and Keshishian, 1996, Bernhardt et al., 1992).

#### 4.2. Advantages of laser ablation

A prerequisite for laser treatment is that the target cell must be identifiable under DIC objectives (Shah and Jay, 1993). Since both ENC1 and its target cells, the ciliated epithelial cells, can be reliably identified *in vivo*, the *Helisoma* embryo provides a

practical system for manipulating either the neuron or the target cells using laser microbeams. Compared to other toxicogenic and genetic knock out techniques, laser ablation has several significant advantages (For a review, Shah and Jay, 1993). First, laser microbeams provide a method for fast cell elimination. The target cell can be killed in minutes to hours, depending on the strength of laser applied. In this study, the morphology of laser treated ENC1 was totally disrupted in 6-24 h. Second, the highly coherent laser beam significantly reduces the area of damage. Theoretically, the diameter of the laser microbeam equals to the wavelength of the laser (Bargmann and Avery, 1995). In our study, for example, the wavelength, and thus the minimum diameter of the laser spot, was 440 nm. This greatly reduced the damage to the surrounding cells, as indicated by our analysis of cells adjacent to the laser-treated ENC1. Third, the pulse intensity and focus of the laser can be precisely controlled. This makes it possible to ablate subcellular compartments of a cell without killing the cell (Beermann and Jay, 1994). In preliminary trials, we were able to sever the primary neurite of ENC1 (**Fig. 11**), while the morphology and serotonin immunoreactivity of the ENC1 soma were unaffected in 72 h. Finally, the treated cell, and those surrounding it, can be continually monitored throughout the treatment process, enabling an ongoing assessment of functional and morphological responses.

#### **4.3. Laser-induced cell death**

The laser treated ENC1 cells underwent morphological changes characterized by a typical necrotic cell death process (**Fig. 48**; Castoldi et al., 2000). Within a few minutes, the laser-treated cell started to bloat and the cell boundary became obscure as a result of membrane rupturing. Because the apical dendrite of ENC1 projects to the embryonic surface, the cytoplasm was occasionally seen to burst out of the dendritic knob, the chemosensory-like surface structure of ENC1 (Diefenbach et al., 1998). The ablated cells were completely eliminated in 6-24 h after laser treatment (**Fig. 48**), possibly through an active process mediated by macrophages or leukocytes (Jones and Corwin, 1996). In addition, most laser-treated ENC1s lost their serotonin immunoreactivity in 6-24 h, along a similar timecourse as seen for the morphological elimination of ENC1.

Although laser-induced cell death was dominated by characteristics of necrosis, it is difficult to determine whether apoptosis was also involved without examining DNA fragmentation or the expression of necrotic proteases and apoptotic caspases. It has been reported that acute necrotic insults cause neuronal apoptosis (Nitatori et al., 1995). Moreover, both necrotic and apoptotic features were observed in the cell death process after necrotic insults in several other studies (Gwag et al., 1997, for reviews, see Martin et al., 1998, Roy and Sapolsky, 1999). It has been proposed that apoptosis and necrosis were simultaneously triggered by acute insults. However, as the cell dies and ATP depletes, the energy-dependent apoptosis process gradually gives way to necrosis (Roy and Sapolsky, 1999).

## **5. ENC1 as a cilioexcitatory motor neuron**

### **5.1. Laser treatment directly demonstrates the motor function of ENC1**

Results from both laser stimulation and laser ablation experiments confirmed the cilioexcitatory motor function of ENC1. First, laser stimulation of ENC1 transiently increases ciliary activity of specific groups of ciliated cells, specifically, the cells of the dorsolateral and pedal ciliary bands. The anatomical association between ENC1 and these ciliary cells has been described previously. As revealed by anti-serotonin immunostaining, electron and DIC microscopy, each ENC1 ventrally projects its primary neurite to the pedal ciliated epithelial cells, where extensive neurite branching occurs (**Fig. 10**; Goldberg and Kater, 1989; Diefenbach et al., 1998; Koss et al., 2002). DIC microscopy and immunohistochemistry also revealed that, on its way to the target pedal ciliated cells, the primary neurite of each ENC1 traverses and sprouts short neuritic processes just below the anterior ciliated cells of the dorsolateral band (**Fig. 9**). Together, these data support the hypothesis that ENC1 functions to regulate ciliary activity. Second, behavioral analysis showed that the average rate of embryonic rotation was reduced and the occurrence of the periodic rotational surges was nearly absent after elimination of ENC1 with laser ablation (**Fig. 21**). These results not only confirm the cilioexcitatory action of ENC1, they also suggest that ENC1 functions to generate the periodic rotational surges displayed by embryos.

Similarly, macrocilia on the lips of the ctenophore were activated from the basal quiescent state by various stimuli via neural pathways (Tamm, 1988). In contrast, neural-mediated periodic arrests of ciliary activity have been reported in other free-swimming molluscan larvae and adult gills (Murakami and Takahashi, 1975; Mackie et al., 1976; Arkett, 1988; Murakami, 1989), events that don't appear to occur in *Helisoma* embryos at stages E20-E30.

## **5.2. ENC1 regulates ciliary activity through release of serotonin**

Cilioexcitatory actions of serotonin have also been shown in many other mollusks, including the pedal ciliated epithelium of *Lymnaea* (Syed and Winlow, 1989) and *Tritonia diomedea* (Audesirk et al., 1979), the gill cilia of bivalves (Gosselin, 1961; Gosselin et al., 1962), and the prototrochal and velar cilia of marine gastropods (Koshtoyants et al., 1961).

In *Helisoma*, previous pharmacological studies have indicated that serotonin stimulates embryonic rotation *in vivo* (Diefenbach et al., 1991) and ciliary beat frequency in cultured ciliated cells (Goldberg et al., 1994; Christopher et al., 1996; 1999). In this thesis, serotonin has been shown to have cilioexcitatory effects specifically on the dorsolateral and pedal ciliary bands *in vivo* (**Fig. 18**). In contrast, the serotonin receptor antagonist mianserin reduces the occurrence of CBF surges displayed by the pedal and dorsolateral ciliary cells (**Fig. 20A**). Taken together with previous results showing that mianserin significantly reduces the occurrence of the periodic surges in embryonic rotation (Diefenbach et al., 1991), these data suggest that endogenously released serotonin generates the episodic surges in ciliary beating and embryonic rotation. Given the serotonergic phenotype and cilioexcitatory action of ENC1, these results suggest that ENC1 endogenously releases serotonin to stimulate the activity of target ciliary cells through generation of periodic accelerations of ciliary beating. The hypothesis is directly supported by results showing that the increase in ciliary activity induced by laser stimulation of ENC1 is attenuated in the presence of mianserin (**Fig. 20C**). Therefore, serotonin receptor activation is involved in the communication between ENC1 and ciliary cells. Together, these data strongly suggest that ENC1 regulates ciliary activity through the release of serotonin (**Fig. 48**).

### 5.3. How are ciliary activity and embryonic rotation regulated in *Helisoma* embryos?

The data shown in this study indicate that different groups of cilia display distinct characteristics of ciliary activity, as has also been shown in the protozoon *Tritrichomonas foetus* (Monteiro-Leal et al., 1995). In *Helisoma*, the dorsolateral, pedal and isolated tufts of cilia differ not only in the overall rate of beating, but also in the presence of periodic beat surges (**Fig. 15**). Furthermore, the dorsolateral and pedal cilia both responded to the cilioexcitatory neurotransmitter serotonin, but the isolated tufts of cilia were unresponsive (**Fig. 18**). These differences may reflect the distinct function and regulatory mechanisms of the three groups of cilia. It has been suggested that embryonic rotation is a complex behavior that contains both a vertical (pitch) component and a horizontal (yaw) component, driven by beating of the pedal and dorsolateral ciliary bands, respectively (Diefenbach et al., 1991). In contrast, the isolated tufts of cilia, which beat at a much faster rate without apparent surges, don't seem to play a major role in driving the embryonic rotational behavior. Instead, the beating of these cilia may function to sweep fluid around the embryonic surface. In addition, the periodic surges of ciliary beating in the dorsolateral and pedal cilia, which generate the surges in embryonic rotation, manifest the neural regulation of ciliary activity (discussed in 5.2). The lack of surges in the isolated tufts of cilia suggests that these cilia are not under neural control. These results are consistent with observations on cultured ciliary cells from mass dissociated *Helisoma* embryos (Goldberg et al., 1994). In that study, a wide range of basal ciliary beat frequencies was recorded and a small percentage of ciliary cells displayed no response to serotonin (Goldberg et al., 1994). It remains to be determined whether the unresponsive cells in culture were in fact the isolated tufts of cilia seen *in vivo*.

The present results suggest that the cilia of dorsolateral and pedal bands are able to beat spontaneously at a basal level, and that the ciliary beat surge is the result of ENC1-mediated regulation of ciliary activity (**Fig. 48**). Stimulated by certain environmental cues, ENC1 periodically releases serotonin to the pedal and dorsolateral ciliated cells to accelerate ciliary beating and thus cause the periodic embryonic rotational surges (**Fig. 48**). It is likely that serotonin is released to all the pedal ciliated cells simultaneously,

because ENC1's extensive network of neurite branching covers most of the pedal band (**Fig. 9C and 14A**). However, the way by which ENC1 activity affects the dorsolateral ciliary bands remains elusive. In addition to the evidence from DIC microscopy and immunohistochemistry showing that the primary neurite of each ENC1 sprout short neuritic processes to the anterior ciliated cells of the dorsolateral band (**Fig. 9B**), transmission electron microscopy revealed that these ciliated cells also send short basal processes to the nearby primary neurite of ENC1 (Koss et al., 2002). These data suggest that the primary neurites of ENC1s directly innervate the anterior ciliary cells of the dorsolateral band through *en passant* serotonergic synapses, whereas excitation of the more posterior ciliary cells requires secondary processes. Since gap junctions have been observed between dorsolateral ciliary cells in *Helisoma* (Koss et al., 2002) and other mollusks (Arkett, 1988), these secondary processes likely include transfer of electrical or chemical signals through gap junctions.

In addition, neurotransmitters other than serotonin might also be involved in mediating the interaction between ENC1 and the dorsolateral ciliated cells. Preliminary evidence suggests that the gaseous nitric oxide (NO) is a likely candidate. In invertebrates, NO has been found in many species as a transmitter, cotransmitter or modulator (for a review, Jacklet, 1997). In *Helisoma*, NO synthase (NOS) activity has been found in ENC1 and the dorsolateral, but not the pedal, ciliated cells (Cole et al., 2002). Moreover, embryo rotation and ciliary beating were stimulated by addition of NO donors, and inhibited by addition of NOS inhibitors (Goldberg et al., 2000; Cole et al., 2002). It has been also shown that a NO pathway is involved in the Ca<sup>2+</sup> induced increase in mammalian tracheal ciliary activity (Uzlaner and Priel, 1999). That mianserin was a more effective antagonist of pedal ciliary activity as compared to dorsolateral activity (**Fig. 20B**) supports the idea that another transmitter, such as NO, contributes to ENC1-dorsolateral ciliary communication. It is possible that upon stimulation, ENC1 releases serotonin along with NO onto the anterior ciliary cells of the dorsolateral band. Because NO readily diffuses to other cells, all cells of the dorsolateral band may respond to NO released from ENC1. Alternatively, serotonin released from ENC1 may induce production of NO in the anterior ciliary cell of the dorsolateral band, which then diffuses to the remaining cells to regulate their ciliary activity.



In conclusion, results from this part show that ENC1s regulate the activity of the dorsolateral and pedal bands of cilia, but not the isolated tufts of cilia, in *Helisoma* embryos. The cilioexcitatory neurotransmitters, serotonin and probably NO as well, are involved in the communication between ENC1 and ciliary cells. Since uncoordinated movements are observed after unilateral elimination of ENC1, how each ENC1 “talks” to its contralateral partner in order to coordinate the rotational behavior is an avenue to explore in the future.

## **6. ENC1 as an O<sub>2</sub>-sensitive chemosensory neuron**

### **6.1. Multiple lines of evidence suggest ENC1 as the O<sub>2</sub> sensor**

Results from developmental correlation, laser ablation experiments, and electrophysiological recordings suggest that ENC1 not only functions to innervate ciliary cells, but also acts directly as the O<sub>2</sub> sensor in *Helisoma* embryos. First, developmental analysis demonstrates that at early stages when ENC1s are morphologically immature, the embryonic response to hypoxia is attenuated (**Fig. 39**). This suggests that the embryonic rotational responsiveness to hypoxia correlates to the development of ENC1. Second, bilateral laser ablation of ENC1s abolishes the hypoxia-elicited enhancement of embryonic rotation (**Fig. 40**), indicating ENC1s are required for mediating the embryonic response to hypoxia. Third, whole-cell recordings show that cultured ENC1s respond to hypoxia with a burst of action potentials and a prolonged depolarization of membrane potentials (**Fig. 43**). Similarly, cell attached recordings demonstrate that the frequency of current spikes increase under hypoxic challenge (**Fig. 42**). These electrophysiological recordings suggest that ENC1s directly respond to hypoxia with increases in electrical activity and subsequently stimulate embryonic rotation.

### **6.2. The dendritic knob is the possible site of O<sub>2</sub> sensing**

Based on several lines of evidence, the site of O<sub>2</sub> sensing is likely located in the dendritic knob of ENC1. First, the dendritic knob is terminated with an array of non-motile stiff cilia and some short microvilli (**Fig. 10**; Diefenbach et al., 1998). This structure shares the morphological features with some typical chemosensory structures reported in larval and adult mollusks (Emery, 1975; 1976; 1992; Yi and Emery, 1995;

Kempf et al., 1997; Marois and Carew, 1997a), as well as in vertebrate olfactory neurons (Muller and Marc, 1984; Menini, 1999). Second, both scanning electron and DIC microscopy indicate that the dendritic knobs are the only chemosensory-like structures on the embryonic surface at stages E15-E30 (Diefenbach et al., 1998; Koss et al., 2002). This reduces the possibility of other embryonic cells as the O<sub>2</sub> sensor. Third, no synaptic terminals from other cells onto the cell body or the apical dendrites of ENC1 were found with transmission electron and DIC microscopy (Goldberg et al., 1996; Koss et al., 2002), suggesting that the electrophysiological response of ENC1 to hypoxia does not result from synaptic activation of ENC1. Despite these lines of anatomical evidence, confirmation that ENC1's dendritic knob is the site of O<sub>2</sub> sensing awaits direct physiological analysis of this cell, such as imaging the hypoxia induced Ca<sup>2+</sup> spikes within individual sensory cilia (Leinders-Zufall et al., 1997; 1998) or laser ablating these chemosensory structures while keeping the soma intact. Finally, the common structure between the dendritic knob of ENC1 and the olfactory cells in adult snails and other animals suggests that ENC1 may also function to detect other chemical stimulants in addition to O<sub>2</sub>. It is possible that the rotational response to glutamine is also mediated by ENC1.

The O<sub>2</sub>-sensitive dendritic knob in snail embryos provides a morphological foundation for the identification of O<sub>2</sub> sensors in other systems. Although internal and external O<sub>2</sub> sensing elements have been reported in air-breathing (Lopez-Barneo et al., 1988; Youngson et al., 1993; Prabhakar, 2000) and aquatic animals (Wyse and Page, 1976; Janse et al., 1985; Burleson and Milsom, 1993), the cellular identity and structure of the O<sub>2</sub> sensors are either unknown or lack characteristic chemosensory-like structural specializations. A common ultrastructural feature of all these O<sub>2</sub>-sensitive cells is the existence of granules in the cytosol. It has been reported that both the glomus (type I) cell in the carotid body and the O<sub>2</sub>-sensitive cells in the blood vessel of fish contain dense core vesicles (Duchen et al., 1988; Kusakabe et al., 1991). Similar particles were also found in the apical region of ENC1's soma (Diefenbach et al., 1998; Koss et al., 2002).

In other marine invertebrate larvae, a group of homologous serotonergic neurons comprise parts of the apical sensory organ (Kempf et al., 1997; Marois and Carew, 1997a; Page and Parries, 2000). Some of these neurons also contain a tuft of apical cilia

at the embryonic surface (Marois and Carew, 1997a, b; Kempf et al., 1997). It would be interesting to test if the ASO also functions to detect environmental O<sub>2</sub> levels and regulate behavioral responses.

## **7. Signaling pathways involved in the rotational response to hypoxia**

The results discussed so far strongly imply that the dendritic knob of ENC1 directly senses decreases in the environmental Po<sub>2</sub> and generates electrical signals in the soma of ENC1. Upon integration of these input signals, action potentials traverse the primary neurite to induce the release of cilioexcitatory neurotransmitters at the nerve terminals. In addition to these cellular mechanisms underlying the hypoxia-induced behavioral response, the thesis also explored some of the molecular mechanisms involved in this sensory-motor reflex. At the chemosensory level, both closure of 4-AP sensitive K<sup>+</sup> channels and inhibition of mitochondrial electron transport chain are involved in the O<sub>2</sub> sensing process. Extracellular Ca<sup>2+</sup> may also be required for O<sub>2</sub> sensing. At the level of motor output, the cilioexcitatory neurotransmitters, serotonin and NO, as well as extracellular Ca<sup>2+</sup>, are involved in mediating the motor response of the ciliary cells.

### **7.1. Mechanisms of O<sub>2</sub> sensing**

Since the discovery that hypoxia reduces a K<sup>+</sup> current in mammalian O<sub>2</sub> chemoreceptors (Lopez-Barneo et al., 1988), K<sup>+</sup> channels have subsequently been implicated in O<sub>2</sub> sensing in many systems (Jiang and Haddad, 1994; Lopez-Barneo, 1994; Haddad and Jiang; 1997). In particular, certain voltage-sensitive K<sup>+</sup> channels that are sensitive to blockage by the pharmacological agent, 4-AP, play an important role in O<sub>2</sub> sensing of several cell types (Yuan et al., 1993; Tristani-Firouzi et al., 1996; Haddad and Jiang, 1997; Archer et al., 1998; Reeve et al., 1998). Experiments in this thesis show that 4-AP stimulates embryonic rotation in a way similar to a hypoxic challenge, but has no effect on the beating of denervated ciliated cells, suggesting that inactivation of K<sup>+</sup> channels is a conserved mechanism underlying O<sub>2</sub> sensing. Further electrophysiological studies on isolated ENC1 are required to demonstrate whether the O<sub>2</sub>-sensitive K<sup>+</sup> channels are specifically located on the surface of this cell.

Although inactivation of  $K^+$  channels is a common mechanism involved in mediating  $O_2$  sensing and acute responses to hypoxia, the molecular sensor for  $O_2$  is thought to be located upstream of the  $K^+$  channels (Haddad and Jiang, 1997; Archer et al., 1999; Lopez-Barneo et al., 2001). One of the prevailing hypotheses suggests that  $K^+$  channel activity can be modulated by the cytosolic redox status (Archer et al., 1999; Fu et al., 2000). Specifically,  $K^+$  channels tend to open when oxidized and close when reduced (**Fig. 1**; Ruppertsberg et al., 1991). However, the molecular identity of the  $O_2$  sensor that initiates the redox signal remains controversial. Mitochondria are the site of cellular respiration and the primary consumer of  $O_2$ . Moreover, function of the mitochondrial electron transport chain (ETC) is sensitive to  $O_2$  supply and affects cytosolic redox status through production of diffusible redox couples (Archer et al., 1999). Inhibitors of the ETC, such as rotenone and cyanide, reduce whole-cell  $K^+$  current and mimic hypoxia in different cell types (Rounds and McMartry, 1981; Burlison and Milsom, 1990; Duchen and Biscoe, 1992; Archer et al., 1993; Yuan et al., 1994; McKenzie and Taylor, 1996; Krumschnabel et al., 1998; Sundin et al., 1999). These lead to the ‘mitochondrial hypothesis’, which proposes the ETC as the  $O_2$  sensor. In this thesis, rotenone mimicked the embryonic rotational response to hypoxia, but had no direct effect on the ciliary effector cells (**Fig. 43**), suggesting that ETC function of chemosensory cells does play a role in  $O_2$  sensing. However, the delayed and slower response to rotenone as compared to the faster and larger response to 4-AP or hypoxia treatment (**Figs. 28 and 45**) argues against the possibility that the ETC is the initial site of  $O_2$  sensing in snail embryos.

It is likely that the mitochondrial ETC contributes to responses to more prolonged hypoxia, whereas the initial site of  $O_2$  sensing is located nearby  $K^+$  channels to enable a more immediate response to hypoxia (Lopez-Barneo, 1994). Specifically, certain membrane-bound proteins, such as NADPH oxidase, may act as the initial site of  $O_2$  sensing. NADPH oxidase catalyzes the production of reactive  $O_2$  species in an  $O_2$  dose-dependent manner (**Fig. 1**). The reactive  $O_2$  species subsequently affects the redox state and therefore determines the opening or closure of the  $K^+$  channels. NADPH oxidase has been implicated in the initial process of  $O_2$  sensing in the carotid body (Cross et al., 1990), pulmonary vasculature (Thomas et al., 1991; Mohazzab and Wolin, 1994) and neuroepithelial body (Fu et al., 2000). Immunohistochemical localization of NADPH

oxidase (Youngson et al., 1993) and pharmacological inhibition of this enzyme with diphenylene iodonium (Fu et al., 2000; Lopez-Barneo et al., 2001) should help to address if NADPH is the initial O<sub>2</sub> sensor in snail embryos. Finally, other O<sub>2</sub> sensing mechanisms, such as that mediated by molecular heme (**Fig. 1**), may also be present in this animal.

## 7.2. Hypoxia-elicited signal transduction

In O<sub>2</sub>-sensitive glomus type I and neuroepithelial cells, the acute hypoxia-induced signaling cascade downstream of K<sup>+</sup> channel closure includes membrane depolarization, Ca<sup>2+</sup> influx through activation of voltage-gated channels, elevation of intracellular Ca<sup>2+</sup>, and finally neurotransmitter release (Lopez-Barneo et al., 2001). Electrophysiological recordings of isolated ENC1s confirmed that hypoxia induces depolarization of these O<sub>2</sub>-sensitive chemosensory cells in snail embryos (**Fig. 43**). In addition, the involvement of extracellular Ca<sup>2+</sup> in mediating the embryonic rotational response to hypoxia was implicated during preliminary experiments with the Ca<sup>2+</sup> chelator EGTA. EGTA completely abolished the hypoxia-elicited enhancement of embryonic rotation (**Fig. 37**). Furthermore, basal embryonic rotation returned to pretreatment level in 30 min after washout of EGTA, whereas hypoxia-elicited embryonic rotation was still attenuated at this time point. These data suggest that Ca<sup>2+</sup> influx is not only required for normal ciliary beating, but also has a prolonged effect on O<sub>2</sub> sensing and hypoxia signaling. However, it remains to be determined whether Ca<sup>2+</sup> influx into ENC1s is a required step in the hypoxia-signaling cascade, since Ca<sup>2+</sup> influx into ciliary cells is necessary for mediating the cilioexcitatory action of serotonin (Christopher et al., 1996). Further examination of hypoxia-induced changes in intracellular Ca<sup>2+</sup> will help elucidate this question.

The final step of the hypoxia-signaling cascade is the release of neurotransmitters from the O<sub>2</sub>-sensitive chemosensory cells (Lopez-Barneo et al., 2001) and other neuronal cells (Fleiderovich et al., 2001). Serotonin immunohistochemistry (**Fig. 9 and 12**; Goldberg and Kater, 1989) and NADPH diaphrase staining (Cole et al., 2002) have indicated the presence of serotonin and NOS in ENC1s. These two cilioexcitatory neurotransmitters (Gosselin, 1961; Jain et al., 1993; Goldberg et al., 1994; 2000; Uzmaner and Priel, 1999; Li et al., 2000) may be released under hypoxic challenge. Results in this

thesis indicated that the serotonin receptor antagonist, mianserin, inhibits the embryonic response to hypoxia (**Fig. 44**), suggesting that release of serotonin from ENC1 is a part of the hypoxia-signaling pathway. Involvement of serotonin and its receptors in O<sub>2</sub> chemoreception has also been reported in the neuroepithelial bodies of rabbits (Youngson et al., 1993; Fu et al., 2002), fish gill (Burlison and Milsom, 1995), and some cells in the carotid body (Herman et al., 2000; Wang et al., 2000). The O<sub>2</sub>-sensitive glomus cells of the carotid body, however, predominantly release dopamine (Montoro et al., 1996), substance P (reviewed in Prabhakar, 2000), acetylcholine and ATP (Fitzgerald et al., 2000; Zhang et al., 2000) onto apposed sensory nerve endings, which result in sensory spikes in the carotid afferent sinus nerve. Therefore, ENC1s may be evolutionarily closer to the serotonergic chemosensory cells in the mammalian neuroepithelial body..

That mianserin alone could not completely block the rotational response to hypoxia suggests that there are additional factors involved in the communication between ENC1 and ciliated cells. NO, which is expressed in the dendrite and soma of ENC1 and plays a role in regulating ciliary activity (Goldberg et al., 2000; Cole et al., 2002), is one likely factor. Preliminary results in this thesis showed that hypoxia-elicited embryonic rotation was reversibly inhibited in the presence of the NO synthase inhibitor, L-NAME (data not shown), suggesting that NO is involved in the hypoxia signaling pathway. NO has also been implicated in the hypoxia-induced signaling cascade in the carotid body (Prabhakar, 1999; 2000) and in mediating the behavioral, cellular and developmental responses to hypoxia in larval *Drosophila* (Wingrove and O'Farrell, 1999). Electrical synapses between ENC1 and ciliated cells (Goldberg et al., 1996; Koss et al., 2002) may also contribute to the hypoxia-elicited enhancement in embryonic rotation observed in this study (see section 5.3).

## **8. General significance of ENC1-ciliary circuits in *Helisoma***

Collectively, I have delineated in this thesis the cellular and some of the molecular components of a sensory-motor neural circuit underlying a behavioral response to hypoxia in *Helisoma* embryos. To piece all the information together, embryonic metabolic O<sub>2</sub> consumption results in localized depletion of O<sub>2</sub> from the medium and an O<sub>2</sub> concentration gradient inside the egg capsule (**Fig. 49**). However, the low O<sub>2</sub> levels

within egg capsules cannot be replenished passively because diffusion of environmental O<sub>2</sub> towards the embryos is hampered by diffusional barriers formed by encapsulation. Therefore, the cilia-driven embryonic rotation serves not only to reduce the O<sub>2</sub> gradient surrounding each embryo, but also to enhance O<sub>2</sub> diffusion into the egg capsule (**Fig. 49**). In *Helisoma*, the ENC1-ciliary neural circuit functions to monitor O<sub>2</sub> levels surrounding the embryos and stimulate embryonic rotation when O<sub>2</sub> level falls, resulting in an enhanced O<sub>2</sub> supply. Given the lack of respiratory and circulatory systems during early developmental stages of the pond snail (Raven, 1958), maintaining an adequate intracapsular O<sub>2</sub> supply is crucial for the continual growth and development of the encapsulated embryos. From a physiological perspective, the function of this neural circuit in mediating embryonic rotation is similar to the neural control of ventilation in adult snails and higher animals.

The ENC1-ciliary cell circuit in *Helisoma* embryo provides a simple and experimentally accessible system to address several types of questions. To date, this system has been particularly useful for investigating the developmental and physiological roles played by neurotransmitters during early embryonic development (Goldberg and Kater, 1989; Goldberg et al., 1991; Goldberg, 1995; 1998; Diefenbach et al., 1995; 1998). The sensory and motor function of ENC1 has been demonstrated in the present study. Further investigations will address the molecular mechanisms of sensory-motor integration and the consequent behavioral responses. Finally, this neuron-ciliary circuit is also useful in answering developmental questions. Given the successful implementation of the cell-ablation and embryo-transplantation techniques in this study, this circuit could be used to investigate neuron-target interactions during neurite pathway formation and synaptogenesis.

ENC1's role in sensing and mediating a behavioral response to hypoxia raises some interesting evolutionary questions. It has been suggested that these cells are derived from the serotonergic cells in the apical sensory organ (ASO) of marine invertebrate larvae (Kempf et al., 1997; Marois and Carew, 1997a, b; Page and Parries, 2000; Hay-Schmidt, 2000). These cells are similar in that they all transiently express serotonin during early developmental stages, and have possible sensory and/or motor functions. In *Aplysia californica* larvae, a group of five apical serotonergic neurons were found to innervate the

velar ciliated cells, as well as muscle and neuronal cells (Marois and Carew, 1997c). Similarly, a group of five serotonergic neurons in the apical sensory organ of some nudibranch species extended axons ventrally into an apical neuropil. Three of these neurons had ciliated apical dendrites (Kempf et al., 1997). Since nudibranches lose their apical sensory organs during metamorphosis, these serotonergic cells are believed to sense environmental stimuli and in turn affect velar function during the larval stage (Kempf et al., 1997; Marois and Carew, 1997a, b). In particular, a recent study indicated that the apical sensory organ of the nudibranch, *Phestilla sibogae*, is responsible for sensing specific settlement cues (Hadfield et al., 2000). Although *Helisoma* embryos directly develop into juveniles without an induced metamorphosis, the serotonin immunoreactivity of ENC1 was lost at later embryonic stages (Diefenbach et al., 1998). It appears that ENC1s in *Helisoma* comprise a simplified apical sensory organ that is adapted to detect O<sub>2</sub> and possibly other stimuli in the capsule environment and control embryonic movements. Conversely, the results of the present study raise the possibility that detection of environmental O<sub>2</sub> is another function of the ASO, possibly mediated by parampullary sensory neurons that share morphological features with ENC1 (Kempf et al., 1997; Marois and Carew, 1997a; b; Page and Parries, 2000; Koss et al., 2002).

Dual function sensory-motor neurons are mostly restricted to lower animals such as cnidarians (Swanson et al., 1999), and are thus considered primitive. It is believed that they were replaced by functionally distinct sensory and motor neurons during nervous system evolution (Swanson et al., 1999). The presence of sensory-motor neurons in embryos (present study) and larvae (Marois and Carew, 1997a) of gastropod molluscs may represent a conservation of primitive features during embryonic development, or a functional adaptation of the nervous system in a simplified cellular environment. From this latter point of view, *Helisoma* embryos provide an excellent opportunity to examine the cellular and molecular mechanisms of O<sub>2</sub> sensing both *in vivo* and *in vitro*, and should provide valuable insights into the development of O<sub>2</sub> sensing.



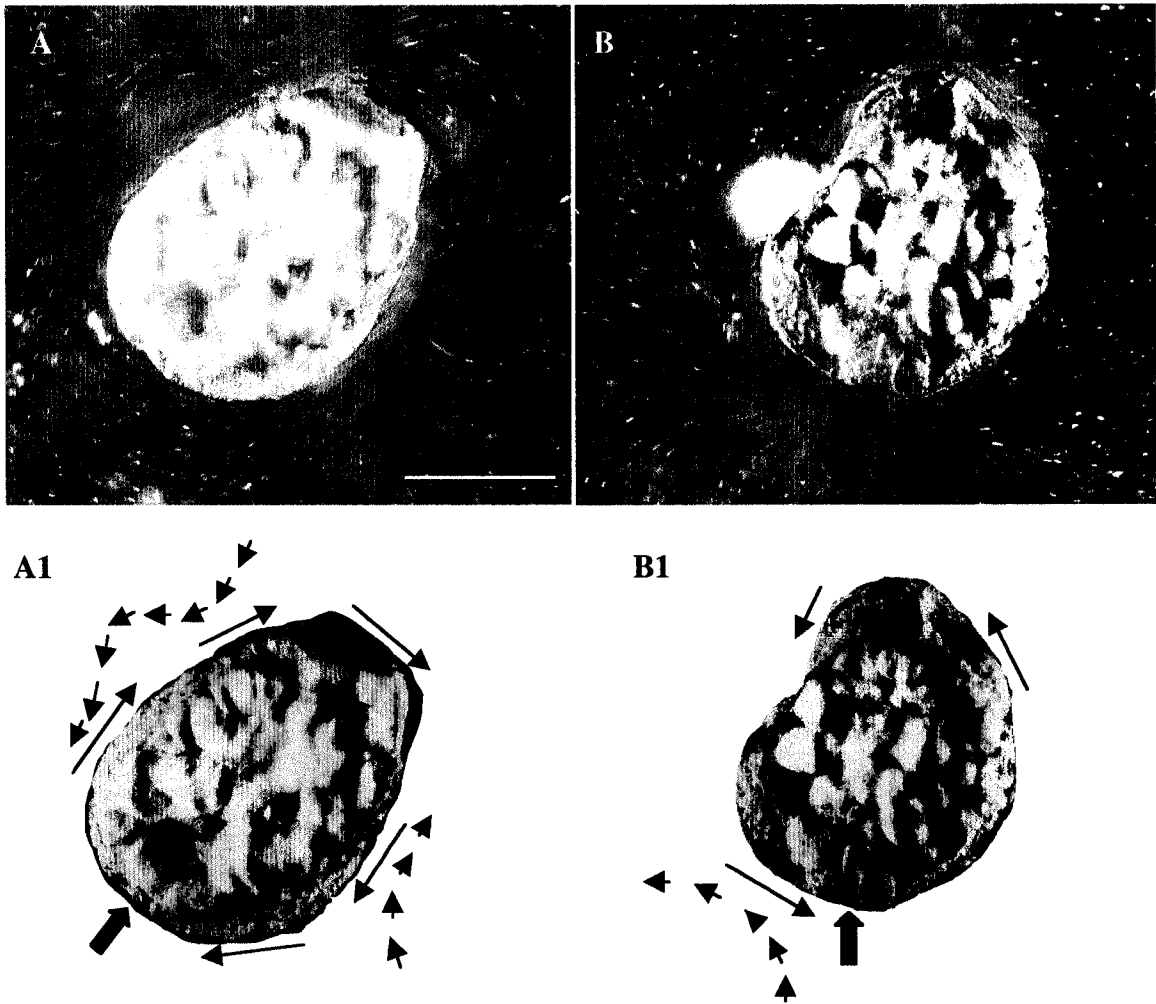


**Figure 47.** Visualization of current flow generated by ciliary beating in *Helisoma* embryos. Color-coated latex beads (diameter: 1  $\mu$ m) were added to the medium bathing a de-capsulated embryo. **A:** dorsal view of the embryo and the motion of particles. The direction of embryonic rotation (long arrows) and direction of current flow (short arrows) are indicated in **A1**. **B** and **B1:** Lateral view of embryonic rotation and current flow generated by ciliary activity. Block arrows indicate the embryonic mouth. Scale bar: 150  $\mu$ m.

**Figure 48.** Laser treatment paradigms. Under control conditions (**0 h**), ENC1 periodically releases cilioexcitatory serotonin (indicated by **red dots**) to a target ciliary cell, causing episodic surge in ciliary beat frequency (**CBF**) in addition to the constitutive basal CBF. Laser beams were focused via the objective lens onto a small area within ENC1. Heat and stress waves released from laser irradiation result in swelling of the cell. As a consequence, membrane permeability to cations (mainly  $K^+$ ,  $Na^+$  and  $Ca^{2+}$ ) increased, resulting in depolarization, generation of action potentials (**AP**) in the short-term (**0-1 h**). Stimulation of ENC1 caused prolonged release of serotonin to the target ciliary cell, resulting in enhanced CBF. Over the long-term (**> 6 h**), laser treatment eventually caused cell death of ENC1 as the cell lost its capability to maintain homeostasis, resulting in denervation and loss of periodic CBF surges in the target ciliary cell. Taking advantage of the laser-induced sequential excitation and cell death, laser beams were used to either stimulate ENC1 over the short-term and ablate this cell over the long-term in this study.

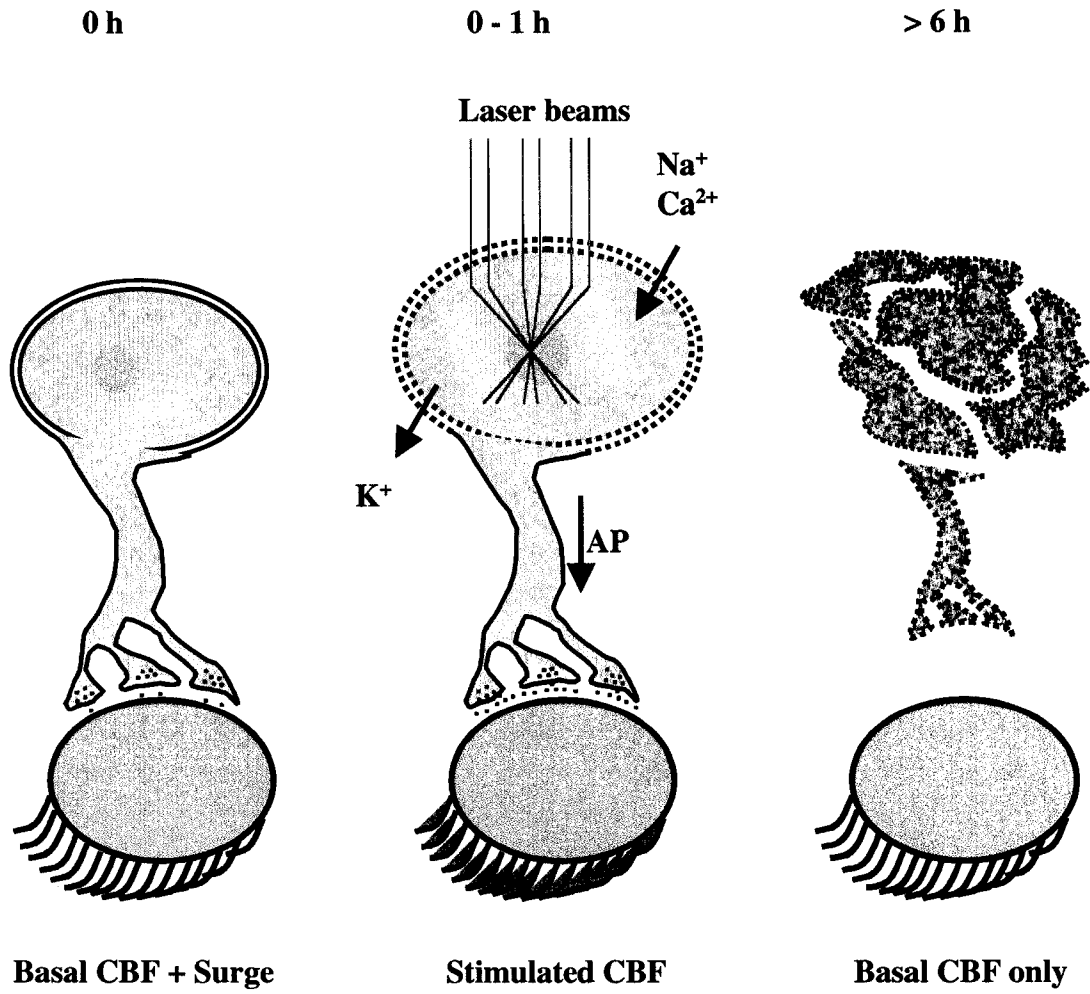
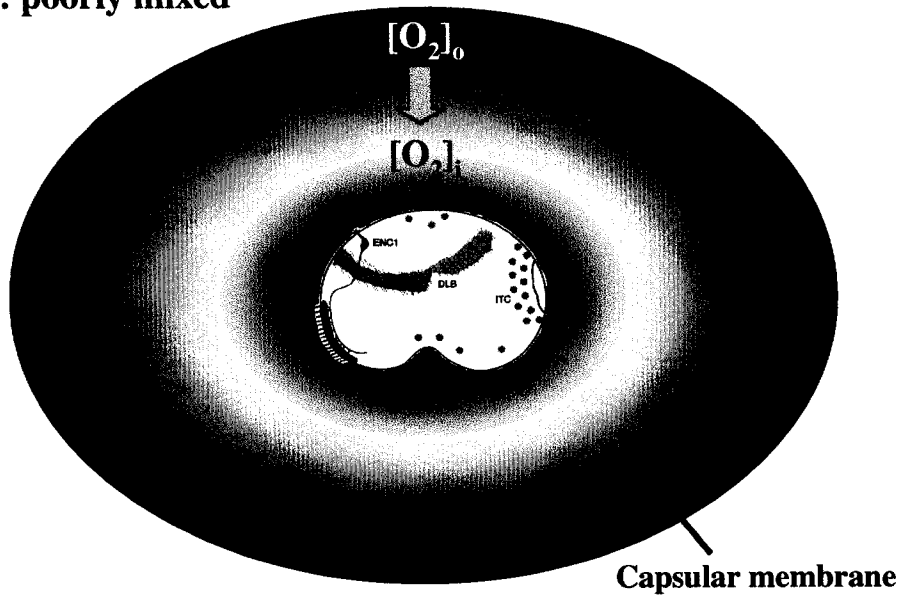
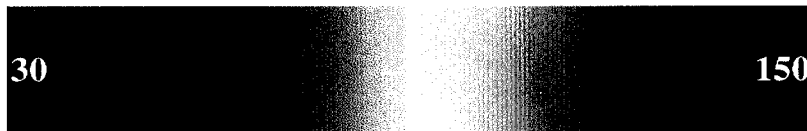
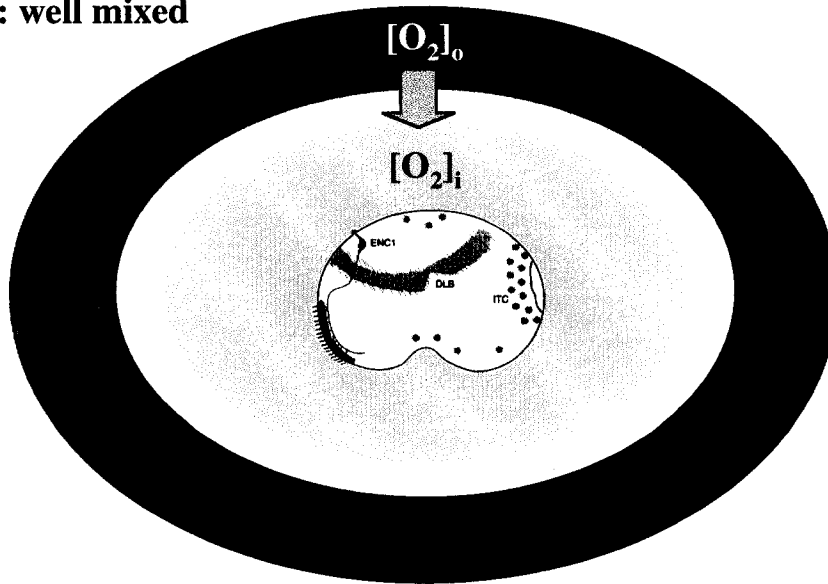


**Figure 49.** Model of the function of the embryonic rotational behavior. **A.** In the absence of rotation, a large intracapsular  $O_2$  concentration ( $[O_2]_i$ ) gradient will form due to the metabolic consumption of  $O_2$  by the embryo and the boundary layer effect. Thus, the capsular fluid immediately surrounding the embryo will be  $O_2$ -depleted with elevated levels of  $O_2$  close to the egg capsular membrane. This higher  $[O_2]_i$  near the egg capsular membrane will reduce the inward diffusion of  $O_2$  since the diffusional rate of environmental  $O_2$  into the egg capsule depends on the concentration gradient of the extracapsular  $O_2$  ( $[O_2]_o$ ) and  $[O_2]_i$ . **B:** Embryonic rotation functions to mix the intracapsular fluid so that the  $[O_2]_i$  gradient will be minimized. As a result, the  $[O_2]_i$  immediately surrounding the embryo will increase whereas the  $O_2$  level near the egg capsular membrane will decrease, thus facilitating the diffusion of environmental  $O_2$  into the egg capsule.

**A: poorly mixed**



**B: well mixed**



$P_{O_2}$  (mm Hg)

## Footnotes

1. A version of this section of the Results has been submitted to the Biological Bulletin for review. Kuang S, Regnier M, Goldberg JI. Long-term culture of decapsulated gastropod embryos: A transplantation study.
2. The technical assistance of Marette Regnier in testing the effect of pH and EGF on the growth and development of de-capsulated embryos is greatly appreciated.
3. A version of this section of the Results has been published. Kuang S, Goldberg JI. 2001. Laser ablation reveals regulation of ciliary activity by serotonergic neurons in molluscan embryos. *J Neurobiol* 47: 1-15.
4. A version of this section of the Results has been published. Kuang S, Doran SA, Wilson RJA, Goss GG, Goldberg JI. 2002. Serotonergic sensory-motor neurons mediate a behavioral response to hypoxia in pond snail embryos. *J Neurobiol* 52: 73-83.
5. I wish to acknowledge the technical assistance of George Braybrook with SEM and Dr. Rich Wilson with measurement of O<sub>2</sub> partial pressure.
6. Thank you Dr. Jeff Goldberg for providing this SEM micrograph (**Fig. 22B**).
7. I thank Dr. Greg Goss for helping me set up the apparatus for hypoxic and hypercapnic treatment.
8. The technical assistance of Shandra Doran in examining the effect of hypoxia on CBF of isolated ciliary cells is highly appreciated.
9. The technical assistance of Dr. Declan Ali in carrying out the patch clamping experiment is greatly appreciated.
10. I thank Dr. Steven Acher for helpful discussion on the mechanisms of O<sub>2</sub> sensing. Shandra Doran tested the effect of rotenone and 4-AP on CBF.

## References

- Agani FH, Kuo NT, Chang CH, Dreshaj IA, Farver CF, Krause JE, Ernsberger P, Haxhiu MA, Martin RJ. 1997. Effect of hyperoxia on substance P expression and airway reactivity in the developing lung. *Am J Physiol* 273: L40-45.
- Aiello E. 1957. The influence of branchial nerve and of 5-hydroxytryptamine on the ciliary activity of *Mytilus edulis gill*. *Biol Bull* 133: 325.
- Ali DW, Drapeau P, Legendre P. 2000. Development of spontaneous glycinergic currents in the Mauthner neuron of the zebrafish embryo. *J Neurophysiol* 84: 1726-1736.
- Archer SL, Huang J, Henry T, Peterson D, Weir EK. 1993. A redox-based O<sub>2</sub> sensor in rat pulmonary vasculature. *Circ Res* 73: 1100-1112.
- Archer SL, Souil E, Dinh-Xuan AT, Schremmer B, Mercier JC, El Yaagoubi A, Nguyen-Huu L, Reeve HL, Hampl V. 1998. Molecular identification of the role of voltage-gated K<sup>+</sup> channels, Kv1.5 and Kv2.1, in hypoxic pulmonary vasoconstriction and control of resting membrane potential in rat pulmonary artery myocytes. *J Clin Invest* 101: 2319-2330.
- Archer SL, Reeve HL, Michelakis E, Puttagunta L, Waite R, Nelson DP, Dinauer MC, Weir EK. 1999. O<sub>2</sub> sensing is preserved in mice lacking the gp91 phox subunit of NADPH oxidase. *Proc Natl Acad Sci USA* 96: 7944-7949.
- Arkett SA. 1988. Development and senescence of control of ciliary locomotion in a gastropod veliger. *J Neurobiol* 19: 612-623.
- Audesirk G. 1978. Central neuronal control of cilia in *Tritonia diamedea*. *Nature* 272: 541-543.
- Audesirk G, McCaman RE, Willows AOD. 1979. The role of serotonin in the control of pedal ciliary activity by identified neurons in *Tritonia diomedea*. *Comp Biochem Physiol* 62C: 87-91.
- Bach KB, Mitchell GS. 1996. Hypoxia-induced long-term facilitation of respiratory activity is serotonin dependent. *Respir Physiol* 104: 251-260.

- Bach KB, Kinkead R, Mitchell GS. 1999. Post-hypoxia frequency decline in rats: sensitivity to repeated hypoxia and  $\alpha$ 2-adrenoreceptor antagonism. *Brain Res* 817: 25-33.
- Bacon NC, Wappner P, O'Rourke JF, Bartlett SM, Shilo B, Pugh CW, Ratcliffe PJ. 1998. Regulation of the *Drosophila* bHLH-PAS protein Sima by hypoxia: functional evidence for homology with mammalian HIF-1 $\alpha$ . *Biochem Biophys Res Commun* 249: 811-816.
- Bainton CR, Kirkwood PA, Sears TA. 1978. On the transmission of the stimulating effects of carbon dioxide to the muscles of respiration. *J Physiol* 280: 249-272.
- Baker TL, Mitchell GS. 2000. Episodic but not continuous hypoxia elicits long-term facilitation of phrenic motor output in rats. *J Physiol* 529: 215-219.
- Balak KJ, Corwin JT, Jones JE. 1990. Regenerated hair cells can originate from supporting cell progeny: evidence from phototoxicity and laser ablation experiments in the lateral line system. *J Neurosci* 10: 2502-2512.
- Ballantyne D, Scheid P. 2000. Mammalian brainstem chemosensitive neurones: linking them to respiration *in vitro*. *J Physiol* 525: 567-577.
- Bargmann CI, Avery L. 1995. Laser killing cells in *Caenorhabditis elegans*. *Methods Cell Biol* 48: 225-250.
- Beadle LC. 1969. Salt and water regulation in the embryos of freshwater pulmonate molluscs. I. The embryonic environment of *Biomphalaria sudanica* and *Lymnaea stagnalis*. *J Exp Biol* 50: 473-479.
- Beermann AEL, Jay DG. 1994. Chromophore-assisted laser inactivation of cellular proteins. *Methods Cell Biol* 44: 715-732.
- Benkendorff K, Davis AR, Bremner JB. 2001. Chemical defense in the egg masses of benthic invertebrates: an assessment of antibacterial activity in 39 mollusks and 4 polychaetes. *J Invertebr Pathol* 78: 109-118.
- Berger F. 1998. Cell ablation studies in plant development. *Cell Mol Biol*. 44: 711-719.



- Bernhardt RR, Nguyen N, Kuwada JY. 1992. Growth cone guidance by floor plate cells in the spinal cord of zebrafish embryos. *Neuron* 8: 869-882.
- Boudko DY, Switzer-Dunlap M, Hadfield MP. 1999. Cellular and subcellular structure of anterior sensory pathways in *Phestilla sibogae* (Gastropoda, Nudibranchia). *J Comp Neurol* 403: 39-52.
- Bradley SR, Pieribone VA, Wang W, Severson CA, Jacobs RA, Richerson GB. 2002. Chemosensitive serotonergic neurons are closely associated with large medullary arteries. *Nat Neurosci* 5:401-402.
- Brodfoehr PD, Debski EA, O'Gara BA, Friesen WO. 1995. Neuronal control of leech swimming. *J Neurobiol* 27: 403-418.
- Bruce EN, Cherniack NS. 1987. Central chemoreceptors. *J Appl Physiol*. 62: 389-402.
- Brunelli M, Castellucci V, Kandel ER. 1976. Synaptic facilitation and behavioral sensitization in *Aplysia*: possible role of serotonin and cyclic AMP. *Science* 194: 1178-1181.
- Bulloch AGM, Syed NI. 1992. Reconstruction of neuronal networks in culture. *Trends Neurosci*. 15: 422-427.
- Bulloch AGM, Ridgway RL. 1995. Comparative aspects of gastropod neurobiology. In: Breidbach O, Kutsch W, editors. *The nervous systems of invertebrates: An evolutionary and comparative approach*. Birkhauser Verlag Basel, Switzerland. p 89-113.
- Bunn HF, Poyton RO. 1996. Oxygen sensing and molecular adaptation to hypoxia. *Physiol Rev* 76: 839-885.
- Burggren W. 1985. Gas exchange, metabolism and ventilation in gelatinous frog egg masses. *Physiol Zool* 58: 503-514.
- Burleson ML, Milsom WK. 1990. Propranolol inhibits O<sub>2</sub>-sensitive chemoreceptor activity in trout gills. *Am J Physiol* 258: R1089-1091.
- Burleson ML, Milsom WK. 1993. Sensory receptors in the first gill arch of rainbow trout. *Respir Physiol* 93: 97-110.

- Burleson ML, Milsom WK. 1995. Cardio-ventilatory control in rainbow trout: II. Reflex effects of exogenous neurochemicals. *Respir Physiol* 101: 289-299.
- Burrell BD, Sahley CL, Muller KJ. 2001. Non-associative learning and serotonin induce similar bi-directional changes in excitability of a neuron critical for learning in the medicinal leech. *J Neurosci* 21: 1401-1412.
- Callaway EM, Katz LC. 1993. Photostimulation using caged glutamate reveals functional circuitry in living brain slices. *Proc Natl Acad Sci USA* 90: 7661-7665.
- Castoldi AF, Barni S, Turin I, Gandini C, Manzo L. 2000. Early acute necrosis, delayed apoptosis and cytoskeletal breakdown in cultured cerebellar granule neurons exposed to methylmercury. *J Neurosci Res* 59: 775-787.
- Chang TN, Keshishian H. 1996. Laser ablation of *Drosophila* embryonic motoneurons causes ectopic innervation of target muscle fibers. *J Neurosci* 16: 5715-5726.
- Chia FS, Buckland-Nicks J, Young CM. 1984. Locomotion of marine invertebrate larvae: a review. *Can J Zool* 62: 1205-1222.
- Christopher KJ, Chang JP, Goldberg JI. 1996. Stimulation of ciliary beat frequency by serotonin is mediated by a  $Ca^{2+}$  influx in ciliated cells of *Helisoma trivolvis* embryos. *J Exp Biol* 199: 1105-1113.
- Christopher KJ, Young KG, Chang JP, Goldberg JI. 1999. Involvement of protein kinase C in 5-HT-stimulated ciliary activity in *Helisoma trivolvis* embryos. *J Physiol* 515: 511-522.
- Cole AG, Mashkournia A, Parries SC, Goldberg JI. 2002. Regulation of early embryonic behavior by nitric oxide in the pond snail, *Helisoma trivolvis*. *J Exp Biol*. in press.
- Crabtree RL, Page CH. 1974. Oxygen-sensitive elements in the book gills of *Limulus polyphemus*. *J Exp Biol* 60: 631-639.
- Cross AR, Henderson L, Jones OT, Delpiano MA, Hentschel J, Acker H. 1990. Involvement of an NAD(P)H oxidase as a  $pO_2$  sensor protein in the rat carotid body. *Biochem J* 272: 743-747.

- Cutz E, Jackson A. 1999. Neuroepithelial bodies as airway oxygen sensors. *Respir Physiol* 115: 201-214.
- Daristotle L, Bisgard GE. 1989. Central-peripheral chemoreceptor ventilatory interaction in awake goats. *Respir Physiol* 76: 383-391.
- Derry MW. 1993. *Air and Water: The Biology and Physics of Life's Media*. Princeton, NJ: Princeton Univ. Press. 341p.
- Dick TE, Coles SK. 2000. Ventrolateral pons mediates short-term depression of respiratory frequency after brief hypoxia. *Respir Physiol* 121: 87-100.
- Diefenbach TJ. 1995. Development of a serotonergic neuron in embryos of *Helisoma trivolvis*: Developmental and behavioral consequences of serotonin expression. Ph. D. thesis. University of Alberta, Edmonton.
- Diefenbach TJ, Koehncke NK, Goldberg JI. 1991. Characterization and development of rotational behavior in *Helisoma* embryos: role of endogenous serotonin. *J Neurobiol* 22: 922-934.
- Diefenbach TJ, Koss R, Goldberg JI. 1998. Early development of an identified serotonergic neuron in *Helisoma trivolvis* embryos: serotonin expression, de-expression, and uptake. *J Neurobiol* 34: 361-376.
- Diefenbach TJ, Sloley BD, Goldberg JI. 1995. Neurite branch development of an identified serotonergic neuron from embryonic *Helisoma*: evidence for autoregulation by serotonin. *Dev Biol* 167: 282-93.
- DiGregorio PJ, Ubersax JA, O'Farrell PH. 2001. Hypoxia and nitric oxide induce a rapid, reversible cell cycle arrest of the *Drosophila* syncytial divisions. *J Biol Chem* 276: 1930-1937.
- Dotz H, Eder M, Frick A, Zieglgansberger W. 1999. Precisely localized LTD in the neocortex revealed by infrared-guided laser stimulation. *Science* 286: 110-113.
- Doukas AG, Flotte TJ. 1996. Physical characteristics and biological effects of laser-induced stress waves. *Ultrasound Med Biol* 22: 151-164.

- Duchen MR, Biscoe TJ. 1992. Mitochondrial function in type I cells isolated from rabbit arterial chemoreceptors. *J Physiol* 450: 13-31.
- Duchen MR, Caddy KW, Kirby GC, Patterson DL, Ponte J, Biscoe TJ. 1988. Biophysical studies of the cellular elements of the rabbit carotid body. *Neuroscience* 26: 291-311.
- Ehrlich JS, Boulis NM, Karrer T, Sahley CL. 1992. Differential effects of serotonin depletion on sensitization and dishabituation in the leech, *Hirudo medicinalis*. *J Neurobiol* 23: 270-279.
- el Manira A, Tegner J, Grillner S. 1994. Calcium-dependent potassium channels play a critical role for burst termination in the locomotor network in lamprey. *J Neurophysiol* 72: 1852-1861.
- Emery DG. 1975. The histology and fine structure of the olfactory organ of the squid *Lolliguncula brevis* Blainville. *Tissue Cell* 7: 357-367.
- Emery DG. 1976. Observations on the olfactory organ of adult and juvenile *Octopus joubini*. *Tissue Cell* 8: 33-46.
- Emery DG. 1992. Fine Structure of Olfactory Epithelia of Gastropod Molluscs. *Microsc Res Tech* 22: 307-324.
- Epstein AC, Gleadle JM, McNeill LA, Hewitson KS, O'Rourke J, Mole DR, Mukherji M, Metzen E, Wilson MI, Dhanda A, Tian YM, Masson N, Hamilton DL, Jaakkola P, Barstead R, Hodgkin J, Maxwell PH, Pugh CW, Schofield CJ, Ratcliffe PJ. 2001. *C. elegans* EGL-9 and mammalian homologs define a family of dioxygenases that regulate HIF by prolyl hydroxylation. *Cell* 107: 43-54.
- Erlichman JS, Leiter JC. 1993. CO<sub>2</sub> chemoreception in the pulmonate snail, *Helix aspersa*. *Respir Physiol* 93: 347-363.
- Erlichman JS, Leiter JC. 1994. Central chemoreceptor stimulus in the terrestrial, pulmonate snail, *Helix aspersa*. *Respir Physiol* 95: 209-226.
- Erlichman JS, Leiter JC. 1997. Comparative aspects of central CO<sub>2</sub> chemoreception. *Respir Physiol* 110: 177-185.

- Eu JP, Sun J, Xu L, Stamler JS, Meissner G. 2000. The skeletal muscle calcium release channel: coupled O<sub>2</sub> sensor and NO signaling functions. *Cell* 102: 499-509.
- Evans JH, Sanderson MJ. 1999. Intracellular calcium oscillations regulate ciliary beat frequency of airway epithelial cells. *Cell Calcium* 26: 103-110.
- Farber IC, Grinvald A. 1983. Identification of presynaptic neurons by laser photostimulation. *Science* 222: 1025-1027.
- Feldman JL, McCrimmon DR. 1999. Neural control of breathing. In: Zigmond MJ, Bloom FE, Landis SC, Roberts JL, Squire LR, editors. *Fundamental neuroscience*. San Diego: Academic Press, p1063-1090.
- Fitzgerald RS, Dehghani GA. 1982. Neural responses of the cat carotid and aortic bodies to hypercapnia and hypoxia. *J Appl Physiol* 52: 596-601.
- Fitzgerald RS, Shirahata M, Wang HY. 1999. Acetylcholine release from cat carotid bodies. *Brain Res* 841: 53-61.
- Fitzgerald RS, Shirahata M, Wang HY. 2000. Acetylcholine is released from *in vitro* cat carotid bodies during hypoxic stimulation. *Adv Exp Med Biol* 475: 485-494.
- Fleiderovich IA, Gebhardt C, Astman N, Gutnick MJ, Heinemann U. 2001. Enhanced spontaneous transmitter release is the earliest consequence of neocortical hypoxia that can explain the disruption of normal circuit function. *J Neurosci* 21: 4600-4608.
- Flores V, Brusco A, Pecci Saavedra J. 1986. The serotonergic system in *Cryptomphalus aspersa*. Immunocytochemical study with an anti-5-HT antiserum. *J Neurobiol* 17: 547-561.
- Fork RL. 1971. Laser stimulation of nerve cells in *Aplysia*. *Science* 171: 907-908.
- Fretter V and Peake J. 1976. *Pulmonates*. Vol. 1. Functional anatomy and physiology. Academic Press, New York. 417p.
- Fu XW, Wang D, Nurse CA, Dinauer MC, Cutz E. 2000. NADPH oxidase is an O<sub>2</sub> sensor in airway chemoreceptors: evidence from K<sup>+</sup> current modulation in wild-type and oxidase-deficient mice. *Proc Natl Acad Sci USA* 97: 4374-4379.

- Fu XW, Nurse CA, Wong V, Cutz E. 2002. Hypoxia-induced secretion of serotonin from intact pulmonary neuroepithelial bodies in neonatal rabbit. *J Physiol* 539: 503-510.
- Fuller DD, Bach KB, Baker TL, Kinkead R, Mitchell GS. 2000. Long term facilitation of phrenic motor output. *Respir Physiol* 121: 135-146.
- Fuller DD, Zabka AG, Baker TL, Mitchell GS. 2001. Phrenic long-term facilitation requires 5-HT receptor activation during but not following episodic hypoxia. *J Appl Physiol* 90: 2001-2006.
- Gilmour KM. 2001. The CO<sub>2</sub>/pH ventilatory drive in fish. *Comp Biochem Physiol A Mol Integr Physiol* 130: 219-240.
- Glover JC, Kramer AP. 1982. Serotonin analog selectively ablates identified neurons in the leech embryo. *Science* 216: 317-319.
- Goldberg JI. 1995. Neuronal development in embryos of the mollusk, *Helisoma trivolvis*: multiple roles of serotonin. *Adv Neural Sci* 2: 67-87.
- Goldberg JI. 1998. Serotonin regulation of neurite outgrowth in identified neurons from mature and embryonic *Helisoma trivolvis*. *Perspect Dev Neurobiol* 5: 373-387.
- Goldberg JI, McCobb DP, Guthrie PB, Lawton RA, Lee RE, Kater SB. 1988. Characterization of cultured embryonic neurons from the snail *Helisoma*. In: Beadle D, Lees G, Kater SB, editors. *Cell Culture Approaches to Invertebrate Neuroscience*. London: Academic Press, p85-108.
- Goldberg JI, Kater SB. 1989. Expression and function of the neurotransmitter serotonin during development of the *Helisoma* nervous system. *Dev Biol* 131: 483-495.
- Goldberg JI, Mills LR, Kater SB. 1991. Novel effects of serotonin on neurite outgrowth in neurons cultured from embryos of *Helisoma trivolvis*. *J Neurobiol* 22: 182-194.
- Goldberg JI, Koehncke NK, Christopher KJ, Neumann C, Diefenbach TJ. 1994. Pharmacological characterization of a serotonin receptor involved in an early embryonic behavior of *Helisoma trivolvis*. *J Neurobiol* 25: 1545-1557.

- Goldberg JI, Tran N, Doran SA, Ahn KC, Eskicioglu C, Mashkournia A. 2000. Regulation of ciliary beating by nitric oxide in cultured ciliated cells from *Helisoma trivolvis* embryos. Soc Neurosci Abs 26: 437.1
- Goldberg MA, Dunning SP, Bunn HF. 1988. Regulation of the erythropoietin gene: evidence that the oxygen sensor is a heme protein. Science 242: 1412-1415.
- Gonzalez C, Lopez-Lopez JR, Obeso A, Perez-Garcia MT, Rocher A. 1995. Cellular mechanisms of oxygen chemoreception in the carotid body. Respir Physiol 102: 137-147.
- Gosselin RE. 1961. The cilioexcitatory activity of serotonin. J Cell Comp Physiol 58: 17-25.
- Gosselin RE, Moore KE, Milton AS. 1962. Physiological control of molluscan gill cilia by 5-hydroxytryptamine. J Gen Physiol 46: 277-294.
- Goudsmit EM. 1976. Galactogen catabolism by embryos of the freshwater snails, *Bulinnaea megasoma* and *Lymnaea stagnalis*. Comp Biochem Physiol 53: 439-442.
- Granzow B, Kater SB. 1977. Identified higher-order neurons controlling the feeding motor program of *Helisoma*. Neurosci 2: 1049-1063.
- Grinvald A, Farber IC. 1981. Optical recording of calcium action potentials from growth cones of cultured neurons with a laser microbeam. Science 212: 1164-1167.
- Groome JR, Clark M, Lent CM. 1993. The behavioural state of satiation in the leech is regulated by body distension and mimicked by serotonin depletion. J Exp Biol 182: 265-270.
- Gwag BJ, Koh JY, DeMaro JA, Ying HS, Jacquin M, Choi DW. 1997. Slowly triggered excitotoxicity occurs by necrosis in cortical cultures. Neurosci 77: 393-401.
- Haddad GG. 2000. Enhancing our understanding of the molecular responses to hypoxia in mammals using *Drosophila melanogaster*. J Appl Physiol 88: 1481-1487.
- Haddad GG, Jiang C. 1997. O<sub>2</sub>-sensing mechanisms in excitable cells: role of plasma membrane K<sup>+</sup> channels. Annu Rev Physiol 59: 23-42.

- Hadfield MG, Meleshkevitch EA, Boudko DY. 2000. The apical sensory organ of a gastropod veliger is a receptor for settlement cues. *Biol Bull* 198: 67-76.
- Hamill OP, Marty A, Neher E, Sakmann B, Sigworth FJ. 1981. Improved patch-clamp techniques for high-resolution current recording from cells and cell-free membrane patches. *Pflugers Arch* 391: 85-100.
- Hardaker LA, Singer E, Kerr R, Zhou G, Schafer WR. 2001. Serotonin modulates locomotory behavior and coordinates egg-laying and movement in *Caenorhabditis elegans*. *J Neurobiol* 49: 303-313.
- Hartness ME, Lewis A, Searle GJ, O'Kelly I, Peers C, Kemp PJ. 2001. Combined antisense and pharmacological approaches implicate hTASK as an airway O<sub>2</sub> sensing K<sup>+</sup> channel. *J Biol Chem* 276: 26499-26508.
- Hay-Schmidt A. 2000. The evolution of the serotonergic nervous system. *Proc R Soc Lond B Biol Sci* 267: 1071-1079.
- Heras H, Garin CF, Pollero RJ. 1998. Biochemical composition and energy sources during embryo development and in early juveniles of the snail *Pomacea canaliculata* (Mollusca: Gastropoda). *J Exp Zool* 280: 375-383.
- Herman JK, O'Halloran KD, Bisgard GE. 2000. Serotonin and the hypoxic ventilatory response in awake goats. *Adv Exp Med Biol* 475: 559-569.
- Hermann PM, van Kesteren RE, Wildering WC, Painter SD, Reno JM, Smith JS, Kumar SB, Geraerts WP, Ericsson LH, Smit AB, Bulloch AG, Nagle GT. 2000. Neurotrophic actions of a novel molluscan epidermal growth factor. *J Neurosci* 20: 6355-6364.
- Hirase H, Nikolenko V, Goldberg JH, Yuste R. 2002. Multiphoton stimulation of neurons. *J Neurobiol* 51: 237-247.
- Horstmann HJ. 1956. Der galaktogengehalt der eier von *Lymnaea stagnalis* L. während der embryonalentwicklung. *Biochem Z* 328: 342-347.
- Hoshi T, Heinemann SH. 2001. Regulation of cell function by methionine oxidation and reduction. *J Physiol* 531: 1-11.



- Hunter T, Vogel S. 1986. Spinning embryos enhance diffusion through gelatinous egg masses. *J Exp Mar Biol Ecol* 96: 303-308.
- Iben SC, Dreshaj IA, Farver CF, Haxhiu MA, Martin RJ. 2000. Role of endogenous nitric oxide in hyperoxia-induced airway hyperreactivity in maturing rats. *J Appl Physiol* 89: 1205-1212.
- Inoue T, Haque Z, Lukowiak K, Syed NI. 2001. Hypoxia-induced respiratory patterned activity in *Lymnaea* originates at the periphery. *J Neurophysiol*. 86: 156-163.
- Ivan M, Kondo K, Yang H, Kim W, Valiando J, Ohh M, Salic A, Asara JM, Lane WS, Kaelin WG Jr. 2001. HIF $\alpha$  targeted for VHL-mediated destruction by proline hydroxylation: implications for O<sub>2</sub> sensing. *Science* 292: 464-468.
- Jaakkola P, Mole DR, Tian YM, Wilson MI, Gielbert J, Gaskell SJ, Kriegsheim Av, Hebestreit HF, Mukherji M, Schofield CJ, Maxwell PH, Pugh CW, Ratcliffe PJ. 2001. Targeting of HIF $\alpha$  to the von Hippel-Lindau ubiquitylation complex by O<sub>2</sub>-regulated prolyl hydroxylation. *Science* 292: 468-472.
- Jacklet JW. 1997. Nitric oxide signaling in invertebrates. *Invert Neurosci* 3: 1-14.
- Jain B, Rubinstein I, Robbins RA, Leise KL, Sisson JH. 1993. Modulation of airway epithelial cell ciliary beat frequency by nitric oxide. *Biochem Biophys Res Commun* 191: 83-88.
- Janse C, van der Wilt GJ, van der Plas J, van der Roest M. 1985. Central and peripheral neurones involved in oxygen perception in the pulmonate snail *Lymnaea stagnalis* (Mollusca, Gastropoda). *Comp Biochem Physiol* 82A: 459-469.
- Jay DG, Keshishian H. 1990. Laser inactivation of fasciclin I disrupts axon adhesion of grasshopper pioneer neurons. *Nature* 348: 548-550.
- Jiang C, Haddad GG. 1994. A direct mechanism for sensing low oxygen levels by central neurons. *Proc Natl Acad Sci USA* 91: 7198-7201.
- Johnson SM, Wilkerson JE, Henderson DR, Wenninger MR, Mitchell GS. 2001. Serotonin elicits long-lasting enhancement of rhythmic respiratory activity in turtle brain stems *in vitro*. *J Appl Physiol* 91: 2703-2712.

- Jones JE, Corwin JT. 1996. Regeneration of sensory cells after laser ablation in the lateral line system: hair cell lineage and macrophage behavior revealed by time-lapse video microscopy. *J Neurosci* 16: 649-662.
- Kamiya H, Muramoto K, Ogata K. 1984. Antibacterial activity in the egg mass of a sea hare. *Experientia* 40: 947-949.
- Kandel ER. 2001. The molecular biology of memory storage: a dialogue between genes and synapses. *Science* 294: 1030-1038.
- Katz LC, Dalva MB. 1994. Scanning laser photostimulation: a new approach for analyzing brain circuits. *J Neurosci Methods* 54: 205-218.
- Katz PS. 1996. Neurons, networks, and motor behavior. *Neuron* 16: 245-253.
- Kemenes G. 1994. Processing of mechano- and chemosensory information in the lip nerve and cerebral ganglia of the snail *Helix pomatia* L. *Neurosci Behav Physiol* 24: 77-87.
- Kemenes G. 1997. *In vivo* neuropharmacological and *in vitro* laser ablation techniques as tools in the analysis of neuronal circuits underlying behavior in a molluscan model system. *Gen Pharmacol* 29: 7-15.
- Kempf SC, Page LR, Pires A. 1997. Development of serotonin-like immunoreactivity in the embryos and larvae of nudibranch mollusks with emphasis on the structure and possible function of the apical sensory organ. *J Comp Neurol* 386: 507-528.
- Kinkead R, Mitchell GS. 1999. Time-dependent hypoxic ventilatory responses in rats: effects of ketanserin and 5-carboxamidotryptamine. *Am J Physiol* 277: R658-666.
- Kodama T, Doukas AG, Hamblin MR. 2002. Shock wave-mediated molecular delivery into cells. *Biochim Biophys Acta* 1542: 186-194.
- Koshiya N, Smith JC. 1999. Neuronal pacemaker for breathing visualized *in vitro*. *Nature* 400: 360-363.
- Koshtoyants KHS, Buznikov GA, Manukhin BN. 1961. The possible role of 5-hydroxytryptamine in the motor activity of embryos of some marine gastropods. *Comp Biochem Physiol* 3: 20-26.

- Koss R, Diefenbach TJ, Kuang S, Doran SA, Goldberg JI. 2002. Coordinated development of identified serotonergic neurons and their target ciliary cells in *Helisoma trivolvis* embryos. *J Comp Neurol*. In press.
- Krumschnabel G, Frischmann ME, Schwarzbaum PJ, Wieser W. 1998. Loss of K<sup>+</sup> homeostasis in trout hepatocytes during chemical anoxia: a screening study for potential causes and mechanisms. *Arch Biochem Biophys* 353: 199-206.
- Kuang S, Goldberg JI. 2001. Laser ablation reveals regulation of ciliary activity by serotonergic neurons in molluscan embryos. *J Neurobiol* 47: 1-15.
- Kuang S, Doran SA, Wilson RJA, Goss GG, Goldberg JI. 2002. Serotonergic sensory-motor neurons mediate a behavioral response to hypoxia in pond snail embryos. *J Neurobiol* 52: 73-83.
- Kurachi M, Kikumoto M, Tashiro H, Komiya Y, Tashiro T. 1999. Real-time observation of the disassembly of stable neuritic microtubules induced by laser transection: possible mechanisms of microtubule stabilization in neurites. *Cell Motil Cytoskeleton* 42: 87-100.
- Kusakabe T, Ishii K, Ishii K. 1991. Dense granule-containing cells in the wall of the branchio-cardiac veins of a fresh water crayfish (*Astacus leptodactylus*). *Anat Embryol (Berl)* 183: 553-557.
- Kuwada JY. 1993. Pathway selection by growth cones in the zebrafish central nervous system. *Perspect Dev Neurobiol* 1: 195-203.
- Lahiri S, DeLaney RG. 1975. Relationship between carotid chemoreceptor activity and ventilation in the cat. *Respir Physiol* 24: 267-286.
- LeBoeuf RA, Kerckaert GA, Poiley JA, Raineri R. 1989. An interlaboratory comparison of enhanced morphological transformation of Syrian hamster embryo cells cultured under conditions of reduced bicarbonate concentration and pH. *Mutat Res* 222: 205-218.
- Lee S, Anderson T, Zhang H, Flotte TJ, Doukas AG. 1996. Alteration of cell membrane by stress waves in vitro. *Ultrasound Med Biol* 22: 1285-1293.

- Leinders-Zufall T, Rand MN, Shepherd GM, Greer CA, Zufall F. 1997. Calcium entry through cyclic nucleotide-gated channels in individual cilia of olfactory receptor cells: spatiotemporal dynamics. *J Neurosci* 17: 4136-4148.
- Leinders-Zufall T, Greer CA, Shepherd GM, Zufall F. 1998a. Imaging odor-induced calcium transients in single olfactory cilia: specificity of activation and role in transduction. *J Neurosci* 18: 5630-5639.
- Leinders-Zufall T, Greer CA, Shepherd GM, Zufall F. 1998b. Visualizing odor detection in olfactory cilia by calcium imaging. *Ann N Y Acad Sci* 855: 205-207.
- Li D, Shirakami G, Zhan X, Johns RA. 2000. Regulation of ciliary beat frequency by the nitric oxide-cyclic guanosine monophosphate signaling pathway in rat airway epithelial cells. *Am J Respir Cell Mol Biol* 23: 175-181.
- Ling L, Fuller DD, Bach KB, Kinkead R, Olson EB Jr, Mitchell GS. 2001. Chronic intermittent hypoxia elicits serotonin-dependent plasticity in the central neural control of breathing. *J Neurosci* 21: 5381-5388.
- Lipton P. 1999. Ischemic cell death in brain neurons. *Physiol Rev* 79: 1431-1568.
- Lopez-Barneo J. 1994. Oxygen-sensitive ion channels: how ubiquitous are they? *Trends Neurosci* 17: 133-135.
- Lopez-Barneo J. 1996. Oxygen-sensing by ion channels and the regulation of cellular functions. *Trends Neurosci* 19: 435-440.
- Lopez-Barneo J, Lopez-Lopez JR, Urena J, Gonzalez C. 1988. Chemotransduction in the carotid body: K<sup>+</sup> current modulated by PO<sub>2</sub> in type I chemoreceptor cells. *Science* 241: 580-582.
- Lopez-Barneo J, Pardal R, Ortega-Saenz P. 2001. Cellular mechanism of oxygen sensing. *Annu Rev Physiol* 63: 259-287.
- Losse G, Greven H. 1993. Structure, composition and permeability of the egg covering in the viviparous prosobranch gastropod *Littorina saxatilis*. *Invert Reprod Dev* 24: 225-236.

- Lucero MT, Horrigan FT, Gilly WF. 1992. Electrical response to chemical stimulation of squid olfactory receptor cells. *J Exp Biol* 162: 231-249.
- Mac Leish PR, Shepherd GM, Kinnamon SC, Santos-Sacchi J. 1999. Sensory transduction. In: Zigmond MJ, Bloom FE, Landis SC, Roberts JL, Squire LR, editors. *Fundamental neuroscience*. San Diego: Academic Press, p671-717.
- Mackie GO, Singla CL, Thiriot-Quievreux C. 1976. Nervous control of ciliary activity in gastropod larvae. *Biol Bull* 151:182-199.
- Makino Y, Cao R, Svensson K, Bertilsson G, Asman M, Tanaka H, Cao Y, Berkenstam A, Poellinger L. 2001. Inhibitory PAS domain protein is a negative regulator of hypoxia-inducible gene expression. *Nature* 414: 550-554.
- Mapara S, Goldberg JI, Gallin WJ. 2001. Cloning, phylogenetic analysis and localization of two serotonin receptors from the pond snail *Helisoma trivolvis*. *Soc Neurosci Abs* 27: 786.4.
- Marois R, Carew TJ. 1997a. Fine structure of the apical ganglion and its serotonergic cells in the larva of *Aplysia californica*. *Biol Bull*. 192: 388-398.
- Marois R, Carew TJ. 1997b. Ontogeny of serotonergic neurons in *Aplysia californica*. *J Comp Neurol* 386: 477-490.
- Marois R, Carew TJ. 1997c. Projection patterns and target tissues of the serotonergic cells in larval *Aplysia californica*. *J Comp Neurol* 386: 491-506.
- Martin LJ, Al-Abdulla NA, Brambrink AM, Kirsh JR, Sieber FE, Portera-Cailliau C. 1998. Neurodegeneration in excitotoxicity, global cerebral ischemia, and target deprivation: A perspective on the contribution of apoptosis and necrosis. *Brain Res Bull* 46: 281-309.
- McCrimmon DR, Zuperku EJ, Hayashi F, Dogas Z, Hinrichsen CF, Stuth EA, Tonkovic-Capin M, Krolo M, Hopp FA. 1997. Modulation of the synaptic drive to respiratory premotor and motor neurons. *Respir Physiol* 110: 161-176.
- McKenzie DJ, Taylor EW. 1996. Cardioventilatory responses to hypoxia and NaCN in the neotenus axolotl. *Respir Physiol* 106: 255-262.

- McPherson DR, Blankenship JE. 1991. Neural control of swimming in *Aplysia brasiliiana*. III. Serotonergic modulatory neurons. *J. Neurophysiol* 66: 1366-1379.
- Menini A. 1999. Calcium signalling and regulation in olfactory neurons. *Curr Opin Neurobiol* 9: 419-426.
- Meshcheryakov VN. 1990. The common pond snail *Lymnaea stagnalis*. In: Dettlaff TA, Vassetzky SG, editors. *Animal species for developmental studies*. Vol. 1. Invertebrates. Consultants Bureau, New York. p69-132.
- Millhorn DE. 1986. Neural respiratory and circulatory interaction during chemoreceptor stimulation and cooling of ventral medulla in cats. *J Physiol* 370: 217-231.
- Millhorn DE, Eldridge FL, Waldrop TG. 1980a. Prolonged stimulation of respiration by a new central neural mechanism. *Respir Physiol* 41: 87-103.
- Millhorn DE, Eldridge FL, Waldrop TG. 1980b. Prolonged stimulation of respiration by endogenous central serotonin. *Respir Physiol* 42: 171-188.
- Mills NE, Barnhart MC. 1999. Effects of hypoxia on embryonic development in two *Ambystoma* and two *Rana* species. *Physiol Biochem Zool* 72: 179-188.
- Mills NE, Barnhart MC, Semlitsch RD. 2001. Effects of hypoxia on egg capsule conductance in *Ambystoma* (Class Amphibia, Order Caudata). *J Exp Biol* 204: 3747-3753.
- Milsom WK. 1995. The role of CO<sub>2</sub>/pH chemoreceptors in ventilatory control. *Braz J Med Biol Res* 28: 1147-1160.
- Mitchell GS, Baker TL, Nanda SA, Fuller DD, Zabka AG, Hodgeman BA, Bavis RW, Mack KJ, Olson EB Jr. 2001. Intermittent hypoxia and respiratory plasticity. *J Appl Physiol* 90: 2466-2475.
- Moerman DG, Hutter H, Mullen GP, Schnabel R. 1996. Cell autonomous expression of perlecan and plasticity of cell shape in embryonic muscle of *Caenorhabditis elegans*. *Dev Biol* 173: 228-242.

- Mohazzab KM, Wolin MS. 1994. Properties of a superoxide anion-generating microsomal NADH oxidoreductase, a potential pulmonary artery PO<sub>2</sub> sensor. *Am J Physiol* 267: L823-831.
- Monteiro-Leal LH, Farina M, Benchimol M, Kachar B, De Souza W. 1995. Coordinated flagellar and ciliary beating in the protozoon *Tritrichomonas foetus*. *J Euk Microbiol* 42: 709-714.
- Montoro RJ, Urena J, Fernandez-Chacon R, Alvarez de Toledo G, Lopez-Barneo J. 1996. Oxygen sensing by ion channels and chemotransduction in single glomus cells. *J Gen Physiol* 107: 133-143.
- Morishita F, Mukai ST, Saleuddin ASM. 1998. Release of proteins and polysaccharides from the albumen gland of the freshwater snail *Helisoma duryi*: effect of cAMP and brain extracts. *J Comp Physiol* 182A: 817-825.
- Moroz LL, Sudlow LC, Jing J, Gillette R. 1997. Serotonin-immunoreactivity in peripheral tissues of the opisthobranch molluscs *Pleurobranchaea californica* and *Tritonia diomedea*. *J Comp Neurol* 382: 176-188.
- Morrill JB. 1982. Development of the pulmonate gastropod, *Lymnaea*. In: Harrison W, Cowdon RF, editors. *Developmental biology of freshwater invertebrates*. Alan R. Liss Inc., New York. p399-483.
- Morrill JB, Norris E, Smith SD. 1964. Electro- and immunoelectrophoretic patterns of the egg albumen of the pond snail *Limnaea palustris*. *Acta Embryol Morph Exp* 7: 155-166.
- Morse DE. 1990. Recent progress in larval settlement and metamorphosis: Closing the gaps between molecular biology and ecology. *Bull Mar Sci* 46: 465-483.
- Mulholland SE, Lee S, McAuliffe DJ, Doukas AG. 1999. Cell loading with laser-generated stress waves: the role of the stress gradient. *Pharm Res* 16: 514-518.
- Muller F, Aschenbach JR, Gabel G. 2000. Role of Na<sup>+</sup>/H<sup>+</sup> exchange and HCO<sub>3</sub><sup>-</sup> transport in pH<sub>i</sub> recovery from intracellular acid load in cultured epithelial cells of sheep rumen. *J Comp Physiol* 170B: 337-343.

- Muller JF, Marc RE. 1984. Three distinct morphological classes of receptors in fish olfactory organs. *J Comp Neurol* 222: 482-495.
- Murakami A. 1989. The control of cilia in metazoa: ciliary functions and Ca-dependent responses. *Comp Biochem Physiol* 94A: 375-382.
- Murakami A, Takahashi K. 1975. Correlation of electrical and mechanical responses in nervous control of cilia. *Nature* 257: 48-49.
- Murphy AD. 2001. The neuronal basis of feeding in the snail, *Helisoma*, with comparisons to selected gastropods. *Prog Neurobiol* 63: 383-408.
- Nagle GT, de Jong-Brink M, Painter SD, Li KW. 2001. Structure, localization and potential role of a novel molluscan trypsin inhibitor in *Lymnaea*. *Eur J Biochem* 268: 1213-1221.
- Nambu JR, Chen W, Hu S, Crews ST. 1996. The *Drosophila melanogaster* similar bHLH-PAS gene encodes a protein related to human hypoxia-inducible factor 1 alpha and *Drosophila* single-minded. *Gene* 172: 249-254.
- Nezlin L, Voronezhskaya E. 1997. GABA-immunoreactive neurones and interactions of GABA with serotonin and FMRFamide in a peripheral sensory ganglion of the pond snail *Lymnaea stagnalis*. *Brain Res* 772: 217-225.
- Nicholls JG, Martin AR, Wallace BG, Fuchs PA. 2001. From neuron to brain (4<sup>th</sup> edition). Sinauer Associates, Inc. Sunderland, MA, USA. p291-314.
- Nitatori T, Sata N, Waguri S, Karasawa Y, Araki H, Shibanaï K, Kominami E, Uchiyama Y. 1995. Delayed neuronal death in CA1 pyramidal cell layer of the gerbil hippocampus following transient ischemia is apoptosis. *J Neurosci* 15: 1001-1011.
- Nonaka S, Tanaka Y, Okada Y, Takeda S, Harada A, Kanai Y, Kido M, Hirokawa N. 1998. Randomization of left-right asymmetry due to loss of nodal cilia generating leftward flow of extraembryonic fluid in mice lacking KIF3B motor protein. *Cell* 95: 829-837.



- Norekian TP, Satterlie RA. 1996. Cerebral serotonergic neurons reciprocally modulate swim and withdrawal neural networks in the mollusk *Clione limacina*. *J Neurophysiol* 75: 538-546.
- O'Farrell PH. 2001. Conserved responses to oxygen deprivation. *J Clin Invest* 107: 671-674.
- Page LR. 2002. Apical Sensory Organ in Larvae of the Patellogastropod *Tectura scutum*. *Biol Bull* 202: 6-22.
- Page LR, Parries SC. 2000. Comparative study of the apical ganglion in planktotrophic caenogastropod larvae: ultrastructure and immunoreactivity to serotonin. *J Comp Neurol* 418: 383-401.
- Pavlova GA, Willows AO, Gaston MR. 1999. Serotonin inhibits ciliary transport in esophagus of the nudibranch mollusk *Tritonia diomedea*. *Acta Biol Hung* 50: 175-184.
- Pechenik JA, Chang SC, Lord A. 1984. Encapsulated development of the marine prosobranch gastropod *Nucella lapillus*. *Mar Biol* 78: 223-229.
- Pellequer JL, Brudler R, Getzoff ED. 1999. Biological sensors: More than one way to sense oxygen. *Curr Biol* 9: R416-418.
- Perrins R, Weiss KR. 1998. Compartmentalization of information processing in an *Aplysia* feeding circuit interneuron through membrane properties and synaptic interactions. *J Neurosci* 18: 3977-3989.
- Plesh B, de Jong-Brink M and Boer HH. 1971. Histological and histochemical observations on the reproductive tract of the hermaphrodite pond snail *Lymnaea stagnalis* (L.). *Neth J Zool* 21: 180-201.
- Prabhakar NR. 1999. NO and CO as second messengers in oxygen sensing in the carotid body. *Respir Physiol* 115: 161-168.
- Prabhakar NR. 2000. Oxygen sensing by the carotid body chemoreceptors. *J Appl Physiol* 88: 2287-2295.

- Prabhakar NR. 2001. Oxygen sensing during intermittent hypoxia: cellular and molecular mechanisms. *J Appl Physiol* 90: 1986–1994.
- Ratcliffe PJ, O'Rourke JF, Maxwell PH, Pugh CW. 1998. Oxygen sensing, hypoxia-inducible factor-1 and the regulation of mammalian gene expression. *J Exp Biol* 201: 1153-1162.
- Raven CP. 1958. Morphogenesis: the analysis of molluscan development. Pergamon Press, New York. 311p.
- Rees BB, Bowman JA, Schulte PM. 2001. Structure and sequence conservation of a putative hypoxia response element in the lactate dehydrogenase-B gene of *Fundulus*. *Biol Bull* 200: 247-251.
- Reeve HL, Weir EK, Archer SL, Cornfield DN. 1998. A maturational shift in pulmonary K<sup>+</sup> channels, from Ca<sup>2+</sup> sensitive to voltage dependent. *Am J Physiol* 275: L1019-1025.
- Rekling JC, Feldman JL. 1998. PreBotzinger complex and pacemaker neurons: hypothesized site and kernel for respiratory rhythm generation. *Annu Rev Physiol* 60: 385-405.
- Richerson GB, Wang W, Tiwari J, Bradley SR. 2001. Chemosensitivity of serotonergic neurons in the rostral ventral medulla. *Respir Physiol* 129:175-189.
- Richoux NB, Thompson RJ. 2001. Regulation of particle transport within the ventral groove of the mussel (*Mytilus edulis*) gill in response to environmental conditions. *J Exp Mar Biol Ecol* 260: 199-215.
- Rossen R, Kabat H, Anderson JP. 1943. Acute arrest of cerebral circulation in man. *Arch Neurol Psychiatry* 50: 510-528.
- Rounds S, McMurtry IF. 1981. Inhibitors of oxidative ATP production cause transient vasoconstriction and block subsequent pressor responses in rat lungs. *Circ Res* 48: 393-400.
- Roy M, Sapolsky R. 1999. Neuronal apoptosis in acute necrotic insults: why is this subject such a mess? *Trends Neurosci* 22: 419-422.

- Ruppersberg JP, Stocker M, Pongs O, Heinemann SH, Frank R, Koenen M. 1991. Regulation of fast inactivation of cloned mammalian  $IK_A$  channels by cysteine oxidation. *Nature* 352: 711-714.
- Saetta M, Mortola JP. 1987. Interaction of hypoxic and hypercapnic stimuli on breathing pattern in the newborn rat. *J Appl Physiol* 62: 506-512.
- Sahley CL. 1994. Serotonin depletion impairs but does not eliminate classical conditioning in the leech *Hirudo medicinalis*. *Behav Neurosci* 108: 1043-1052.
- Satir P, Sleight MA. 1990. The physiology of cilia and mucociliary interactions. *Annu Rev Physiol* 52: 137-155.
- Satterlie RA, Norekian TP. 1996. Modulation of swimming speed in the pteropod mollusc, *Clione limacina*: role of a compartmental serotonergic system. *Invert Neurosci* 2: 157-165.
- Satterlie RA, Norekian TP, Pirtle TJ. 2000. Serotonin-induced spike narrowing in a locomotor pattern generator permits increases in cycle frequency during accelerations. *J Neurophysiol* 83: 2163-2170.
- Sawin ER, Ranganathan R, Horvitz HR. 2000. *C. elegans* locomotory rate is modulated by the environment through a dopaminergic pathway and by experience through a serotonergic pathway. *Neuron* 26: 619-631.
- Semenza GL. 1999. Perspectives on oxygen sensing. *Cell* 98: 281-284.
- Semenza GL, Koury ST, Nejfelt MK, Gearhart JD, Antonarakis SE. 1991. Cell-type-specific and hypoxia-inducible expression of the human erythropoietin gene in transgenic mice. *Proc Natl Acad Sci USA* 88: 8725-8729.
- Shah EM, Jay DG. 1993. Methods for ablating neurons. *Curr Opin Neurobiol* 3: 738-42.
- Sillar KT, Kiehn O, Kudo N. 1997. Chemical modulation of vertebrate motor circuits. In: Stein PSG, Grillner S, Selverston AI, Stuart DG, editors. *Neurons, Networks, and Motor Behavior*. Cambridge, MA: MIT press. p183-193.

- Smith JC, Ellenberger HH, Ballanyi K, Richter DW, Feldman JL. 1991. Pre-Botzinger complex: a brainstem region that may generate respiratory rhythm in mammals. *Science* 254: 726-729.
- Smotherman WP, Robinson SR. 1987. Stereotypic behavioral response of rat fetuses to acute hypoxia is altered by maternal alcohol consumption. *Am J Obstet Gynecol* 157: 982-986.
- Soliman S. 1983. Pharmacological control of ciliary activity in the young sea urchin larva. Effects of monoaminergic agents. *Comp Biochem Physiol* 76C: 181-191.
- Stea A, Jackson A, Nurse CA. 1992. Hypoxia and N<sub>6</sub>, O<sub>2</sub>'-dibutyryl adenosine 3',5'-cyclic monophosphate, but not nerve growth factor, induce Na<sup>+</sup> channels and hypertrophy in chromaffin-like arterial chemoreceptors. *Proc Natl Acad Sci USA* 89: 9469-9473.
- Stockmann-Bosbach R, Althoff J. 1989. A correlated morphological and biochemical study of capsular fluid of *Nucella lapillus* (Gastropoda: Prosobranchia: Muricidae). *Mar Biol* 102: 283-289.
- Sundin LI, Reid SG, Kalinin AL, Rantin FT, Milsom WK. 1999. Cardiovascular and respiratory reflexes: the tropical fish, traïra (*Hoplias malabaricus*) O<sub>2</sub> chemoresponses. *Respir Physiol* 116: 181-199.
- Swanson LW, Lufkin T, Colman DR. 1999. Organization of nervous system. In: Zigmond MJ, Bloom FE, Landis SC, Roberts JL, Squire LR, editors. *Fundamental neuroscience*. San Diego: Academic Press, p9-37.
- Syed NI, Winlow W. 1989. Morphology and electrophysiology of neurons innervating the ciliated locomotor epithelium in *Lymnaea* (L.). *Comp Biochem Physiol* 93A: 633-644.
- Syed NI, Bulloch AG, Lukowiak K. 1990. *In vitro* reconstruction of the respiratory central pattern generator of the mollusk *Lymnaea*. *Science* 250: 282-285.
- Syed NI, Harrison D, Winlow W. 1991. Respiratory behavior in the pond snail *Lymnaea stagnalis* I. Behavioral analysis and the identification of motor neurons. *J Comp Physiol* 169A: 541-555.

- Syed NI, Ridgway RL, Lukowiak K, Bulloch AG. 1992. Transplantation and functional integration of an identified respiratory interneuron in *Lymnaea stagnalis*. *Neuron* 8: 767-774.
- Tamm SL. 1988. Calcium activation of macrocilia in the ctenophore *Beroë*. *J Comp Physiol* 163A: 23-31.
- Taylor BL, Zhulin IB, Johnson MS. 1999. Aerotaxis and other energy-sensing behavior in bacteria. *Annu Rev Microbiol* 53: 103-128.
- Taylor EW. 1982. Control and coordination of ventilation and circulation in crustaceans: response to hypoxia and exercise. *J Exp Biol* 100: 289-319.
- Taylor HH. 1973. The ionic properties of the capsular fluid bathing embryos of *Lymnaea stagnalis* and *Biomphalaria sudanica* (Mollusca: Pulmonata). *J Exp Biol* 59: 543-564.
- Teppema LJ, Dahan A, Olievier CN. 2001. Low-dose acetazolamide reduces CO<sub>2</sub>-O<sub>2</sub> stimulus interaction within the peripheral chemoreceptors in the anaesthetised cat. *J Physiol* 537: 221-229.
- Teshiba T, Shamsian A, Yashar B, Yeh SR, Edwards DH, Krasne FB. 2001. Dual and opposing modulatory effects of serotonin on crayfish lateral giant escape command neurons. *J Neurosci* 21: 4523-4529.
- Thom SR, Bhopale V, Fisher D, Manevich Y, Huang PL, Buerk DG. 2002. Stimulation of nitric oxide synthase in cerebral cortex due to elevated partial pressures of oxygen: An oxidative stress response. *J Neurobiol* 51: 85-100.
- Thomas HM 3rd, Carson RC, Fried ED, Novitch RS. 1991. Inhibition of hypoxic pulmonary vasoconstriction by diphenylethylidenehydrazide. *Biochem Pharmacol* 42: R9-12.
- Thompson C, Page CH. 1975. Nervous control of respiration: oxygen-sensitive elements in the prosoma of *Limulus polyphemus*. *J Exp Biol* 62: 545-554.

- Tristani-Firouzi M, Reeve HL, Tolarova S, Weir EK, Archer SL. 1996. Oxygen-induced constriction of rabbit ductus arteriosus occurs via inhibition of a 4-aminopyridine-, voltage-sensitive potassium channel. *J Clin Invest* 98: 1959-1965.
- Tsuchiya M, Kensler CJ. 1959. The effects of autonomic drugs and 2-amino-2-methyl propanol, a choline antagonist, on ciliary movement. *Fed Proc* 18: 453.
- Uzlaner N, Priel Z. 1999. Interplay between the NO pathway and elevated  $[Ca^{2+}]_i$  enhances ciliary activity in rabbit trachea. *J Physiol* 516: 179-190.
- van der Baan B. 2000. Ciliary function. *Acta Otorhinolaryngol Belg* 54: 293-298.
- van Mier P, Joosten HW, van Rheden R, ten Donkelaar HJ. 1986. The development of serotonergic raphespinal projections in *Xenopus laevis*. *Int J Dev Neurosci* 4: 465-475.
- van Raaij MT, Pit DS, Balm PH, Steffens AB, van den Thillart GE. 1996. Behavioral strategy and the physiological stress response in rainbow trout exposed to severe hypoxia. *Horm Behav* 30: 85-92.
- Voet D, Voet JG. 1995. *Biochemistry* (2<sup>nd</sup> ed). John Wiley & Sons, Inc. New York. 1360p.
- Vogan KJ, Tabin CJ. 1999. A new spin on handed asymmetry. *Nature* 397: 295-298.
- Waggoner LE, Zhou GT, Schafer RW, Schafer WR. 1998. Control of alternative behavioral states by serotonin in *Caenorhabditis elegans*. *Neuron* 21: 203-214.
- Wagner PG, Eldridge FL. 1991. Development of short-term potentiation of respiration. *Respir Physiol* 83: 129-139.
- Walczak CE, Nelson DL. 1994. Regulation of dynein-driven motility in cilia and flagella. *Cell Motil Cytoskeleton*. 27: 101-107.
- Walker RJ. 1986. Transmitters and modulators. In: Wilbur EM, editor. *The Mollusca*. Vol. 9 Neurobiology and Behavior, part 2 (Willows AOD volume editor). Academic Press, Inc. New York, p279-485.

- Wang ZY, Keith IM, Beckman MJ, Brownfield MS, Vidruk EH, Bisgard GE. 2000. 5-HT<sub>5a</sub> receptors in the carotid body chemoreception pathway of rat. *Neurosci Lett* 278: 9-12.
- Wannamaker CM, Rice JA. 2000. Effects of hypoxia on movements and behavior of selected estuarine organisms from the southeastern United States. *J Exp Mar Biol Ecol* 249: 145-163.
- Weiss KR, Koch UT, Koester J, Rosen SC, Kupfermann I. 1982. The role of arousal in modulating feeding behavior of *Aplysia*: neural and behavioral studies. In: Hoebel BG, Novin D, editors. *The neural basis of feeding and reward*. Haer Institute, Brunswick. p25-27.
- Wenger RH. 2000. Mammalian oxygen sensing, signalling and gene regulation. *J Exp Biol* 203: 1253-1263.
- Wijsman TCM, van Wijck-Batenburg H. 1987. Biochemical composition of the eggs of the freshwater snail *Lymnaea stagnalis* and oviposition-induced restoration of albumen gland secretion. *Int J Invert Reprod Dev* 12: 199-212.
- Wingrove JA, O'Farrell PH. 1999. Nitric oxide contributes to behavioral, cellular, and developmental responses to low oxygen in *Drosophila*. *Cell* 98: 105-114.
- Withers PC. 1992. *Comparative Animal Physiology*. Saunders College Publishing, Harcourt Bruce Jovanovich College Publishers. New York.
- Wright WG, Jones K, Sharp P, Maynard B. 1995. Widespread anatomical projections of the serotonergic modulatory neuron, CB1, in *Aplysia*. *Invert Neurosci* 1: 173-183.
- Wyse GA, Page CH. 1976. Sensory and central nervous control of gill ventilation in *Limulus*. *Fed Proc* 35: 2007-2012.
- Yeh SR, Fricke RA, Edwards DH. 1996. The effect of social experience on serotonergic modulation of the escape circuit of crayfish. *Science* 271: 366-369.
- Yeoman MS, Kemenes G, Benjamin PR, Elliott CJ. 1994. Modulatory role for the serotonergic cerebral giant cells in the feeding system of the snail, *Lymnaea*. II. Photoinactivation. *J Neurophysiol* 72: 1372-1382.

- Yi H, Emery DG. 1991. Histology and ultrastructure of the olfactory organ of freshwater pulmonate *Helisoma trivolvis*. *Cell Tissue Res* 265: 335-344.
- Youngson C, Nurse C, Yeger H, Cutz E. 1993. Oxygen sensing in airway chemoreceptors. *Nature* 365: 153-155.
- Yuan XJ, Goldman WF, Tod ML, Rubin LJ, Blaustein MP. 1993. Hypoxia reduces potassium currents in cultured rat pulmonary but not mesenteric arterial myocytes. *Am J Physiol* 264: L116-1123.
- Yuan XJ, Tod ML, Rubin LJ, Blaustein MP. 1994. Deoxyglucose and reduced glutathione mimic effects of hypoxia on K<sup>+</sup> and Ca<sup>2+</sup> conductances in pulmonary artery cells. *Am J Physiol* 267: L52-63.
- Zaitseva OV. 1999. Principles of the structural organization of the chemosensory systems of freshwater gastropod mollusks. *Neurosci Behav Physiol* 29: 581-593.
- Zhang M, Zhong H, Vollmer C, Nurse CA. 2000. Co-release of ATP and ACh mediates hypoxic signalling at rat carotid body chemoreceptors. *J Physiol* 525: 143-158.
- Zhu H and Bunn HF. 2001. How do cells sense oxygen? *Science* 292: 449-451.
- Zufall F, Leinders-Zufall T. 2000. The cellular and molecular basis of odor adaptation. *Chem Sense* 25: 473-481.